Assessment of computational methods, *Drosophila* assays and mouse model for identifying antigenotoxic phytochemicals

Thesis submitted to Jawaharlal Nehru University
for the award of the degree of

DOCTOR OF PHILOSOPHY

ISHA NAGPAL

School of Life Sciences
Jawaharlal Nehru University
New Delhi-110067
India

2017

SCHOOL OF LIFE SCIENCES

JAWAHARLAL NEHRU UNIVERSITY

NEW DELHI-110067

INDIA

CERTIFICATE

This is to certify that the research work embodied in this thesis entitled as **"Assessment of computational methods, *Drosophila* assays and mouse model for identifying antigenotoxic phytochemicals"** submitted for the award of Degree of Doctor of Philosophy has been carried out by Ms. Isha Nagpal under the guidance and supervision of Dr. Suresh K. Abraham at the School of Life Sciences, Jawaharlal Nehru University, New Delhi-110067, India. This work is original and has not been submitted so far, in part or in full for award of any other degree or diploma of any other university.

Isha Nagpal

(Candidate)

Dr. Suresh K. Abraham

20/12/14

(Supervisor)

Prof. B.C. Tripathy

(Dean)

Dedicated...

To

My

Beloved Family

Acknowledgement

A journey is easier when you travel together. Interdependence is certainly more valuable than independence. This thesis is the result of hard work whereby I have been accompanied and supported by many. It is pleasant that I now have the opportunity to express my gratitude for all of them. The feeling of completion of Ph.D. and this thesis is just like a lifetime achievement award. It was a long journey, and I have forgotten what I was doing before my Ph.D. period. Just like an old man, now I see back in time and think, "It was just a whole life." More or less I enjoyed this period, learned many things, made new friends and most of all I enjoyed the lifestyle of JNU. I know I am going to miss them. Along with these beautiful memories, some bad things also come with Ph.D. Many times, I was hunted down by frustration, hopelessness and many other adjectives with "ness" suffix. But I was fortunate that I have many well-wishers, who always saved me and brought me back on track. I want to express my gratefulness to all of them because without them this journey was not possible.

The first person I would like to thank is my guide ***Dr. Suresh K, Abraham (UGC Research Scientist "C")****. I wish to place my most sincere and profound sense of gratitude and profound thanks for his valuable guidance and encouragement throughout the course of this study. I indebted to him for providing me the golden opportunity to start my Ph.D. studies when I was facing the hardest time of my life. He not only supported me professionally, but also helped me in developing myself as an independent personality and granted me the serenity to accept the things I can not change, and courage to change the things which I can and enough wisdom to know the differences! I am heartily grateful to him for instilling confidence in me as a researcher and have made my approach toward science more refined and also supported me with his able guidance, honest criticism, suggestions and constant encouragement. It is his enthusiasm in mentoring the students which enticed me to decide*

about my future goals as a researcher and a teacher to keep the torch lit for times and generations ahead.

My heartfelt and sincere thanks to Prof. B.C. Tripathy, Dean of School of Life Sciences and Prof. B.N. Mallick, Prof. Neera Bhalla Sarin, Prof. R. Madhubala former Deans of School of Life Sciences, for providing the infrastructure facilities in the school for this research work.

I am thankful to Dr. Jayshree Paul for creating research environment in the laboratory and for her inspiring nature. I am also thankful to Naresh sir, Anil sir, Reena mam and Ishani for good research environment in lab

I would like to acknowledge Council of Scientific & Industrial Research (CSIR) for providing Senior Research Fellowship (SRF) for my research. I would also like to mention UGC non-NET, UGC-NETWORKING, and DST -PURSE for infrastructure support.

Teamwork divides the task and multiplies the success. During this work I have collaborated with many colleagues for whom I have great regard, and I wish to extend my warmest thanks to all those who have helped me with my work in the Department. Heartfelt thanks to my lab members Apurva, Sarpras for their help and support. A good friend is like a four-leaf clover, hard to find and lucky to have. I thank Dr. Nidhi Dwivedi and Lokesh Nigam for their valuable advice and friendly help. Their extensive discussions around my work and interesting explorations in my research work have been very helpful in this study. I will always remember my seniors Ashmita Samadder and Nidhi Khandelwal for their updates and encouragements.

Research is a mammoth task that can't be achieved alone and I am very grateful to the many people who have helped me along the way.

Great friends are hard to find, difficult to leave, and impossible to forget. I would also like to gratefully acknowledge the support of some very special individuals. They helped me immensely by giving me encouragement and friendship. I am thankful to my friends Vinod Singh ,Arpita Chakraborty, Neelu Singh, Shilpa Mukherjee, Ashutosh Singh, and Jogendra pawar for their help and moral support.

I am also grateful to Mrs. Bhawana Arora for her parental care and moral support when I was away from my home. Her words were sufficient to make me calm whenever I felt depressed and disturbed.

My acknowledgment remains incomplete without mentioning the care and affection provided by my parents especially in the testing times. Words fail to express my humble gratitude and profound regards to my parents and my all family members including my elder sister and brothers for their affectionate encouragement, co-operation and blessings, which always being a source of inspiration, without which it could not have been possible to achieve my objectives.

I would like to take this opportunity to beg mercy from the Almighty for the animals that had to be sacrificed during my research work. It is with heaviness in my heart that I bow my head in tribute to those creatures of God which had to sacrifice their lives for humanity's cause.

I am indebted to my parents for living, but to my teacher for living well. Even a plethora of words are not sufficient to express my feelings for my teachers. I am dedicating my Ph.D. to my all teachers who met me in different phases of life and taught me to make differences between good and bad.

Isha Nagpal

Table of Contents

List of Figures

List of Tables

List of abbreviations

.mol2	A tripos Mol2 file
.pdb	A protein data bank file
.ps	Post script file
.sdf	Spatial data file
Abs	Absorbance
AChE	Acetylcholinesterase
ANOVA	Analysis of Variance
Bax	Bcl-2 associated X protein
Bak	Bcl-2 homologous antagonist/killer protein
BC	Beta carotene
Bcl-2	B-cell lymphoma 2 protein
BRCA1	Breast cancer 1
BRCA2	Breast cancer 2
BSA	Bovine serum albumin
CAT	Catalase
cDNA	Complementary DNA
CDNB	1-chloro-2,4-dinitrobenzene
CF	Coffee
CPH	Cyclophosphamide
CvdW	coulomb and vander Waal
CYP450/cyt P450	Cytochrome P450
D. melanogaster	*Drosophila melanogaster*
DAPI	4',6-diamidino-2-phenylindole
DCA	Dichloroacetic acid
DCPIP	2,6-Dichlorophenolindophenol
DCF	2',7'-Dichlorofluorescein
DNA	Deoxyribonucleic acid
DTD	Dimethylthiarum disulfide
DTNB	5,5'-Dithiobis (2-nitrobenzonate)

DTT	Dithiothreitol
EDTA	Ethylene diamine tetra-acetic acid
Emodel	Energy Score based on Glide scoring function
EPA	Environmental Protection Agency
FBS	Fetal bovine serum
FITC	Fluorescein isothiocyanate
GA	Gallic acid
gm	Gram
GPx	Glutathione peroxidise
GR	Glutathione reductase
GSH	Glutathione
GSSG	Glutathione disulfide
GST	Glutathione-S-transferase
H_2DCFDA	2',7'-dihydrofluorescein diacetate
H_2O_2	Hydrogen peroxide
H&E	Hematoxylin and Eosin
HETATM	Hetero atom
HPF	High power field
HRP	Horse radish peroxidase
Hsp	Heat shock protein
IARC	International Agency for Research on Cancer
IC_{50}	Inhibitory concentration of maximal 50%
$K_2Cr_2O_7$	Potassium Dichromate
L	Litre
LDH	Lactate dehydrogenase
Lim	Limonene
LPO	Lipid peroxidation
M	Molar
MDA	Malondialdehyde
mg	Milligram
Min	Minute

ml	Millilitre
mM	Millimolar
Mol. Wt	Molecular weight
NAD^+	Nicotinamide adenine dinucleotide
NADH	Nicotinamide adenine dinucleotide
NADP	Nicotinamide adenine dinucleotide phosphate
NADPH	Nicotinamide adenine dinucleotide phosphate
NaOH	Sodium hydroxide
NBT	Nitroblue tetrazolium
ng	Nanogram
Nmoles	Nanomoles
$O_2^{\cdot -}$	Superoxide anion radica
$^{\cdot}OH$	Hydroxyl radical
$ONOO^-$	Peroxynitrite anion
PARP	Poly (ADP-ribose) polymerase protein
PBS	Phosphate buffer saline
PDB	Protein data bank
PI	Propedium Iodide
PMS	Phenazine methosulphate
PVDF	Polyvinylidene difluoride
QC	Quercetin
QSAR	Quantitative structure-activity relationship
RNA	Ribonucleic acid
RNAi	RNA interference
ROS	Reactive oxygen species
SDS	Sodium do-decyl sulphate
sec	Second
SLRL	Sex-linked recessive lethal test
SMART	Somatic mutation and recombination test
SOD	Superoxide dismutase Thermophilus
TAX	Taxifolin

TCA	Trichloroacetic acid
TEMED	Tetramethyethylenediamine
TBA	Thiobarbituric Acid
TP	Tea polyphenol
URE	Urethane
WHO	World Health Organization
µg	Microgram
µl	Microlitre
µm	Micrometer
µM	Micromolar

Chapter 1 : Introduction

DNA damage is a spontaneous process that the cells encounter during their normal cellular activities. Often mutations arise due to spontaneous DNA damage. Conversely, the frequencies of such mutations are relatively small, and imperatively cells have their repair mechanisms to encounter such DNA damages which may otherwise result in a fatal outcome. There are several environmental agents broadly characterized as physical and chemical agents that contribute to DNA damage

1.1. Physical agents causing DNA damage

Radiations, such as γ and X-rays, UV light, and particulate radiation (neutrons, α and β particles) are the most common physical agents that cause mutations. Most of these radiations are ionizing radiations with potential to ionize molecules. DNA is most susceptible to such ionizing radiations and gets damaged upon chronic exposure to these radiations. About 30-40% of this damage is direct and forms DNA adducts, cyclobutane pyrimidine dimers (CPDs), 6-4 photoproducts (6-4 PPs) (Morley et al., 2005), chromosome aberrations and rearrangements, point mutations while remaining 60-70% of DNA damage is indirect (Santivasi and Xia, 2014). Indirect DNA damage causes free radical generation like ROS and RNS which interacts with DNA and leads to base release and damage, crosslinking, polymerization, single stranded and double stranded DNA breakages (Ward, 1988). Perhaps, DNA damage also occurs due to the radiation-induced bystander effect, where cells with damaged DNA also induces DNA damage in the neighboring cells and thus amplifies the impairment (Mothersill and Seymour, 2001). In the last few decades, exposure to harmful levels of radiations has increased

due to ozone depletion (Sinha and Häder, 2002), radiation based clinical diagnosis, and radiotherapy for cancer treatment (Goldstein and Kastan, 2015). Also, studies have shown that radiotherapy is responsible for "bystander effect" (Havaki et al., 2015).

1.2. Chemical agents causing DNA damage

In addition to environmental factors, a wide variety of chemical agents also modulates genomic stability. These chemicals agents are mainly metal, aromatic hydrocarbon derivatives, pesticides, biphenyls, volatile organic compounds/organic solvents, food adulterants, and synthetic drugs.

Cyclophosphamide, an inactive prodrug with anticarcinogenic efficacy is commonly used as an adjuvant to various chemotherapeutic regimens including blood and marrow transplantations due to its immunosuppressive activity (Kanakry et al., 2013). Once administered, cyclophosphamide gets chemically and enzymatically metabolized into active 4-hydroxycyclophosphamide and aldophosphamide (both exist as tautomer) by cytochrome P450 in the liver. These two tautomers diffuse into cells where aldophosphamide further decomposes into phosphoramide mustard and acrolein. Phosphoramide mustard then induces inter and intra strands DNA crosslinks causing DNA damage (Emadi et al., 2009). Acrolein is a strong electrophilic α1 β-unsaturated aldehyde which forms acrolein-GSH adducts and results in oxidative stress by depleting cellular glutathione. Acrolein also reacts with cysteine, lysine, histidine residues in proteins and with deoxyguanosine (dG), and forms adducts with proteins and DNA (Stevens and Maier, 2008). Also, acrolein is reported to induce lipid peroxidation (Adams, 1993). Cyclophosphamide, besides an anticancer drug, is also reported to increase mutation frequency rates (Dubrova, 2016). Furthermore, there are many other

toxic effects associated with cyclophosphamide administration which include suppression of bone marrow, cardiotoxicity, failure of gonads (particularly in females), hemorrhagic cystitis, cancer of the bladder, secondary acute leukemia, and skin cancer.

Urethane, a carbamic acid ester is another hazardous chemical (Group 2A carcinogen) which is known to induce many types of toxic effects including carcinogenesis (Field and Lang, 1988). Urethane has multiple applications and used as an intermediate in the synthesis of amino resins in the textile industry (IARC, 1974). It is also used as a co-solvent and solubilizing agent in pesticide, cosmetics, and fumigants and as an adjuvant in pharmaceuticals and biomedical research. Urethane is also produced as a secondary metabolite by fermenting microorganisms, and thus levels of urethane are reported in many fermented products like bread, cheese, and beverages including beer, wine (Jiao et al., 2014). Urethane is metabolized mainly via three pathways amongst which the predominant one occur in the liver by microsomal esterase, where urethane is broken down into ammonia, ethanol, and CO_2. The other two metabolic pathways of urethane metabolism involve cytochrome P450 isoform CY2E1, which results in the production of vinyl carbamate (VC) and N-hydroxyurethane. CY2E1 itself subsequently oxidizes the produced VC into electrophilically more potent and highly reactive VC epoxide which reacts with adenosine and forms 1, N6-ethenoadenosine adducts. The second product N-hydroxyurethane produced during urethane metabolism depurinates thymine and cytosine (Williams and Nery, 1971). While the metabolic products of urethane induce DNA damage, urethane itself produce an increase in the frequency of sister chromatid exchange in bone marrow, somatic tissues, and germ cells and contributing disturbances in cellular DNA integrity (Jiao et al., 2014).

Human exposure to numerous such environmental agents may lead to induction of severe genetic modifications associating point mutation, chromosome rearrangement and breakage, chromosome loss or gain and gene silencing. Further pooling of such lethal mutations is often associated with severe pathophysiological conditions (Trimble and Doughty, 1974) like mutations in mitochondrial DNA also causes many human diseases (Tuppen et al., 2010) and further induces carcinogenesis. Chemoprevention is one of the most common approaches to prevent invasive carcinogenesis. Several chemical based compounds are used as chemotherapeutic drugs for the treatment of cancers like breast cancer (Choudhary et al., 2016), and other types of cancers (Hill et al., 2016) and many of them are under clinical trials (Boone et al., 1990). Even with the availability of myriads of chemical based drugs, not a single drug is completely efficient and thus, efforts are being made to develop a combinatorial regimen of such drugs to treat cancers (Lu, 2015). Nevertheless, besides not being completely efficient, synthetic compounds also pose severe side effects. Thus, there is an urge to define chemotherapeutic agents with higher potency and least side effects.

1.3. Dietary phytochemical as better alternative chemotherapeutics

Phytochemicals are naturally occurring secondary metabolites of plant origin and are known to exert inhibitory effects against chemical mutagenesis and carcinogenesis both in *in vitro* and *in vivo* test systems. These inhibitors are widely available in dietary plants and have the potentials to impede the dangerous effects and provide protection against both physical and chemical mutagens (Abraham et al., 1993). Phytochemicals offer minimal side effects and also their production cost is very less as compared to chemically synthesized anti-mutagens. Thus, the ongoing research is nowadays more

focused towards the study of antioxidative effects of phytochemicals. Phytochemicals exert their effects by different mechanisms; some interact with proteins and enhance their activity (Gertz et al., 2012), while some inhibit the activity of certain proteins. However, the most common protective mode of action of phytochemicals against the effects of both physical and chemical mutagens implicate chelation and scavenging free radicals generated due to exposure to such mutagens. Besides, phytochemicals also induce upregulation of mRNAs of antioxidant enzymes like catalase, glutathione *s*-transferase leading to overexpression of such antioxidant enzymes *in vivo* (C Jagetia, 2007) and rescuing cells from induced oxidative stress. Several phytochemicals have been studied and explored for their beneficial role in the prevention of DNA damage caused due to mutagenic agents. The most common of these include phytochemicals flavonoids, carotenoids, and saponins which are present in tea, coffee, fruits, vegetables, and herbs.

1.3.1. Tea polyphenols

Tea, one of the most common beverages is consumed throughout the world. It is extracted from the leaves of plant *Camellia sinensis* and consumed as green, black, or Oolong tea. Green tea is produced by steaming, which destroys the enzymes responsible for degrading phytochemicals and thus preserves them. Many beneficial effects of green tea are reported so far which include anti-tumor and anti-proliferative effects, protection against degenerative diseases, prevention from hepatoxicity and oxidative stress (Pastore et al. 2006). Green tea prevents oxidative stress by protecting cells from detrimental effects of free radicals. Based on Oxygen Radical Absorbance Capacity (ORAC) data analysis, tea and tea polyphenols have been reported to exert very high

antioxidant potentials (Khan and Mukhtar, 2007). Green tea reduces the concentration of nitric oxide and malondialdehyde in plasma. Catechins, phytochemicals present in tea are believed to enhance the activity of vitamin C, and vitamin E. Consumption of green tea also increases the activities of superoxide dismutase and catalase (Chacko et al., 2010). Reports from *in vivo* studies suggest that tea polyphenols reduce oxidization of DNA base 8-OHdG in skin, colon, lung, liver and pancreatic cancers (Frei and Higdon, 2003). Green tea polyphenols are also reported to inhibit mutagen induced reverse mutations (Wang et al., 1989). Recently Morey et al. using alkaline comet assay demonstrated that epigallocatechin gallate (EGCG), a bioactive phytochemical present in green tea can reduce UVR-induced DNA damage in cultured human cells and peripheral leucocytes (Cinkilic et al., 2014).

1.3.2. Beta-carotene

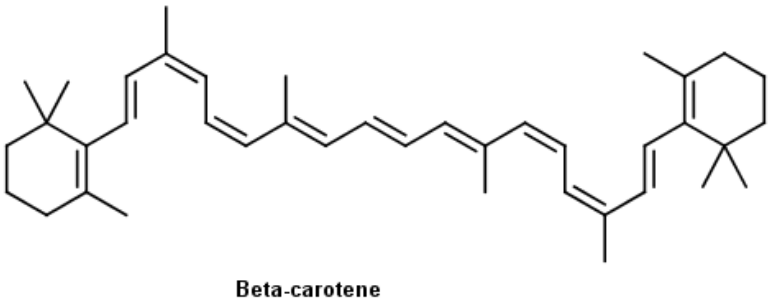

Figure 1.1: Chemical structure of Beta-carotene

Beta-carotene is a member of carotenoids family which comprises of more than 600 members. Carotenoids are naturally produced by plants, non-photosynthetic bacteria, and fungi with two primary functions of photosynthesis and photoprotection. The conjugated polyene structure of carotenoids enables them to absorb light and quench singlet oxygen species as well. β-carotene is found in fruits and vegetables and is the

chief source of vitamin A. β-carotene due to its photoprotective effect is also called as sun protectant (Biesalski and Obermueller-Jevic, 2001). β-carotene demonstrates various health effects including chemopreventive effects in the formation of preneoplastic lesions, antioxidant effects by scavenging singlet oxygen and prevention of peroxide compounds oxidation (Dias et al., 2009). It significantly reduces radiation-induced damage, and under different studies, β-carotene exerts radioprotective effects in partial and total body irradiation, chromosomal damage, micronuclei frequency in mice and radiation-induced weight loss in rats. Supplementation of β-carotene in cancer patients and children exposed to Chernobyl reactor demonstrates a lower prevalence of micronuclei and lipid peroxidation (Ben-Amotz et al., 1998). It is reported to reduce frequencies of micronucleated polychromatic erythrocytes (MN-PCEs) and associated chromosomal damage in mouse models exposed to γ radiation (Abraham et al., 1993). It is also reported to induce protection against reduction in the frequencies of micronuclei development in both somatic and germ cells of mouse exposed to X-rays (Salvadori et al., 1996). β-carotene has been reported to induce protective effects in doxorubicin-induced genotoxicity in somatic cells of *Drosophila melanogaster* (Dias et al., 2009). Owing to its photoprotective and antioxidant properties, supplementation of β-carotene has been reported for inducing protective effects in various disorders including photosensitivity disorder, cardiovascular disease, age-related macular degeneration and senile cataract (Mayne, 1996).

1.3.3. Quercetin

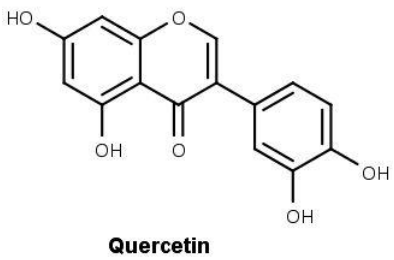

Figure 1.2: Chemical structure of Quercetin

Quercetin, a flavonoid widely present in fruits and vegetables especially in onions, apples, cranberries and blueberries. Quercetin is known for its antioxidant potentials, owing to the reduction potential of its phenolic hydroxyl group and scavenges ROS and RNS species (Boots et al., 2008). Quercetin is also reported to inhibit malignant cell growth by inducing cell cycle arrest in the late G_2 phase of the cell cycle. It also attenuates signal transduction pathways and inhibits intracellular Ca^{2+} release by inhibiting protein tyrosine kinases and also inhibits various serine/threonine protein kinases (Csokay et al., 1997). Besides its antioxidant properties, quercetin also poses other health benefits including antiviral, anticarcinogenic, anti-inflammatory, cardioprotective and neuroprotective properties. It is also reported to enhance mitochondrial biogenesis and thus may exert profound beneficial effects on performance and health (Davis et al., 2009).

1.3.4 Taxifolin

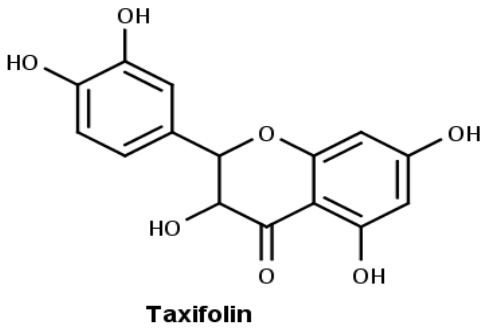

Figure 1.3: Chemical structure of Taxifolin

Taxifolin, also called as dihydroquercetin is a flavonoid and commonly found in red onions, Jeffery pine (Kurth and Chan, 1951), milk thistle, French maritime bark, etc. (Weidmann, 2012). The chemical structure of taxifolin is similar to quercetin and the only difference is presence of two additional hydrogen atoms (Kurth and Chan, 1951) and the absence of a double bond in the C-ring, which makes taxifolin more potent quenching agent than quercetin (Salah et al., 1995; Ghosh et al., 2002). Taxifolin is reported to inhibit production of superoxide and cytochrome P450 activity (Haraguchi et al., 1996). It activates the genetic activator antioxidant response element (ARE) (Lee et al., 2007) which is localized in the promoter region of two phase II enzyme genes namely: NADPH: quinone oxidoreductase-1 (Favreau and Pickett, 1991) and glutathione S-transferase A2 (Friling et al., 1990). These enzymes play crucial roles in signal transduction, proliferation, survival and immunological defense of cell. Also, they help in the elimination of xenobiotic products of phase I cytochrome enzymes (Lee et al., 2007). Taxifolin helps in prevention of cardiovascular diseases by inhibiting cholesterol biosynthesis, and liver diseases mainly by inhibiting lipid peroxidation (Weidmann, 2012).

1.3.5 Gallic acid

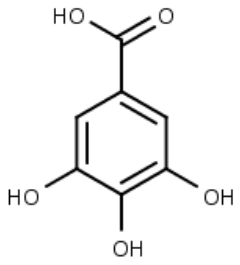

Gallic acid

Figure 1.4: Chemical structure of Gallic acid

Gallic acid is another phytochemical profoundly distributed in varieties of fruits and plants. In plants, the gallic acid may occur in a free state or conjugated form. Commercially, gallic acid is obtained by solvent extraction of either nutgalls or japanese gall. Commercial applications of the gallic acid include as a precursor for paints and inks, as the developer of color, in pharmaceuticals and as anti-oxidant in packaged foods. Gallic acid is reported to exert antimicrobial and is more potent against fungi and Gram-positive bacteria by interfering with the ATP synthesis pathways of the microbiota. It is also reported to induce apoptosis in cancer cells and selectively inhibits metastatic tumors and poses no such effect in healthy cells. Few studies suggest that the gallic acid induces protection against radiation and reduces lipid peroxidation in exposed mice thus protecting both membrane and DNA damage (Gandhi and Nair, 2005). It is also reported to inhibit tyrosinase (polyphenol oxidase), which is a copper-containing monooxygenase and a regulatory enzyme in melanin biosynthesis (Kim, 2007). Gallic acid is also reported to affect different isoforms of drug metabolizing enzyme CYP both *in vitro* and *in vivo*. Gallic acid and its derivatives also induce anti-mutagenic and anti-carcinogenic properties by interacting with proteins involved in the

metabolization of chemical mutagens, particularly they enhance the intracellular level and expression of glutathione S-transferase, a phase II metabolizing enzyme and attenuates the activity of phase I enzyme CYP450 (Ow and Stupans, 2003).

1.3.6 Limonene

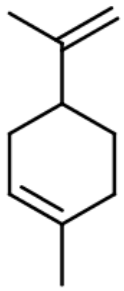

D-Limonene

Figure 1.5: Chemical structure of D-Limonene

D-limonene (1-methyl-4-(1-methylethenyl) cyclohexane) is a monoterpene present in oils of citrus fruits like orange, lemon, and grapefruit. D-limonene is commercially used as flavoring and fragrance agent in beverages, chewing gums, food products, soaps, and perfumes. D-limonene is a potent anti-genotoxic agent as it quenches free radicals generated by oxidative stress (Romero-Jiménez et al., 2005). It is reported to inhibit mutations arising due to exposure to ultraviolet-C radiations in *Escherichia coli*, *Salmonella typhimurium*, and *Saccharomyces cerevisiae* (Bakkali et al., 2008). D-limonene also shows anti-carcinogenic activity in rats mammary carcinogenesis induced by exposure to dimethylbenz[a]anthracene (DMBA) by elevating the levels of hepatic glutathione S-transferase, a phase II metabolizing enzyme (Elegbede et al., 1993). In another study, D-limonene inhibited the development of gastric cancers in wistar rats exposed to *N*-methyl-N^1-nitro-*N*-nitrosoguanidine (MNNG) by accelerating

apoptosis and lowering DNA synthesis (Uedo et al., 1999). D-limonene in combination with 4-hydroxyandrostrenedione has been reported to reduce up to 83% of NMU-induced mammary tumors in the rat (Chander et al., 1994). Many other clinical applications of D-limonene are reported which include dissolution of human gallstones, gastroesophageal reflux disorder (GERD) (Sun, 2007), enhancing immunity, blood regeneration and as a diuretic (Djilani and Dicko, 2012).

1.3.7 Coffee

Coffee, one of the most commonly consumed beverages worldwide is known to exert antigenotoxic and anticarcinogenic effects against a variety of mutagens in both *in vitro* and *in vivo* test systems. Coffee has been reported to induce antigenotoxic properties against somatic mutations and mitotic recombinations induced in *Drosophila melanogaster* by exposure to three different chemical mutagens: cyclophosphamide (CPH), mitomycin C (MMC) and urethane (URE) (Abraham and Graf, 1996). Coffee is also reported to attenuate ROS-induced lipid peroxidation in rats (Devasagayam et al., 1996) and exerts protective effects against oxidative and DNA damage in human cell culture. A Recent report suggests that coffee is beneficial against cellular mutagens, and it exerts antimicrobial properties against foodborne pathogenic microorganisms (Monente et al., 2015).

1.4. Models for screening of phytochemicals and other chemotherapeutics

Human health can be protected by detection and minimization of human exposure to mutagens. In this regard, screening of mutagens and antimutagens is required for both newly synthesized and already prevalent compounds. Several factors like sensitivity and the capacity of the test system to detect mutagens and promutagens, time needed for the

assay and cost of the test influence the choice of the test system employed. Many *in vitro* and *in vivo* screening and test systems are reported for the screening of mutagens and antimutagens including yeast, S*almonella typhimurium* (Ames, 1971), *E.coli* (Rosenkranz et al., 1976), *Bacillus subtilis* (Kada et al., 1972), mammalian cells (Chu, 1974). However, none of the test systems facilitate whole organism study and each of these have their own drawbacks.

With the recent development and advancement of computer-aided tools, large genotoxic datasets can be analyzed and thus computational application came to light for screening and development of chemotherapeutic agents (Ekins, 2007) including phytochemicals. Thus *in silico* approach offers many advantages like less cost, time and technical staff, reproducibility of results, reduced use of animals for experimental validation (3R approach), less exposure to chemicals (Snyder, 2009). The *in silico* approach can be helpful in understanding the molecular interactions between the both mutagens and antimutagens with different biomolecules including DNA, proteins, and enzymes. Using the knowledge of these interactions, the underlying chemistries and the structural-activity relationships (SAR), a chemical compound can be developed into a potent antigenotoxic agent by simply modifying functional groups.

Drosophila is a robust model for studying genetics and mutations. With the recent findings of the genome and biochemical similarities with human, use of *Drosophila* in the screening of drugs is nowadays more common (Giacomotto and Ségalat, 2010). The small genome of *Drosophila* allows easy manipulation and thus can be used for development for different disease models. Several disease models are reported to screen drugs like an antiepileptic drug (Stilwell et al., 2006), nadolol, fosfanol, and

levonordefrin (Pandey and Nichols, 2011). The benefit of using *Drosophila* in screening includes low cost and maintenance, short generation time and screening of promutagens. One of the major advantages of using *Drosophila* in the studies is the identifying mutations by different phenotypic characters including the color of eye and wing hair mutations. Based on these phenotypes, many anti-cancer drugs have been tested using SMART test in *Drosophila* (Phillips, 1990). Also, the use of two different test systems mainly the SLRL and SMART assay, one can even determine that whether the genotoxicity of the drug is in somatic cells or germ cells (Frei et al., 1992). The model can also be used in cases where other models cannot be used due to certain drawbacks (life cycle, availability of mutants, mode of administration of test agents, etc.). For example, *Drosophila* SMART test was successfully used to investigate the genotoxicity of tamoxifen, a drug used in the treatment of breast cancer. Since tamoxifen is an anti-estrogen, its pathway requires estrogen receptor. However, *Drosophila* lacks estrogen receptor and thus it provides an added advantage where genotoxicity of tamoxifen is identified due to its cellular attributes and not influenced by estrogen receptor pathway (Heres-Pulido et al., 2004).

Use of animal models (*in vivo*) in drug screening is one of the most commonly employed model systems due to its anatomical, physiological and genetic similarities with the human system (Giacomotto and Ségalat, 2010). Mouse models are largely used for the study of cancer development and its prevention due to its ability to generate xenografts and solid tumors. The other advantage of mouse model is that genetic alterations (Toupet et al., 2008) can be done and, immunological (Lötscher et al., 2007), developmental and stem cell research can be carried out in an efficient way. However,

the mouse model is suitable for various studies, yet there is an urge to minimize the use of mouse models, and preferential use of other alternative models is appreciated considering the high cost, maintenance and the 3Rs approach (Olsson et al. 2011).

The prime objective of the planned work is to emphasize the useful properties of screened phytochemicals which are naturally packaged with least known adverse effects on human body. In the proposed study, phytochemicals were screened with the aid of modern computing based technology blended with tests using *Drosophila* model as it is ideal for large-scale screening and a much-needed tool to bridge the gap between the traditional *in vitro* and preclinical animal assays. Considering cost and time constraint for testing large chemical libraries, the *in vivo* screening using whole-animal tumor models is not feasible, and only the potent inhibitors undergo *in vivo* assessment using animal models. Such an effort including all aspects of phytochemical properties may yield a new generation of drugs which will be effective but least toxic and may also give other benefits. Thus this study may help to prove and establish Indian culture of medication which has been using these phytochemicals in their crude form for the cure of various disorders.

Chapter 2 : Computational screening of dietary phytochemicals

2.1. Introduction

Computational screening of small molecules also called virtual screening is an effective method often used in the modern world for the screening, development and optimization of novel molecules against a target protein. Virtual screening offers many advantages over traditional high throughput screening which scrutinizes different combinatorial chemicals with the aid of highly advanced robotics and engineering. Earlier high throughput screening was the only choice for the rational and systematic selection of lead molecules in the drug development industry. This methodology involves higher expenditure and intensive techniques for a long duration of time yet resulting in very low output and high cost for the newly developed drugs. Besides being costly in terms of time, money and technical staff, high throughput screening may also sometimes lead to false-positives and negatives (Keseru & Makara 2006) or otherwise non-specific binding of test compound leading to fatal side effects (Harrow 2002). Furthermore, if a test compound shows high efficacy, its exact mode of action, may remain unclear, and it can be deciphered only with further structural biology experiments (Ramesha 2000).

In recent years, virtual screening has emerged as an alternative to high-throughput screening, where large sets of compound libraries can be screened against a target molecule with predicted binding properties. Virtual screening methods are performed using computer algorithms, requires less cost, time and technical staff. Moreover, since the entire process is carried out in a virtual environment based on the binding, chemical

and entropic properties of the target and the compounds, only the final scrutinized compounds are needed to be synthesized, unlike high throughput screening where a whole set of compounds are first synthesized and later tested for their effect. Virtual screening of compounds requires an X-ray crystal structure or solution (NMR) structure of the target protein and considering the 'hot spot' residues of the target, molecule libraries of different chemicals can be screened (Bohacek et al. 1996). One chemical can be screened within just five seconds based upon its chemical interactions, accessing the void cavity and solvent accessible area within the target molecule. In recent years, even if the three-dimensional structure of a particular target protein is unavailable, utilizing bioinformatics and molecular modeling tools, one can model the structure of the target protein, which can be further minimized, optimized and can be used for screening diverse set of compounds. *In silico* screening and designing methods can also be employed in the development of lead molecule from a screened dataset. Using 3D-pharmacophore methods like QSAR, one can alter the functional groups of a top lead compound and can further rationally refine and optimize the lead with all possible potentials to be developed as a new and promising drug. Various computer-based docking tools based on varying algorithm and scoring functions are used for virtual screening of chemical compound libraries against a target protein (Harrow 2002). These include GLIDE (based on incremental and simulation search), GOLD (based on genetic algorithm search), DOCK (based on incremental and simulation search), AUTODOCK (based on Monte Carlo search) and Hammerhead (based on incremental and simulation search) (Kitchen et al. 2004).

In our studies, we used virtual screening approach, which is a computer-aided approach to screen compounds based on the predicted binding affinity between compounds and a target protein. Different *in silico* screening tools have been employed in screening libraries of chemical compounds and proved beneficial in scrutinizing a lead compound against a particular protein (Kitchen et al. 2004). Phytochemicals are natural compounds, reported to exhibit myriads of effects in cellular biology. In the present study, we have computationally screened phytochemical library from quality phytochemical database against p53, Mdm2, Bcl-2 and PARP as our target proteins.

2.1.1. The p53-Mdm2 interaction

The p53 tumor suppressor gene also acts as a transcription factor, which is associated with many cellular functions. Amongst many of these functions (Vousden & Lane 2007), p53 functions are also associated with maintaining DNA integrity (Meek 2004). Under normal conditions, cellular DNA gets damaged, which is either repaired or eliminated by concomitant expression of p53. However, under various pathophysiological conditions like DNA damage, chromosome alterations (arising due to certain external factors or due to altered cellular conditions), p53 homeostasis is altered. Cellular levels of p53 are tightly regulated by p53 associated protein called as Murine Double Minute 2 (MDM2). Expression of both p53 and Mdm2 is autoregulated in a negative feedback loop, where p53 transcribes Mdm2 gene, while Mdm2 degrades p53 (Wu et al. 1993). Mdm2 protein contains many domains and regions including a nuclear localization signal (NLS) sequence, p53 binding domain, acidic domain, zinc finger and ring finger motifs which contribute to p53 turnover (Lozano & Montes de Oca Luna 1998). The interaction between these two protein is made by p53 binding

domain at its N-terminal end which forms a deep hydrophobic binding pocket, into which a α-helix of p53 comprising of residues 18-26 amino acids that governs its interaction (Iwakuma & Lozano 2003). Amongst these residues, Phe-19, Trp-23 and Leu-26 form hydrogen bonds with the hydrophobic cavity of Mdm2 (Moll & Petrenko 2004). Once p53 binds to Mdm2, it is then degraded by 26s proteasome complex (Michael & Oren 2003).

2.1.2. The Bcl-2 protein

Bcl-2 was first introduced as a unique oncogene in B-cell lymphomas that inhibits cell death (Tsujimotoet al., 1985), and comprises a family of proteins on the basis of their homology domains (BH1 to BH4). The Bcl-2 family is further characterized into three sub-groups on the basis of their roles in apoptosis and the BH region: (1) The anti-apoptotic group containing BH3 or BH4 region includes Bcl-2, Bcl-xL, Bcl-w, Bcl-B, A1, and Mcl-1. (2) The pro-apoptotic group containing BH2 or BH4 region and includes Bax, Bak, Bcl-x s, Bok, and Bcl-GL. (3) The BH3 protein group which shares only its BH3 domain and includes Bad, Bid, Bim, Bik, Noxa, Puma, Bcl-Gs, Blk, Bmf and Hrk. The Bcl-2 protein family is associated with the mitochondrial apoptotic pathway, also known as an intrinsic pathway. The Bcl-2 is a 26kDa mitochondrial membrane protein (Hockenbery et al. 1990) and is also localized in the intracellular membrane of endoplasmic reticulum (ER), and perinuclear membrane. The functional role of Bcl-2 in the nuclear membrane is yet not clear but it’s presence in ER is associated with induction of apoptosis via calcium signaling (Kirkin et al. 2004).

2.1.3. PARP protein

PARP (Poly (ADP-ribose) polymerase) is one of the most ubiquitous families of protein which is associated with DNA repair, recombination, cell proliferation and apoptosis. PARP family consists of 18 members including PARP1, PARP2, PARP4, Tankyrase-1 and Tankyrase-2, PARP3, PARP6, TIPARP, and PARP-8, etc. The PARP-1 enzyme is an 113kDa nuclear protein which catalyzes the biogenesis of ADP-ribose from nicotinamide and ribose. PARP-1 protein structure can be dissected into three functional domains; N-terminal DNA binding domain, catalytic C-terminal domain, and core auto modification domain. The major function of PARP is implicated in DNA repair, chromatin relaxation, the progression of cell cycle and apoptosis (Vyas & Chang 2014) and PARP-induced NAD^+ depletion leading to cellular necrosis (Ying et al. 2016).

2.1.4. Rationale for selecting p53, Mdm2, Bcl-2 and PARP as target proteins

We have computationally screened a phytochemical library against p53, Mdm2, Bcl-2 and PARP proteins. These proteins are associated with maintenance of DNA integrity, which when compromised leads to altered cellular conditions. Cellular p53 concentration is regulated by Mdm2, however, under stress conditions, this regulation is disturbed, and thus, p53 levels goes down within the cell, leading to different pathophysiological conditions including DNA damage and abnormal cellular growth. We targeted p53-Mdm2 interaction by screening phytochemicals against a binding region of p53 and Mdm2 in order to rescue cellular p53 with an approach to restore normal cellular functioning. Bcl-2 is another crucial protein that maintains cellular integrity. Overexpression of Bcl-2 has been reported in various symptoms associated with DNA damage including tumor development and maintenance (Tse et al. 2008).

Besides this, Bcl-2 alterations have also been reported to induce resistance against various chemopreventive drugs (Vogler et al. 2009). One of the key functions of Bcl-2 is direct interaction with pro-apoptotic proteins Bax/Bak, where Bcl-2 attenuates their oligomerization. Bax/Bak oligomerization is important for induction of apoptosis when the cell is exposed to stress. Thus, overexpression of Bcl-2 prevents apoptosis in altered cells. Moreover, Bcl-2 RNA silencing studies have shown enhanced levels of p53 and have induced apoptosis in both normal and colorectal carcinoma (Kirkin et al. 2004). Therefore, these findings indicate that inhibition of Bcl-2 activity in cells encountering stress may restore normal cellular activities. As discussed earlier, PARP1 is crucial enzyme for DNA maintenance, recently it has been found that PARP1 is associated with abnormal growth of cells with mutated BRCA1 and BRCA2 genes (which are tumor suppressor genes and once mutated, cause DNA damage) and inhibition of PARP1 selectively kills the cells harboring mutated or null BRCA1/2 genes (Ye et al. 2013).

Targeting protein with a chemical inhibitor is one of the common strategies in drug development; however, most of these synthetic drugs fail in clinical trials mostly due to their toxic effects. We have screened a library of dietary phytochemicals and targeted certain crucial proteins which are associated with DNA damage/repair mechanisms. Since phytochemicals are natural plant products, they pose minimum toxic effects and also exert various health benefits. Followed by *in silico* screening, we have also studied the effects of top-ranked phytochemicals in mice models, and our findings suggests that the screened phytochemicals validated well with the *in vivo* studies (as discussed in Chapter-3)

2.2. Materials

2.2.1. Protein structures

The crystal structures of p53 (PDB ID: 1YCR), Mdm2 (PDB ID: 1RV1), Bcl-2 (PDB ID: 4AQ3) and PARP (PDB ID: 4HHY) proteins were downloaded from the PDB database (www.rcsb.org).

2.2.2. Ligand molecules

Phytochemical libraries were downloaded from "Quality phytochemical database." For *in silico* docking, these molecules were converted into 3D format (.pdb/.sdf) using CORINA program for virtual screening against active site of p53, Mdm2, Bcl-2 and PARP proteins.

2.2.3 Docking algorithm

Glide is a well-known protein-ligand docking program developed by Schrodinger, LLC. GLIDE v9.5 program was used for molecular docking with the aim to screen and select the phytochemicals against a suitable target and computed with higher rankings as per the algorithm employed in the GLIDE docking program. Cross-validation of the top-ranked phytochemicals (obtained from GLIDE docking) was conducted using GOLD docking program.

2.2.3.1. GLIDE: Grid-based Ligand Docking with Energetics

GLIDE calculates all possible interactions between protein receptor grid and ligands (Halgren et al. 2004). GLIDE computation is based on filters of hierarchical cascades in order to identify all best possible poses of the ligand in the receptors cavity. In GLIDE calculations, the structural features and chemical properties of the receptor are localized

in a prescribed region called as a grid. To attain more accurate scoring, different poses of the ligand are generated on the basis of its position, orientation, and the conformation of the core and associated rotamers. Once the grid is defined, different conformations of ligands are selected based upon their computed minimal torsion angle space. The selected ligand is then minimized by computing custom energy functions of molecular mechanics within the receptor grid (Friesner et al. 2004). Finally up to six lowest energy conformations of the ligands were computed for minimal torsion by employing Monte Carlo minimization calculations (Figure 2.1)

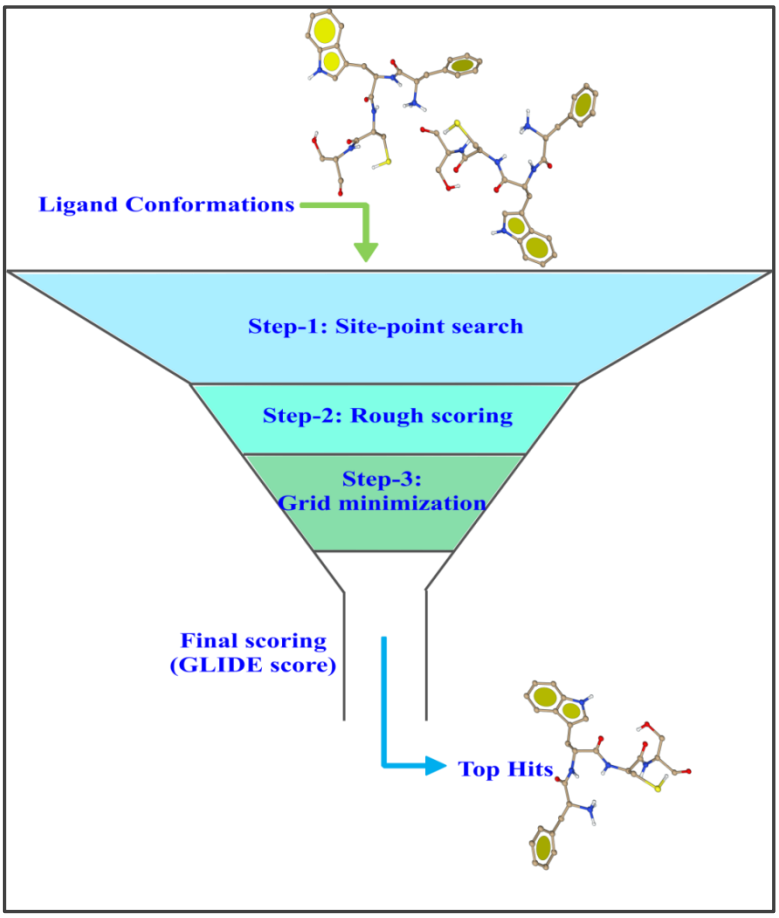

Figure 2.1: Docking methodology used in GLIDE to filter a library of compounds.

2.2.3.1.1 Glide scoring function

The GLIDE scoring function is based on chem-score function described as follows.

$$\Delta G_{bind} = C_0 + C_{lipo}\sum f(r_{lr}) + C_{hbond}\sum g(\Delta r)h(\Delta R) + C_{metal}\sum f(r_{lm}) + C_{rotb}H_{rotb}$$

Where the terms defined by chemscore as lipophilic (2nd term in the equation), hydrogen-bonding interactions (3rd term in the equation) and metal ion interaction (4th term in the equation). The functions: **f**, **g**, and **h** in the equation provide a full score (1.00) for angles and distances that recline in minimal limits and a fraction of the score (ranging between 1.00-0.00) to those that recline outside those limits.

$$\begin{aligned}\Delta G_{bind} = {} & C_{lipo-lipo}\sum f(r_{lr}) \\ & + C_{hbond-neut-neut}\sum g(\Delta r)h(\Delta\alpha) \\ & + C_{hbond-neut-charged}\sum g(\Delta r)h(\Delta\alpha) \\ & + C_{hbond-charged-charged}\sum g(\Delta r)h(\Delta\alpha) \\ & + C_{max-metal-ion}\sum f(r_{lm}) + C_{rotb}H_{rotb} \\ & + C_{polar-phobic}V_{polar-phobic} + C_{coul}E_{coul} + C_{vdw}E_{vdw} \\ & + Solvation\ terms\end{aligned}$$

In the GLIDE scoring function equation, the lipophilic-lipophilic and hydrogen-bonding expressions are defined as in Chem-Score. However, the hydrogen-bonding expression is segregated into different components on the basis of associated donors and acceptors

where both of them are neutral, one neutral and other charged, and both of them are charged. The metal-ligand interaction function differs in three ways from Chem-Score function. Firstly, it assesses anionic interactions only. Secondly, it considers only the best interaction when two or more metal bonds are found, and thirdly GLIDE computes net charge on the metal ion in the apoprotein. While in conditions where metal ion is neutral, the metal ion function is suppressed. The use of coulomb and vander Waal (vdW) interaction energies is another major aspect in GLIDE scoring function as both, coulomb and vdW energies play a major contribution in ligand binding. The salvation function is used to explicitly dock water molecules into the binding cavity for every pose of the ligand as the presence of water molecule plays a crucial role in the ligand-protein interaction. The salvation function in GLIDE allows the users to reject false positives (Friesner et al. 2004).

2.2.3.2 GOLD: Genetic Optimization for Ligand Docking

GOLD v3.1.1 (CCDC, Cambridge, UK.) is another molecular docking software which is based on genetic algorithm, and screen ligands on the basis of complete conformational flexibility including acyclic and partial cyclic flexibility against the partially flexible active site of the protein site, and satisfies the fundamental requirement that the ligand must displace loosely bound water on the binding.

2.2.3.2.1 GOLD scoring function:

$$\boldsymbol{GOLDFitness = S_{hb\_ext} + S_{vdv\_ext} + S_{hb\_int} + S_{vdw\_int}}$$

Where, $\mathbf{S_{hb\_ext}}$ is hydrogen-bond score and $\mathbf{S_{vdv\_ext}}$ is van der Waals score between protein-ligand bindings. $\mathbf{S_{hb\_int}}$ is intra-molecular hydrogen bonds and $\mathbf{S_{vdw\_int}}$ represents to intra-molecular strain in the ligand.

To dock the ligand in the binding cavity of the protein, GOLD uses fitting point methodology. Where, GOLD adds fitting points for both hydrogen and hydrophobic bond forming groups in both ligand and protein as well. For screening of ligands, GOLD uses a genetic algorithm. The algorithm optimizes dihedral rotatable bonds and ring geometries of ligands, along with protein dihedrals (OH and NH^{3+}) of proteins and maps the fitting points (Verdonk et al. 2003).

2.3. Post-docking analysis

In order to cross-validate the docking experiments, the post-docking analysis was performed. We employed two post-docking analysis tools for this purpose. These programs are discussed below:

2.3.1. X-Score v1.2.1

Different docking tools use different algorithms associated with specific scoring functions. Thus, it is necessary to compare the scores of different docking tools in order to minimize false positives and to screen the best-predicted ligand against a target protein. To compare the docking scores of different docking tools, X-Score is a benchmark program with high accuracy in comparing the scores of two or more docking programs. The X-Score program computes post-docked poses of the ligand within the binding site of protein. X-Score computes the negative logarithm (-log Kd) of ligand dissociation constant against the target protein. The X-Score scoring function is

based on calculating the average of three consensus scoring functions namely; HPScore, HMScore and HSScore and computes the predicted binding energy of the docked ligand in terms of kcal/mol with an accuracy of ± 2.2 kcal/mol.

2.3.2. Ligplot V 4.4

Ligplot is a program that defines and extrapolates hydrogen bonds and hydrophobic interacting residues between ligand-protein complexes (Wallace et al. 1995). The hydrogen bonds are depicted as dashed lines while hydrophobic interactions are represented as an arc of spokes protruding towards the ligand from the associated residue. The program is simple and produces a 2D interaction diagram of ligand-protein interaction without stacking atoms over each other. The 2D interaction diagram can be colored or in grayscale as well. The color diagram helps in distinguishing ligand atoms with accessibility to the solvent with other atoms. Ligplot can not only be employed for understanding protein-ligand interacting forces but can also be applied to other interactions involving protein and nucleic acids (Laskowski & Swindells 2011).

2.3. Methods

2.3.1. Docking of ligands to the target proteins

To perform protein docking, some pre-processing is required which includes removal of HETATM and water molecules from the PDB structures. After pre-processing the protein structures, computational screening of phytochemicals library was conducted against each protein using GLIDE software (of Schrödinger Suite) and the top hits were further checked with GOLD docking software. (Figure 2.2)

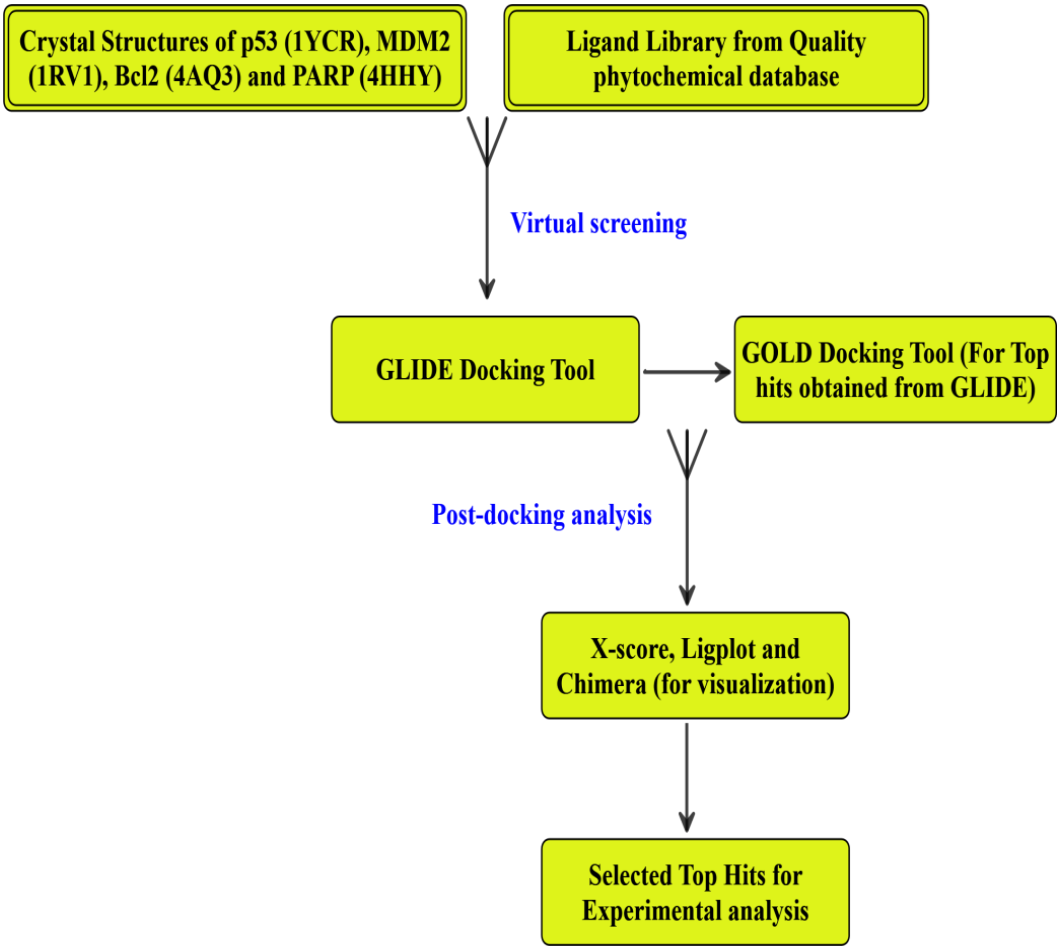

Figure 2.2: Schematic presentation of the screening protocol of phytochemical library against target proteins.

2.3.1.1. GLIDE Grid-based ligand docking with energetics

Docking in GLIDE employs sequential processes described as follows.

2.3.1.1.1. Protein preparation

In the PDB file of the crystal structure of protein, there may be heavy atoms, waters molecules, cofactors, and metal ions. Also, the structure may be multimeric and possess no information on topologies, bond orders, or atomic charges. Since X-ray structure analysis fails to differentiate between O_2 and NH_2, thus terminal amides may be misaligned, and also the tautomeric and ionized states of the amino acids are

unassigned. Thus, protein preparation is required. GLIDE computes all-atom force field hence it requires the proper assignment of ionic states and bond orders.

The Protein preparation in GLIDE is carried out using "Protein Preparation Wizard". The subsequent steps are listed below.

1. Import PDB file into Maestro project table.
2. Remove redundant binding sites in case of multimeric protein (if any).
3. Delete undesired water molecules.
4. Add hydrogen atoms.
5. Minimize protein using specific force field based upon requirement (we used impref minimization using OPLS-2005 molecular mechanics force field).

2.3.1.1.2. Ligand preparation

Similar to protein preparation, GLIDE implements certain criteria (lipinski filter) for ligand preparation. Ligprep wizard of the GLIDE was employed for ligand preparation which involves; appending hydrogen atoms, deletion of unwanted molecules, neutralizing charged groups, generating ionization states, tautomers, chiralities, low-energy conformers and optimizing ligands geometry.

2.3.1.1.3. Receptor grid generation

A Grid can be defined as a cube around the binding region of protein within which the ligand interacts. GLIDE grid preparation wizard was used for the preparation of grid with a grid size of 17Å, and all the amino acid residues that are crucial for protein-ligand interaction were incorporated into the grid. The different residues that we used for the Grid generation are as follows:

p53 active site residues: Phe-19,Trp-23, Lys-24, Leu-26, Pro-27, Glu-28, Asn-29.

Mdm2 active site residues: Leu-54, Phe-55, Gly-58, Ile-61, Met-62, Gln-72.

Bcl-2 active site residues: Tyr-67, Phe-71, Leu-96, Asn-102, Gly-104, Arg-105, Ala-108.

PARP active site residues: Asp-105, His- 201, Gly-202, Arg-217, Ala-219, Pro-220, Tyr-228, Tyr-235, Ser-243, Tyr-246.

2.3.1.1.4. Ligand Docking

Once proteins, ligands, and grids are prepared, docking of different ligands was performed against target proteins. Screening of ligands is a three step process that involves three different protocols:

1. High Throughput Virtual Screening (HTVS).

2. Standard Precision docking (SP).

3. Extra Precision docking (XP).

Using HTVS, the entire phytochemical library was initially screened and top 25% of phytochemicals with highest Glide Score were then subjected to second docking protocol; the SP (Standard Precision) mode of docking. Post SP docking, the top phytochemicals on the basis of Glide Score were further introduced to XP mode of GLIDE docking. Finally, top 30 molecules were selected for cross-validation using GOLD tool.

2.3.2.1. GOLD: Genetic Optimization for Ligand Docking

For docking of ligand (phytochemicals) using GOLD software, the ligand input structures were extracted in mol2 format. The active site in GOLD can be defined in two ways, where employing one approach user can just define one residue around which GOLD itself defines a grid of 10 Å which is considered as an active site for that target protein. Whereas, in the other mode of defining the active site, the user provides the residue numbers or the list of active site atoms. We prepared the list of atoms involved in active site formation in a file named "act_site atoms" (separately for p53, Mdm2, Bcl-2, and PARP) and defined as an active site in GOLD. The GLIDE screened top ranking phytochemicals for p53, Mdm2, Bcl-2 and PARP were then screened using the "standard default" settings. GOLD employs genetic algorithm (GA) to predict the optimal binding pose of the ligand against receptor protein, Since GA is a heuristic algorithm, it assists multiple individual GA runs for each molecule at three different settings offered by GOLD i.e. "library screening" setting, "3-times-up" setting and "standard default" settings. We employed "standard default" (parameters for which are given in Table 1) settings with 10 GA runs. The best-ranked docked structure was written in SDF format output file. Once docking is completed, a file named

"bestranking.lst" is generated enlisting all the best-ranked solutions with their corresponding GOLD Fitness score for a given molecule. The various parameters used for the default settings are listed in Table 2.1 below

Table 2.1: Standard docking parameters employed in GOLD

PARAMETERS	STANDARD SETTINGS
Population size	100
Number of islands	5
Niche size	2
Selection pressure	1.100
Migrate	2
Number of operators	100 000
Mutate	95
Crossover	95

2.3.2.2. X-Score v1.2.1

Post-docking, all the top ranking phytochemicals that were filtered through GLIDE and later cross-validated with GOLD were then subjected to X-Score analysis. X-Score calculates the dissociation binding constants and binding energy of ligand with its

respective protein; it was used to verify the results generated by GLIDE and GOLD. X-Score requires that the input files of protein and docked ligands must be fixed in .mol2 format. Thus, the .pdb files for both ligand and protein were fixed in .mol2 format for X-Score computation, and the output results were tabulated.

2.3.2.3. Ligplot V 4.4

Ligplot requires both protein and ligand docked complex in one single file as input for calculation. All the top ligands with corresponding proteins were appended in single individual files and were then subjected to ligplot calculations. The output .ps files were then analyzed for the associated interactions between ligand-protein complexes.

2.4. Results

2.4.1. *In silico* screening of phytochemicals library and post-docking analysis

We have carried out *in-silico* screening of a library of dietary phytochemicals from "Quality photochemical database" against the catalytic site of p53, Mdm2, Bcl-2, and PARP using Glide docking program of Schrödinger suite. The top screened molecules obtained from GLIDE were then docked with GOLD docking tool. Finally, the docking results obtained from both GLIDE and GOLD docking programs were analyzed using a consensus scoring function of 'X-Score' and 'LIGPLOT" to calculate the binding affinity and other protein-ligand interactions for top-ranking compounds. On the basis of these analysis, we finally selected two compounds Taxifolin (TAX) and Limonene (Lim) against each protein (i.e. p53, Mdm2, Bcl-2, and PARP) which could be high-affinity inhibitors and were tested further using mouse model.

2.4.2. Docking of TAX to p53, Mdm2, Bcl-2, and PARP proteins

2.4.2.1. Docking studies with p53-TAX

Glide docking score for docking of TAX to p53 was computed to be **-5.20 kcal/mol** and the corresponding E-model and CvdW values for this docked pose were **-54.4** and **-38.7 kcal/mol** respectively. p53-TAX docking with Gold was computed to be **49.59.** The X-Scores for Glide and Gold docked complexes were **-6.92 kcal/mol** and **-7.41 kcal/mol** respectively **(Table 2.2)**. Protein-ligand interactions were calculated using ligplot to determine the interacting forces between the docked ligand-protein complexes. Ligplot calculations for p53-TAX docking revealed participation of four hydrogen bonds and one hydrophobic interaction **(Table 2.3) (Figure 2.3)**

p53-Taxifolin

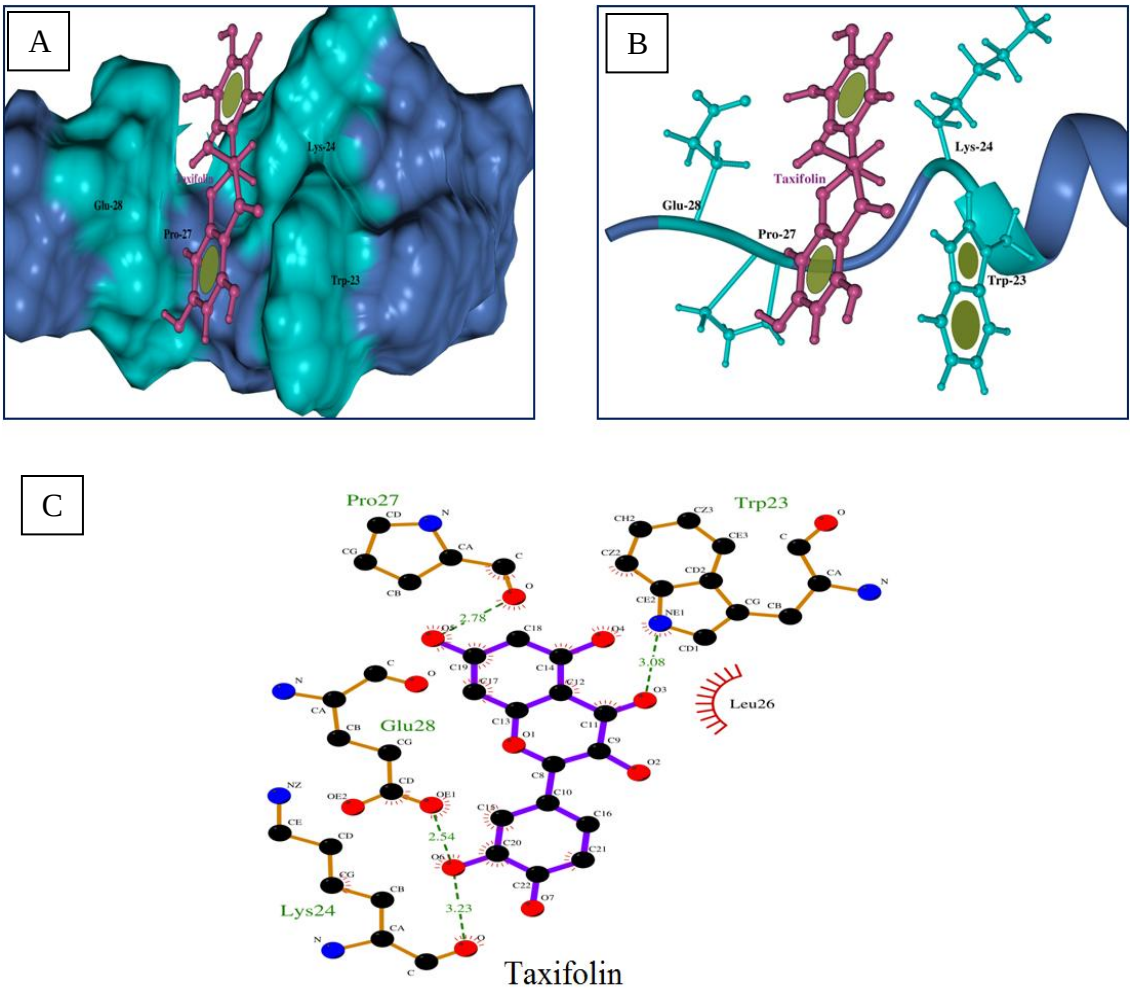

Figure 2.3: Docking of TAX to p53 protein is colored blue, and the active site residues are colored cyan: A) Surface structure of the p53-TAX complex. B) The secondary structure of the p53-TAX complex. C) Ligplot interaction diagram of a p53-TAX complex hydrogen bond is indicated by green dashed lines and amino acid residues forming hydrogen (Trp-23, Lys-24, Pro-27, Glu-28) bonds are labeled green. Hydrophobic interaction is indicated by a red arch with spokes towards ligand, amino acid forming hydrophobic interaction (Leu-26) is labeled black

2.4.2.2. Docking studies with Mdm2-TAX

Glide docking score for docking of TAX to Mdm2 was the computed to be **-4.94 kcal/mol** and the corresponding E-model and CvdW values for this docked pose were **-31.24** and **-33.3 kcal/mol** respectively. Mdm2-TAX docking with Gold was computed to be **40.08.** The X-Scores for Glide and Gold docked complexes were **-7.43 kcal/mol** and **-6.82 kcal/mol** respectively **(Table 2.2).** Protein-ligand interactions were calculated using ligplot to determine the interacting forces between the docked ligand-protein complexes. Ligplot calculations for Mdm2-TAX docking revealed participation of one hydrogen bond and five hydrophobic interactions **(Table 2.3) (Figure 2.4)**

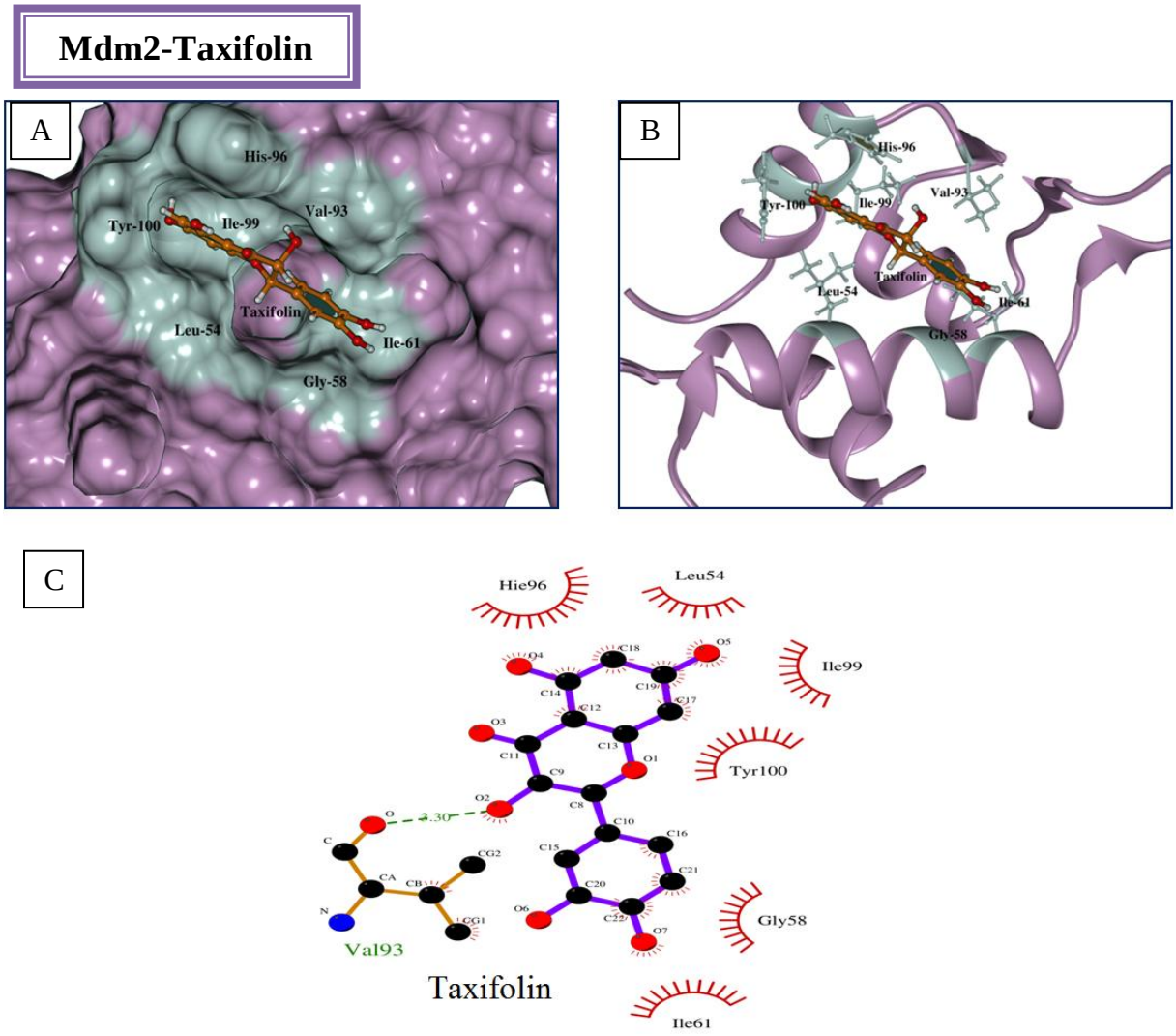

Figure 2.4: Docking of TAX to Mdm2 protein is colored purple, and the active site residues are colored mud gray: A) Surface structure of Mdm2-TAX complex. B) The secondary structure of Mdm2-TAX complex. C) Ligplot interaction diagram of Mdm2-TAX complex hydrogen bond is indicated by green dashed lines and amino acid residue forming hydrogen (Val-93) bond is labeled green. Hydrophobic interaction is indicated by a red arch with spokes, amino acids forming hydrophobic interactions (Leu-54, Glu-58, Ile-61, His-96, Ile96, Tyr-100) are labeled black.

2.4.2.3. Docking studies with Bcl-2-TAX

Glide docking score for docking of TAX to Bcl-2 was the computed to be **-5.58 kcal/mol** and the corresponding E-model and CvdW values for this docked pose were **-40.0** and **-29.90 kcal/mol** respectively. Bcl-2-TAX docking with Gold was computed to be **40.72.** The X-Scores for Glide and Gold docked complexes were **-7.4 kcal/mol** and **-7.39 kcal/mol** respectively **(Table 2.2)**. Protein-ligand interactions were calculated using ligplot to determine the interacting forces between the docked ligand-protein complexes. Ligplot calculations for Bcl-2-TAX docking revealed participation of one hydrogen bond and four hydrophobic interactions **(Table 2.3) (Figure 2.5)**

Bcl-2-taxifolin

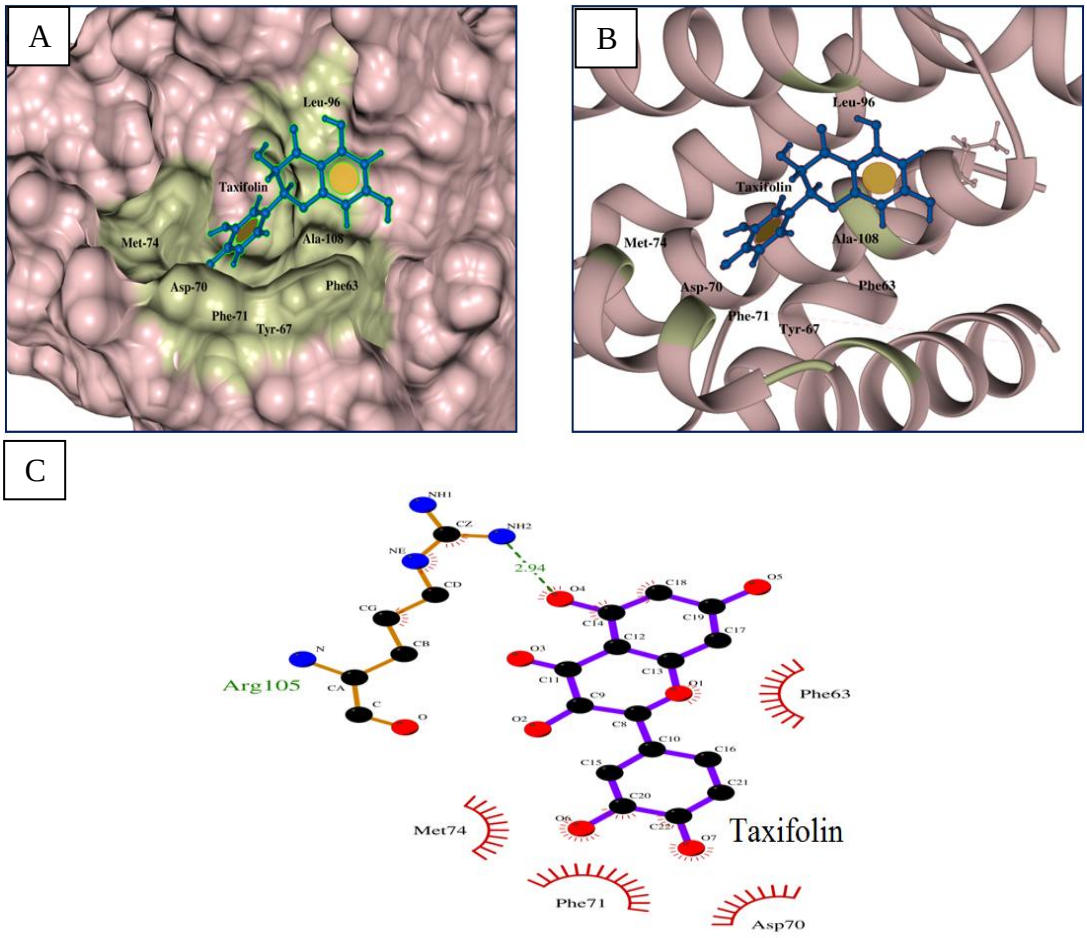

Figure 2.5: Docking of TAX to Bcl-2 protein is colored dull pink, and the active site residues are colored golden yellow: A) Surface structure of Bcl-2-TAX complex. B) The secondary structure of Bcl-2-TAX complex. C) Ligplot interaction diagram of Bcl-2-TAX complex hydrogen bond is indicated by green dashed lines and amino acid residue forming hydrogen (Arg-105) bond is labeled green. Hydrophobic interaction is indicated by a red arch with spokes towards ligand, amino acids forming hydrophobic interactions (Phe-63, Asp-70, Phe-71, Met-74) are labeled black

2.4.2.4. Docking studies with PARP-TAX

Glide docking score for docking of TAX to PARP was the computed to be **-9.28 kcal/mol** and the corresponding E-model and Cvdw values for this docked pose were **-70.20** and **-48.8 kcal/mol** respectively. PARP-TAX docking with Gold was computed to be **58.43.** The X-Scores for Glide and Gold docked complexes were **-7.74 kcal/mol** and **-7.90 kcal/mol** respectively **(Table 2.2)**. Protein-ligand interactions were calculated using ligplot to determine the interacting forces between the docked ligand-protein complexes. Ligplot calculations for PARP-TAX docking revealed participation of three hydrogen bond eight hydrophobic interactions **(Table 2.3) (Figure 2.6).**

PARP-taxifolin

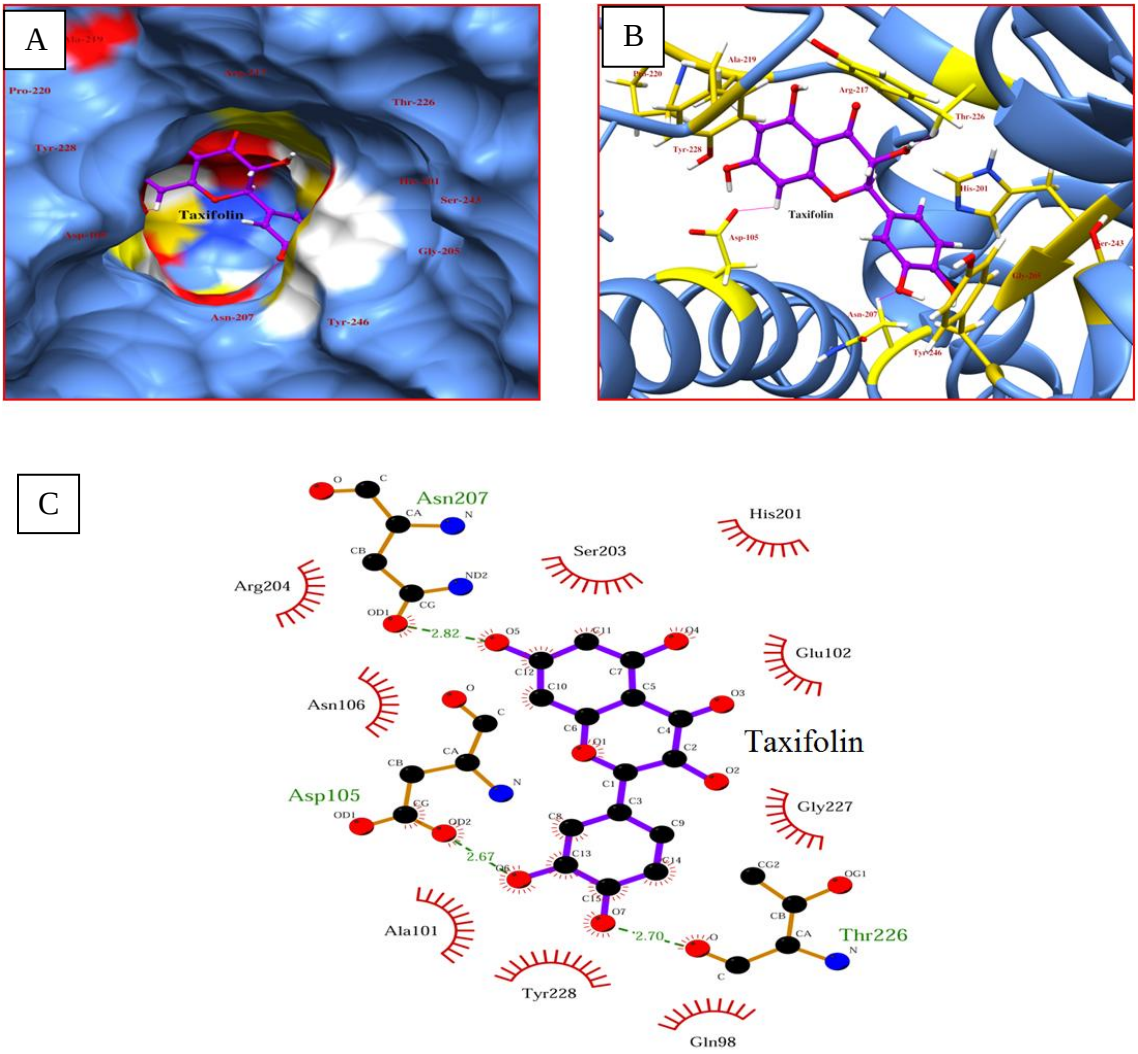

Figure 2.6: Docking of TAX to PARP protein is colored blue, and the active site residues are colored yellow: A) Surface structure of PARP-TAX complex. B) The secondary structure of PARP-TAX complex. C) Ligplot interaction diagram of PARP-TAX complex hydrogen bond is indicated by green dashed lines and amino acid residue forming hydrogen (Asp-105, Asn-207, Thr-226) bond is labeled green. Hydrophobic interaction is indicated by a red arch with spokes towards ligand, amino acids forming hydrophobic interactions (Gln-92, Ala-101, Glu-102, Asn-106, His-201, Ser-203, Arg-204, Tyr-228) are labeled black.

Table 2.2: Docking and post-docking scores for TAX against p53, Mdm2, Bcl-2 and PARP protein targets

Phytochemicals	Glide Score (kcal/mol)	Gold Score (Fitness)	CvdW (kcal/mol)	X Score (kcal/mol)		E model (kcal/mol)
				Glide	Gold	
p53-TAX	-5.20	49.59	-38.7	-6.92	-7.41	-54.4
Mdm2-TAX	-4.94	40.08	-33.3	-7.43	-6.82	-31.24
Bcl-2-TAX	-5.58	40.72	-29.9	-7.47	-7.39	-40
PARP-TAX	-9.28	58.43	-48.8	-7.74	-7.90	-70.2

Table 2.3: Hydrogen bonds and hydrophobic interactions of TAX with p53, Mdm2, Bcl-2 and PARP target proteins

Phytochemicals	Hydrogen Bonds	Hydrophobic Interactions
p53-TAX	Trp-23, Lys-24, Pro-27, Glu-28	Leu-26
Mdm2-TAX	Val-93	Leu-54, Glu-58, Ile-61, Ile-99, His-96, Tyr-100
Bcl-2-TAX	Arg-105	Phe-63, Asp-70, Met-74, Phe-71
PARP-TAX	Asp-105, Asn-207, Thr-226	Gln-92, Ala-101, Glu-102, Asn-106, His-201, Ser-203, Arg-204, Tyr-228

2.4.3. Docking of Lim to p53, Mdm2, Bcl-2, and PARP proteins

2.4.3.1 Docking studies with p53-Lim

Glide docking score for docking of Lim to p53 was the computed to be **-5.20kcal/mol** and the corresponding E-model and Cvdw values for this docked pose were **-32.4** and **-20.4 kcal/mol** respectively. p53-Lim docking with Gold was computed to be **42.3.** The X-Scores for Glide and Gold docked complexes were **-6.92 kcal/mol** and **-7.29 kcal/mol** respectively **(Table 2.4)**. Protein-ligand interactions were calculated using ligplot to determine the interacting forces between the docked ligand-protein complexes. Ligplot calculations for p53-Lim docking revealed participation of five hydrophobic interactions **(Table 2.5) (Figure 2.7).**

p53-limonene

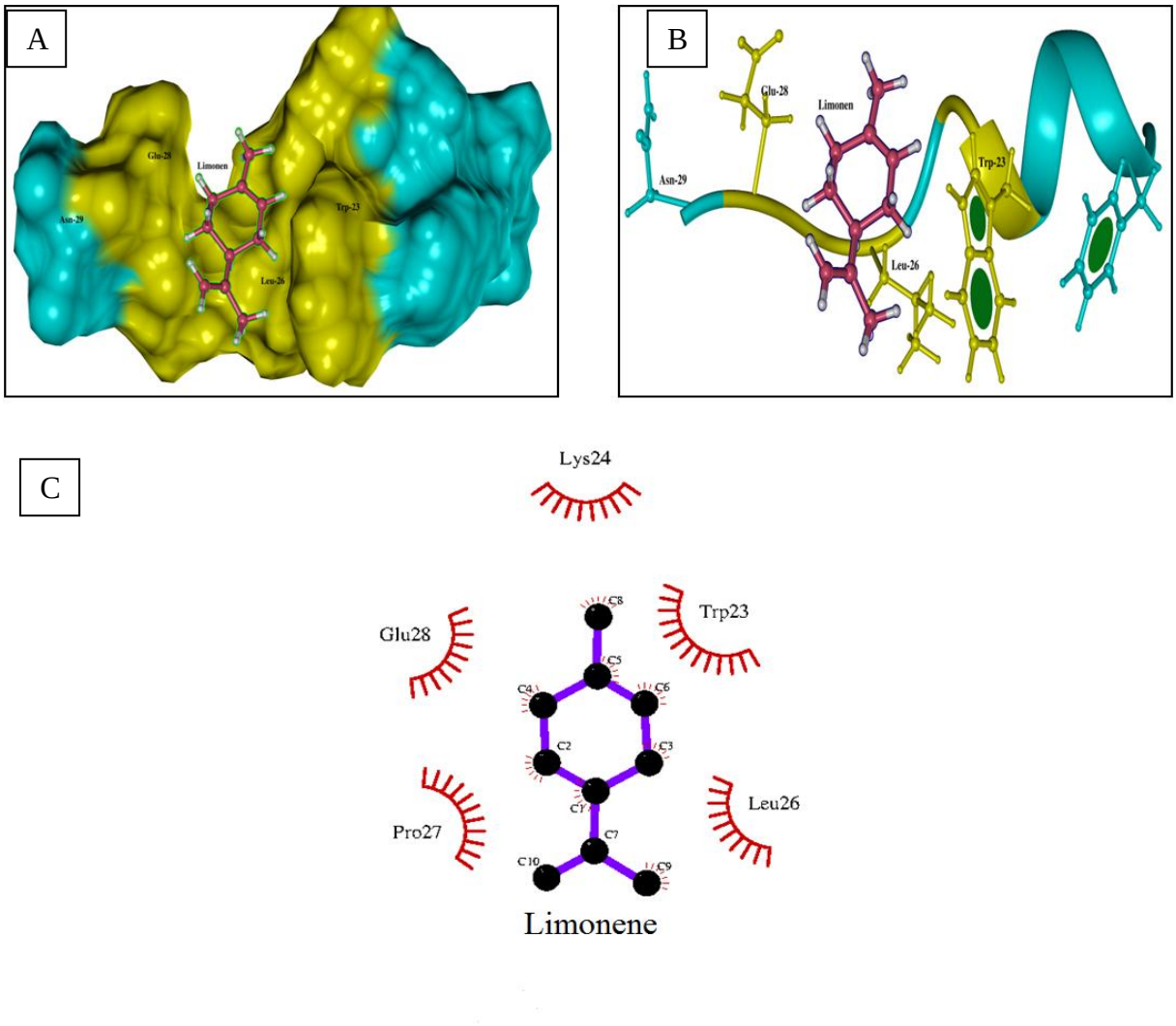

Figure 2.7: Docking of Lim to p53 protein is colored sea green and the active site residues are colored in golden yellow. A) The surface structure of the p53-Lim complex. B) The secondary structure of the p53-Lim complex. C) Ligplot interaction diagram of p53-Lim complex. Hydrophobic interaction is indicated by a red arch with spokes towards ligand, amino acids forming hydrophobic interaction (Trp-32, Lys-24, Leu-26, Pro-27, Glu-28) are labeled black

2.4.3.2. Docking studies with Mdm2-Lim

Glide docking score for docking of Lim to Mdm2 was the computed to be **-4.8kcal/mol** and the corresponding E-model and CvdW values for this docked pose were **-20.3** and **-17.6 kcal/mol** respectively. Mdm2-Lim docking with Gold was computed to be **36.6.** The X-Scores for Glide and Gold docked complexes were **-7.39 kcal/mol** and **-6.93kcal/mol** respectively **(Table 2.4)**. Protein-ligand interactions were calculated using ligplot to determine the interacting forces between the docked ligand-protein complexes. Ligplot calculations for Mdm2-Lim docking revealed participation of nine hydrophobic interactions **(Table 2.5) (Figure 2.8).**

Mdm2-limonene

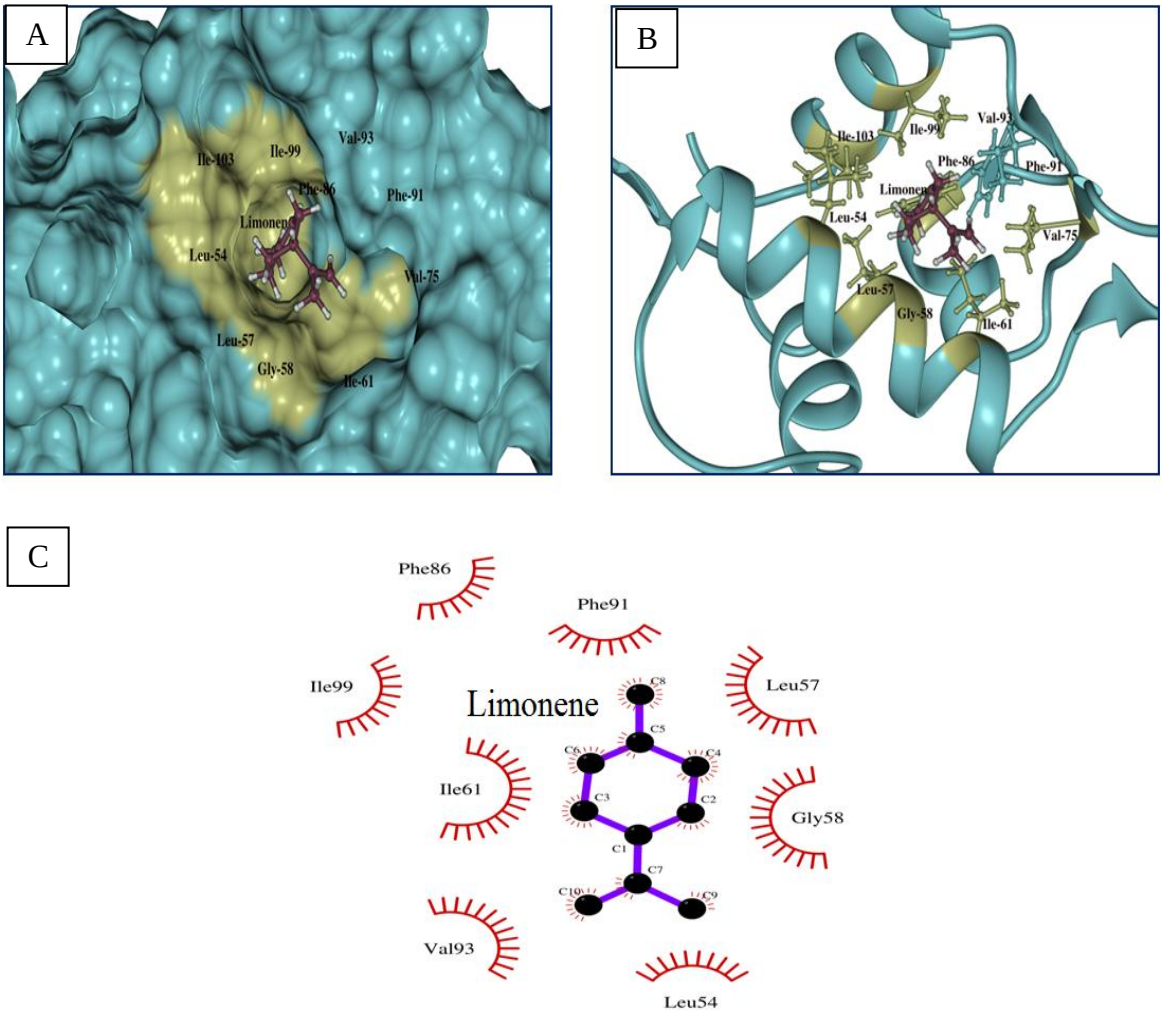

Figure 2.8: Docking of Lim to Mdm2 protein is colored dull sea blue, and the active site residues are labeled in dull green color. A) The surface structure of Mdm2-Lim complex. B) The secondary structure of Mdm2-Lim complex. C) Ligplot interaction diagram of Mdm2-Lim complex. Hydrophobic interaction is indicated by a red arch with spokes towards ligand, amino acids forming hydrophobic interaction (Leu-54, Leu-57, Gly-58, Ile-61, Phe-86, Phe-91, Val-93, Ile-99) are labeled black.

2.4.3.3. Docking studies with Bcl-2-Lim

Glide docking score for docking of Lim to Bcl-2 was the computed to be **-6.64 kcal/mol** and the corresponding E-model and CvdW values for this docked pose were **-50.1** and **-37.6 kcal/mol** respectively. Bcl-2-Lim docking with Gold was computed to be **52.1.** The-Scores for Glide and Gold docked complexes were **-7.21 kcal/mol** and **-7.42 kcal/mol** respectively **(Table 2.4)**. Protein-ligand interactions were calculated using ligplot to determine the interacting forces between the docked ligand-protein complexes. Ligplot calculations for Bcl-2-Lim docking revealed participation of nine hydrophobic interactions **(Table 2.5) (Figure 2.9).**

Bcl2-Limonene

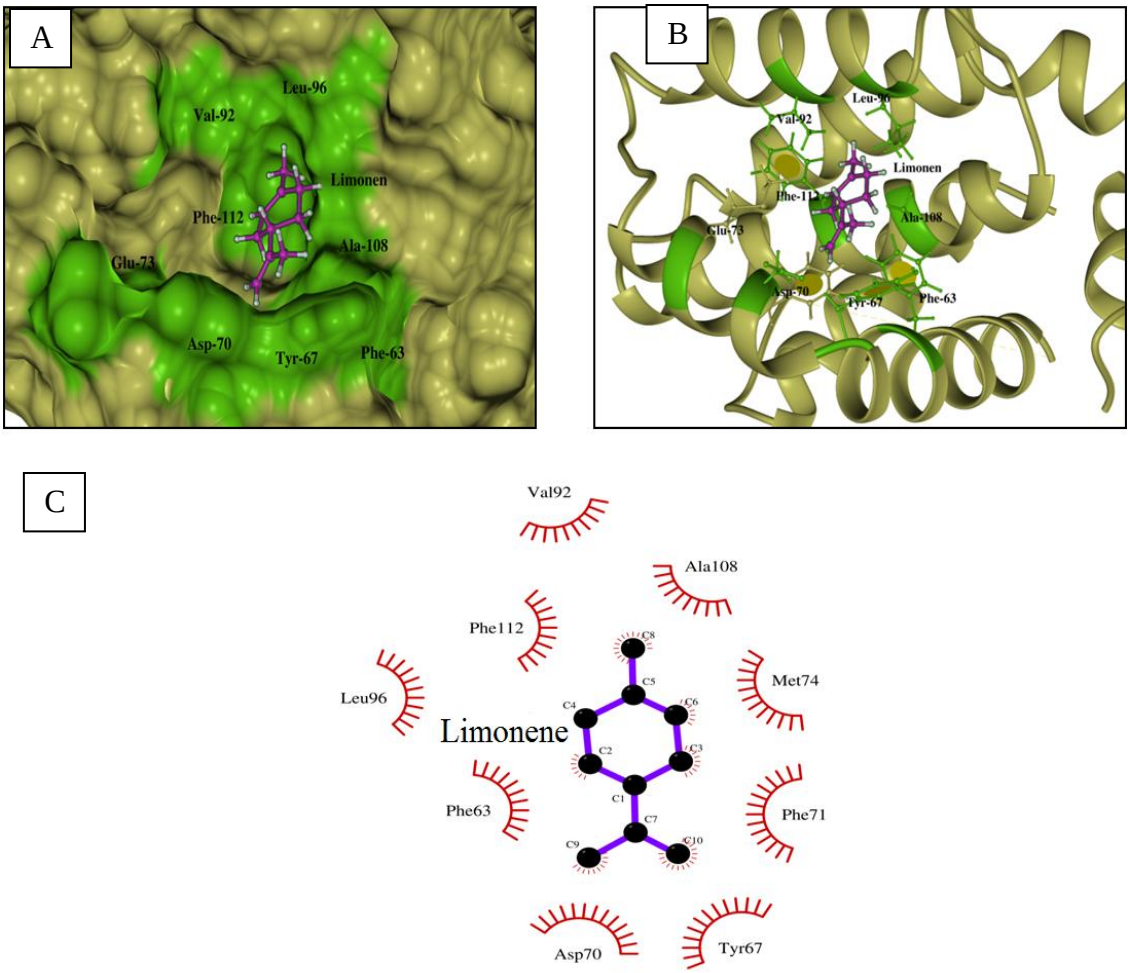

Figure 2.9: Docking of Lim to Bcl-2 protein is colored dull green, and the active sites are labeled in colored bright green. A) The surface structure of Bcl-2-Lim complex. B) The secondary structure of Bcl-2-Lim complex. C) Ligplot interaction diagram of Bcl-2-Lim complex. Hydrophobic interaction is indicated by a red arch with spokes towards ligand, amino acids forming hydrophobic interaction (Phe-63, Tyr-67, Asp-70, Phe-71, Met-74, Leu-96, Val-92, Ala-108, Phe-112) are labeled black.

2.4.3.4. Docking studies with PARP-Lim

Glide docking score for docking of Lim to PARP was the computed to be **–5.91 kcal/mol** and the corresponding E-model and CvdW values for this docked pose were **-49.1** and **-35.5 kcal/mol** respectively. PARP-Lim docking with Gold was computed to be **49.32.** The X-Scores for Glide and Gold docked complexes were **-6.84 kcal/mol** and **-7.21 kcal/mol** respectively **(Table 2.4)**. Protein-ligand interactions were calculated using ligplot to determine the interacting forces between the docked ligand-protein complexes. Ligplot calculations for PARP-Lim docking revealed participation of eight hydrophobic interactions **(Table 2.5) (Figure 2.10).**

PARP- limonene

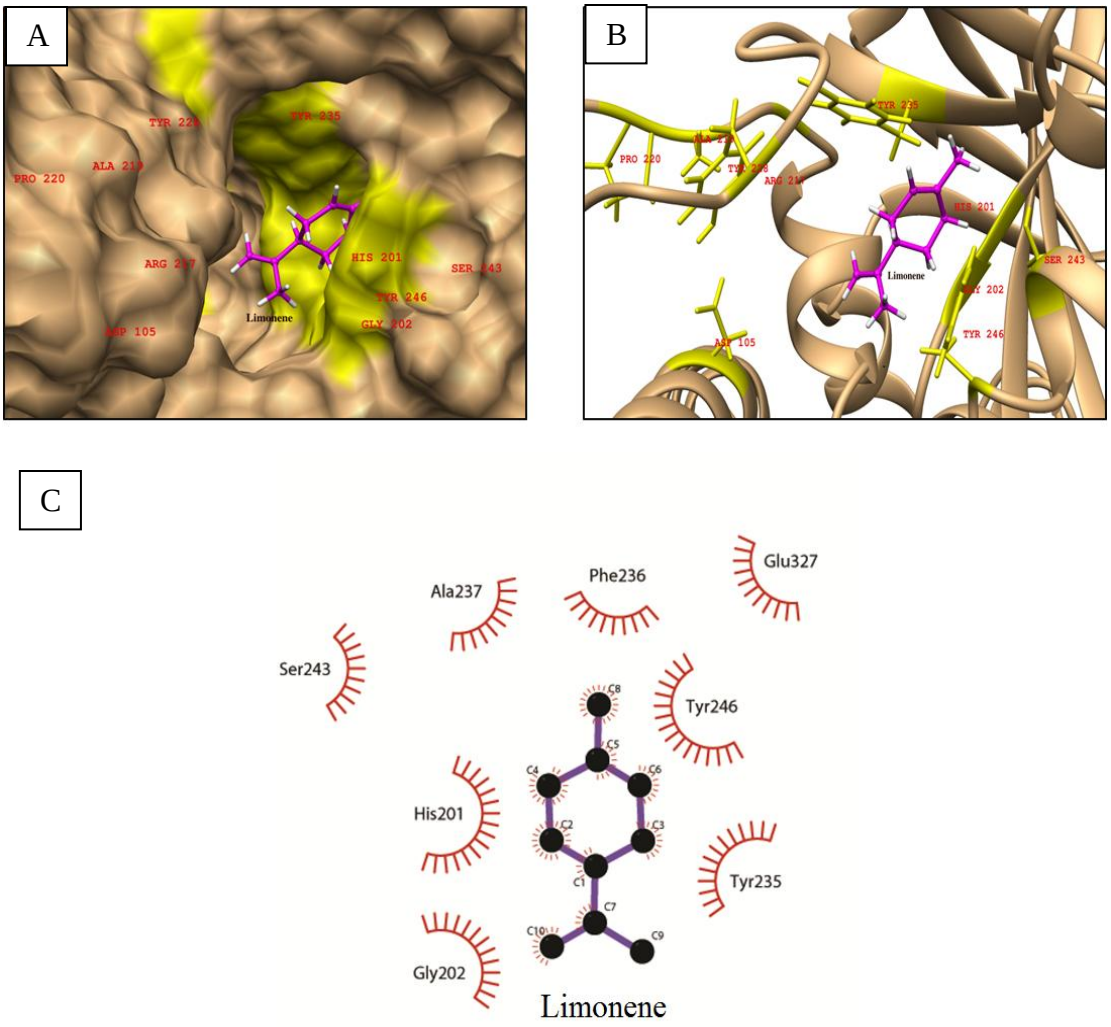

Figure 2.10: Docking of Lim to PARP protein is colored dull gold, and the active sites are labeled in colored yellow. A) The surface structure of PARP-Lim complex. B) The secondary structure of PARP-Lim complex. C) Ligplot interaction diagram of PARP-Lim complex. Hydrophobic interactions are indicated by a red arch with spokes towards ligand, amino acids forming hydrophobic interaction (His-210, Gly-202Tyr-246, Tyr-235, Phe-236, Ala-237, Ser-243, Glu-327) are labeled black.

Table 2.4: Docking and post-docking scores for Lim against p53, Mdm2, Bcl-2 protein targets

Phytochemicals	Glide Score (kcal/mol)	Gold Score (Fitness)	CvdW (kcal/mol)	X-Score (kcal/mol)		E model (kcal/mol)
				Glide	Gold	
p53-Lim	-5.2	42.3	-20.4	-6.92	-7.29	-32.4
Mdm2-Lim	-4.8	36.6	-17.6	-7.39	-6.93	-20.3
Bcl-2-Lim	-6.64	52.1	-37.6	-7.21	-7.42	-50.1
PARP-Lim	-5.91	49.32	-35.5	-6.84	-7.21	-49.1

Table 2.5: Hydrophobic interactions of Lim with p53, Mdm2, Bcl-2 target proteins.

Phytochemicals	Hydrogen Bonds	Hydrophobic Interactions
p53-Lim	Nil	Trp-23, Lys-24, Leu-26, Pro-27, Glu-28
Mdm2-Lim	Nil	Leu-54, Leu-57, Gly-58, Ile-61, Phe-86, Phe-91, Val-93, Ile-99
Bcl-2-Lim	Nil	Phe-63, Tyr-67, Asp-70, Phe-71, Met-74, Val-92, Leu-96, Ala-108, Phe-112
PARP-Lim	Nil	His-210, Gly-202Tyr-246, Tyr-235, Phe-236, Ala-237, Ser-243, Glu-327

2.5. Discussion

The p53 protein is one of the most studied cancer related protein. Studies show that mutations in the p53 gene are the 'hot-spots' of cancer generation (Nigro et al. 1989). The p53 protein has versatile functions (Vogelstein et al. 2000) and thus its endogenous concentration is under tight regulation. Mdm2 is a negative regulator of p53 which controls p53 turnover in an autoregulatory feedback loop (Wu et al. 1993). Mdm2 protein binds with p53 and leads to degradation of both by ubiquitin-mediated pathway (Michael & Oren 2003). This protein-protein interaction of Mdm2-p53 is governed by a strong hydrophobic cleft of Mdm2 (Grasberger et al. 2005), into which one of the helix of p53 transactivation domain docks. Many synthetic inhibitors of p53-Mdm2 interactions are being developed by exploiting this protein-protein interaction including Nutlin family inhibitors (Vassilev et al. 2004), benzodiazepinedione inhibitors (Grasberger et al. 2005), RITA (Issaeva et al. 2004; Vassilev 2007). Bcl-2 is a family of proteins categorized on the basis of BH1-BH4 domains which are required for the functional specificities of these proteins. Bcl-2 is an anti-apoptotic protein localized in the inner mitochondrial membrane (Hockenbery et al. 1990) and is associated with many other functions (Siddiqui et al. 2015). Under normal conditions, there is a stringent homeostasis between the anti-apoptotic and pro-apoptotic function of Bcl-2 which is regulated by Bim protein via protein-protein interaction mediated by BH3 domain (O'Connor et al. 1998). A separate class of synthetic inhibitors called as BH3 mimetic have been developed which target the hydrophobic binding pocket of BH1-BH3 of Bcl-2 protein to rescue cells from malignancies (Lugovskoy et al. 2002;Vogler 2014). Poly(ADP-ribosyl)ation protein (PARP) is a DNA repair protein (D'Amours et

al. 1999) which catalyzes Poly(ADP-ribosyl)ation reactions using NAD^+ as a cofactor. Over-activation of PARP is reported to induce mitochondrial oxidative stress (Orsucci et al. 2008) and is implicated in the generation of many other pathological conditions (Virág & Szabó 2002). Several synthetic inhibitors of PARP are being studied and evaluated for their effects (Vyas & Chang 2014) and recently Olaparib; a PARP inhibitor has been approved for the treatment of advanced stages of ovarian cancer with mutated *BRCA* gene (Murata et al. 2016).

We have performed molecular docking of a library of dietary phytochemicals from "Quality photochemical database" against p53, Mdm2, Bcl-2 and PARP protein targets. For screening of the 'Quality phytochemical library,' we employed HTVS mode of Glide followed by the SP and XP mode of docking. Finally, top 30 molecules with highest Glide docking score were selected for cross-validation using GOLD tool. Also, we have validated the docking results produced from both Glide and Gold docking tools by computing X-Scores of the docked complexes. The associated molecular forces involved in protein-ligand complexes were determined using ligplot which computes the number of hydrogen bonds and hydrophobic interactions and the amino acid residues involved in such interactions. From our *in silico* screening and docking protocols using Glide and Gold docking tools, we finally selected two phytochemicals, TAX and Lim for our further experimental validations in *in vivo* model (discussed in Chapter 3) as both of these phytochemicals were amongst top ranked molecules against p53, Mdm2, Bcl-2 and PARP as target proteins.

TAX showed a high binding affinity for p53 and Mdm2 proteins; these findings are in concurrence with the molecular docking and simulation studies (Verma et al. 2013a).

According to these studies, residue 24 and 26 of p53 play an important role in binding to Mdm2 by the formation of hydrogen bonds between the duo, and disruption of the hydrogen bonds between p53 and Mdm2 will lead to disruption of p53-Mdm2 interaction. In our docking studies, TAX forms a hydrogen bond with residues 23, 24, 27 and 28 of p53 and residue 93 of Mdm2 (Verma et al. 2013a) indicating that its presence will disrupt p53-Mdm2 interaction. In our studies, TAX interacts with Mdm2 with a higher number of hydrophobic interactions (six in number) while p53-TAX complex has only one hydrophobic interaction. These findings are also in concurrence with docking and simulation studies which report that the Mdm2-TAX complex interacts with strong hydrophobic interactions while the p53-TAX hydrophobic interaction is less (Verma et al. 2013b).

TAX also interacts with Bcl-2 protein with good binding affinity. Based on structural domains, Bcl-2 has four domains namely BH1, BH2, BH3, and BH4. Studies have shown that various conditions like stress, ubiquitin-dependent degradation, and phosphorylation induce disturbance in the charge distribution of the Bcl-2 protein which disrupts its oligomerization (Ruvolo et al. 2001) and heteromerization (Shitashige et al. 2001). These disturbances thus result in flipping the anti-apoptotic activity of Bcl-2 protein to pro-apoptotic activity (Zacarías-Lara et al. 2016). To inhibit the pro-apoptotic activity of Bcl-2, BH3 mimetics are being developed which can bind into the hydrophobic pocket of Bcl-2. We have screened phytochemicals, targeting this hydrophobic cleft of Bcl-2 protein. Since p53 binds to this hydrophobic cleft by its transactivation domain (Ji-Hyang Ha et al. 2013) and it also binds to Mdm2 using the same domain (Chen et al. 1993), TAX can also act as a dual inhibitor (Wang & Song

2106). In our docking studies, TAX interacts with the residues of BH3 domain (which ranges from residues 96-106) of Bcl-2 (Sathishkumar et al. 2012) and p53 also interact with Bcl-2 in the region from BH1-BH3 domains (Wang & Song 2106), suggesting that TAX can inhibit p53-Bcl-2 interaction. Also, TAX showed interaction with the same binding region of the Bcl-2 protein as most of the synthetic inhibitors of ABT family, which includes ABT-199 (Kamath et al. 2016), ABT-737, and ABT-263 (Zacarías-Lara et al. 2016). However, in Bcl-2-TAX complex, TAX does not interact with the same residues as the inhibitors of ABT families interact. This could be due to the smaller size of TAX as compared to large ABT moieties.

In our docking studies, highest Glide docking score was computed in PARP-TAX interaction. The number of hydrogen bonds and hydrophobic interactions for the complex were also higher than most of other protein interactions of TAX. The Glide docking score for TAX was computed to be -9.28 Kcal/mol. In different studies using Glide, workers have shown that the known inhibitors of PARP with IC_{50} values in the nM range also docked with similar kind of Glide scores (Salmas et al. 2015; Ekhteiari Salmas et al. 2016). The post-docking analysis of PARP-TAX complex indicates that Gly-202 forms hydrophobic interaction. Studies based on X-ray crystallography also suggest that Gly-863 (which is Gly-202 in our structure) is important for inhibition of PARP activity (Ye et al. 2013). PARP protein requires NAD^+ as a cofactor for catalyzing Poly(ADP-ribosyl)ation reaction. The interaction of PARP with NAD^+ is mediated by serine amino acid (Steffen et al. 2013). This Ser 864 (Ser-203 in our structure) is thus important for PARP activity. In our studies, TAX forms a hydrophobic interaction with Ser-203 residue rendering it unavailable for the NAD^+-PARP

interaction. Based on similar docking studies on known chemical inhibitors of PARP carried out using Glide, the residues involved in interaction with PARP protein complexes were also involved in interaction in our docking studies with the PARP-TAX complex (Salmas et al. 2015; Ekhteiari Salmas et al. 2016). These findings indicate that TAX may inhibit PARP protein with strong affinity, as the chemical inhibitors used in docking studies with similar Glide scores had IC_{50} values in nM ranges (Salmas et al. 2015; Salmas et al. 2016).

In our docking studies with Lim against p53, Mdm2, Bcl-2 and PARP proteins, Lim also showed a higher binding affinity for p53 and Mdm2. Since Lim is hydrophobic in nature, it did not show hydrogen bond interactions with any of the target proteins. However, the strong interaction of Lim with these proteins is governed by its capability of forming many hydrophobic interactions with hydrophobic binding sites of the corresponding targets and its small size. The p53-Lim complex forms hydrophobic interactions with the residues that are crucial for Mdm2-p53 interactions (Verma et al. 2013b) suggesting that Lim can block Mdm2-p53 binding. The Mdm2 binding pocket comprises of many hydrophobic residues which are crucial for p53-Mdm2 protein-protein interactions. In an independent study, it has been demonstrated that synthetic hydrophobic D-peptide interacts strongly with this hydrophobic binding region of Mdm2 with greater affinity and displaces native p53-helix that interacts with Mdm2 (Liu et al. 2010). The Mdm2-Lim complex forms hydrophobic interactions with almost all the same hydrophobic residues of Mdm2 binding pocket for p53 (Liu et al. 2010) and the residues that stabilize p53-Mdm2 complex (Verma et al. 2013b). The Bcl-2-Lim complex also forms strong hydrophobic interactions. The BH3 region of Bcl-2 protein

along with BH1 and BH2 domains forms a hydrophobic cavity for protein-protein interactions (O'Connor et al. 1998). Lim occupies the hydrophobic binding cleft of Bcl-2 and thus may inhibit protein-protein interactions. Lim forms hydrophobic interactions with the residues that are reported to be crucial for interactions of BH3 inhibitors (Kamath et al. 2016). Docked complex of Lim with PARP showed interaction with eight hydrophobic interactions. In the complex, Lim interacted with glycine (202) residue which is involved in the formation of a hydrogen bond with many other PARP inhibitors (Ye et al. 2013) suggesting that Lim can also inhibit PARP activity. In a recent report on molecular docking of PARP with other inhibitors, it is demonstrated that Gly863, Asp770, Ser864, His862, Tyr907, and Tyr896 are important for PARP inhibition (Ekhteiari Salmas et al. 2016). In our docking studies, Lim showed interaction with Gly202, His201 (corresponding to Gly863 and His862). Lim also occupies the hydrophobic pocket of PARP and interacts hydrophobically with residues that are reported to be important for the interaction of other known PARP inhibitors (Steffen et al. 2013). These results suggest that Lim interacts with a hydrophobic binding pocket of PARP and thus can be a potent inhibitor of PARP activity.

The binding affinity of protein-ligand complexes is governed by the formation of hydrogen bonds and hydrophobic interactions. Moreover, the nature and size of binding pocket also contribute in the accessibility of protein to ligand along with the nature of the ligand. In our computational screening and docking studies of dietary phytochemicals from "Quality photochemical database" against crucial proteins (p53, Mdm2, Bcl-2, and PARP) involved in response to DNA damage, we screened out two phytochemicals TAX and Lim. In our docking studies, both TAX and Lim interacted

with the target proteins by occupying the active binding sites and forming hydrophobic interactions and hydrogen bond interactions. On analyzing the interactions of TAX and Lim with different target proteins and comparing them with the interactions of known inhibitors of the same, we observed that both of them are interacting with the crucial residues as the known synthetic inhibitors. The data suggests that TAX and Lim may inhibit the target proteins with strong binding affinities and may serve the dual function of antioxidants as well as potential inhibitors.

Chapter 3 : Role of *Drosophila* model for identifying antioxidant and antimutagenic activity of dietary phytochemicals against physical and chemical mutagens

3.1 Introduction

Drosophila, the common fruit fly, has gained an immense importance as a model organism in biomedical research. It is used to study a diverse range of processes in areas like genetic and environmental toxicology, developmental biology, behavioral studies and learning, aging, neurobiology, endocrinology and metabolic disorders (Jennings, 2011). The predominant expansion in the history of *Drosophila* and genetics emanated in the early 20^{th} century for its use as a research model when Morgan demonstrated that genes are localized in the chromosomes (Morgan, 1909, 1910). Later in 1929, Muller demonstrated the X-rays induced mutations in fruit flies, and the frequencies of such genetic mutations are dose dependent (Muller and Altenburg, 1929). Charlotte Auerbach and coworkers reported for the first time the induction of mutagenesis by chemical agents like mustard gas (Auerbach, 1947) by studying the development of lethal mutations using SLRL test. Since then, *Drosophila* has been used to evaluate the mutagenic effects of radiations such as γ rays (Ives, 1959), UV light, particulate radiations (neutrons, α and β particles) along with various chemical agents including drugs, narcotics, cosmetics, food additives, preservatives, pesticides, contaminants, industrial wastes, and other abiotic pollutants (Lee, 1975).

Drosophila has always been a role model of genetics and mutation studies. In toxicological research, this model is widely used to test the mutagenicity and

antimutagenicity of environmental toxicants (Würgler, 1980; Würgler and Graf, 1985). It offers rapid and efficient *in vivo* system (alternate to higher animal models) to assess any induced genetic aberration by physical or chemical mutagens in somatic as well as germ cell stages. *Drosophila* shares 60% genome similarity to the human genome (Adams et al., 2000) and 75% of genes associated with diseases in humans shows pattern similarities with *Drosophila* genome (Reiter et al., 2001). Moreover, their similarities in core proteome, aging, cancer, Alzheimer's, Parkinson's and biochemical pathways has led to the development of *Drosophila* as more robust and versatile model for various kinds of studies (Bernards and Hariharan, 2001; Bier and McGinnis, 2008; Pandey and Nichols, 2011). Several *Drosophila* strains related to human diseases are developed by altering the *Drosophila* homolog genes which are associated with disease genes in humans (Reiter and Bier, 2002). Using these approaches, *Drosophila* models of human Parkinson's (Greene et al., 2003), Alzheimer's (Greeve et al., 2004), Huntington's (Jackson et al., 1998), spinocerebellar ataxia (Bonini, 1999), cancer (Tapon et al., 2002) and for screening of drugs (Steffan et al., 2001) have been developed. Thus, development of *Drosophila* models for human disease genes offers insights to understand the underlying mechanism of disease pathogenesis (Brumby and Richardson, 2005; Botas, 2007). It can also be used to assess genetic alteration by its phenotype and also in identifying potential therapeutic agents to supersede the cause (Giacomotto and Ségalat, 2010; Ugur et al., 2016).

3.1.1. Drosophila and its role in mutation studies

Drosophila has been a role model for the study and assessment of different types of mutations for several decades. Using *Drosophila*, different kinds of DNA lesions have

been detected by studying chromosomal aberrations like translocations, deletions and duplications, non-disjunctions (Sobels, 1974), genetic mutations (like forward mutations, reverse mutations and multiple specific locus), induced recombination, sister chromatid exchange and / or DNA repair (Wienberg, 1977). Furthermore, *Drosophila* model is often employed to study mutations induced by exposure of both, directly and indirectly acting chemical mutagens (Sobels and Vogel, 1976a; b).

Drosophila offers a test model system for analysis of mutations in both somatic and germ cells. Somatic mutations in *Drosophila* can be determined by somatic mutation and recombination test (SMART), a very sensitive and efficient, one generation test. It was first described by Graf and co-workers where they identified mutagenic and recombinogenic effects of varieties of chemical mutagens by scoring pattern of spots on the wings of fly (Graf et al., 1984; Graf and Singer, 1992). SMART test also allows the user to study antigenotoxic effects of various compounds and complex mixtures (Abraham, 1994; Abraham and Graf, 1996). The test also provides information to the user whether the antigenotoxic effect is due to its antimutagenic activity or its anti-recombinogenic activity (Graf et al., 1998). Although SMART is an excellent and sensitive method to detect genetic aberrations. It is restricted to only one generation of the fly, and the test cannot be applied to detect any heritable mutations in germ cells (recessive lethal). Analysis of mutations in germ cells is carried out by performing the sex-linked recessive lethal test (SLRL) (Abrahamson and Lewis, 1971; Lee et al., 1983a; Vogel, 1984).

3.1.2. Sex-linked recessive lethal test (SLRL)

The sex-linked recessive lethal (SLRL) test in *Drosophila melanogaster* is far more reliable and widely employed for the detection of almost all types of genetic mutations exerting recessive lethal effects (Sobels and Vogel, 1976b). It can be used to study the genotoxic effects of various physical and chemical mutagens (Sobels and Vogel, 1976a; Szabad et al., 1983; Abraham, Singh, et al., 1993). The test can be used to screen recessive lethal mutations at almost 800 different loci on the X chromosome, which represents 80% of the X chromosome and one-fifth of the entire *Drosophila melanogaster* genome (Abrahamson, 1980). Since *Drosophila* model exhibits the higher activity of xenobiotic drug metabolizing enzymes like cytochrome P450 and aryl hydrocarbon hydroxylase (Baars, 1980; Gladstone and Su, 2011), the SLRL test can be used to detect mutagens and promutagens with very short half-lives (Würgler, 1980; Yang et al., 2007). Promutagens are mostly activated in spermatids (Hothorn, 1991), and SLRL can be used to analyze induced mutations in specific stages of germ cells (Abraham, Singh, et al., 1993). Thus, SLRL can be considered as the best tool for the assessment of promutagens (Lee et al., 1983b). The sex-linked recessive lethal (SLRL) test is highly sensitive assay system for the detection of mutation frequency occurring per locus ranging from 3.3×10^{-6} to 2.5×10^{-6} which is almost equal to double of mutation frequency occurring in humans which ranges from 5×10^{-6} to 5×10^{-7} (Livingstone, 1973).

Thus, with the ability of SLRL to detect both mutagens and promutagens, detection of different types of DNA lesions and high levels of sensitivity at low cost makes it an excellent choice for the detection of genotoxicity.

3.1.3. Drosophila and its role in oxidative stress

Oxidative stress is one of the major mechanisms to cause DNA damage. Several mutagens increase cellular stress by the generation of free radicals which ultimately causes DNA damage. Cells possess an antioxidative defense system, and this machinery is conserved in most of the eukaryotes including *Drosophila* and humans (Missirlis et al., 2003). Intracellular levels of ROS and RNS, lipid peroxidation and altered activities of antioxidant enzymes viz superoxide dismutase (SOD), catalase, glutathione S-transferase (GST) are key biomarkers of oxidative stress (Missirlis et al., 2001). *Drosophila* model is used in research studies to detect these oxidative stress levels to study the effect of radiations, and different natural and synthetic compounds on oxidative stress (Singh et al., 2009).

3.1.4. Drosophila and its role in drug screening

The similarities in the genome and regulatory metabolic pathways between human and *Drosophila* has encouraged the development of *Drosophila* models of human diseases. Successful development of such models has encouraged workers to use *Drosophila* model in the screening of potential drug candidate (Giacomotto and Ségalat, 2010; Willoughby et al., 2013). Its short life cycle, generation of large progeny, easy culture conditions, and convenience in the mode of feeding the test agents provides an added advantage for using *Drosophila* as a useful model for screening drugs (Gladstone and Su, 2011). Successful screening of drugs such as histone deacetylase inhibitors for the treatment of various neurodegenerative disorders has been reported using *Drosophila* (Steffan et al., 2001). Similarly, treatment of 'indomethacin' has shown to induce gain of function in transgenic *Drosophila* model against human colon cancer (Bhandari and

Shashidhara, 2001). The treatment of drug; ZD6474 has been used in *Drosophila* model of human multiple endocrine neoplasia-2 (MEN2) (Vidal et al., 2005). *Drosophila* as a whole organism offers many advantages. Initially, both validation of drug and associated toxicity can be tested in one single experiment. Since the whole organism is used, it provides insights to find all possible targets for the drug. Furthermore, use of transgenic models enables to understand and decipher the molecular mechanism of complex pathways and potential targets for a drug (Nazir et al., 2001).

3.1.5. Drosophila and its role in antimutagenic studies

Various species of plants, fruits, spices, and herbs are used in diet and predominantly in traditional medicines for their beneficial health effects. It is essential that systematic studies of such phytochemicals must be carried out to characterize their antimutagenic effects and other beneficial or hazardous effects. To analyze these effects, several well established *in vitro* and *in vivo* test systems are used, such as bacteria (Simić et al., 1998), yeast (Vuković-Gačić et al., 2006), mammals (Vujosević and Blagojević, 2004). However, one of the most limiting features of all these models is that with these models, one can test the compounds only in its pure form, but *Drosophila* model gives an added advantage to screen variety of compounds even in their crude form along with several mixtures if needed. Another important advantage of *Drosophila* is to screen the different concentrations of test agents by choosing different modes of administration of the test agents like feeding, injecting (Frei et al., 1992) and even in the form of vapors (aerosols) (Bownes and Seiler, 1977). It can also be used to detect mutagens present in various body fluids like urine, plasma, tissue homogenates and peritoneal fluids (Zimmermann, 1973). Furthermore, mutagenic and antimutagenic potentials of test

agents can be evaluated in both somatic cells (Negishi et al., 1989; Frölich and Würgler, 1990), and germ cells (Stamenkovic-Radak et al., 2005) of *D.melanogaster*. Using SMART and SLRL test systems in *Drosophila*, several phytochemicals like sage tea (Patenkovic et al., 2009), coffee (Abraham, 1994), fennel and parsley extracts (Fakiha and Bibars, 2010), essential oils from *Origanum compactum* (Mezzoug et al., 2007), *Helichrysum italicum*, *Ravensara aromatica* and *Ledum groenlandicum* (Idaomar et al., 2001) have been evaluated for their antimutagenic potentials.

Drosophila has been considered as the most studied model in the field of genetics and mutations. Its application in the study of genotoxicity and antigenotoxicity has been practiced for almost decades. Due to its various advantages and applications, *Drosophila* has attracted importance amongst researchers for their experimental studies, and this can be understood by the fact that three Nobel prizes are associated with *Drosophila melanogaster* (T. H.Morgan -1933, H. Muller -1946 and Ed Lewis, C. N.Volhard and E.Wieschaus -1995).

The objective of this study is to evaluate potential mammalian genotoxic and antigenotoxic agents in *Drosophila* with the rationale that *Drosophila* can be used as an alternative model organism which can be used in reduction, refinement and replacement (3Rs) of laboratory animals for better experimental studies (Vogel, 1987; Abolaji et al., 2013).

The present exploration employs the use of *Drosophila* to study potential antigenotoxic and antioxidant effects of certain phytochemicals which are already established as potent chemoprotective agents in higher animals.

The objectives of our studies are:

a) To check the antimutagenic and antioxidant effect and of quercetin, gallic acid, and Lim against urethane induced DNA damage.

b) To check the antimutagenic and antioxidant effect of tea polyphenol and β-carotene against γ radiation induced DNA damage.

c) To check the antimutagenic and antioxidant effect of coffee against cyclophosphamide induced DNA damage

d) To check the modulatory effects of selected phytochemicals on the life span of *Drosophila* male flies.

3.2. Materials and Methods

3.2.1. Chemicals

The chemicals used in the experiments were: polyphenol 60 from green tea (TP), β-carotene (BC), quercetin (QC), gallic acid (GA), limonene (Lim), coffee (CF), urethane (URE) and cyclophosphamide (CPH), 1-chloro-2, 4-dinitrobenzene, 5 (CDNB), 5'-di thiobis (2-nitrobenzoic acid) (DTNB) and glutathione reduced (GSH). All these chemicals were purchased from Sigma-Aldrich chemical company (India), and all other reagents and chemicals were of analytical grade and procured from SRL and Himedia.

3.2.2. *Drosophila* stocks and culture conditions

Two strains of *D.melanogaster* were used in the present study: **Oregon K** (wild type) and **Muller-5** (or Basc) stock *In(1)*s^{s1L} sc^{8R} + *S*, sc^{s1} sc^{8} $w^{a}B$). These stocks were obtained from *Drosophila* stock center of Mysore University (India).

The above symbols have been explained by (Lindsley and Grell, 1968).

The stocks mentioned above are maintained at 25±2ºC on a standard culture medium containing:

1) Agar	10gm
2) Yeast	11gm
3) Corn flour	75gm
4) Jaggery	50gm
5) Water	750ml
6) Propionic Acid	2.5ml

This standard culture medium was prepared by dissolving the above ingredients in water. The mixture was boiled for 15-20 min. Once the mixture was cooled down, propionic acid was added as a mould inhibitor.

3.2.3. Irradiation

Culture vials containing adult flies and larvae of *Drosophila* were exposed to γ radiations at a dose rate of 0.03Gy/sec in a gamma chamber (source ^{60}Co, 204TBq, 5500Ci) obtained from Bhaba Atomic Research Centre (BARC), Mumbai, India. The dose rate was determined using Fe^{2+}/Fe^{3+} dosimetry.

3.2.4. Test for detecting mutagenicity

3.2.4.1. Muller-5 (Basc) test for detecting sex-linked recessive lethal mutation

Control and treated wild-type males are allowed to mate with Muller-5 (Basc) females, which is homozygous for the genetic markers on the X-chromosome. The F_1 progeny which emerged comprised of males with *Basc* phenotypes (bar white apricot eyes) and females heterozygous for the X chromosomes, shows kidney shaped red eyes. The F_1 progeny was allowed to intercross, and the F_2 generation which emerged comprised of wild-type males having round red eyes (wild type phenotypes) and bar white apricot eyes (Basc phenotypes) and females with kidney shaped red eyes and bar white apricot eyes (Basc phenotypes). The absence of wild-type males in the F_2 generation confirms the occurrence of SLRL mutation. (Figure.3.1)

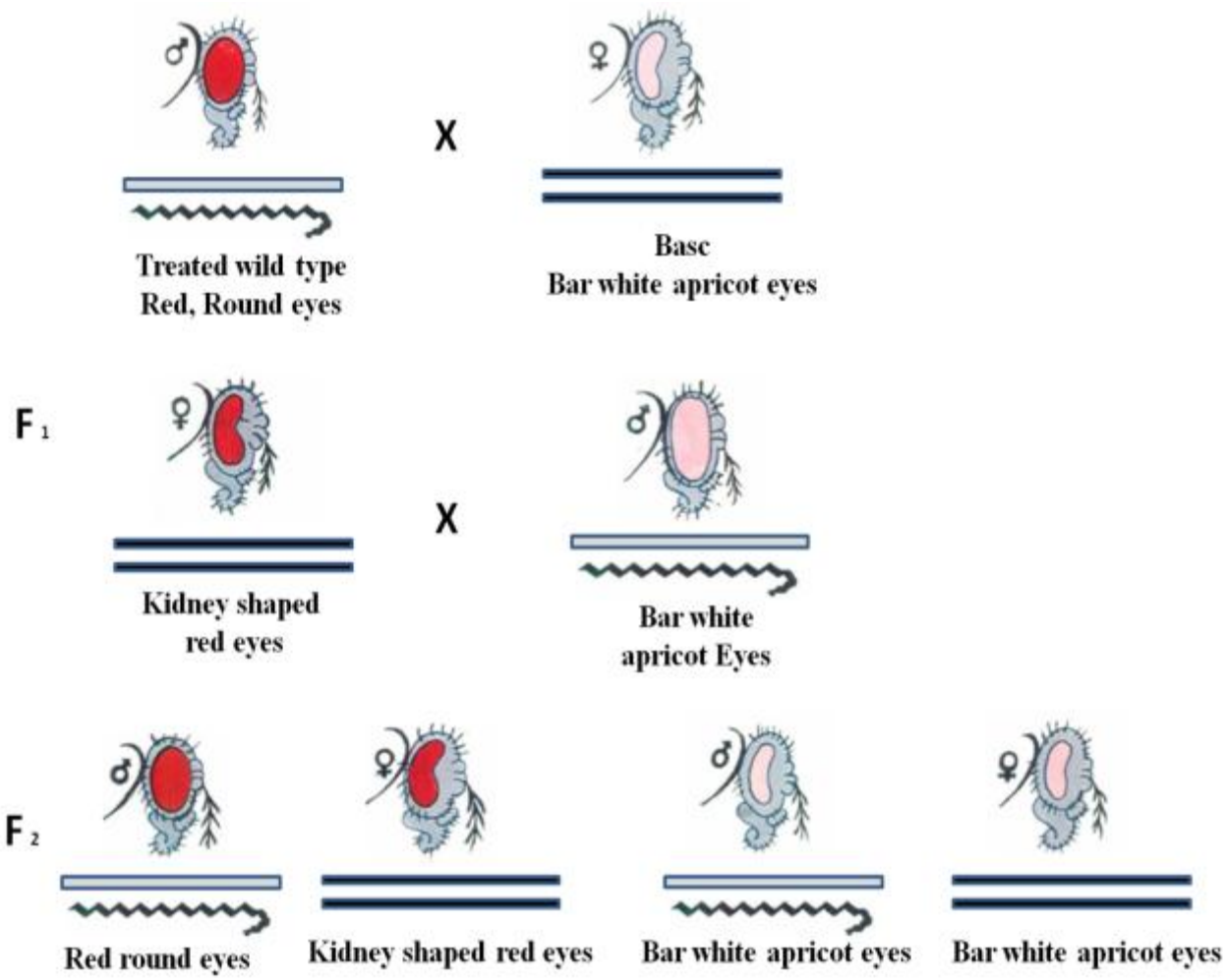

Figure 3.1: Test procedure for sex-linked recessive lethal test (SLRL test)

3.2.4.2. Administration of test agents

Adult feeding experiments

Four days old adult male flies (ORK) were starved for 6-8h and transferred into a glass vial containing filter paper soaked with test agents and mixed with 10% sucrose solution (as a negative control) for 72h. The filter paper was renewed once every 12h.

Larval feeding experiments

Inseminated females (ORK) were allowed to lay eggs on the culture medium for 8-10h. After this, the females were discarded, and 3 days later, the larvae were transferred to glass vials containing test solution mixed with instant *Drosophila* culture medium (Carolina Biological Supply, Burlington, USA). After 24h, one batch of the third instar larvae were harvested to check the enzymatic activity whereas emerging one-day old adult males were mated individually with a set of 3 to 5 *Basc* females in order to conduct SLRL test. (Figure 3.2)

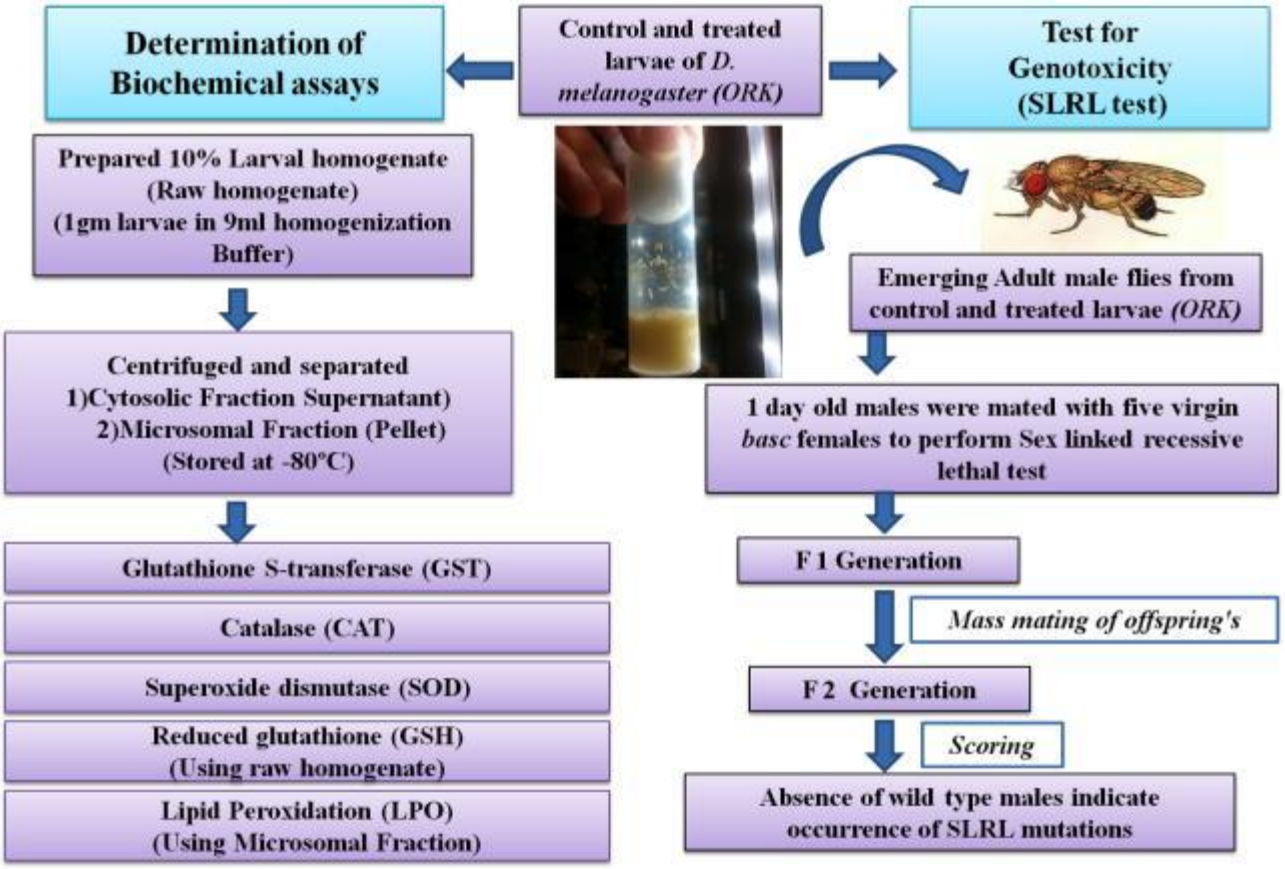

Figure 3.2: Flow chart of the methodology followed for larval feeding experiments

3.2.4.3. Toxicity testing for selecting concentration of each phytochemical

i. **Adult feeding experiments:** Each group comprising of ten vials containing 20 flies (n=200) were fed with the test agents for 72h, The adult flies that survived at the highest possible concentration were used for the final experimental studies.

ii. **Larval feeding experiments:** *Drosophila* larvae were fed on different concentrations of test agents, to select those which did not show lethality or delay in the normal development of larvae.

3.2.4.4. Test agents, their concentrations and treatment schedule

Table 3.1: Experimental design **a)** Concentrations of the test agents (QC, GA and Lim) against URE (positive control) in larval and adult flies of *Drosophila*. **b)** Concentrations of the test agents (BC and TP) against γ-irradiation (positive control) in larval and adult flies of *Drosophila***. c)** Concentrations of the test agents CF against CPH (positive control) in larval and adult flies of *Drosophila*

Table 3.1a: Experiment 1

Phytochemicals	**Positive Control**	**Selected doses (after toxicity test)**	
		Adult	**Larval**
Quercetin (QC)	Urethane (20mM)	0.25% (w/v)	0.25% (w/v)
Gallic acid (GA)		1.0% (w/v)	0.50% (w/v)
Limonene (Lim)		0.25% (v/v)	0.25% (v/v)

Table 1b: Experiment 2

Phytochemicals	Positive Control	Selected doses (After toxicity test)	
		Adult	Larval
β-carotene (BC)	γ-irradiation (10 Gy)	0.25%, 0.5%, 1% (w/v)	0.25%, 0.5%, 1% (w/v)
Tea polyphenols (TP)		1% (w/v)	1% (w/v)

Table 1c: Experiment 3

Phytochemicals	Positive Control	Selected doses (After toxicity test)	
		Adult	Larval
Coffee (CF)	Cyclophosphamide (3mM)	2.0% (w/v)	2.0% (w/v)

3.2.4.5. Brood test to assess the sensitivity of successive germ cell stages

According to the test procedure, four, 3- day broods were sampled to assess the sensitivity of successive germ cell stages which roughly corresponds to four different broods in adult flies of *D. melanogaster*. However, the chemical and physical mutagens exhibit stage specificity, therefore, it is essential to analyze the progeny in all the germ cell stages (in postmeiotic (spermatozoa and spermatids), meiotic (spermatocytes) and premeiotic (spermatogonia) cells (**Figure 3.3).** Each treated male was allowed to mate with five virgin *Basc* females for three days resulting in brood I. After three days, the same male fly was allowed to mate with another set of five virgin females (Muller-5) to produce brood II. The same pattern was repeated until brood IV to check the

antimutagenic effect of test agents. These four broods correspond to mature sperm, mid or late-stage spermatids, spermatids, spermatocytes, and spermatogonia (Figure 3.3).

For both the adult and larval feeding experiments, the F_1 flies were mass mated and allowed to raise the F_2 generation which was scored for the absence of wild-type males indicating the occurrence of SLRL mutation.

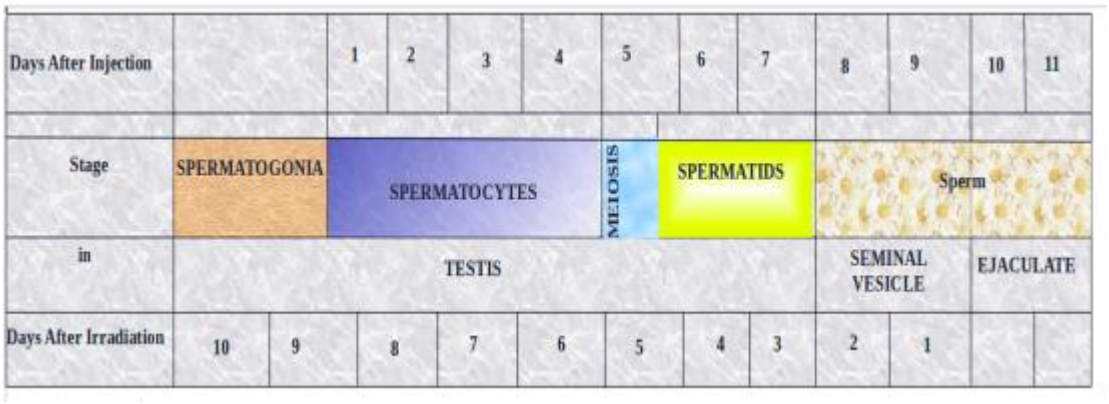

Figure 3.3: Timing of spermatogenesis in *Drosophila melanogaster* and the scheme for brood pattern analysis of the genetic effect of radiation in mature sperms, spermatids, spermatocytes, and spermatogonia. (Chandley and Bateman, 1962)

3.2.5. Assay of oxidative stress markers

For evaluating oxidative damage in control and treated third instar larvae, biochemical, enzymatic assays were carried out to estimate reduced glutathione content (GSH), glutathione S-transferase (GST), catalase (CAT), superoxide dismutase (SOD) and lipid peroxidation (LPO). All the assays were performed on 10% larval homogenate.

3.2.5.1. Preparation of tissue homogenate

Larval homogenate (10%) from control and treated larvae were prepared (Potter Elvehjem homogenizer) using phosphate buffer (0.1M/pH-7.4) along with 0.15M KCl.

After centrifugation at 9000 x g for 30 mins, the supernatant was again centrifuged at 1,05000 x g for 1h and the supernatant (cytosolic content) was used for further biochemical assays. The pellet containing microsomes was again resuspended with buffer mixture containing 0.1M phosphate buffer pH 7.25, 20% (v/v) glycerol, 0.25 mM PMSF, 0.01 M EDTA and 0.1M DTT. The microsomal and cytosolic samples were stored at -80°C until further use (Singh et al., 2009).

3.2.5.2. Determination of glutathione S-transferase activity (GST)

Glutathione S-transferase (GST) activity determined by the method of Habig et al., (1974) with some minor modifications using 5mM of 1-chloro-2,4 dinitrobenzene (CDNB) as substrate. The reaction mixture comprised of 25 µl of the larval cytosolic sample, 1.975ml of sodium phosphate buffer (0.2M), 1ml reduced glutathione (1mM) and 10 µl of CDNB (5.0 mM). The formation of CDNB-GSH conjugate was measured at 340nm for 3 min at an interval of 30 seconds. The GST activity was expressed as nmol CDNB reduced/min/mg protein using molar extinction coefficient of 6.25×10^3 $M^{-1}cm^{-1}$.

3.2.5.3. Determination of superoxide dismutase activity (SOD)

SOD activity was estimated in control and treated 10% larval homogenate as reported by Nishikimi et al., (1972) with some minor modification, The reaction mixture comprises of 25µl of larval homogenate, 0.175 ml of double distilled water, 1.2 ml of sodium pyrophosphate buffer (0.052M, pH 8.3) 100µl of phenazine methosulfate (186µM), 300µL nitroblue tetrazolium (300µM). The above reaction mixture was incubated for 2 min. The reaction was terminated by addition of 200 µl of reduced nicotinamide adenine dinucleotide (NADPH) (780µM), and 1 ml glacial acetic acid. A

colored product was obtained after addition of n-butanol which was measured at 560nm. One unit of enzymatic activity is defined as the protein concentration required for inhibiting the chromogen production by half in a time interval of 1 min and the SOD activity is expressed as U/min/mg protein.

3.2.5.4. Determination of catalase activity (CAT)

Catalase activity was measured in control and treated 10% larvae homogenate, as described by Sinha, (1972), and is defined as the ability to dissociate H_2O_2 in 1 min of incubation time. The assay mixture consisting of 100µl of the larval cytosolic sample, 400µl of distilled water and 1ml of sodium phosphate buffer (0.01M, pH 7.0), was incubated with 500µl of H_2O_2 (0.2M) for 1 min at 37°C. This reaction was stopped by addition of 2ml of dichromate acetic acid mixture (DAA) (5% $K_2Cr_2O_7$ with glacial acetic acid, 1:3 by volume), forming a blue colored unstable precipitate, which was further heated and cooled down to get a stable green colored product (chromic acetate) and absorbance was measured at 570 nm. The enzymatic activity is expressed as µmoles of H_2O_2/min/mg larval protein.

3.2.5.5. Estimation of reduced glutathione (GSH Content)

GSH content was measured by the method of Ellman, (1959) with some minor modifications. Equal amounts of 10% larval homogenate and 5% trichloroacetic acid were vortexed and centrifuged. The reaction mixture consist of the supernatant was mixed with Ellman's reagent (0.2M phosphate buffer (pH 8.0), 0.01% 5,5′-dithiobis-2-nitro benzoic acid (DTNB). The reaction is monitored immediately at 412nm, and the GSH content was expressed as nmol/mg larval protein.

3.2.5.6. Assay for lipid peroxidation (LPO)

Malondialdehyde (MDA) content was measured as a marker of lipid peroxidation (LPO) by the method of Ohkawa et al., (1979), using tetra ethoxy propane (TEP) as an external standard. The assay mixture consists of 25µl of the larval microsomal sample, 0.825 ml double distilled water, 150µl of 10% sodium dodecyl sulfate (SDS). This reaction mixture was incubated in test tubes for 4 min at 25°C. After incubation, 1 ml of acetic acid (20%, pH 3.5) was added. This mixture was incubated for 5 mins at 37°C, to which 0.8% thiobarbituric acid (TBA) was added The assay mixture was kept in boiling water (80-90°C) for 1h, 5ml of n-butanol was added to the above mixture centrifuged at 4000 x g for 15 mins at 25°C and the absorbance of the top organic layer was measured at 532 nm against n-butanol. MDA content was expressed as moles MDA formed/h/mg protein.

3.2.5.7. Protein estimation

The protein concentration in control and treated larval homogenates were estimated by the method of Lowry et al., (1951) using bovine serum albumin (BSA) as the external standard. The 10% larval homogenate (cytosolic and microsomal) was mixed with equal volumes of 1% CuSO4 and 2% $KNaC_4H_4O_6 \cdot 4H_2O$ along with 2%Na_2CO_3 in 0.1N NaOH solution). After vortexing, 1 N Folin's reagent was added, and absorbance was measured at 670 nm after 30 min incubation, protein concentration was expressed as mg/ml homogenate.

3.2.6. Longevity assay

In order to check the effect of dietary phytochemicals and mutagens, the longevity assay was performed in adult flies of *D. melanogaster* (ORK) as described by Nazir et al.,

(2001). Newly eclosed male flies (25 flies/vial) were housed in 10 vials (n=250) for each group and were fed on a basal diet (normal control), as well as a diet containing test agents (test phytochemicals along with positive controls). The flies were exposed to test agents from day 1 of their emergence. After counting the dead flies, the remaining live flies were transferred to the fresh media on every alternate day.

3.2.7. Statistical analysis

i. The enzyme activity and longevity results were statistically analyzed by ANOVA (Newman's Keuls as post hoc test), using the software Graph pad PRISM (V.5.0).

ii. Kastenbaum and Bowman tables (Würgler et al., 1975) were used for SLRL test with further validation using Z-Test for a test of difference in proportion.

3.3. Results

The results are divided into the following sections:

- Evaluation of antimutagenic potential of test phytochemicals
- Evaluation of antioxidant capacity of test phytochemicals
- Effect of test agents on the longevity of *D. melanogaster* flies

3.3.1. Sex-linked recessive lethal mutation: Test for genotoxicity

In our study, using SLRL assay, we determined the antimutagenic potential of various phytochemicals (QC, GA, Lim against URE; TP and BC against γ radiation and CF against CPH) Overall, we observed a significant reduction in the incidence of SLRL mutation frequencies with phytochemical treatment against lethal mutations of genotoxic agents. The results were expressed in terms of % lethal from the adult, and larval SLRL experiments.

3.3.1.1. Antimutagenic potential of QC, GA, and Lim against URE induced mutations

i. Adult feeding experiments

In the adult feeding experiments, SLRL frequencies were found to decrease significantly when the flies were treated with the mixture of test agents (QC, GA, and Lim) and carcinogen (URE) as compared to carcinogen exposure (URE alone). Significant reductions were observed in the incidence of SLRLs by 65.20% (with URE + QC 0.25%), > 62.03% (URE + GA 1%) > and 60.79% (URE + Lim 0.25%) as compared to URE alone (Table 3.2).

ii. Larval feeding experiments

A similar trend has been observed in the larval feeding experiments with a slight difference in the doses, where URE + QC 0.25%, URE + GA **0.5%** and URE + Lim 0.25% has significantly reduced the SLRLs by 57.66%, 54.16% and 48.13% respectively (Table 3.3).

Table 3.2: Adult feeding experiments: Induction of SLRLs by URE and its modulation by QC, GA, and Lim in *Drosophila* adult flies.

Treatment	Broods	Days after treatment	No: of X-chromosomes	Lethal (n)	Lethal (%)
Sucrose 10% (Negative Control)	I	0-3	802	2	0.249
	II	3-6	771	1	0.129
	III	6-9	516	1	0.193
	IV	9-12	412	1	0.243
	I-IV	**0-12**	**2501**	**5**	**0.200**
QC 0.25%	I	0-3	737	1	0.136
	II	3-6	573	1	0.175
	III	6-9	534	1	0.187
	IV	9-12	388	1	0.258
	I-IV	**0-12**	**2232**	**4**	**0.179**

GA 1%	I	0-3	796	2	0.251
	II	3-6	758	1	0.132
	III	6-9	562	1	0.178
	IV	9-12	401	0	0.000
	I-IV	**0-12**	**2517**	**4**	**0.159**
Lim 0.25%	I	0-3	775	1	0.129
	II	3-6	686	1	0.146
	III	6-9	522	1	0.192
	IV	9-12	335	1	0.299
	I-IV	**0-12**	**2318**	**4**	**0.173**
URE 20mM	I	0-3	766	19	2.480***
	II	3-6	620	13	2.097***
	III	6-9	507	9	1.775***
	IV	9-12	330	4	1.212*
	I-IV	**0-12**	**2223**	**45**	**2.024*****

	I	0-3	966	9	0.932**
	II	3-6	515	5	0.971
	III	6-9	428	2	0.467*
URE 20mM + QC 0.25%	IV	9-12	363	0	0.000***
	I-IV	**0-12**	**2272**	**16**	**0.704****
	I	0-3	789	9	1.141**
	II	3-6	579	4	0.691**
URE 20mM + GA 1%	III	6-9	449	3	0.668
	IV	9-12	395	1	0.253
	I-IV	**0-12**	**2212**	**17**	**0.768****
	I	0-3	666	8	1.201*
	II	3-6	574	5	0.871*
URE 20mM + Lim 0.25%	III	6-9	441	2	0.454*
	IV	9-12	335	1	0.299
	I-IV	**0-12**	**2016**	**16**	**0.794****

* *p≤0.10, ** p≤0.05, *** p≤0.01* (Compared to positive control, URE)

Table 3.3: Larval feeding experiments: Induction of SLRLs by URE and its modulation by QC, GA, and Lim in Drosophila larvae.

Treatment	No: of X-chromosomes	Lethal (n)	Lethal (%)
Control	1724	4	**0.232**
QC 0.25%	1016	2	**0.197**
GA 0.5%	1021	2	**0.196**
Lim 0.25%	1092	2	**0.183**
URE 20mM	1251	36	**2.878*** **
URE 20mM + QC 0.25%	985	12	**1.218*** **
URE 20mM + GA 0.5%	1137	15	**1.319*** **
URE 20mM + Lim 0.25%	1005	15	**1.493****

**p≤0.10, **p≤0.05, ***p≤0.01* (Compared to positive control, URE)

3.3.1.2. Antimutagenic potential of TP and BC against γ radiation (10Gy) induced mutations

i. Adult feeding experiment

Data from adult feeding experiments demonstrates that γ radiation + BC 0.5% has significantly reduced γ radiation (10 Gy) induced mutation frequency in all the germ cell stages (brood I-IV). Co-exposure of γ radiation + TP 1% has significantly decreased the SLRL frequencies by 70.1%. In other experiment, we tested BC at varying concentrations, combination of γ radiation + BC 0.5% has significantly reduced the SLRL mutation by 70.3% followed by γ radiation + BC 0.25% (69.8%). At higher concentration of BC, combination effect (γ

radiation + BC 1%) showed hormesis effect where we found induction in the incidence of lethal mutations by 29.1% as compared to γ radiation exposure alone (Table 3.4).

ii. Larval Feeding experiment

Results obtained from larval feeding experiments showed that co-exposure of γ radiation + TP 1% has significantly reduced the mutation frequencies by 43.4%. Co-exposure of γ radiation + BC 0.25%, γ radiation + BC 0.5% and γ radiation + BC 1% has significantly reduced the SLRL mutations by 40.7%, 39.4% and 32.5% respectively (Table 3.5).

Table 3.4: Adult feeding experiments: Induction of sex-linked recessive lethal (SLRLs) by γ radiation (10Gy) and its modulation by TP and BC in *Drosophila* adult males.

Treatment	Brood	Days after treatment	No: of X-Chromosomes	Lethal	Lethal (%)
10% Sucrose (Negative Control)	I	0-3	913	1	0.110
	II	3-6	837	2	0.239
	III	6-9	682	1	0.147
	IV	9-12	554	1	0.181
	I-IV	**0-12**	**2986**	**5**	**0.167**
TP 1%	I	0-3	781	2	0.256
	II	3-6	746	1	0.134
	III	6-9	614	1	0.163
	IV	9-12	517	0	0.000
	I-IV	**0-12**	**2658**	**4**	**0.150**
BC 0.25%	I	0-3	869	1	0.115
	II	3-6	684	2	0.292
	III	6-9	577	0	0.000
	IV	9-12	461	1	0.217
	I-IV	**0-12**	**2591**	**4**	**0.154****
BC 0.5%	I	0-3	889	2	0.225
	II	3-6	702	1	0.142
	III	6-9	693	0	0.000

	IV	9-12	415	1	0.241
	I-IV	**0-12**	**2699**	**4**	**0.148**
BC 1%	I	0-3	902	2	0.222
	II	3-6	819	1	0.122
	III	6-9	674	1	0.148
	IV	9-12	529	1	0.189
	I-IV	**0-12**	**2924**	**5**	**0.171**
γ Radiation	I	0-3	752	31	4.122***
	II	3-6	732	27	3.689***
	III	6-9	717	15	2.092*
	IV	9-12	665	2	0.301
	I-IV	**0-12**	**2866**	**75**	**2.617*** **
γ Radiation + TP 1%	I	0-3	825	8	0.970***
	II	3-6	782	5	0.639***
	III	6-9	645	5	0.775
	IV	9-12	562	4	0.712
	I-IV	**0-12**	**2814**	**22**	**0.782****
γ Radiation + BC 0.25%	I	0-3	810	7	0.864***
	II	3-6	711	6	0.844***
	III	6-9	512	4	0.781
	IV	9-12	499	3	0.601
	I-IV	**0-12**	**2532**	**20**	**0.790****

γ Radiation + BC 0.5%	I	0-3	788	7	0.888***
	II	3-6	651	5	0.768***
	III	6-9	582	4	0.687
	IV	9-12	558	4	0.717
	I-IV	**0-12**	**2579**	**20**	**0.775****
γ Radiation + BC 1%	I	0-3	704	8	1.136***
	II	3-6	688	7	1.017***
	III	6-9	662	7	1.057
	IV	9-12	522	4	0.766
	I-IV	**0-12**	**2576**	**26**	**1.009****

* *p≤0.05, ** p≤0.01, *** p≤0.001* (Compared to positive control, γ radiation)

Table 3.5: Larval feeding experiments: Induction of sex-linked recessive lethal (SLRLs) by γ radiation (10Gy) and its modulation by TP and BC in *Drosophila* larvae.

Treatment	**No: of X chromosomes**	**Lethal (n)**	**Lethal (%)**
Control	1808	4	0.221
TP 1%	1095	2	0.183
BC 0.25%	935	2	0.214
BC 0.5%	1167	3	0.257
BC 1%	1218	4	0.328
γ Radiation	1315	27	2.053**
γ Radiation + TP 1%	1121	13	1.160**
γ Radiation + BC 0.25%	986	12	1.217**
γ Radiation + BC 0.5%	885	11	1.243**
γ Radiation + BC 1%	722	10	1.385**

** $p \leq 0.05$, ** $p \leq 0.01$, *** $p \leq 0.001$* (Compared to positive control, γ radiation)

3.3.1.3. Antimutagenic potential of CF against CPH induced mutations

i. Adult feeding experiment

Data from adult feeding experiments demonstrates that CPH + CF2% has significantly reduced the CPH (3mM) induced mutation frequencies in all the germ cell stages (Brood I-IV). Combination exposure to CPH + CF2% has significantly decreased the SLRL frequencies by 62.4% (Table 3.6).

ii. Larval feeding experiments

Results obtained from larval feeding experiments demonstrate that co-exposure of CPH + CF2% has significantly reduced the mutation frequencies by 75% (Table 3.7).

Table 3.6: Adult feeding experiments: Induction of SLRLs by CPH and its modulation by CF in *Drosophila* adult flies.

Treatment	Broods	Days after treatment	No: of X-chromosomes	Lethal (n)	Lethal (%)
Sucrose 10% Negative Control	**I**	0-3	820	2	0.244
	II	3-6	763	2	0.262
	III	6-9	656	1	0.152
	IV	9-12	545	1	0.183
	I-IV	**0-12**	**2784**	**6**	**0.216**
CF 2%	**I**	0-3	653	2	0.306
	II	3-6	571	1	0.175
	III	6-9	562	1	0.178
	IV	9-12	488	1	0.205
	I-IV	**0-12**	**2274**	**5**	**0.220**
CPH 3mM	**I**	0-3	665	12	1.805***
	II	3-6	588	8	1.361***
	III	6-9	492	6	1.220**
	IV	9-12	395	4	1.013**
	I-IV	**0-12**	**2140**	**30**	**1.402*** **

	I	0-3	687	6	0.873*
	II	3-6	566	3	0.530*
CPH + CF	**III**	6-9	457	1	0.219**
	IV	9-12	379	1	0.264*
	I-IV	**0-12**	**2089**	**11**	**0.527*** **

** p≤0.10, ** p≤0.05, *** p≤0.01* (Compared to positive control, CPH)

Table 3.7: Larval feeding experiments: Induction of SLRLs by CPH and its modulation by CF in Drosophila larvae.

Treatment	**No: of X-chromosomes**	**Lethal (n)**	**Lethal (%)**
Control	1781	4	**0.225**
CF 2%	1269	3	**0.236**
CPH 3mM	1422	25	**0.196*** **
CPH + CF	1022	8	**0.783*** **

** p≤0.10, ** p≤0.05, *** p≤0.01* (Compared to positive control, CPH)

3.3.2. Antioxidative stress parameters

3.3.2.1. Modulation of oxidative stress levels by QC, GA and Lim against URE in third instar larvae of *D. melanogaster*.

A significant enhancement was observed in the overall antioxidant enzyme activity when the third instar larvae were treated with test agents in combination with URE 20mM. (Figure 3.4)

1) Effects on reduced glutathione (GSH) levels and glutathione S-transferase (GST) activity: As compared to negative control group, GSH levels, and GST activity were reduced significantly in URE treated group. However, the co-exposure of test agents (QC, GA, and Lim) with URE had significantly increased the GSH content and GST activity as compared to URE group alone. Although the maximum elevation in the GSH levels was observed with URE 20mM + Lim 0.25% and prominent increase in GST activity was observed with URE 20mM + GA 0.5%.

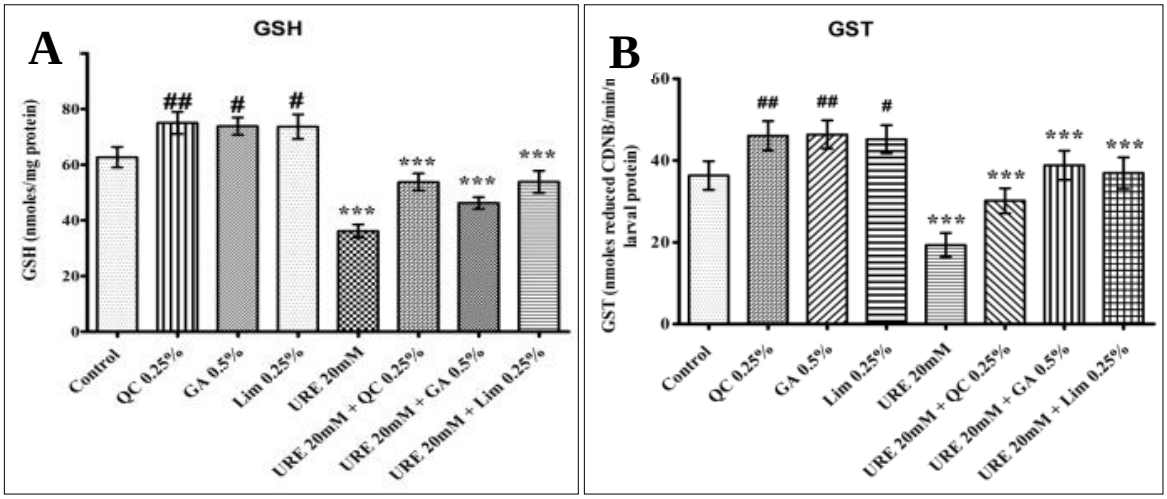

2) Effects on catalase (CAT) activity and superoxide dismutase (SOD):

As compared to negative control group, CAT and SOD activities decreased significantly in URE treated group while the co-exposure of test agents (QC, GA, and Lim) with URE has significantly increased the CAT and SOD activity. The maximum increase in the SOD activity was observed with URE 20mM + QC 0.25% and maximum increase in catalase activity was observed with URE 20mM + GA 0.5%.

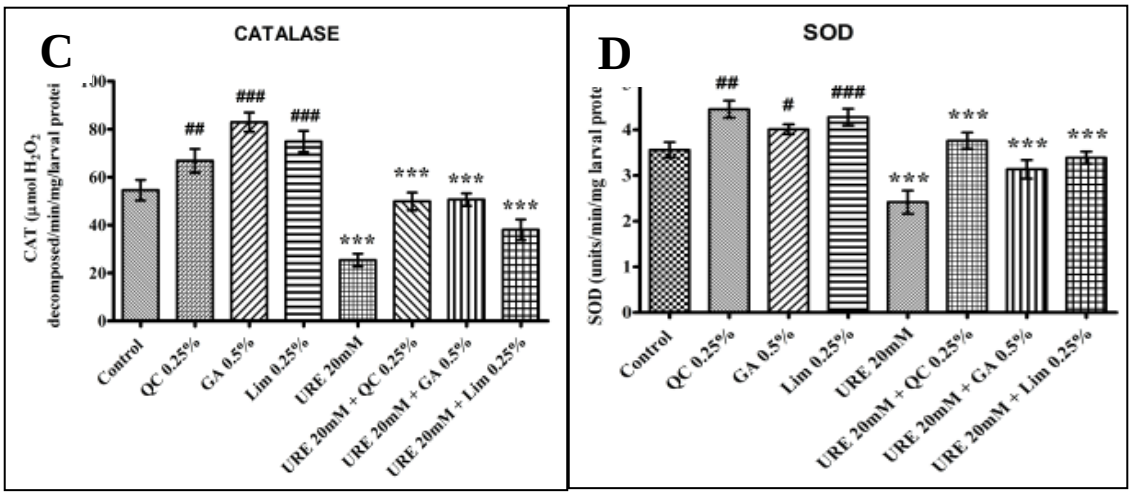

3) Effects on lipid peroxidation (MDA content): As compared to negative control group, MDA content was found to increase significantly in URE treated group. The co-exposed group of test agents (QC, GA, and Lim) with URE has shown significant depletion in the MDA content. The prominent depletion in MDA content was observed in URE 20mM + Lim 0.25% co-exposed group as compared to other two test agents.

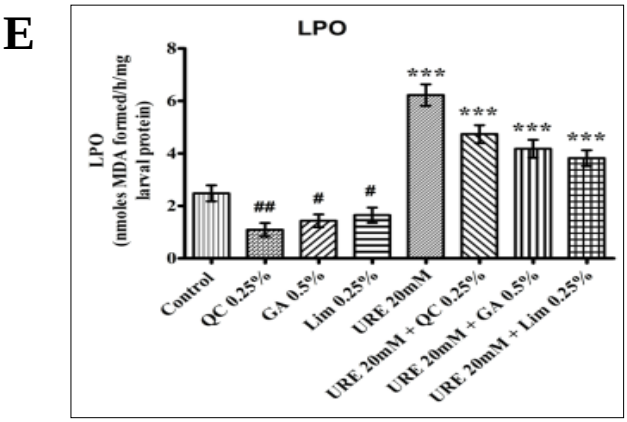

Figure 3.4: Measurement of oxidative stress endpoints: Modulatory effects of QC, GA, and Lim against URE induced oxidative stress on *Drosophila* larvae (A) Glutathione content (GSH), (B) Glutathione S-transferase (GST), (C) Catalase (CAT), (D) Superoxide dismutase (SOD), (E) Lipid peroxidation (in terms of MDA). Data represented as mean ± SD (N=3). ***p ≤ 0.01, **p ≤ 0.05 *p ≤ 0.10 as compared to positive control (URE) and ### p ≤0.01, ##p ≤0.05, #p ≤0.10 as compared to normal control

3.3.2.1.1. Correlation among different stress parameters

A correlation was drawn between the different sets of oxidative stress markers (GSH, GST, CAT, SOD, and LPO) for URE induced adverse effects in the exposed organism. A significant negative correlation of MDA content (lipid peroxidation) and positive correlation of GSH content was observed with different sets antioxidant enzymes (GST, CAT, and SOD) (Table 3.8).

Table 3.8: Correlation analysis: a) Correlation between different sets of oxidative stress markers (GSH, GST, SOD, CAT, and LPO) when the larvae were fed with QC 0.25% and URE 20mM + QC 0.25%. b) Correlation between different sets of oxidative stress markers (GSH, GST, SOD, CAT, and LPO) when the larvae were fed with GA and URE 20mM + GA (0.5%). C) Correlation between the different sets of oxidative stress markers (GSH, GST, SOD, CAT, and LPO) when the larvae were fed with Lim and URE 20mM + Lim (0.25%)

Table 3.8a:

QC	**GSH**	**GST**	**SOD**	**CAT**	**LPO**
GSH	1				
GST	0.998	1			
SOD	0.947	0.940	1		
CAT	0.988	0.978	0.977	1	
LPO	-0.979	-0.983	-0.862	-0.937	1

Table 3.8b:

GA	GSH	GST	SOD	CAT	LPO
GSH	1				
GST	0.846	1			
SOD	0.980	0.933	1		
CAT	0.941	0.949	0.970	1	
LPO	-0.985	-0.906	-0.996	-0.948	1

Table 3.8c:

Lim	GSH	GST	SOD	CAT	LPO
GSH	1				
GST	0.963	1			
SOD	0.990	0.984	1		
CAT	0.970	0.886	0.953	1	
LPO	-0.993	-0.955	-0.973	-0.945	1

3.3.2.2. Modulation of oxidative stress levels by BC and TP against γ-irradiation (10 Gy) in third instar larvae of *D. melanogaster.*

A significant enhancement was observed in the overall antioxidant enzyme activity when the third instar larvae were treated with test agents in combination with γ radiation (10 Gy) (Fig. 5)

1) Effects on reduced glutathione (GSH) levels and glutathione s-transferase (GST) activity: As compared to negative control group, GSH levels, and GST activity was depleted significantly in γ radiation treated group. A significant decrease in GSH content and GST activity was observed in group co-exposed to test agents (TP and BC) with γ radiation as compared to individual γ radiation group. However, the prominent increase in the GSH levels and GST levels was observed in γ radiation + TP 1% and γ radiation + BC 0.5% co-exposed group respectively .

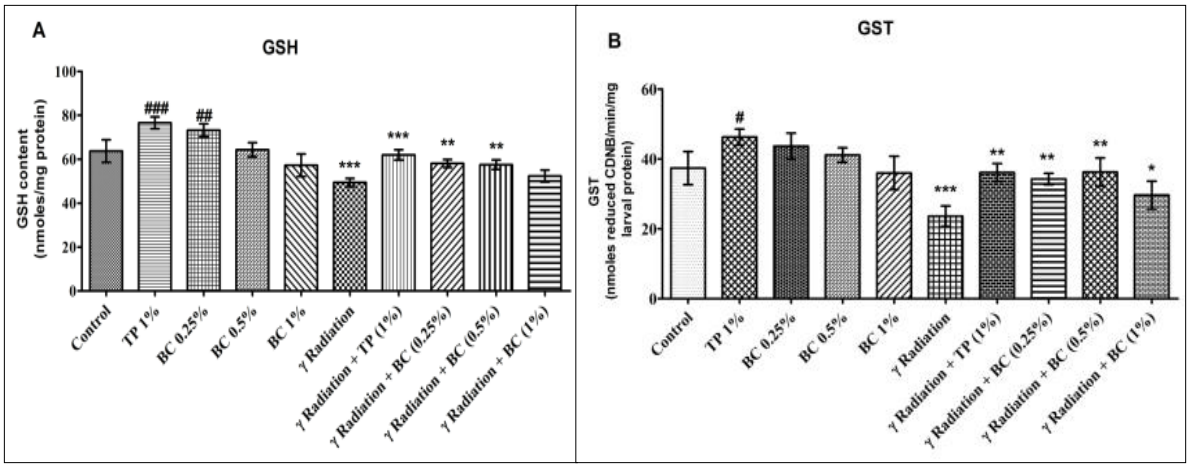

2) Effects on catalase (CAT) and superoxide dismutase (SOD) activities: As compared to negative control group, CAT and SOD activities was found to decrease significantly in γ-irradiation treated group. The co-exposure of test agents (BC and TP)

with γ-irradiation has significantly increased the CAT and SOD activity. Where the maximum increase in the catalase activity was observed with γ radiation + TP 1% and maximum increase in SOD activity was observed with γ radiation + BC 0.25%.

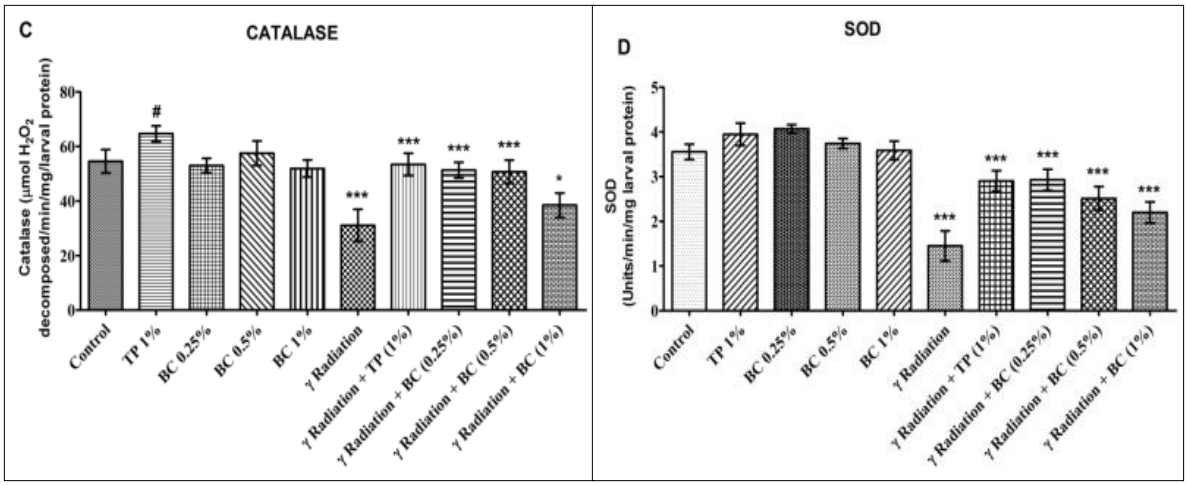

3) Effects on lipid peroxidation (MDA content): As compared to negative control group, MDA content was found to increase significantly in γ-irradiation treated group. The coexposure of test agents (BC and TP) with γ-irradiation has significantly decreased the MDA content. However, the maximum depletion in the MDA content was observed in γ radiation + BC 0.25% group.

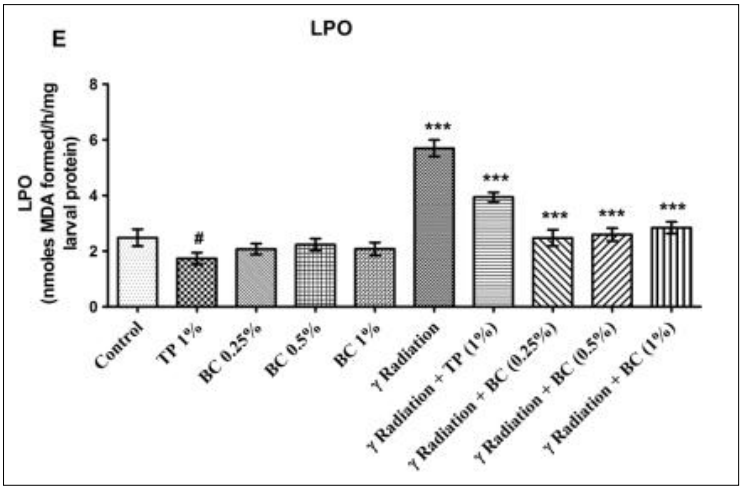

Figure 3.5: Measurement of oxidative stress endpoints. Modulatory effects of TP and BC against γ-irradiation induced oxidative stress on *Drosophila* larvae (A) Glutathione content (GSH), (B) Glutathione *S*-transferase (GST), (C) Catalase (CAT), (D) Superoxide dismutase (SOD), (E) Lipid peroxidation (in terms of MDA). Data represented as mean ± SD (N=3). ****p ≤ 0.01,* ***p ≤ 0.05* **p ≤ 0.10* as compared to positive control (γ-irradiation) and $^{###}$p *≤0.01,* $^{##}$p *≤0.05,* $^{#}$p *≤0.10* as compared to normal control.

3.3.2.2.1 Correlation among different stress parameters

A correlation was drawn between the different sets of oxidative stress markers (GSH, GST, CAT, SOD, and LPO) for γ radiation induced adverse effects in the exposed organism. A significant negative correlation of MDA content (lipid peroxidation) and positive correlation of GSH content was observed with different sets antioxidant enzymes (GST, CAT, and SOD) (Table 3.9).

Table 3.9: Correlation analysis: a) Correlation between the different sets of oxidative stress markers (GSH, GST, SOD, CAT & LPO) when the larvae were fed with TP and γ radiation + TP (1%). b) Correlation between the different sets of oxidative stress markers (GSH, GST, SOD, CAT & LPO) when the larvae were fed with a different dose range of BC and γ radiation + BC

Table 3.9a

TP	**GSH**	**GST**	**SOD**	**CAT**	**LPO**
GSH	1				
GST	0.938	1			
SOD	0.965	0.934	1		
CAT	0.820	0.917	0.896	1	
LPO	-0.742	-0.842	-0.825	-0.864	1

Table 3.9b

BC	**GSH**	**GST**	**SOD**	**CAT**	**LPO**
GSH	1				
GST	0.943	1			
SOD	0.961	0.933	1		
CAT	0.820	0.912	0.901	1	
LPO	-0.747	-0.851	-0.834	-0.864	1

3.3.2.3. Modulation of oxidative stress levels by CF against CPH in third instar larvae of *D. melanogaster.*

A significant enhancement was observed in the overall antioxidant enzyme activity when the third instar larvae were treated with test agents in combination with CPH. (Figure 3.6)

1) Effects on reduced glutathione (GSH) levels and glutathione S-transferase (GST) activity: As compared to negative control group, GSH levels, and GST activity was reduced significantly in CPH treated group. However, the co-exposure of CF with CPH had significantly increased the GSH content and GST activity as compared to CPH group alone.

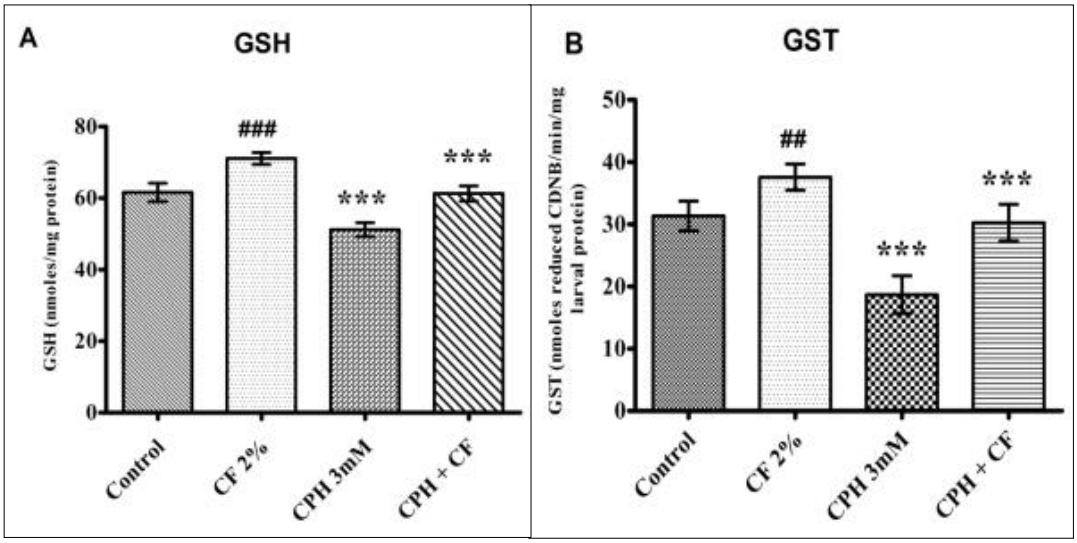

2) Effects on catalase (CAT) and superoxide dismutase (SOD) activities: As compared to negative control group, CAT and SOD activities was found to decrease significantly in CPH treated group. The co-exposure of coffee with CPH has significantly increased the CAT and SOD activity.

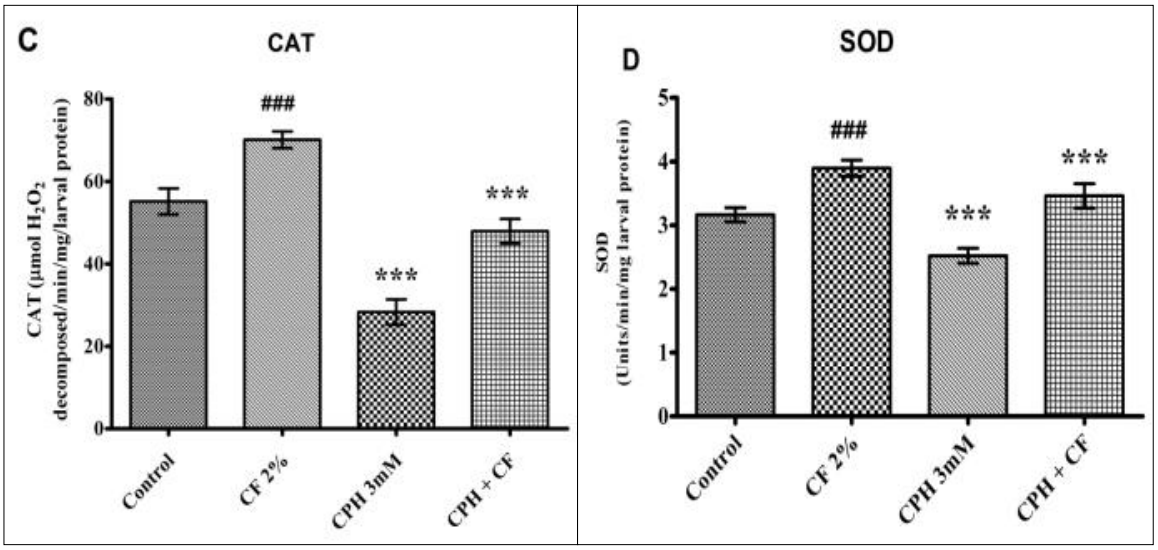

3) Effects on lipid peroxidation (MDA content): As compared to negative control group, MDA content was found to increase significantly in CPH treated group. The co-exposure of CF with CPH has significantly decreased the MDA content.

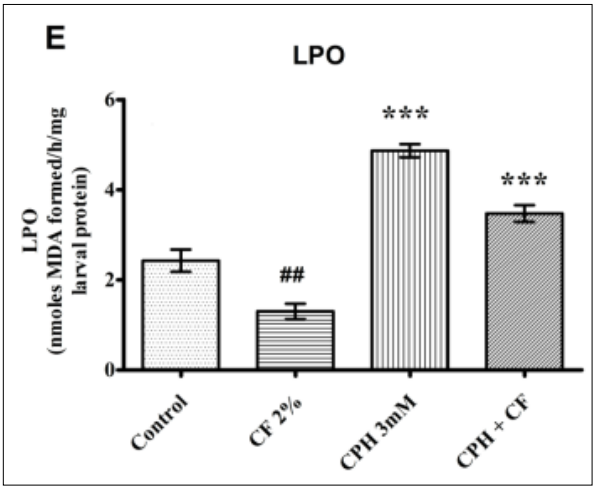

Figure 3.6: Measurement of oxidative stress endpoints Modulatory effects of CF2% against CPH (3mM) induced oxidative stress on *Drosophila* larvae (A) Glutathione content (GSH), (B) Glutathione S-transferase (GST), (C) Catalase (CAT), (D) Superoxide dismutase (SOD),(E) Lipid peroxidation (in terms of MDA). Data represented as mean ± SD (N=3). ****p ≤ 0.01, **p ≤ 0.05 *p ≤ 0.10* as compared to positive control (CPH) and $^{###}$p *≤0.01,* $^{##}$p *≤0.05,* $^{#}$p *≤0.10* as compared to normal control.

3.3.2.3.1. Correlation among different stress parameters

A correlation was drawn between the different sets of oxidative stress markers (GSH, GST, CAT, SOD, and LPO) for CPH induced adverse effects in the exposed organism. A significant negative correlation of MDA content (lipid peroxidation) and positive correlation of GSH content was observed with different sets antioxidant enzymes (GST, CAT, and SOD) Table 3.10.

Table 3.10: Correlation analysis: Correlation between the different sets of oxidative stress markers (GSH, GST, SOD, CAT, & LPO) when the larvae were fed with CF and CPH + CF.

	GSH	**GST**	**SOD**	**CAT**	**LPO**
GSH	1				
GST	0.984	1			
SOD	0.971	0.961	1		
CAT	0.987	0.987	0.927	1	
LPO	-0.964	-0.964	-0.878	-0.993	1

3.3.3. Longevity Assay

3.3.3.1. Effect of QC, GA, and Lim on the longevity of ORK flies

QC,GA and Lim alone as well as in combination with URE showed a significant increase in the mean lifespan *ORK* (wild-type) male flies. Where, URE + Lim 0.25% and URE + QC 0.25% has extended the mean lifespan by 10 days. URE + GA 0.5% has shown 6 days extension. (Figure 3.7)

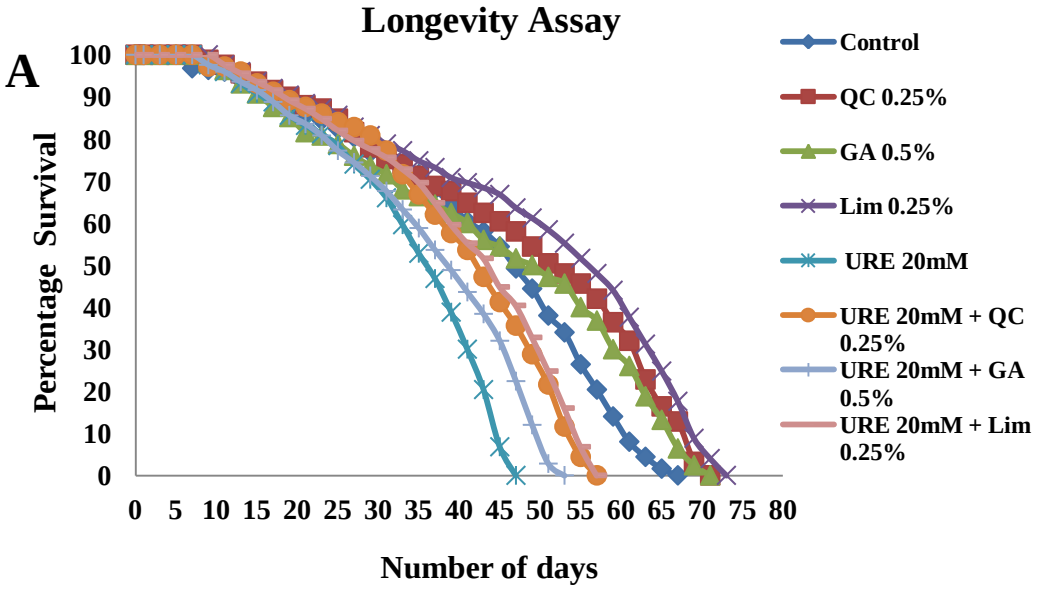

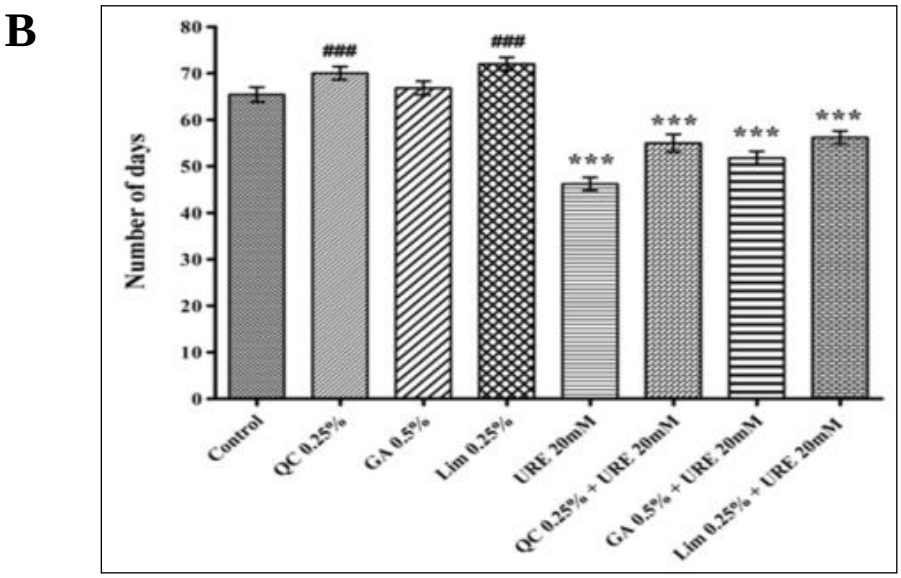

Figure 3.7: Effect of QC, GA and Lim on the life span of wild-type males: (A) Lifespan curve and (B) Mean life span of ORK flies, fed with control diets, diets containing test agents alone (QC 0.25%, GA 0.5% and Lim 0.25%) and diets containing combination of test agents and positive control, URE. Co-treatment of test agents with URE has significantly enhanced the mean lifespan of fruit flies by 10days (QC 0.25 % and Lim 0.25%) and 6 days (GA 0.5%) compared to URE treatment alone. Data were recorded until the last fly died. Newman's Keuls test was used to check significance ***$p \leq 0.001$ vs. positive control (URE); $^{###}p<0.001$ *vs.* normal control.

3.3.3.2. Effect of TP and BC on the longevity of ORK flies

TP and BC alone as well as in combination with γ radiation has shown a significant increase in the mean lifespan ORK (wild-type) male flies. Where, γ radiation + TP 1% extended the mean lifespan by 12 days followed by 10 days extension with γ radiation + BC 0.5%. (Figure 3.8)

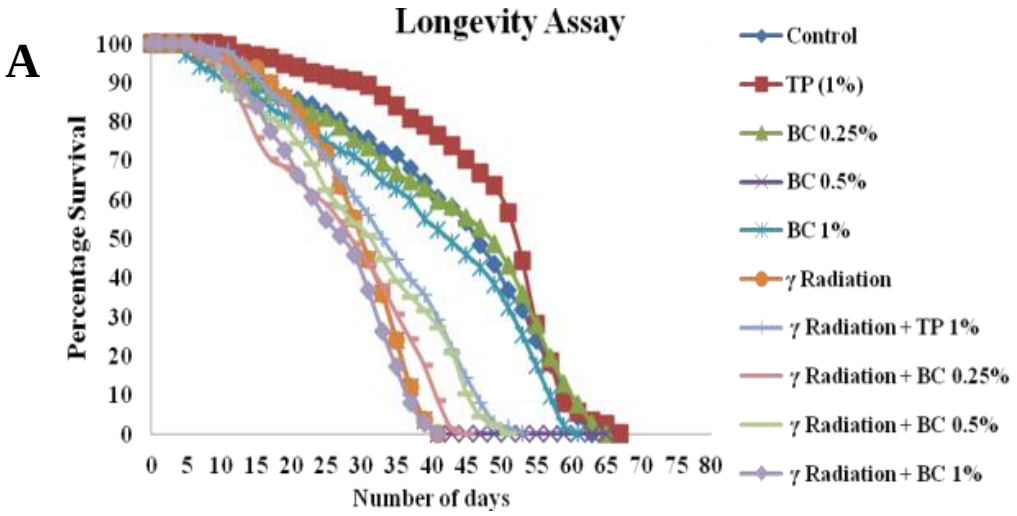

B

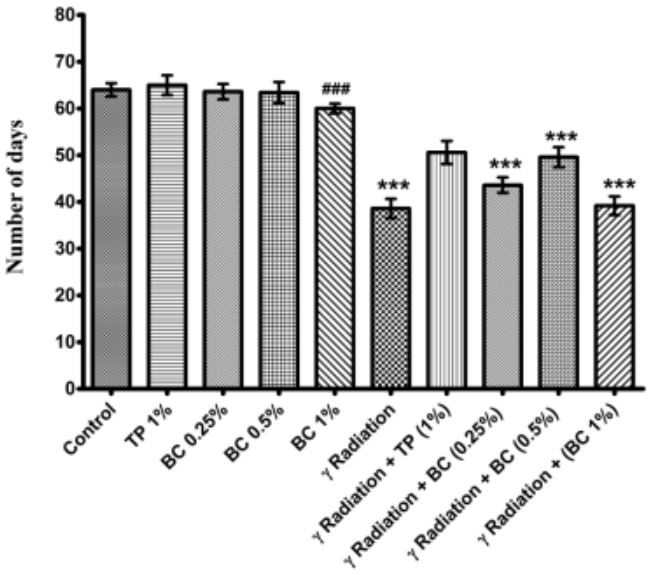

Figure 3.8: Effect of BC and TP on the life span of wild-type males: **(A)** Lifespan curve and **(B)** Mean life span of ORK flies, fed with control diets, diets containing test agents alone (TP 1%, BC 0.25%, BC 0.5% and BC 1%) and diets containing combination of test agents and positive control, γ radiation. Co-treatment of test agents with γ radiation has significantly enhanced the mean lifespan of fruit flies by 12days (γ radiation + TP 1%) and 10 days (γ Radiation + BC 0.5%) compared to γ radiation treatment alone. Data were recorded until the last fly died. Newman's Keuls test was used to check significance ***$p \leq 0.001$ vs. positive control (γ radiation); ###$p<0.001$ *vs.* normal control.

3.3.3.3. Effect of CF on the longevity of ORK flies

.CF alone as well as in combination with CPH has shown a significant increase in the mean lifespan *ORK* (wild-type) male flies. Where, in comparison to CPH 3mM, CPH + CF 2% extended the mean lifespan by 8 days (Figure 3.9)

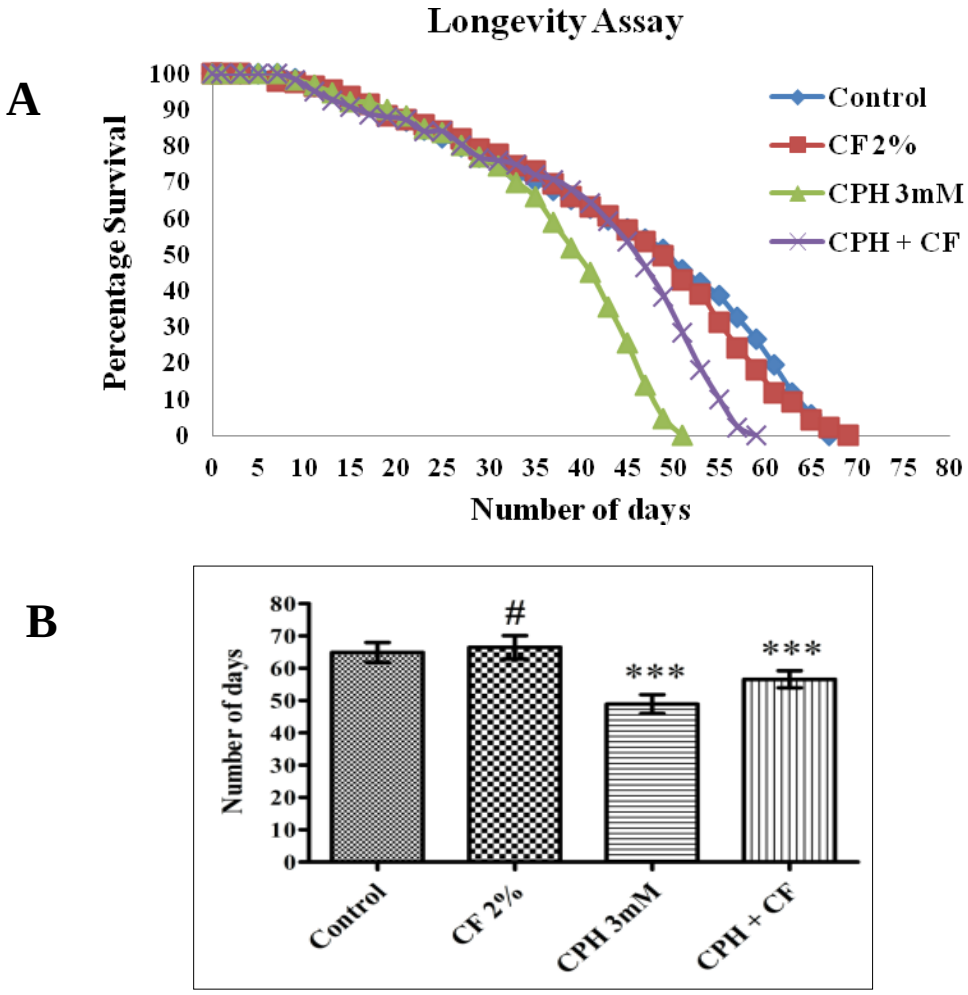

Figure 3.9: Effect of CF on the life span of wild-type males: **(A)** Lifespan curve and **(B)** Mean life span of ORK flies, fed with control diets, diets containing test agent alone (CF 2% and diets containing a combination of test agent and positive control, CPH. Co-treatment of the test agent (CF 2%) with CPH (3mM) has significantly enhanced the mean lifespan of fruit flies by 8 days. Newman's Keuls test was used to check significance ***$p \leq 0.001$ vs. positive control (URE); $^{###}p<0.001$ *vs.* normal control.

3.4. Discussion

Drosophila, an *in vivo* model, is often used to study genotoxic and antigenotoxic properties of various compounds and mixtures (Abraham and Graf, 1996; Stanić et al., 2011). The similarity of metabolic pathways between *Drosophila* and mammals makes the results of this test widely applicable and provides the possibility to utilize active compounds in the prevention and treatment of human health (Apidianakis and Rahme, 2011). The present study was performed to evaluate the antimutagenic effects of different varieties of natural agents (phytochemicals) present in our daily diet. We determined the antimutagenic effect and antioxidant activities of QC, GA, and Lim against URE; TP and BC against γ-irradiation and CF against CPH induced DNA damage.

To evaluate the antimutagenic activity of test compounds against the mutagens, we employed SLRL test. An important feature of SLRL test is that the effect of mutagenicity and antimutagenicity of test agents is assayed at each germ cell stage (Würgler and Graf, 1985) which differ in sensitivity and chemical mutagens can exhibit stage specificity. Therefore, it is essential to analyze the progeny in all the germ cell stages (from treated spermatozoa, late and early spermatids, spermatocytes, and spermatogonia). According to the test procedure, successive germ cell stages were sampled which roughly corresponds to four different broods; the first brood gives the effect in treated mature sperm, the second brood on mid or late-stage spermatids, third brood on early spermatids, spermatocytes, and fourth brood on spermatogonia at the time of treatment.

Free radicals like ROS and RNS are biologically important for cell survival. Moderate levels of ROS/RNS may provide necessary signals to cell proliferation and survival, whereas elevated levels ROS/RNS may be fatal for cells. Under physiologic conditions, there is homeostasis in generation and elimination of ROS/RNS which regulates the normal function of redox-responsive signaling proteins (Manna et al., 2010). This homeostasis enables cells to respond according to several endogenous and exogenous stimuli. Perturbations in redox homeostasis lead to oxidative stress which further induces DNA damage (Cooke et al., 2003), aberrant cellular conditions and may contribute to the development of many disorders (Trachootham et al., 2008). Disturbed redox homeostasis is often observed under conditions like stress, exposure to radiations and mutagens, microbial infections, severe tissue injuries and several types of malignancies. Thus, monitoring redox homeostasis by assessment of activities of regulatory enzymes and proteins associated with oxidative stress can be a major strategy involving both prevention and cure.

Both DNA damage and oxidative stress enhance the process of aging. Also, the metabolic rate and ROS generation are linked together (Khazaeli et al., 2005), thus monitoring the process of aging can be useful in the studies associated with life span. *Drosophila* from a very long time has been used to study longevity and other associated behavioral parameters (Joshi and Mueller, 1997). The advantage of short life span, greater generation number, and sequence homology with human genome at various levels of biochemical pathways makes *Drosophila* an excellent in vivo model to study longevity. *Drosophila* has been used to develop an assay system involving dynamics of expression of particular marker genes and their effects on longevity (Bauer

et al., 2004). Many different studies like effects of calorie restriction (Bordone and Guarente, 2005), metabolic rate (Khazaeli et al., 2005), irradiation (Seong et al., 2011), resveratrol (Bass et al., 2007), citrus juice (Fernández-Bedmar et al., 2011), glucose (Galenza et al., 2015) on longevity in *Drosophila* have been conducted.

Both environmental and chemical factors may induce DNA lesions. However, cells possess mechanisms to counteract such damages, but conditions such as over exposure to mutagens may cause lethal effects. In recent years, human exposure to harmful levels of radiations has increased due to ozone depletion (Sinha et al., 2002), radiation based clinical diagnosis, and radiotherapy for cancer treatment (Goldstein and Kastan, 2015). Also, studies have shown that radiotherapy is responsible for "bystander effect" (Havaki et al., 2015). Similarly, exposure to chemical agents also causes mild to severe DNA damage. Exposure to such harmful chemicals is mainly due to their applications/presence in various products.

Ionizing radiations such as γ radiation have the potential to penetrate cells and interact with DNA. It has been reported that even lower doses of γ radiation can exert mutagenic effects in *Drosophila* adult flies (Caspari and Stern, 1948; Suzuki et al., 1967), as well as in oocytes (Markowitzz, 1970). Chemical mutagens in combination to γ radiation are reported to exert enhanced lethal mutations in *Drosophil*a (Abraham, Singh, et al., 1993). Previous literature demonstrated that γ radiation induces mutation, but recent reports in *Drosophila* suggests that exposure to very low doses of γ radiation results in reduced frequency of lethal mutations (Ogura et al., 2009) and may even be associated with enhanced longevity (Seong et al., 2011).

CPH is a chemotherapeutic drug which is also used in transplantation immunology due to its immunosuppressive properties (Huyan et al., 2011). CPH metabolism (in the liver) produces highly toxic byproducts which form DNA adducts (Kushner et al., 1996) and also interfere with normal functioning of various proteins. Studies showed that CPH causes concentration independent lethal mutations in *Drosophila* germ cells (Vogel, 1975; Sadiq and Al-Quraishe, 2005) and also reported as a potential teratogen while studying various drug metabolizing enzyme pathways (Bournias-Vardiabasis and Flores, 1983).

URE is mainly found in fermented products, and commercially possess varieties of application. URE, a Group 2A carcinogen (Field and Lang, 1988) itself increases the frequency of sister chromatid exchange (Cheng et al., 1981) which leads to genetic damage (Schlatter and Lutz, 1990). Also, the metabolic products of URE cause DNA damage and forms DNA adducts (Williams and Nery, 1971). Studies on mutagenic effects of URE in somatic cells of *Drosophila* have been carried out using wing spot test, and it is reported to have potent recombinogenic activity (Frölich and Würgler, 1990).

Studies on the biological effects of phytochemicals strongly suggest that phytochemicals have a variety of beneficial properties. There are reports which show that chemoprevention by these compounds was due to their interference at various stages of cancer development like chelation of free radicals, stimulation of immune system (Craig, 1997), neutralization of xenobiotic and carcinogens (Sotibrán et al., 2011).

QC is reported to provide protection against DNA damage induced by hydrogen peroxide (Duthie et al., 1997), and radiations like UV-A (Erden Inal et al., 2001) and γ radiation (Devipriya et al., 2008). It is also reported to exert multiple biological effects including antioxidant, anti-carcinogenic (Csokay et al., 1997), neuroprotectant (Ho and Chang, 2004), anti-inflammatory, and antiviral effects (Davis et al., 2009). In *Drosophila*, quercetin is reported to reduce genotoxicity by various detrimental environmental agents (Singh et al., 2011) and carcinogens, ethyl methanesulfonate (EMS) (Mladenović et al., 2013).

GA, a known antioxidant (Rice-Evans, 1995; Salah et al., 1995) with additive antimutagenic (Hour et al., 1999) anticarcinogenic (Ferguson, 2001) antifungal, and antiviral properties. GA is also known to exhibit effects on phase I and phase II drug metabolizing enzymes (Ow and Stupans, 2003). GA is reported to reduce lipid peroxidation and DNA damage (Gandhi and Nair, 2005) and it restores locomotor and enhanced longevities in iron and paraquat exposed flies (Jimenez-Del-Rio et al., 2010). Also, studies on Parkinson's disease model of *Drosophila* suggest that GA reduces oxidative stress, restores locomotor activities and enhances the longevity in fly models with neurodegenerative diseases (Ortega-Arellano et al., 2011).

Lim is a potent anticancerous agent and is reported to be beneficial against various kinds of tumors and cancers including mammary tumors (Maltzman et al., 1989; Chander et al., 1994), gastric cancer (Uedo et al., 1999), and colon cancer (Jia et al., 2013). Lim is also reported to exert antiparasitic effects against Leishmania parasites, in both *in vitro* and *in vivo* studies (Arruda et al., 2009). Lim enhances the viability of lymphoma-bearing mice by restoration of host immunosuppressive machinery (Del

Toro-Arreola et al., 2005) and modulates viability and activity of T-lymphocytes (Lappas and Lappas, 2012). Using SMART test in *Drosophila*, it was demonstrated that Lim exerts antigenotoxic and antimutagenic effects in somatic cells (Idaomar et al., 2001), and also induces longevity in *Drosophila* (Fernández-Bedmar et al., 2011).

BC belongs to the members of carotenoids family with potential to scavenge singlet oxygen species/free radicals (El-Habit et al., 2000). It is a natural precursor of vitamin A, and most efficiently converted into vitamin A as compared to other provitamins (Gul et al., 2015). Studies on the anticarcinogenic property of BC are widely reported. However, the results of such studies are discrepant (Mayne, 1996). Many studies on the consumption of high doses of dietary BC in reducing cancer progression in both early and late phases of its development are reported (Gul et al., 2015). BC is a potent antioxidant, and studies demonstrate that BC significantly reduces radiation-induced DNA damage including γ radiation (El-Habit et al., 2000) and UV radiations (Sinha et al., 2002). In 1993, our group also demonstrated protective efficacy of BC against γ radiation induced chromosomal damage in mouse bone marrow cells (Abraham, Sarma, et al., 1993). In *Drosophila,* BC is reported to modulate the mutagenic effects of harmful chemicals and mutagens such as CPH (Salvadori et al., 1992) and doxorubicin (Dias et al., 2009).

Tea is one of the most common beverages consumed as green tea or black tea. Both forms of tea contain active ingredients commonly called as tea polyphenols which are strong antioxidants (Rice-Evans, 1995); however green tea is reported to be more potent (Chacko et al., 2010). Besides being antioxidant, tea polyphenols have myriads of beneficial effects on various pathophysiological conditions including arthritis (Haqqi et

al., 1999), cancer (Kavanagh et al., 2001), bacterial infections, inflammation (Donà et al., 2003), cardiovascular disease (Sueoka et al., 2001) and neurodegeneration (Weinreb et al., 2004). Tea polyphenols are also reported to delay the onset of neurodegenerative Huntington's disorder in *Drosophila* model (Ehrnhoefer et al., 2006) and restore locomotor ability and enhance longevity in flies exposed to toxicants like iron and paraquat (Jimenez-Del-Rio et al., 2010).

Coffee is another commonly consumed beverage and contains active components which are effective antioxidants (Delgado-Andrade et al., 2005; Cämmerer and Kroh, 2006). It is also a strong antigenotoxic agent. Data based on *in vivo* studies showed that coffee inhibits genotoxic effects of chemicals like cyclophosphamide, procarbazine, mitomycin C and adriamycin (Abraham, 1989). Similarly, studies on *Drosophila* using SMART test also demonstrated the antigenotoxic potentials of coffee against genotoxic agents like CPH, diethylnitrosamine (DEN), mitomycin C, procarbazine and URE (Abraham, 1994). Coffee also exhibits antigenotoxic effects against such genotoxic agents, that can traverse through the placenta and induce developmental genotoxicity in mice (Abraham, 1995) with an induction in intracellular levels of thiol (-SH), glutathione *s*-transferase activity (Abraham and Singh, 1999) and inhibition of lipid peroxidation under *in vivo* experimental conditions (Devasagayam et al., 1996). Besides being antigenotoxic, different studies on the consumption of coffee report its multiple effects including minimization of heart stroke, lowering the risk of type II diabetes and different types of malignancies (Bhatti et al., 2013).

We have studied antimutagenic and antigenotoxic effects of different phytochemicals against physical mutagen (γ radiations) and chemical mutagens (URE and CPH). In this

study, we have used *Drosophila* as our test model to evaluate these effects using SLRL assay, biochemical and longevity assays.

3.4.1. SLRL assay for the study of antimutagenic effects of Lim, QC, and GA against URE

SLRL data demonstrates that Lim (0.25%) when given together with URE, has significantly reduced URE induced SLRL frequencies in larval treatment by 48.1% and in adult flies by 60.7% respectively, where the maximum reduction in SLRLs was found in the premeiotic stage, brood IV (75.3%). Similarly, QC (0.25%) + URE has reduced SLRL mutation by 57.6% in larvae and 65.2% in adult. We observed no trace of SLRL mutation in premeiotic stages (i.e. brood IV) followed by 73.6% reduction in brood III. GA (0.5%) + URE reduced SLRL mutation by 54.1% in larvae and with GA (1%) + URE, by 62.0% in adult flies. Maximum reduction was again found in the premeiotic stage, brood IV by 79.1% followed by brood II (67.0%) (mid-late spermatid). All these phytochemicals were found to reduce the SLRL frequencies from the postmeiotic stages (brood IV) to premeiotic ones (brood I).

3.4.2. SLRL assay for the study of antigenotoxic effects of BC and TP against γ radiations (10Gy)

SLRL data obtained from the study clearly suggests that supplementation of BC and TP has reduced the SLRL frequencies in both larval as well as in the adult flies where the maximum reduction of mutation frequencies (43.4%) in larvae was observed with supplementation of γ radiation + TP (1%), followed by γ radiation + BC 0.25% (40.7%) as compared to γ radiation. In the case of adult germ cells, a significant reduction was observed in all the successive germ cell stages (i.e. Brood IV to I) when flies were

treated with γ radiation + BC 0.5% (70.3%) followed by γ radiation + TP 1% (70.1%). We also studied the effects of different concentrations of BC along with γ radiation (10Gy) in both adult and larvae of flies and compared the observed SLRL frequencies with γ radiation alone. In adult feeding experiments, we observed that treatment with γ radiation + BC 0.5% has significantly reduced (70.3%) the SLRL mutations followed by γ radiation + BC 0.25% (69.8%) However, at higher concentration of BC 1%, we did not observe any significant antimutagenic effect (29.1%). Similarly, in larval feeding experiments, significant reduction in the incidence of lethal mutations was observed (40.7%) with the lower dose of BC, (γ radiation + BC 0.25%) followed by γ radiation + BC 0.50% (39.4%) and γ radiation + BC 1% (32.5%) respectively. The optimal concentration of BC which reduces SLRL frequencies is different in both adult and larval stages which may be due to differences in metabolic rates in both stages. However, further experimental validations will be needed to support the hypothesis.

3.4.3. SLRL assay to test antigenotoxic effects of Coffee against CPH

In *Drosophila*, antimutagenic effects of coffee against CPH in somatic cells of *Drosophila* larvae was already reported in our lab (Abraham, 1994). However, in the present study, we investigated the antimutagenic effects of coffee in germ cells by using SLRL test and a similar trend has been observed, and we found that the supplementation of CPH + CF has significantly reduced the SLRL frequencies by 75% in larvae and 62.4% in adult flies. SLRL mutation was reduced from the postmeiotic stages (brood IV) to premeiotic ones (brood I) as 51.60% (brood I), 61.04% (brood II), 82.06% (brood III), and 73.94% (brood IV) against CPH.

3.4.4. Modulation of oxidative stress levels by assessment of oxidative stress markers

In our studies, we have further determined antioxidative potentials of the selected phytochemicals against γ radiations, URE and CPH in third instar larvae. Since oxidative stress is associated with DNA damage and mutations, our aim was to analyze the effects of selected phytochemicals on the levels/activities of GSH, GST, catalase, SOD and LPO which are considered as markers of oxidative stress and antioxidative properties as well. Further, we also determined the correlations between these markers in flies exposed to γ radiations, URE and CPH.

3.4.5. Modulatory effects of QC, GA and Lim supplementation against URE induced oxidative stress

To analyze the effects of QC, GA and Lim supplementation on the generation of ROS, we performed biochemical analysis of LPO and GSH and also evaluated antioxidant enzymatic activities of CAT, GST, and SOD in *Drosophila* larvae. Like SLRL test results, all these phytochemicals significantly altered the levels of oxidative stress parameters in a way that it clearly indicates that supplementation of these phytochemicals decreases ROS generation. In our study, maximum induction in the GST activity was observed with the supplementation of URE + GA 0.5% followed by URE + Lim 0.25% and URE + QC 0.25% respectively. Maximum levels of GSH were observed in URE + Lim 0.25% followed by URE + QC 0.25% and URE + GA 0.5%. On analyzing SOD, we observed maximum SOD activity with the supplementation of URE + QC 0.25% followed by URE + Lim 0.25% and URE + GA 0.5%. While the trend of maximum catalase activity was observed with supplementation of URE + GA

0.5%, URE + QC 0.25% and URE + Lim 0.25%. Lipid peroxidation is expressed in terms of formation of malondialdehyde content. The lower the MDA content, the stronger is the antioxidant capacity. The reduction in MDA content was observed highest with URE + Lim 0.25% , URE + GA 0.5% and then with URE + QC 0.25%. Thus on analyzing the overall effects on antioxidative potentials, all the three phytochemicals in combination with URE remarkably lowered down the URE induced toxicity.

3.4.6. Modulatory effects of BC and TP supplementation against γ radiation (10Gy) induced oxidative stress

In the present study, γ radiation has significantly decreased (as compared to normal control) the antioxidant enzymatic activities of GST, CAT, and SOD along with a reduction in biochemical levels of GSH and induction in the level of LPO. After evaluating antioxidative effects of TP1% and different concentrations of BC in combination with γ radiation, we observed that maximum GSH levels and catalase activity was induced by γ radiation + TP 1%. The maximum activities of GST and SOD were observed in γ radiation + BC 0.5% and γ radiation + BC 0.25% respectively. While the maximum reduction in MDA content was observed with γ radiation + BC 0.25%. Within different concentrations of BC, we observed that γ radiation + BC 0.25% was the most optimal dose as it maximally increases GSH levels, SOD and catalase activities, and reduce MDA content in comparison to doses of γ radiation + BC 0.5% and γ radiation + BC 1% respectively.

3.4.7. Modulatory effects of coffee supplementation against CPH induced oxidative stress

As compared to CPH (3mM) combination of CPH + CF has significantly increased GSH levels, GST, SOD, and catalase while it significantly decreases MDA content. Although, the maximum elevation was observed in catalase activities followed by GST and SOD activities.

3.4.8. Longevity assay

Using longevity assay, we have determined the effects of phytochemicals and mutagens on the lifespan of ORK flies. Our findings clearly indicate that amongst three mutagens, exposure to γ radiation is most lethal by restricting the mean life span of flies to 41 days. Phytochemicals supplementation increased the mean lifespan of the flies by 53 days (12 day's extension) in γ radiation + TP 1% group and by 45 days (4 day's extension) with γ radiation + BC 0.25%. In another experiment mean life span of flies reduced to 47 days by URE, while the co-exposure of URE + QC 0.25%, and URE + Lim 0.25% has extended the mean lifespan by 57 days (10 day's extension). Lastly, CPH was found to show less effect on the mean life span of flies (51 days) which was also extended (59 days- 8 day's extension) with the supplementation of CF 2%. These findings suggest that ionizing radiations directly interact with DNA are more mutagenic and thus lethal as compared to promutagens like URE and CPH which indirectly induce mutations.

3.5. Conclusion

In conclusion, this study explored a variety of dietary phytochemicals (QC, GA, Lim, TP, BC, and CF) against different mutagens (γ radiation, URE, and CPH) and studied

their antigenotoxic and antimutagenic effects. Our findings clearly demonstrate that all these phytochemicals have potent activities against both genotoxicity and oxidative stress. These findings support the use of such phytochemicals in our daily diet to counteract various pathophysiological conditions that may arise due to DNA damage and oxidative stress. Our study also demonstrates the suitability of *Drosophila* as an alternative model for evaluating the antigenotoxic activity of a diverse range of dietary phytochemicals as the organism can be used at the same time to assess DNA associated damage (in pre-meiotic and post-meiotic germ cell stages), biochemical effects and associated outcomes on the lifespan of the organism. Experiments performed using this *in vivo Drosophila* model can generate valuable information on antimutagenicity and antioxidant effects of dietary phytochemicals against directly and indirectly acting environmental carcinogens/mutagens

Chapter 4 : Validation of *in silico* methods using mouse model

4.1. Introduction

Phytochemicals are natural compounds with potentials to scavenge free radicals and to reduce oxidative stress. In the earlier chapter of our study, we have computationally screened phytochemicals against proteins associated with DNA damage and oxidative stress (p53, Mdm2, Bcl-2, and PARP) with the aim to identify potential phytochemicals that can interact with the selected target proteins. In the present study, we aim to validate our *in silico* studies using mouse models experimentally. Thus, by using these two different methodologies we aim to find out those phytochemicals which are potent antioxidants and which can also inhibit the function of certain crucial proteins associated with DNA damage and associated pathophysiology.

4.1.2. Apoptosis and DNA damage

Apoptosis is a normal cellular mechanism of homeostasis to keep a check on cellular population within tissues and is vital for cellular turnover, development, immune system functioning, embryonic development, chemically induced cell death and hormone-dependent atrophic changes (Elmore, 2007). Kerr and Currie (1972) proposed the term "apoptosis" to illustrate inherently controlled and morphologically different forms of cell death which characterized by specific energy-driven biochemical processes and structural features (Kerr and Currie, 1972). Structural changes associated with induction of apoptosis takes place at two distinct stages. The first involves

pyknosis (chromatin condensation) (Van Cruchten and Van den Broeck, 2002) and cell shrinkage followed by the second phase of apoptosis which involves karyorrhexis (nuclear fragmentation) (Majno and Joris, 1995) and blebbing of the plasma membrane. Post second phase of apoptosis, the cell is disintegrated into apoptotic bodies in which cell organelles with or without nuclear fragments are tightly bound with cytoplasm in an intact plasma membrane. These apoptotic bodies are then digested by macrophages or other phagocytic cells (Saraste and Pulkki, 2000). Deregulation of apoptosis leads to many pathophysiological conditions including autoimmune disorders, neurodegenerative diseases many types of cancers.

4.1.3. Molecular mechanism of apoptosis

Apoptosis machinery includes complex and energy dependent cascades of the proteins belonging to protease family. There are two major pathways of apoptosis namely intrinsic and extrinsic pathways. The extrinsic pathway is triggered by the crosstalk between cell surface receptors called as death receptors with their corresponding ligand. The death receptors belong to tumor necrosis factor receptor (TNFR) superfamily while the ligands fall into a family of related cytokines called as TNF family (Sheikh and Fornace, 2000). The intrinsic apoptotic pathway also called as mitochondrial apoptotic pathway (Marchenko and Moll, 2014) which is triggered by an intracellular signal, in response to different stress conditions that involves mainly DNA damage, hypoxia, chemotherapeutic agents and high levels of Ca^{+} ions.

4.1.4. DNA damage and intrinsic pathway

Several intrinsic and extrinsic factors induce DNA damage. DNA damage response mechanisms are triggered by cells to maintain DNA integrity for replication. These

responses either lead to the repair of DNA or cell cycle arrest (Zhang et al., 2016). Many potential conditions like oxidative stress, exposure to genotoxic agents or mutagens and irradiation can cause severe DNA damage (Collins, 1999). In response to such stimuli, changes in the inner mitochondrial membrane occur, and mitochondrial permeability transition pores (MPT) are opened. Through these, MPTs pro-apoptotic proteins are released from the intermembrane space of mitochondria into the cytoplasm. Once released these mitochondrial proteins triggers cascades of interactions of different caspases which lead to an event called apoptosis (Elmore, 2007).

4.1.5. Oxidative stress, DNA damage and induction of apoptosis

Cells encounter endogenous oxidative stress during aerobic respiration, by the activities of peroxisomes and enzymes like cytochrome P450. Environmental sources of oxidative stress include exposure to radiation and genotoxic agents, mutagens and pro-mutagens and various other chemicals with xenobiotic potentials (Sosa et al., 2013). The reactive species induce oxidative stress and based on the associated atoms, they are characterized into four categories as reactive oxygen species (ROS), reactive nitrogen species (RNS), reactive sulfur species (RSS) and reactive chloride species (RCS). Out of these, ROS and RNS are the predominant source of free radicals which induces oxidative stress and includes superoxide anion ($O2^{\bullet-}$), singlet oxygen (O_2), hydroxyl radical ($^{\bullet}OH$), hydrogen peroxide (H_2O_2), ozonide (O^{3-}), and nitric oxide ($^{\bullet}NO$) (Halliwell, 1991). Excess of oxidative stress predominantly induces lipid peroxidation, disturbs calcium homeostasis and various metabolic pathways (Slater, 1987) leading to the development of various diseases including Alzheimer's and Parkinson's, diabetes mellitus, autoimmunity, and different types of cancers (Kannan and Jain, 2000).

4.1.6. Free radicals and DNA damage

One of the common cause of DNA damage is by its interaction with free radicals. There are various modes by which free radicals react and induce DNA damage. Free hydroxyl radicals react with DNA bases, deoxyribose sugars, and oxidize purinyl radicals and form adducts with DNA (Simic et al., 1989). Increased oxygen stress induces chromosomal aberrations (Maser et al., 1997). Excessive ROS generation attenuates repair of damaged nuclear and mitochondrial DNA (Weyemi and Dupuy, 2012) and causes modification of cellular and mitochondrial histone proteins (Shaughnessy et al., 2015). Studies have shown that ROS also directly or indirectly induces methylation and demethylation of DNA (Siomek et al., 2014).

4.1.7. Free radicals and apoptosis

ROS can trigger both extrinsic and intrinsic pathways of apoptosis by activating Jun kinase (JNK) receptor by modulating the interaction of signal-regulating kinase 1 (ASK1) and proteasomal degradation of FLIPL (Circu and Aw, 2010). ROS activates the intrinsic apoptotic pathway by inducing mitochondrial DNA damage and leading to release of intermembrane proteins into the cytosol and triggering caspases (Trachootham et al., 2007). Also, ROS can induce apoptosis by oxidizing GSH and by attenuating cellular redox balance (Merad-Boudia et al., 1998).

4.1.8. Regulatory proteins associated with apoptosis and DNA damage and their role in oxidative stress

Poly (ADP-ribose) polymerase (PARP), p53 and Bcl-2 family of proteins are key regulatory proteins associated with apoptosis and DNA damage.

4.1.8.1. Poly (ADP-ribose) polymerase (PARP) protein

PARP is a member of the superfamily of 17 different poly(ADP-ribose) polymerases which are associated with a cellular process like DNA repair, transcription, and apoptosis (Scovassi, 2014). Amongst all the members of the family, PARP-1 is the most abundant isoform. This 113 kDa protein has three structural domains: The N-terminal domain, the auto modification and C-terminal domain (D'Amours et al., 1999). Functionally PARP is associated with ADP-ribosyl transfer reactions, where it catalyzes Poly(ADP-ribosyl)ation. The transfer of ADP-ribosyl is carried out on glutamate, aspartate, or lysine residues of target proteins which are called as 'acceptors' (Bürkle, 2005). Upon DNA damage (both single stranded and double stranded breaks), PARP-1 via its two zinc finger (Eustermann et al., 2011) in the DNA binding domain binds to DNA and forms homodimers. Once PARP-1 binds to DNA it cleaves nicotinamide and ADP-ribose from NAD^+ and catalyzes Poly(ADP-ribosylation onto the acceptor proteins including histones, DNA repair proteins, transcription factors, and chromatin modulators PARP-1 itself (Pacher and Szabó, 2007). Activation of PARP is reported in several studies where, DNA damage is induced by oxidative stress (Huang and Shen, 2009) by ROS and NOS, ionizing radiations and alkylating agents. PARP-1 also plays a pivotal role in dissecting cell fate from DNA repair or cell death, by either encouraging cellular flux to apoptosis or necrosis (Eustermann et al., 2011).

4.1.8.2. The p53 protein

During early 1980's research was going on simian virus 40 (SV-40) a small antigen called "Tau antigen" with molecular weight was identified (Chang et al., 1979). Later the protein was termed as p53 as its molecular weight was around 53 kDa by *Deleo et*

al. (DeLeo et al., 1979). The p53 protein contains 393 amino acids residues and structurally it is comprised of the N-terminal region which contains transcriptional and transactivation domain, a central region containing DNA-binding domain, and a C-terminal region which contains oligomerization/tetramerization domain (Soussi and May 1996). Functionally, p53 is a transcription factor. However, it has versatile functions in cellular biology including cell cycle regulation, autophagy, DNA repair, apoptosis, and regulation of ROS, etc. p53 regulates both development and attenuation of cellular stress by regulating the production of ROS. It is reported to upregulate expression of NADPH oxidase also called as respiratory burst oxidase, neutrophil cytosol factor 1, neutrophil cytosol factor 2, xanthine oxidase, 5-Lipoxegenase and PIG's which increases cellular ROS (Budanov, 2014). Also on the other hand p53 is also reported to induce expression of an enzyme like aldehyde dehydrogenase 4 (Liu et al., 2008), glutaminase-2 (Budanov, 2014), glutathione peroxidase, manganese superoxide dismutase (MnSOD) (Jänicke et al., 2008) that quench cellular ROS. Also, p53 can induce apoptosis mostly by mitochondrial pathway. However, it can also induce apoptosis by death receptors. The mitochondrial mode of p53 dependent apoptosis is mediated through its transcriptional activity where p53 regulates expression of pro-apoptotic genes like BH-3, PUMA, NOXA and Bax (Amaral et al., 2010).

4.1.8.3. The Bcl-2 protein

Tsujimotoet et al. first described Bcl-2 and its function as an oncogene. (Tsujimoto et al., 1985). Since then much has been reported about Bcl-2 family which based on its function, is mainly characterized as anti-apoptotic and pro-apoptotic (Hockenbery et al., 1990). The anti-apoptotic members of the Bcl-2 family include Bcl-2, $Bcl_{-XL,}$ Bcl-w,

Mcl-1, A1/Bfl-1 (Kirkin et al., 2004). Amongst all these, Bcl-2 is widely studied due to its central function in modulating apoptosis regulation. The anti-apoptotic function of Bcl-2 proteins is due to their potential to attenuate dimerization of Bax or Bak which is a crucial step in caspase activation. Also, anti-apoptotic Bcl-2 protein controls mitochondrial swelling and prevents rupture of mitochondrial membrane and thereby blocking the release of cytochrome c as well as other mitochondrial proteins that trigger activation of caspase cascade (Siddiqui et al., 2015).

4.1.8.4. Interaction of PARP with p53

Interaction of p53 and PARP were first reported by Vaziri et al. (1997). PARP-1 was reported to ribosylate p53 and regulate its activity in neurons with damaged DNA and studies show that inactivation of PARP at genetic levels or by pharmacological agents alter p53 activity (Ying et al., 2016). Alternatively, regulation of PARP by p53 has been reported by Montero et al. In their study, they have demonstrated that mutated p53 failed to activate PARP and suggested that mutation of p53 resulted in the loss of function of p53. However, the wild type of p53 successfully activated PARP (Montero et al., 2013); (Wiman, 2013).

4.1.8.5. Interaction of p53 with Mdm2 and Bcl-2 proteins

Mdm2 is a p53 regulatory protein which maintains cellular p53 in an autoregulatory feedback fashion (Wu et al., 1993). Mdm2 regulates the nuclear activity of p53 protein. In the nucleus, p53 acts as a transcription factor and to maintain its transcriptional function; Mdm2 binds to p53 by forming a protein-protein complex. This complex is translocated into the cytoplasm where p53 and Mdm2 are degraded (Eischen and Lozano, 2009). p53 as a transcriptional function directly downregulate the expression

of the anti-apoptotic Bcl-2 gene (Toshiyuki and Reed, 1995). It also directly interacts with Bcl-2 protein and regulates Bcl-2 activity (Mihara et al., 2003).

In our present study, we have explored the antimutagenic and antigenotoxic effects of screened dietary phytochemical (TAX and limonene) against chemical mutagen (URE), As discussed earlier; phytochemicals exert antimutagenic effects by quenching free radicals. Thus, the rationale of the present work is to validate our computational findings (Chapter-1) and also to establish that the selected phytochemicals exert protective effects.

4.2. Materials and Methods

4.2.1. Chemicals

TAX, D-limonene, urethane, bovine serum albumin (BSA), reduced glutathione (GSH), 5,5′-dithiobis (2-nitrobenzoic acid) (DTNB), thiobarbituric acid (TBA), oxidized glutathione (GSSG), reduced nicotinamide adenine dinucleotide (NADH), reduced nicotinamide adenine dinucleotide (NADH), acridine orange (AO), ethidium bromide (EtBr), propidium iodide (PI), annexinV-FITC were purchased from Sigma-Aldrich (India), Primary mouse antibody (p53, Mdm2, Bcl2, cleaved PARP) and secondary anti-mouse antibody (IgG-HRP) were procured from Santa Cruz Biotechnology, India. Fetal bovine serum (FBS) was purchased from HiMedia Laboratories, Mumbai, India. All other analytical laboratory chemicals and reagents were purchased from Merck (Germany) and SRL (India).

4.2.2. Animals

Randomly bred male Swiss Albino mice (6-7 week old) of 25-30 g body weight were used in the present study. The animals were housed in standard cages in an air-conditioned room in university animal house with the temperature maintained at 22 ± 2.5 °C and 12 h light/dark cycle; RH, 65%). Mice were allowed a standard chow diet throughout the experiment and drinking water *ad libitum*. All the experimental studies were approved and carried out under the guidelines of the Committee for the Purpose of Control and Supervision of Experiments on Animals (CPCSEA), constituted by the Animal Welfare Division, Government of India and Institutional Animal Ethics Committee (IAEC) on the use of animals.

4.2.3. Experimental Design

Fourty two Swiss albino mice were randomized into seven groups of five mice each and were treated as below on alternate days for up to 12 weeks:

Group I - Control - Saline 0.9% (intraperitoneal)

Group II - Solvent control (for limonene only) (Olive oil, per os)

Group III - Urethane (700 mg/kg b.wt, intraperitoneal, with time interval of 30 min)

Group IV - TAX (5mg/kg b.wt, per os)

Group V - TAX (oral) + Urethane (intraperitoneal, with time interval of 30 min)

Group VI - Lim (10%, per os)

Group VII - Lim (10%, per os) + Urethane (intraperitoneal)

4.2.4. Dissection

The animals were dosed on alternate days through oral route for TAX and limonene while it was an intraperitoneal injection for Urethane. After 12 weeks, experimental

animals, i.e., control and treated animals were euthanized and sacrificed (within 24h of the last dose) by cervical dislocation. Cells from bone marrow were obtained by flushing both the femurs containing 1ml FBS and thus sorted in a single cell suspension. All the organs viz liver (after perfusion with 10% saline), lungs, kidney, testis, and intestine were quickly excised and washed in chilled homogenizing solution [0.15M Tris-KCl buffer (pH7.4)], Liver and lungs were blotted dry, enclosed in aluminum foil and stored at -80^{o}C for various biochemical assays. For the histopathological examination, one part of the above mentioned organs was stored immediately in 10% buffered formalin.

4.2.5. Preparation of tissue homogenates

After liver perfusion, 10% liver homogenate (w/v) was prepared in homogenizing solution using Potter-Elvehjem homogenizer. This crude homogenate (0.5 ml) was used for estimating acid soluble sulfhydryl content (S-H) while the remaining homogenate was further centrifuged at 10,000 x g for 20 min using RC5C Sorvall Centrifuge. The supernatant obtained was re-centrifuged at 105,000 x g for 60 min (Beckman Type 50 Ti rotor) and the resulting supernatant was used for assaying cytosolic enzymes such as DT-diaphorase, superoxide dismutase, glutathione s-transferase, lactate dehydrogenase, and catalase. Whereas, the pellet was resuspended in 1ml microsomal dilution buffer and was used to estimate lipid peroxidation and CYP 450 content in control and treated group.

4.2.6. Biochemical assays

4.2.6.1. Determination of protein content

The protein concentration of all the samples was determined by the method of Lowry et al., (1951).

Principal: Protein in the sample makes peptide bonds with copper sulphate ($CuSO_4$) and gives a blue color when folin ciocalteu reagent was added to it.

Assay: To 1ml of sample aliquot (BSA or test sample), a freshly prepared alkaline mixture of 2.5ml copper sulphate reagent, comprised of sodium carbonate (2%), copper sulphate (1%), and sodium potassium tartrate (2%) was added. Followed by incubation of 10min, 1N folin ciocalteu reagent was added and allowed to incubate for 30min; this blue colored mixture was measured at 660 nm against blank and protein content for all the samples were calculated using bovine serum albumin (BSA) as a standard curve and expressed in mg/ml.

4.2.6.2. Determination of reduced glutathione content (GSH)

GSH content of the liver and lungs tissue was determined by the method as described by Moron et. al., (1979).

Principal: GSH is considered as the acid soluble sulfhydryl group as it contributes to total 90% of the non-protein thiols, GSH forms a yellow colored complex when reacts to DTNB and absorbance was read at 412nm.

Reduced Glutathione + DTNB ⟹ **5-thio-2 nitrobenzoate (yellow)**

Assay: To 500µl of crude liver and lungs homogenate of each sample, 100µl of 25% TCA was added. This mixture was immediately centrifuged at 5000 rpm for 5 min to allow sedimentation of tissue debris. After centrifugation, 100µl of the supernatant was added to a mixture containing 2ml DTNB (0.6mM) and 0.9ml of 0.2M sodium phosphate buffer (pH 8.0). The yellow color complex obtained was measured at 412nm against a reference blank that contained 100µl of 5% TCA. GSH content of all the samples was calculated with the help of GSH standard curve graph and were expressed as nmol/gm tissue.

4.2.6.3. Measurement of specific activity of glutathione s-transferase (GST)

Glutathione-S-transferase activity was measured by the method of Habig et al., (1974).

Principal: GST catalyzes the reaction of GSH and CDNB conjugate formed during the reaction which was measured at 340nm.

CDNB + GSH ⟹ CDNB - GSH conjugate

Assay: The assay mixture consists of sodium phosphate buffer (0.1M/ pH 6.5), 1mM CDNB (freshly prepared in ethanol) and 1mM GSH. The reaction mixture (3ml) was incubated for 10 min at room temperature followed by addition of the cytosolic sample. The enzyme reaction was measured at 340 nm for 5min at a time interval of 30sec. The specific activity of the enzyme (GST) was calculated as µmoles of CDNB-GSH conjugate formed/min/mg protein.

$$\textbf{Specific activity} = \frac{\textbf{OD/min x 3 x dilution}}{\textbf{9.6 x protein conc. (mg/ml)}}$$

Extinction coefficient = 9.6 mM^{-1} cm^{-1} and 3 is the total volume of reaction mixture

4.2.6.4. Measurement of catalase activity (CAT)

Catalase activity was measured as described by the method of Aebi, (1984).

Principle: Catalase is an enzyme that catalyzes the H_2O_2 to produce oxygen and water.

$$2H_2O_2 \xrightarrow{CAT} 2H_2O + O_2$$

Assay: The cytosolic samples were treated with chilled ethanol (10 ml/ml) for 30 min at 4ºC. To this, Triton X-100 (1%) was mixed gradually and incubated for 30 min at 4ºC. After incubation, 0.05M sodium phosphate buffer (pH 7.0) and 10mM H_2O_2 was added, and absorbance was measured at 240 nm. One unit of catalase activity is defined as the amount of enzyme required to decompose one mole of H_2O_2 per min. (extinction coefficient = 0.04 $mmole^{-1}$ cm^{-1}).

4.2.6.5. Measurement of superoxide dismutase (SOD) activity

SOD activity was determined by the method of Marklund and Marklund, (1974).

Principal: SOD catalyzes the dismutation of superoxide radical to give H_2O_2 and O_2. This activity is based on the amount of enzyme required to inhibit auto-oxidation of pyrogallol.

Assay: The assay mixture was comprised of 0.05M sodium phosphate buffer (pH 8.0),0.1mM EDTA and 0.27mM pyrogallol (prepared in 10mM HCl). To the above assay mixture (1ml), a cocktail of cytosolic samples already incubated (30 min) with Triton X-100 (1%) was added, and the enzyme activity was measured immediately at 420 nm for 5min. One unit of enzymes is defined as the amount of SOD required for

inhibition of auto-oxidation of pyrogallol by half (50%) and was expressed as Units/mg protein.

4.2.6.6. Measurement of lipid peroxidation (LPO)

Lipid peroxidation was estimated by the method of Varshney and Kale, (1990) and is expressed in terms of formation of malondialdehyde (MDA) content per mg protein.

Assay: The reaction mixture (3ml) was comprised of 1600µl Tris KCl (0.15M KCl + 10mM Tris-HCI, pH 7.4), 400µl of the microsomal sample, 500µl of TCA (30%) and 500µl of TBA (52mM). This reaction mixture was then incubated in a boiling water bath at 80°C for 45min, after cooling; the tubes were kept for cooling and then centrifuged at 3,000 rpm for 10min. The absorbance of the supernatant was measured at 532nm.

$$\textbf{MDA Content (nmoles)} = \frac{\textbf{V x OD x protein conc. (mg/ml)}}{\textbf{0.152}}$$

Where, V= final volume of test solution (ml),

and, extinction coefficient = 0.152

4.2.6.7. Measurement of lactate dehydrogenase (LDH)

The specific activity of LDH was estimated by the method of Bergmeyer HU, Bernt E, (1974) The assay is a measurement of enzyme activity to oxidize the NADH molecules.

Equation: $\textbf{Pyruvate} + H^+ \xrightarrow{\textbf{LDH}} \textbf{Lactate} + NAD^+$

Assay: The reaction mixture (1ml) consist of potassium phosphate buffer (50mM | pH7.5), 0.5mM sodium pyruvate and the cytosolic fraction of the sample. The reaction was initiated by the addition of 0.1mM NADH at 25°C. The enzyme activity was

measured by the rate of oxidation of NADH at 340nm. The enzyme activity is defined as the oxidation of 1µmol of NADH per min.

Formula:

$$\textbf{Specific activity of LDH} = \frac{\textbf{OD/min x 1000 x 1}}{\textbf{6.22 x protein conc. (mg/ml)}}$$

Where, 1 is the total reaction volume and 6.22 $mM^{-1}cm^{-1}$ = extinction coefficient

4.2.6.8. Measurement of DT- diaphorase activity

Principle: DT -diaphorase activity was assayed according to Ernster et al., (1962). This assay is based on the measurement of catalytic activity of enzyme DT-diaphorase required for the reduction of the DCPIP and oxidation of NADH.

Assay: The reaction mixture consists of Tris-HCI buffer (50mM, pH 7.5), 0.5mM NADH, 40µM DCPIP and 0.8% Triton X-100 as an activator in a final volume of 1ml. The reaction was initiated by the addition of cytosolic sample at 25°C. The rate of reduction of DCPIP was measured at 600nm. One unit of enzyme activity is defined as the amount of enzyme required to reduce one micromole of DCPIP per min.

$$\textbf{Specific activity} = \frac{\textbf{OD/min x 1 x dilution}}{\textbf{21 x mg protein in sample}}$$

In which, 1 is the volume in ml, Extension coefficient: 21mM^{-1} cm^{-1}.

4.2.6.9. Measurement of glutathione reductase (GR)

GR assay was performed according to the method of Carlberg and Mannervik (1975).

Principle: Glutathione reductase catalyzes the NADPH-dependent reduction of glutathione disulfide to glutathione.

Assay: The reaction mixture (1ml) comprised of 825µl of phosphate buffer, (0.125M, pH 7.4) 100µl NADPH (0.1mM) and 25µl GSSG (1mM). The reaction was initiated by the addition of 50µl of the sample, and the enzyme activity was measured by the oxidation of NADPH spectrophotometrically for 5 min at 340 nm with a time interval of 30sec. One unit of enzyme activity is defined as nmoles of NADPH oxidized/min/mg protein.

$$\textbf{Specific activity} = \frac{\textbf{OD/min x 1000 x 1}}{\textbf{6.22 x mg protein in sample}}$$

where, 1 is the volume of the reaction mixture (in ml), and 6.22 mM^{-1} cm^{-1} is the extinction coefficient for NADPH.

4.2.6.10. Measurement of glutathione peroxidase (GPx)

The specific activity of glutathione peroxidase (GPx) was determined by the method by Paglia and Valentine, (1967).

Principle: Glutathione disulfide (oxidized form) is usually produced as a result of GPx activity which is immediately reduced by an excess glutathione reductase (GR), thereby maintaining a constant level of glutathione (reduced form) in the reaction system. The assay takes advantage of the depletion of NADPH by GR, which is measured at 340 nm.

$$2H_2O_2 + 2GSH \xrightarrow{\textbf{GPX}} 2H_2O + GSSG$$

$$GSSH + 2NADPH \xrightarrow{\textbf{GR}} 2GSH + 2NADP^{+}$$

Assay: The assay mixture (1ml) comprised of 50mM sodium phosphate buffer (pH 7.0) 0.1M EDTA, 0.24 V/ml yeast glutathione reductase, 0.3mM glutathione reduced, 0.2mM NADPH, 1 mM sodium azide and 1.5mM H_2O_2 and cytosolic sample. The reaction was started by addition of NADPH and the decrease in absorbance was monitored at 340 nm for 5 min. One unit of enzyme activity has been defined as nmoles of NADPH consumed/min/mg protein.

$$\textbf{Specific activity} = \frac{\textbf{OD/min x 1000 x 1}}{\textbf{6.22 x mg protein in sample}}$$

where, 1 is the volume of the reaction mixture (in ml), and 6.22 mM^{-1} cm^{-1} is the extinction coefficient for NADPH.

4.2.6.11. Measurement of cytochrome P450

The cytochrome P450 content was determined by the method of Omura and Sato, (1964).

Principle: This assay is based on the measurement of the rate with which cytochrome P450 interacts with carbon monoxide molecules and gives a characteristic absorption pattern of CO difference spectrum at 450 nm.

Assay: The assay mixture comprised of 500µl microsomal samples mixed with 4.3ml Tris-HCI buffer (50mM, pH 7.4) and a pinch sodium dithionite (to reduce hemoprotein). This assay mixture was then divided into two equal parts, and a baseline correction was done between 400 to 500nm by a double beam spectrometer. The sample cuvette was then saturated with 30-40 bubbles of carbon monoxide (1 bubble/sec), and absorption spectra were recorded between 400-500 nm. The cytochrome P450 content

was then determined using molar extinction coefficient of $91mM^{-1}cm^{-1}$ between 450 and 490 nm and was expressed as moles/mg protein.

4.2.7. Determination of apoptosis by acridine orange and ethidium bromide (AO/EtBr) staining

Fluorescent DNA and RNA binding dyes, acridine orange and ethidium bromide (AO/EB) were used to detect morphological changes by urethane-induced apoptosis in cells (Darzynkiewicz et al., 1994). Freshly collected bone marrow cells (in FBS) from both the femurs (($1x10^6$) were immediately washed with ice cold PBS and centrifuged at 200 x g for 5 min. The cell pellet obtained was then resuspended in 1ml PBS and incubated with ice cold buffered paraformaldehyde for 15 min. The cells were again centrifuged (200 x g, 5 min) and the cell pellet was again resuspended in 5 ml PBS. The above step was repeated twice, and finally, cell pellet was suspended in the mixture of 1ml PBS and ice cold 70% ethanol (9ml) for 4h. The mixture was centrifuged (200 x g, 5 min) again and the cell pellet was mixed with 20µl of fluorescent dye mixture (with 1:1 ratio of AO (200µg/ml PBS) and EtBr (200µg/ml PBS)). After incubation for 5-7 min, the cells were visualized under a fluorescence microscope (Olympus BX51, Olympus Microscopes, Tokyo, Japan) using the 40x objective. Two hundred cells per sample were counted in triplicate for each dose. Four types of cells were differentiated on the basis of fluorescence emission. (1) normal cells (live-green); (2) early apoptotic cells (yellow); (3) late apoptotic cells (bright orange to red); (4) necrotic cells (dark orange to red).

4.2.8. Annexin and PI apoptotic assay: Flow cytometry

Annexin-V/PI stained cells were analyzed by FACS study according to Vermes et al. (1995). To detect apoptosis, bone marrow cells (1×10^6) were processed similarly as above experiment(AO/EtBr), washed with 1X PBS, from the resulting cell pellet, 100ul of cell suspension was incubated with 200µl of staining solution (FITC-conjugated Annexin-V and PI) for 30 min in the dark at room temperature. After incubation, the cells were filtered and analyzed using a BD FACS Verse flow cytometer. Fluorescence intensity of the cells was recorded at FL1 (515-545nm) and FL2 (564-601nm) band pass filter after excitation at 488 nm. BD cell quest software was used for analysis of data.

4.2.9. Analysis of DNA fragmentation by single cell gel electrophoresis

This method is most commonly called as '**comet assay'.**Using comet assay we observed the single and double strand DNA damage. (Singh et al., 1988; Tice et al., 2000)

1. Blood was drawn from the retro-orbital plexus using a glass capillary and collected in the heparinized tube.
2. The cell suspension was prepared by mixing 25µl of blood cells ($1.0x10^5$ cells) with 75 µl of 1% low melting agarose (LMA) (prepared in ion-free PBS, pH 7.5).
3. This cell suspension was then spread over the frosted slide which was already coated with 0.5% normal melting agarose (NMA).
4. After solidification, another layer of LMA was added to cover the cells.
5. Once the LMA layers were solidified, slides were kept in chilled lysing solution (2.5M NaCl, 100mM EDTA, 10mM Tris (pH 10), freshly added 10% DMSO and 1% Triton X-100) for 3-4h at 4ºC.

6. In a horizontal gel electrophoresis tank, slides were dipped in electrophoresis buffer (1mM Na_2EDTA and 300mM NaOH, pH >13) at 24 volts for 30 min at 4ºC (to allow DNA unwinding). After incubation, power supply was turned on, and electrophoresis was carried out for another 30 min at 4ºC.
7. After electrophoresis, the slides were washed twice with cold neutralization buffer (0.4M Tris, pH 7.5)
8. Drained slides were stained with 75 µl EtBr (20µg/ml) for 5 min and rinsed with cold water to remove the excess stain. The slides were covered with fresh coverslips and examined using Olympus fluorescence microscope within 3-4h. Slides were prepared in triplicates, and from each slide, 70-100 cells were analyzed by using ImageJ 1.x software.

4.2.10. Analysis of protein expression by western blot

4.2.10.1 Preparation of cell lysate

For single cell suspension, liver tissue samples were weighed and were homogenized in 1ml 1% lysis buffer (150mM sodium chloride, 1.0% IGEPAL ® CA-630 Sigma-Aldrich, 0.5% sodium deoxycholate, 0.1% SDS, 50mM Tris, pH 8.0, protease inhibitors) by use of downs homogenizer at 4ºC. The tissue sample was placed in a rocker for 60 min at 4^0C. After lysis, the tissue lysate was centrifuged at 13000 rpm for 10min at 4ºC. The supernatant was again centrifuged at 5000 rpm for 10 mins at 4ºC. The resulting supernatant containing protein extract was collected in sterile tubes and stored in -80ºC until further use.

4.2.10.2. Protein estimation

Protein estimation was done by using Quick Start Bradford Protein kit (Biorad, Hercules, California, USA). The quantification was done as per as the manufacturer instruction.

4.2.10.3. Western blot assay

Control and treated cells (45-50µg protein) were mixed with 2X Laemmli buffer (4% SDS, 10% 2-mercaptoehtanol, 0.004% bromophenol blue, 20% glycerol and 0.125 M Tris-HCl, pH 6.8). The samples were immediately heated at 90^0C for 10 min.Thereafter, the samples (mixed with dye) were loaded into wells of polyacrylamide gel (PAGE),and electrophoresis was conducted at 40 volts, once the dye reaches the end of stacking gel, the voltage was increased to 60 volts. After the electrophoresis step, the gel was taken out carefully and transferred to a nitrocellulose membrane (NCM) (65 volts, 60 min). Once the protein was transferred to the membrane, it was treated (blocking) with 5% BSA (PBS, 0.1% Tween 20) for 90 min at room temperature. The membrane was then incubated with primary antibody (diluted in PBS, 0.1%Tween 20) for 8-10h at 4^0C. After incubation, the membrane was washed with 5X PBST (PBS, 0.1 % Tween 20) twice at an interval of 10 min, placed on a rocker machine. The membrane was finally re-incubated with the HRP-secondary antibody for 60 min. After incubation, the membrane was washed twice with 5X PBST (PBS, 0.1% Tween 20) for 10min. After washing, protein band was developed into X-ray film by using ECL reagent kit.

4.2.11. Histopathological observations

To observe the morphological changes in tissue by modulatory effects of test agents, hematoxylin and eosin (H & E) staining was performed. Histopathological examination

in liver, lung, kidney, intestine and testes were carried out in both control and treated animals by H & E staining as described below:

1. **Fixation:** After dissection, soft organs viz liver, lung, kidney, intestine and testes were excised carefully and kept in cold normal saline solution, washed with distilled water, blotted dry and fixed in 10% buffered formalin solution.
2. **Dehydration:** Formalin-fixed tissues were dehydrated in series of percent ethanol (100%, 95%, 80%, 70%, and 50% ethanol) and finally treated with xylene to complete dehydration processing.
3. **Block preparation:** A section of all the tissues were embedded in molten paraffin after processing. The sections of 5µm thickness were cut for all the organs using microtome (Leica Biosystems) to carry out H & E staining.
4. **Staining:** Hematoxylin and eosin staining were performed in this study. To begin with H&E staining, the first step is to deparaffinized the paraffin-embedded sections in a water bath (60-65ºC),then treated with xylene and further downgraded with different grades of alcohol to water (absolute alcohol- 90% alcohol- 70 % alcohol- water). Sections were slightly overstrained with hematoxylin (20-25min) and rehydrated (10min). Then the slides were destained in acidic alcohol till the blue nuclei became clearly visible (hematoxylin stains cell nuclei blue). Slides are then rinsed in tap water to remove excess acid and dehydrated in 70% and 90% alcohol. After dehydration, slides were dipped in eosin for 1 min, and then passed through different grades of alcohol 90% alcohol (1-2 dips), absolute alcohol (5min) and finally in xylene for clearing the sections from excess stains and finally allow the slides to dry for 30 min.

5. **Mounting**: Once the staining procedure was done, the stained sections were mounted in DPX under a cover slip, and histopathological evaluation of sections was carried out using a microscope (400x).

4.2.12. Immunohistochemistry

For immuno-histopathological studies, paraffin embedded tissues were first cut into 5µm thick section using a cryostat (Leica Biosystems). To avoid nonspecific binding of cells; the sections were dipped in blocking buffer (10% primary antibody serum, 0.3% Triton X-100) for 45 min at room temperature. After blocking, the sections were treated with primary monoclonal antibody (1:500 dilution in BSA (1%), antibody host serum (1%), Triton X-100 (0.3%), and sodium azide (0.01%)) for 1h, washed with 0.1% BSA (in PBS) and incubated with fluorescent-conjugated secondary antibody (1:700 diluted with BSA (1%), antibody host serum (1%), Triton X-100 (0.3%), and sodium azide (0.01%)) for 1h in dark. The slides were washed twice with washing buffer for 5 min. Cells/tissue were stained with 100-400µl of DAB signal stain solution for 5 min at room temperature (3µM in PBS). After staining, tissue/cells once rinsed with PBS. Semi-dried section/cells mounted with anti-fade mounting media and visualized under the fluorescence microscope (Olympus BX51, Olympus Microscopes, Tokyo, Japan).

4.3. Results

4.3.1. Experiments with TAX

In these experimental studies, the effects of TAX on URE induced toxicity in male Swiss albino mice have been examined.

4.3.1.1. Body weight profile

Table 1 depicts the toxic effects of URE on body weight in mice. Body weight had significantly decreased in animals exposed to URE as compared to normal control; Animals co-exposed to URE+TAX showed a significant increase in body weight as compared to animals, exposed to URE alone. There was no significant increase in body weight when the mice were exposed to TAX. (Figure 4.1)

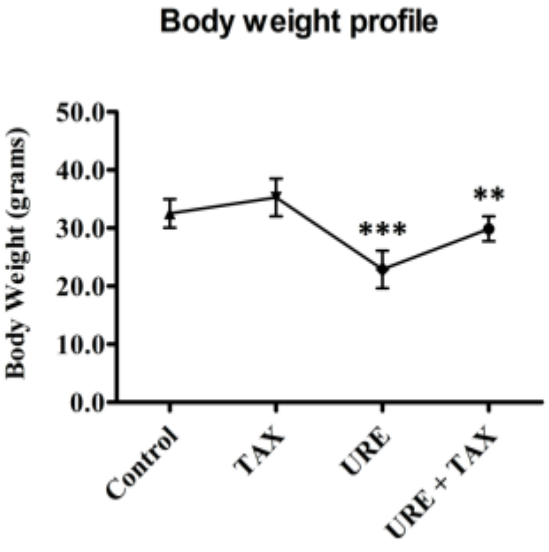

Figure 4.1: Body weight profile (gms) in mice among different treatment groups

Table 4.1: Body weight of Swiss albino mice exposed to URE, TAX, and URE + TAX

Treatment	Mean Body weight	SD
Control	32.52	2.45
TAX	33.89	3.25
URE	22.87***	3.02
URE + TAX	28.85**	2.14

4.3.1.2. Biochemical assays in lungs and liver to study effects of TAX on URE induced oxidative stress

4.3.1.2.1. Modulatory effects of TAX and URE on GSH levels

As compared to negative control, administration of URE has significantly decreased the GSH levels in liver and lung by 43.8% and 33.1% respectively. Co-administration of TAX with URE has significantly increased the GSH levels up to 87% and 85.4% respectively as compared to positive (URE) control. (Figure 4.2)

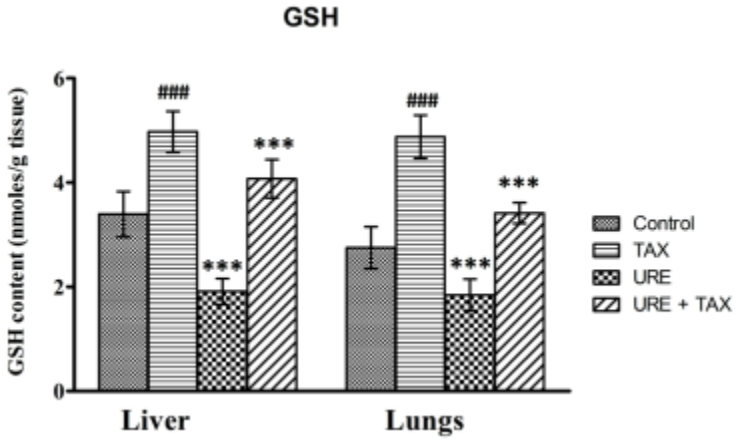

Figure 4.2:Reduced glutathione level among different treatment groups of mice GSH content in nmole/g of tissue. Data presented as mean ± SD; (n = 5). Data was also analyzed for statistical comparison using ANOVA followed by Bonferroni test. A significance of (***) P< 0.01 and (###) P< 0.01 was considered significant

4.3.1.2.2. Modulatory effects of TAX and URE on GST activity

As compared to negative control, administration of URE has significantly decreased the GST activity in liver and lungs by 43.1% and 30.4% respectively. Co-administration of TAX with URE has significantly increased the GST activity to 135% and 52.4% respectively as compared to positive (URE) control (Figure 4.3).

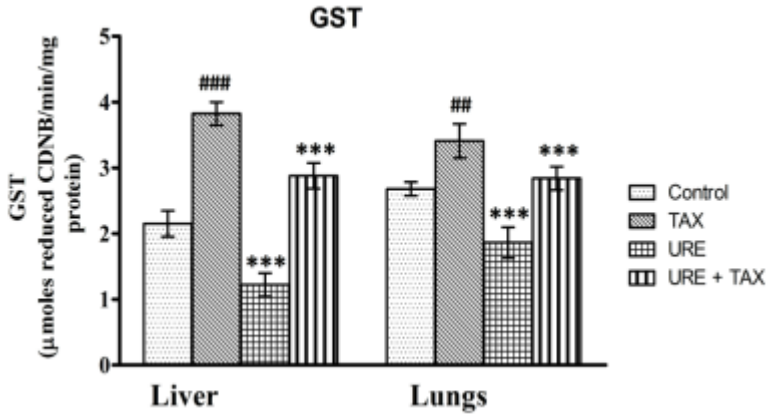

Figure 4.3: Glutathione S-transferase levels in different treatment groups of mice. GST activity is calculated as µ moles of reduced CDNB/min/mg of protein. Data presented as mean ± SD; (n = 5). Data was also analyzed for statistical comparison using ANOVA followed by Bonferroni test. A significance of (***) P<0.01, (###), P<0.01 and (##), P< 0.05 was considered significant.

4.3.1.2.3. Modulatory effects of TAX and URE on Catalase activity

As compared to negative control, administration of URE has significantly decreased the CAT activity in liver and lungs by 34.1% and 42.3% respectively. Co-administration of TAX with URE has significantly increased the CAT activity to 37.7% and 82.9% respectively as compared to positive (URE) control (Figure 4.4).

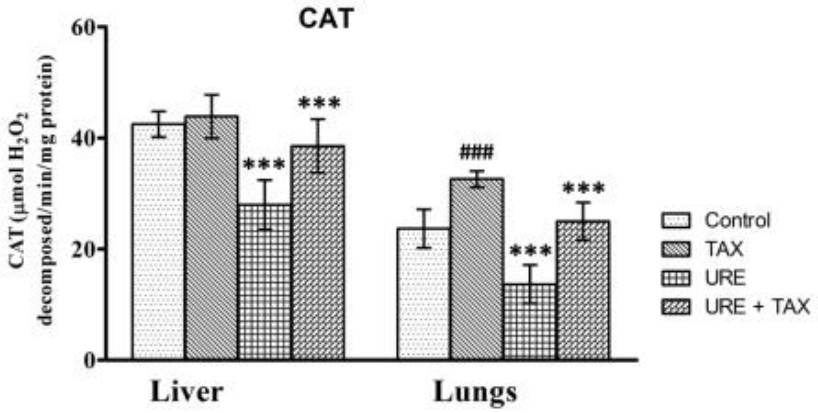

Figure 4.4: Catalase activity in different treatment groups of mice: Catalase activity calculated as decomposition of H2O2 in µ mol/mg of protein. Data presented as mean ± SD; (n = 5). Data was also analyzed for statistical comparison using ANOVA followed by Bonferroni test. A significance of (***) P<0.01, (###), P<0.01 and (##), P< 0.05 was considered significant.

4.3.1.2.4. Modulatory effects of TAX and URE on SOD activity

As compared to negative control, administration of URE has significantly decreased the CAT activity in liver and lungs by 34.7% and 76.5% respectively. Co-administration of TAX with URE has significantly increased the CAT activity to 47.5% and 302.9% respectively as compared to positive (URE) control (Figure 4.5).

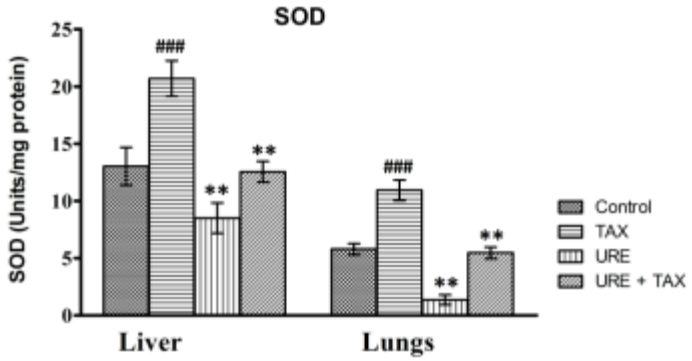

Figure 4.5:Superoxide dismutase activity in different treatment groups of mice. SOD activity in Units/mg of protein. Data presented as mean ± SD; (n = 5). Data presented as mean ± SD; (n = 5). Data was also analyzed for statistical comparison using ANOVA followed by Bonferroni test. A significance of (***) P<0.01, (###), P<0.01 and (##), P< 0.05 was considered significant.

4.3.1.2.5. Modulatory effects of TAX and URE on GR activity

As compared to negative control, administration of URE has significantly decreased the CAT activity in liver and lungs by 50.7% and 56.3% respectively. Co-administration of TAX with URE has significantly increased the CAT activity to 114.6% and 76.1% respectively as compared to positive (URE) control (Figure 4.6)

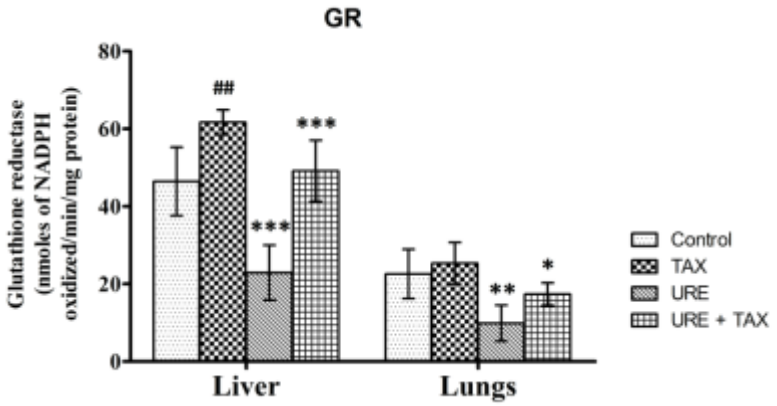

Figure 4.6: Glutathione reductase activity in different treatment groups of mice. GR activity in nmoles NADPH oxidation/min/mg of protein. Data presented as mean ± SD; (n = 5). Data was also analyzed for statistical comparison using ANOVA followed by Bonferroni test. A significance of (***) P<0.01, (###), P<0.01 and (##), P< 0.05 was considered significant.

4.3.1.2.6. Modulatory effects of TAX and URE on GPx activity

As compared to negative control, supplementation of URE has significantly decreased the CAT activity in liver and lungs by 32.5% and 41.0% respectively. Co-supplementation of TAX with URE has significantly increased the CAT activity to 49.0% and 31.0% respectively as compared to positive (URE) control (Figure 4.7).

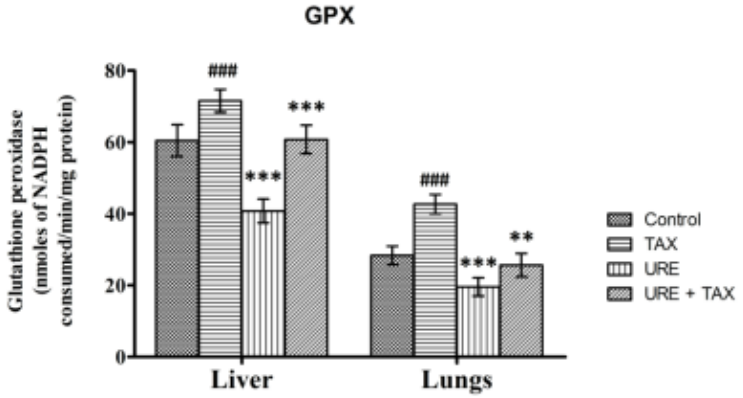

Figure 4.7: Glutathione peroxidase activity in different treatment groups of mice . Glutathione peroxidase activity in nmoles NADPH reduction/min/mg of protein. Data presented as mean ± SD; (n = 5). Data was also analyzed for statistical comparison using ANOVA followed by Bonferroni test. A significance of (***) P<0.01, (###), P<0.01 and (##), P< 0.05 was considered significant.

4.3.1.2.7. Modulatory effects of TAX and URE on DTD activity

As compared to negative control, administration of URE has significantly decreased the DTD activity in liver and lungs by 31.6% and 52.7% respectively. Co-administration of TAX with URE has increased the DTD activity to 27.0% and 70.4% (significantly) respectively as compared to positive (URE) control (Figure 4.8).

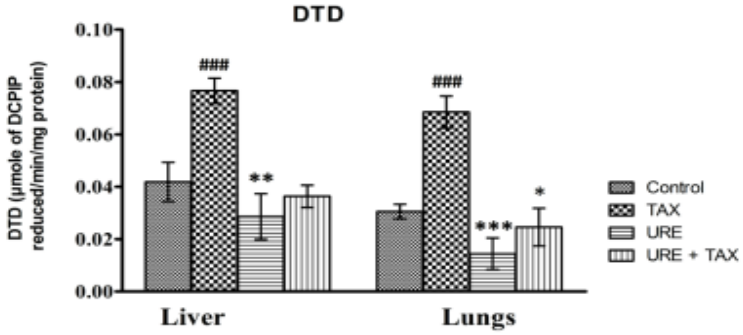

Figure 4.8: DT-diaphorase activity in different treatment groups of mice, DT-diaphorase activity in µ mole of DCPIP reduction/min/mg of protein. Data presented as mean ± SD; (n = 5). Data was also analyzed for statistical comparison using ANOVA followed by Bonferroni test. A significance of (***) P<0.01, (###), P<0.01 and (##), P< 0.05 was considered significant.

4.3.1.2.8. Modulatory effects of TAX and URE on CYP450 levels

As compared to negative control, administration of URE has significantly decreased the CYP450 activity in liver and lungs by 46.2% and 52.2% respectively. Co-administration of TAX with URE has increased the CYP450 activity to 80.9% and 99.4% (significantly) respectively as compared to positive (URE) control (Figure 4.9).

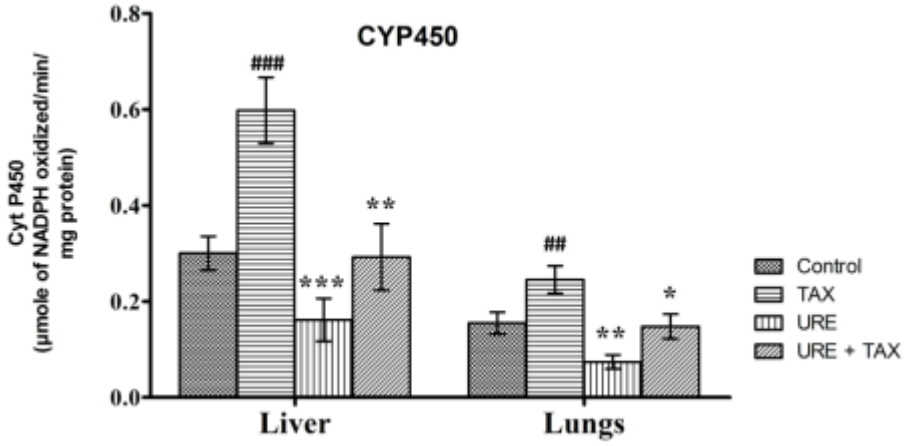

Figure 4.9: Cytochrome P450 level in different treatment groups of mice. CYP450 activity in µmoles NADPH oxidation/min/mg of protein. Data was also analyzed for statistical comparison using ANOVA followed by Bonferroni test. A significance of (***) P<0.01, (###) P< 0.01, (**) P< 0.05, (##) P< 0.05 and (*) P < 0.10 was considered significant.

4.3.1.2.9. Modulatory effects of TAX and URE on LPO (MDA content)

As compared to negative control, supplementation of URE has significantly increased the LPO activity in liver and lungs by 34.1% and 42.3% respectively. Co-supplementation of TAX with URE has significantly decreased the LPO activity to 37.7% and 82.9% respectively as compared to positive (URE) control (Figure 4.10).

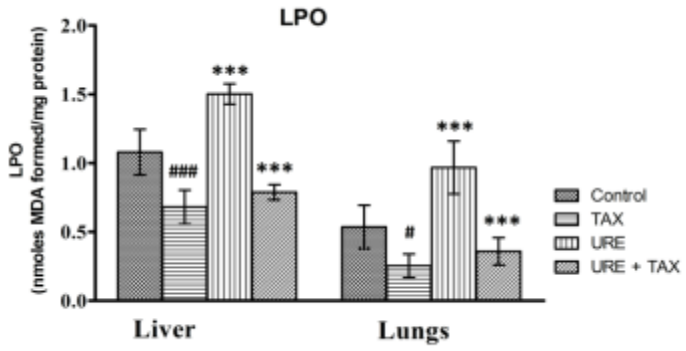

Figure 4.10: Lipid peroxidation levels in different treatment groups of mice. Lipid peroxidation levels in nmoles of MDA formed /mg of protein. Data was also analyzed for statistical comparison using ANOVA followed by Bonferroni test. A significance of (***) P< 0.01, (###) P< 0.01, and (#) P< 0.10 was considered significant.

4.3.1.2.10. Modulatory effects of TAX and URE on LDH activity

As compared to negative control, administration of URE has significantly increased the LDH activity in liver and lungs by 132.2% and 85.6% respectively. Co-administration of TAX with URE has significantly decreased the LDH activity to 68.8% and 58.2% respectively as compared to positive (URE) control (Figure 4.11).

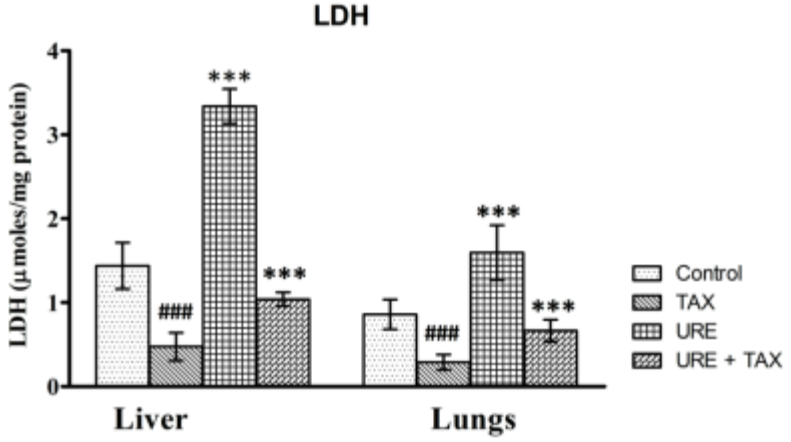

Figure 4.11: Lactate dehydrogenase level in different treatment groups of mice. Lactate dehydrogenase levels in µmoles/mg of protein. Data was also analyzed for statistical comparison using ANOVA followed by Bonferroni test. A significance of (***) P< 0.01 and (###) P< 0.01 was considered significant.

4.3.1.3. Visualization of the apoptosis by AO/EtBr staining

Apoptosis data obtained from AO/EtBr staining method is shown. The results analysis showed that percentage of apoptotic and dead cells were reduced in combined treatment of URE + TAX (15.0 ± 3.7) as compared to URE (24.3 ± 3.1) alone group. AO penetrates into living cells, emitting green fluorescence after intercalation with DNA, the results analysis showed that in control and Tax group, the ratio of live cells were more as compared to URE group (1.3 fold increase) where the cells were stained with orange-yellow and red due to loss of membrane integrity and shrunken nuclear material

which allows penetration of EtBr stain. The combined treatment of URE + TAX has significantly reduced the apoptotic cells (0.6 fold decrease).

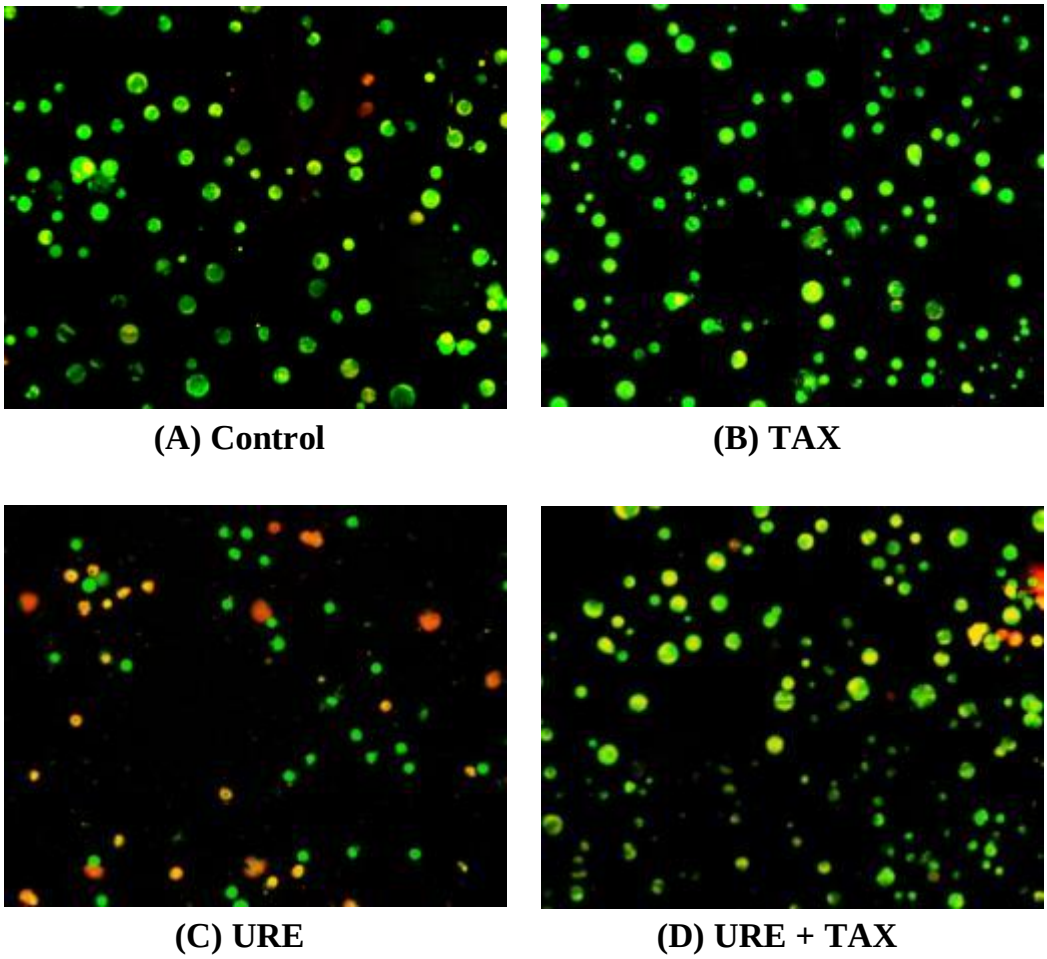

(A) Control **(B) TAX**

(C) URE **(D) URE + TAX**

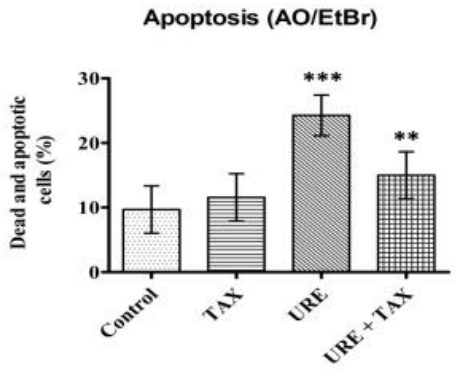

Table 4.2: Effect of TAX and URE on apoptosis of bone-marrow cells (a) photomicrographs depicting live, apoptotic and dead cells. (b) bar diagram showing percentage of apoptotic and dead cells. Each data point represents mean ± SD of 1000 cells from five independent experiments. (*) $p < 0.10$ vs control; (**) $p < 0.05$; (***) $p < 0.01$ represents the linear (pairwise) change.

4.3.1.4. Histopathological studies

The histopathological analysis was carried out using H&E staining in lungs, liver, kidney, intestines and testis of mice for all the control and treated groups

The histopathological changes in **lungs** of control, URE and TAX exposed mice (individually or in combination) are shown in Figure 4.12. URE treated lung showed alveolar spaces filled with edema fluid as compared to normal control and TAX treated mice where lungs section showed normal bronchiole and alveolar spaces and no infiltration or edema is seen. On the other hand, combined doses of URE + TAX treated lung showed significant changes where alveolar spaces were partially filled with edema fluid.

The hepatic section from the URE treated **liver** showed portal triad with damaged hepatocytes in the periportal area with the presence of inflammatory cells as compared to control and TAX treated mice, where, portal triad showed normal hepatocytes and no inflammatory cells were observed. The combined treatment of URE + TAX has significantly reduced the damaged hepatocytes in the portal area with no evidence of inflammatory cells (Figure 4.13).

The histopathological changes in **testis** of control, URE and TAX treated mice are shown in Figure 4.14. URE treated testis showed few apoptotic bodies (2 to 4/HPF) in the basal layers of the seminiferous tubules in comparison to control and TAX treated groups which did not show any significant changes in the morphology. The combined effect of URE+ TAX has significantly reduced the degree of apoptosis and restored the normal tissue morphology.

The histopathological changes in **intestines** of control, URE and TAX, treated mice are shown in Figure 4.15. URE treated animal showed a significant increase in the number of apoptotic bodies (8 to 10 /HPF) in epithelial cells of intestinal crypts as compared to control and TAX treated group, which showed few (1 to 2 / HPF) apoptotic bodies in epithelial cells. The presence of apoptotic bodies were significantly reduced (3 to 5 /HPF) when mice were treated with the combined dose of URE + TAX.

The histopathological changes in kidneys of control, URE, TAX treated mice are shown in Figure 4.16. In case of renal tissue of control and TAX treated mice, the glomerulus surrounded by renal tubules showed normal histological morphology as compared to URE treated group animal where the periglomerular space show presence of hyaline casts indicating the leakage of proteinaceous material through the glomerulus. However, unlike in URE treated group, animals treated with URE + TAX resulted in the restoration of the normal cortical architecture (evidenced by the clear and occasional tubules that showed the presence of small hyaline casts with a lesser degree of protein leakage through the glomerulus.

4.3.1.4.1. Histopathological observation in lungs

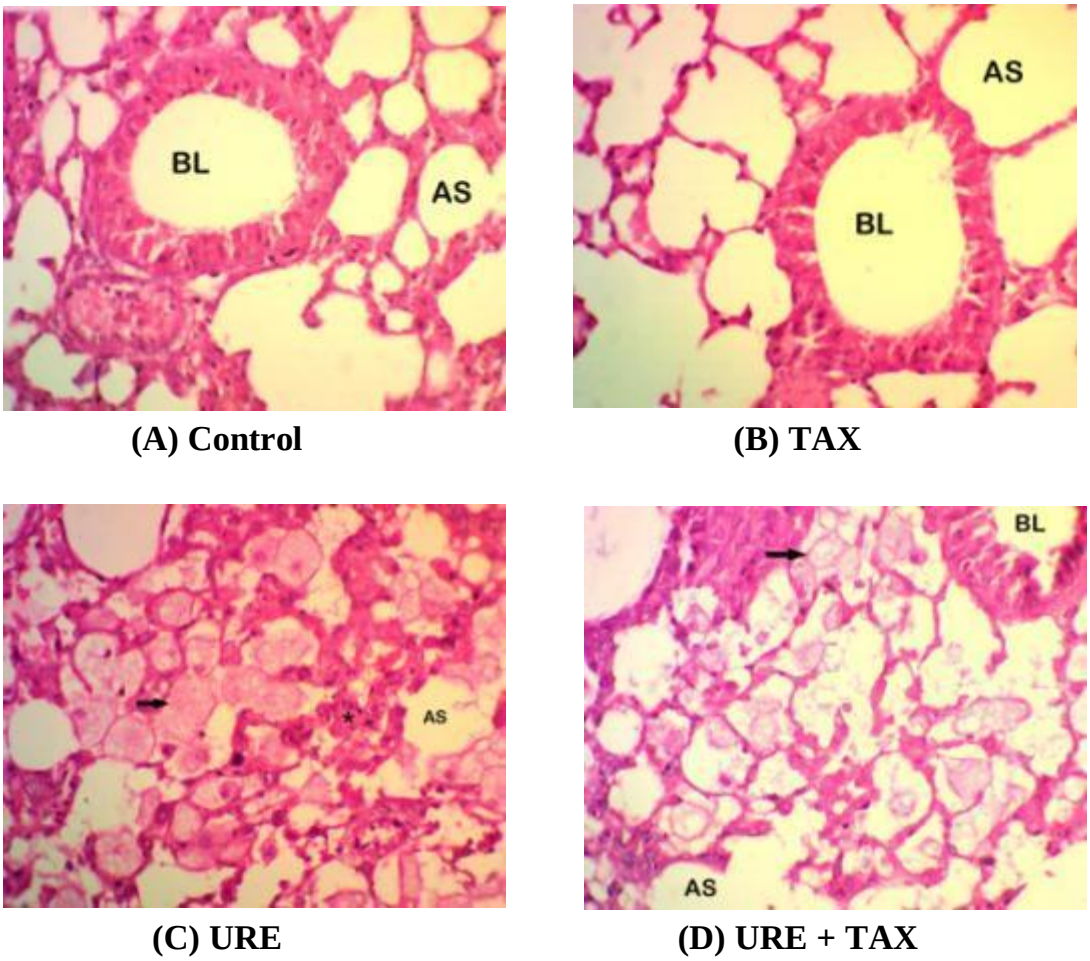

(A) Control **(B) TAX**

(C) URE **(D) URE + TAX**

Figure 4.12: High power photomicrograph of histopathological analysis of control, URE and TAX treated mice lung tissue, (H&E X 40x). High power photomicrograph of histopathological analysis of control, URE and TAX treated mice lung tissue, (H&E X 40x). A and B: Control and TAX group showed normal bronchiole and adjacent alveolar spaces. No infiltration or edema is seen. C) URE treated lung showed alveolar spaces filled with edema fluid (Arrow). D) URE + TAX treated lung showed alveolar spaces partially filled with edema fluid (Arrow). The changes seen in this sample are less than that seen in URE treated animals. BL = Bronchial Lumen, AS = Alveolar Space.

4.3.1.4.2. Histopathological observation in liver

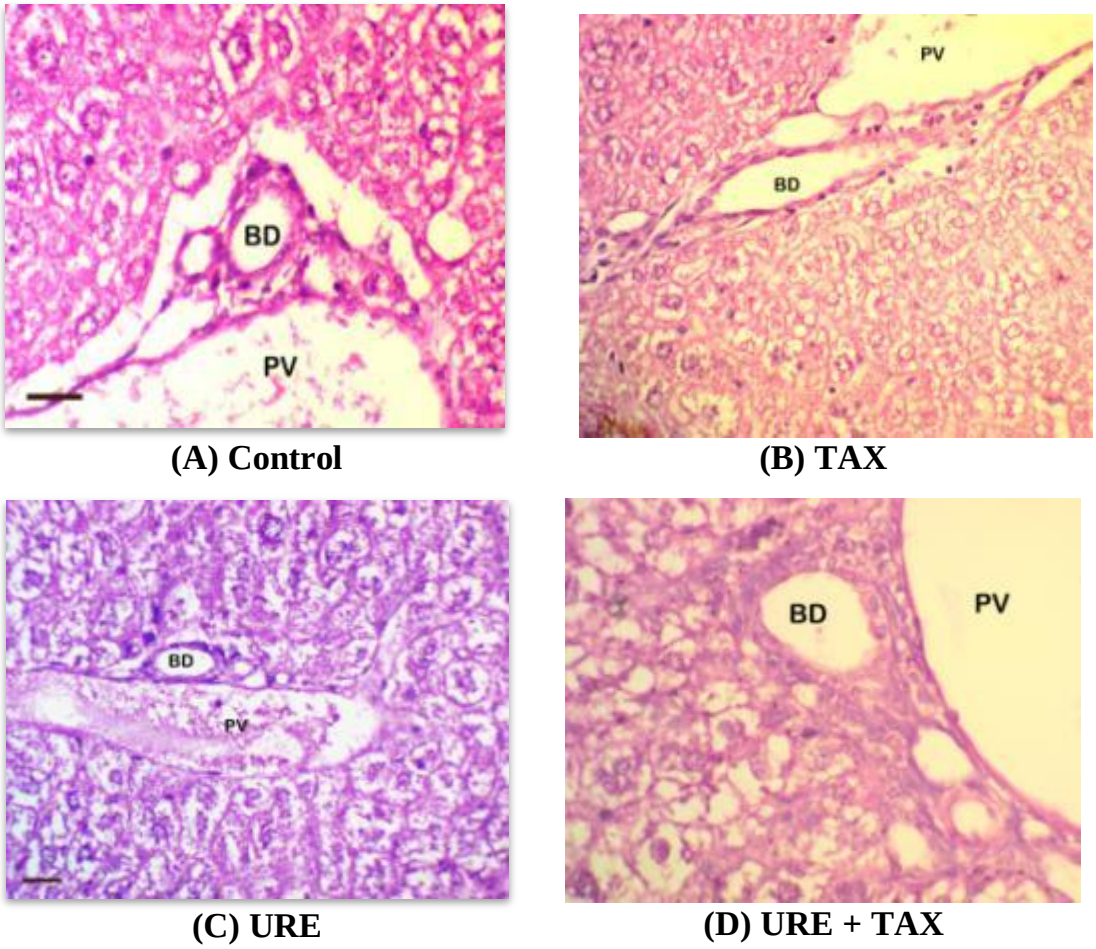

(A) Control **(B) TAX**

(C) URE **(D) URE + TAX**

Figure 4.13: High power photomicrograph of histopathological analysis of control, URE and TAX treated mice liver tissue, (H&E X 40x). A and B: Portal triad from the control and TAX treated liver showed normal portal triad structures with adjacent normal hepatocytes in the periportal area. No inflammatory cells are present. C) URE: URE treated liver showed portal triad with damaged hepatocytes in the periportal area. Inflammatory cells are present. D) URE + TAX: Liver showed portal triad with attenuated hepatocytes in the periportal area. No inflammatory cells are present. PV = Portal Vein, BD = Bile Duct.

4.3.1.4.3. Histopathological observation in testis

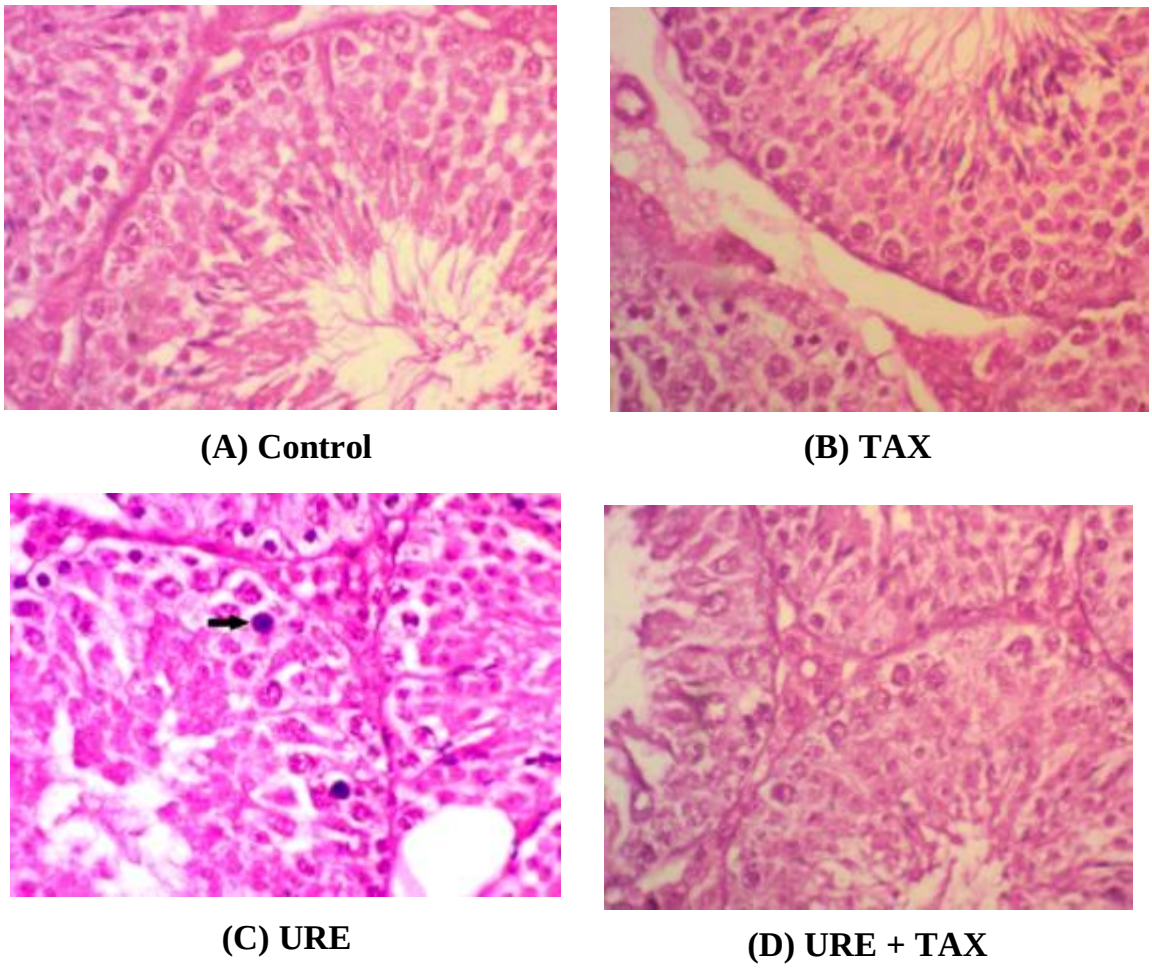

Figure 4.14: High power photomicrograph of histopathological analysis of control, URE and TAX treated mice testes, (H&E X 40x) A and B: Testis from control group animal showed the normal histological appearance of seminiferous tubules. No apoptotic bodies were seen. B) TAX: Testis from animal treated with TAX showed the normal histological appearance of seminiferous tubules. No apoptotic bodies were seen. C) URE: Testis from URE treated animal showed few apoptotic bodies (2 to 4/HPF) in the basal layers of the seminiferous tubules. D) URE + TAX: Testis from URE + TAX treated animals showed the normal histological appearance of seminiferous tubules. No apoptotic bodies were seen.

4.3.1.4.3. Histopathological observation in intestines

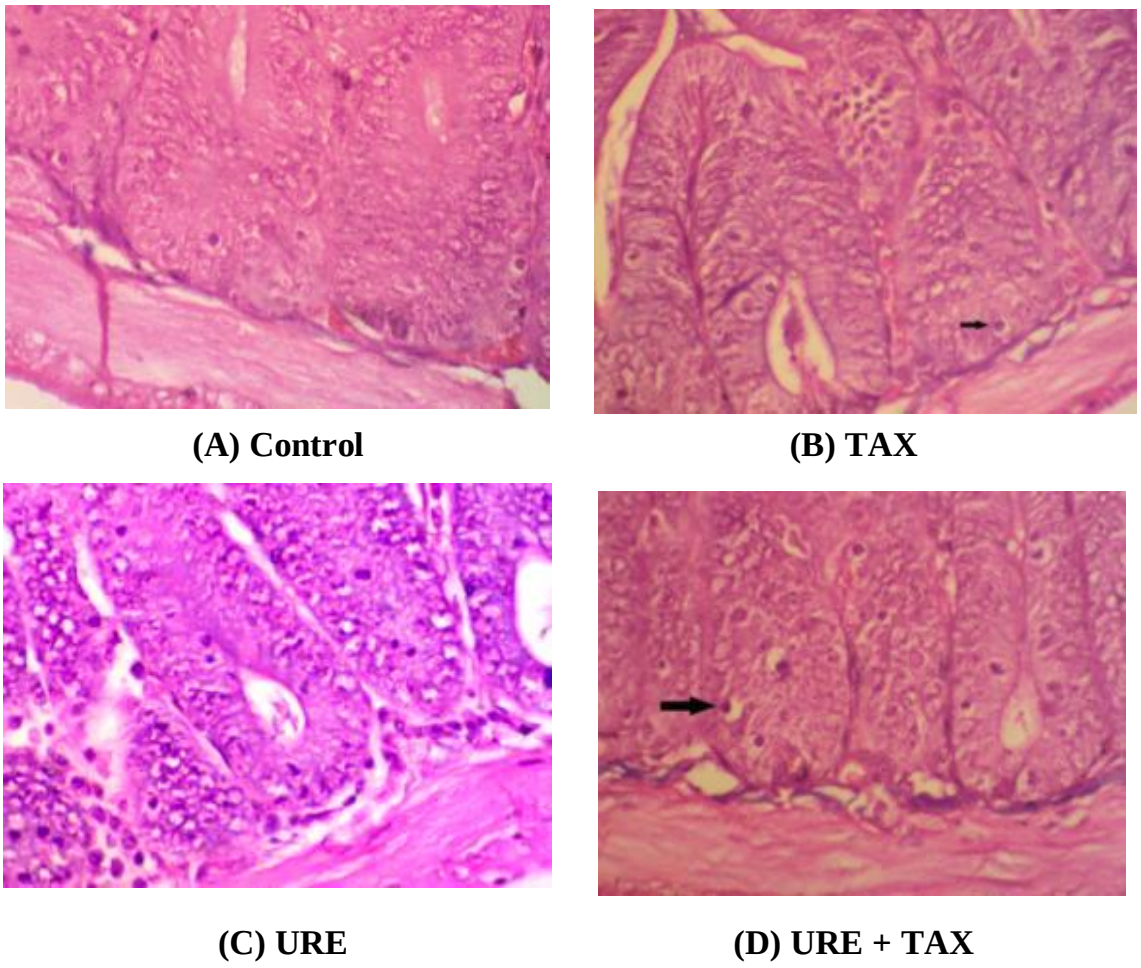

(A) Control **(B) TAX**

(C) URE **(D) URE + TAX**

Figure 4.15: High power photomicrograph of histopathological analysis of control, URE and TAX treated mice intestines, (H&E X 40x). A and B: Intestinal crypts from the animal in control and TAX showed few (1 to 2 / HPF) apoptotic bodies in epithelial cells. C) URE: Intestinal crypts from the animal in URE group showed an increase in a number of apoptotic bodies (8 to 10 /HPF) in epithelial cells. D) URE + TAX: Intestinal crypts from animal in URE + TAX group showed comparatively reduced number of apoptotic bodies (3 to 5 /HPF) in epithelial cells.

4.3.1.4.4. Histopathological observation in kidneys

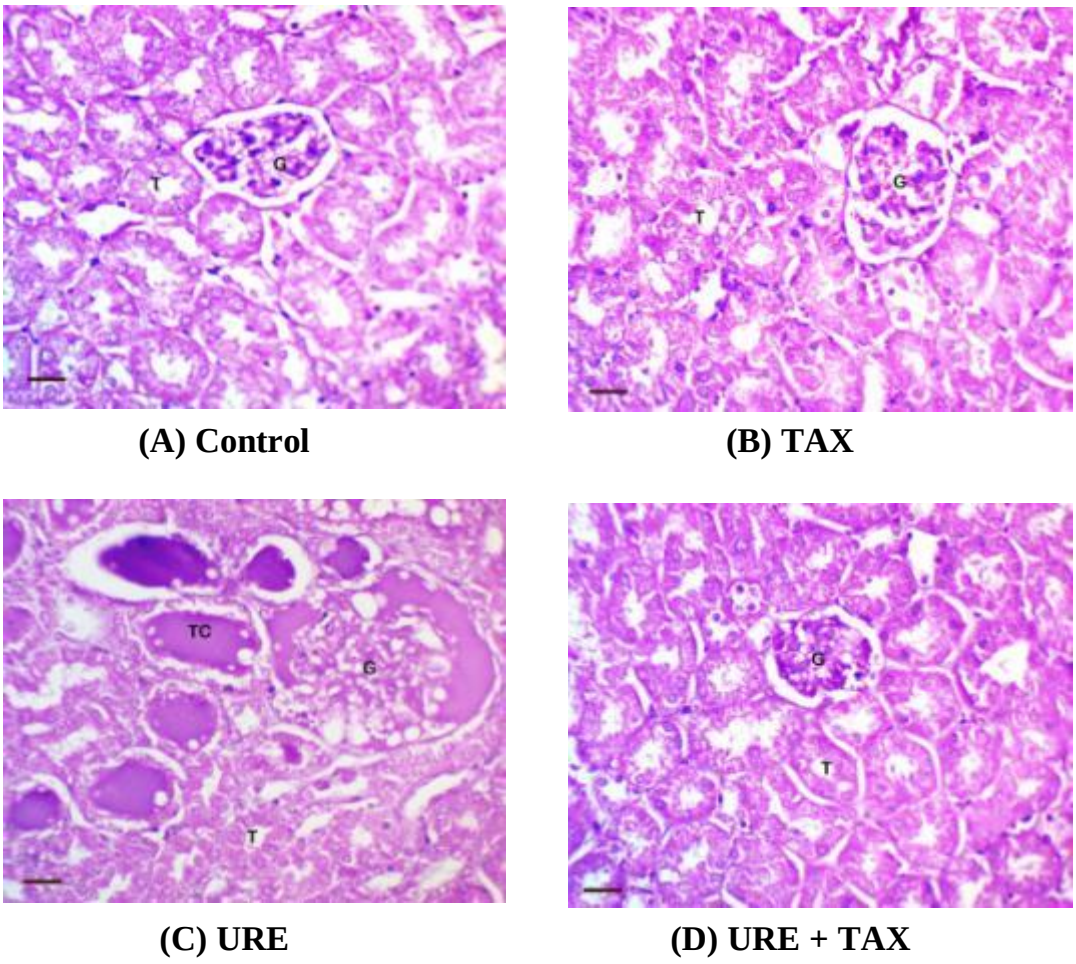

(A) Control **(B) TAX**

(C) URE **(D) URE + TAX**

Figure 4.16: High power photomicrograph of histopathological analysis of control, URE and TAX treated mice kidneys, (H&E X 40x). A) and B): Kidney from control and TAX group animal showed normal renal tissue with a glomerulus surrounded by renal tubules. C) URE: Kidney from URE treated group animal showed renal tissue with a glomerulus surrounded by renal tubules. The periglomerular space and several tubules show the presence of hyaline casts indicating leakage of proteinaceous material through the glomerulus. D) URE + TAX: Kidney from URE +TAX treated group animal showed normal renal tissue with a glomerulus surrounded by renal tubules. The periglomerular space is also clear. G = Glomerulus, T = Tubules, TC = Tubular Cast.

4.3.1.4. Evaluation of DNA damage by comet assay

The genotoxic potential of normal and exposed animals was evaluated by performing comet assay using the whole blood from mice as shown in Figure 4.18. In control group animals, no comets were observed indicating an intact DNA structure as compared to URE treated mice which showed a significant increase (2.8 fold) in the comet length, measured in the form of the olive tail moment. Co-administration of URE and TAX significantly reduced (1.36 fold) the DNA damage as compared to URE treatment alone, indicated by comparatively reduced comet tail length (Figure 4.17).

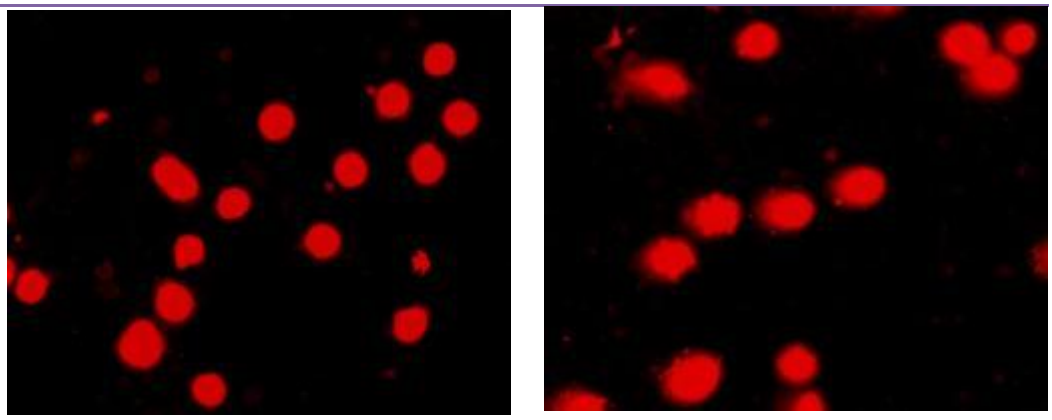

(A) Control **(B) TAX**

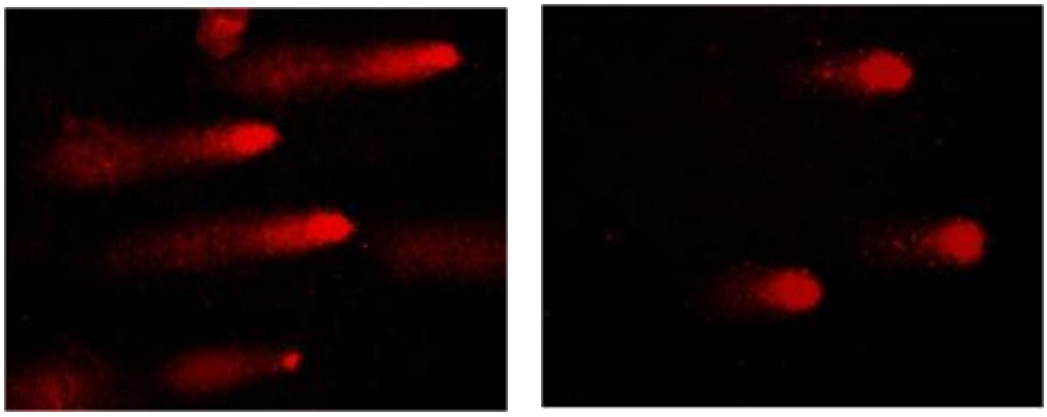

(C) URE **(D) URE + TAX**

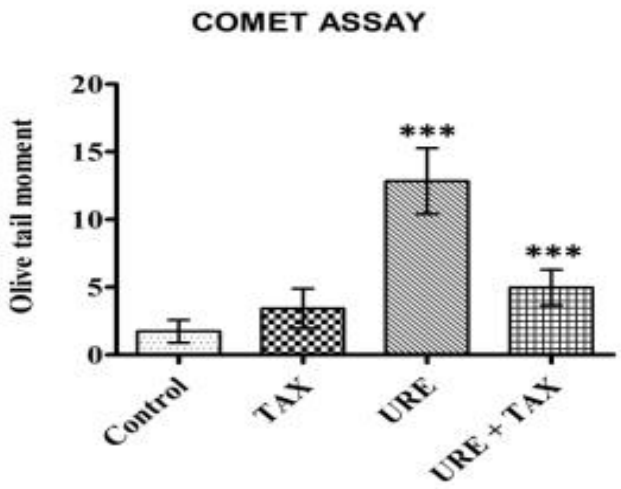

Figure 4.17: Effect of TAX on URE-induced DNA damage in mice. a)- A) Control, (B) TAX, (C) URE, (D) URE + TAX. b) Bar graph showing the olive tail moment of comets observed in different treatment groups. Each data point represents mean ± SD of 250 cells from fi five independent experiments. (*) $p < 0.10$ vs control; (**) $p < 0.05$; (**) $p < 0.01$ represents the linear (pairwise) change

4.3.1.5. Evaluation of apoptosis by Annexin V (FITC) and PI staining method

The extent of apoptosis in bone marrow cells was evaluated by flow cytometric method using FITC-conjugated Annexin V/PI. The apoptotic rate by different treatment groups was quantified by Annexin V and PI staining. Treatment with URE resulted in significant increase in apoptosis by 61.2 % (only Annexin V positive) as compared to control group. Co-treatment of URE + TAX has significantly reduced the percentage of apoptotic cells by 64.2%. (Figure 4.18)

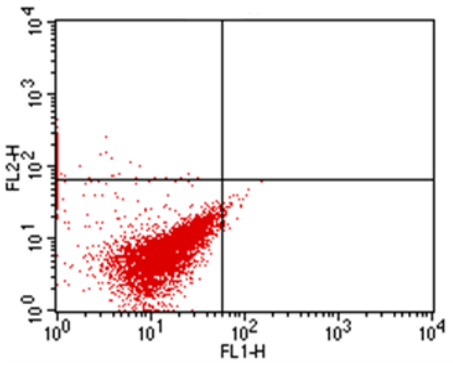

(A) Control

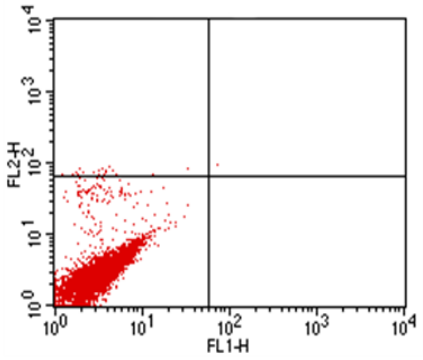

(B) TAX

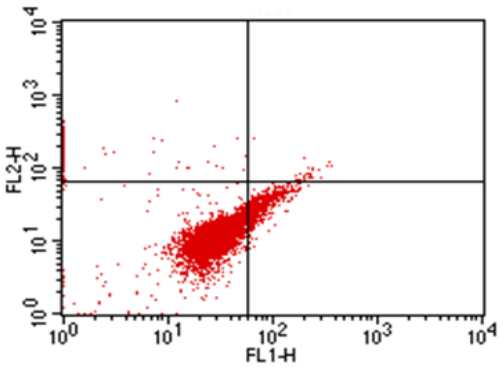

(C) URE

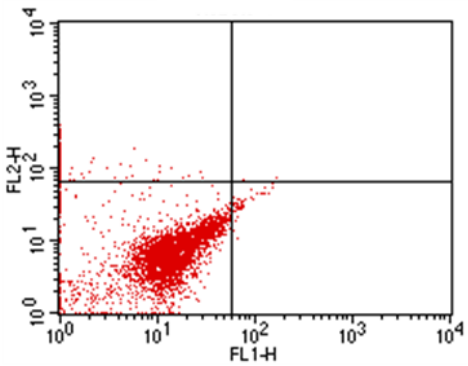

(D) URE + TAX

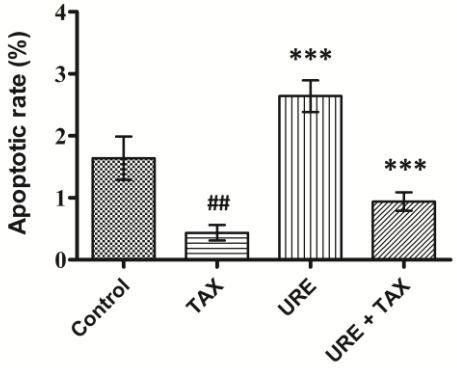

Figure 4.18: Annexin V–PI staining: Effects of control, URE, TAX and its combination (URE+ TAX) exposure on apoptosis. The X-axis depicts Annexin- V positive cells and Y axis depicts PI positive cells. Each data point represents mean ± SD; (n=5). (*) $p<0.10$ vs. control; (**) $p<0.05$; (***) $p<0.01$ represents the linear (pairwise) change

4.3.2. Experiments with Limonene

In these set of experiments, the effects of Lim on URE induced toxicity in male swiss albino mice has been examined. Supplementation of olive oil (solvent control) did not show any significant change as compared to results obtained with normal control. therefore, we are comparing our experimental agents with normal control.

4.3.2.1. Body weight profile

Table 1 depicts the toxic effects of URE on body weight in mice. Body weight had significantly decreased in animals exposed to URE as compared to normal control; Animals co-exposed to URE + Lim showed a significant increase in body weight as compared to animals exposed to URE alone. There was no significant increase in body weight when the mice were exposed to Lim (Figure 4.19).

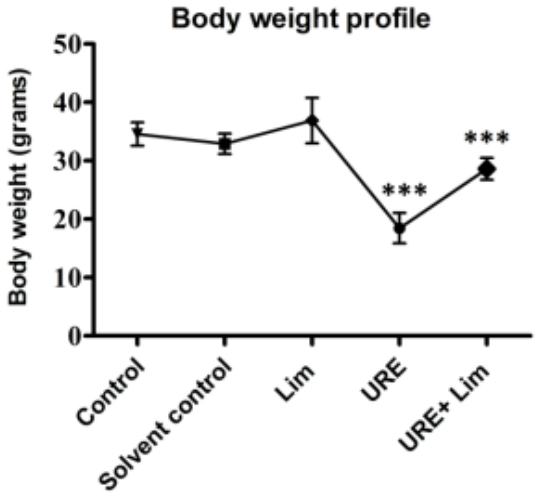

Table 4.3: Body weight of Swiss albino mice exposed to URE, Lim, and URE + Lim

Treatment	Mean Body weight	SD
Control	34.56	2.45
Sol. Control	32.56	1.74
Lim	36.87	3.89
URE	18.45	2.61
URE + Lim	27.45	1.87

Figure 4.19: Body weight gain (gms) in mice in different treatment groups

4.3.2.2. Biochemical assays in liver and lungs

4.3.2.2.1. Modulatory effects of Lim and URE on GSH levels

As compared to negative control, administration of URE has significantly decreased the GST activity in liver and lungs by 52% and 44% respectively. Co-administration of Lim with URE has significantly increased the GSH levels to 39.2% and 44.4% respectively as compared to positive (URE) control (Figure 4.20).

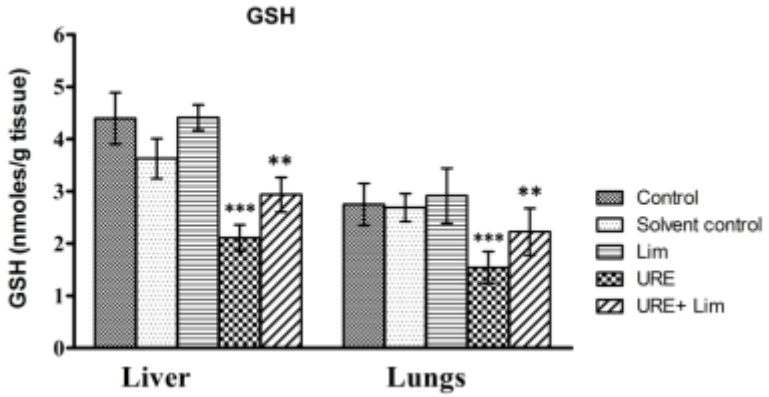

Figure 4.20: Reduced glutathione level among different treatment groups of mice. GSH content in nmole/g of tissue. Data presented as mean ± SD; (n = 5). Data was also analyzed for statistical comparison using ANOVA followed by Bonferroni test. A significance of (***) P< 0.01 and (###) P< 0.01 was considered significant.

4.3.2.2.2. Modulatory effects of Lim and URE on GST activity

As compared to negative control, administration of URE has significantly decreased the GST activity in liver and lungs by 52.5% and 62.7% respectively. Co-administration of Lim with URE has significantly increased the GST activity to 80.9% and 124% respectively as compared to positive (URE) control (Figure 4.21).

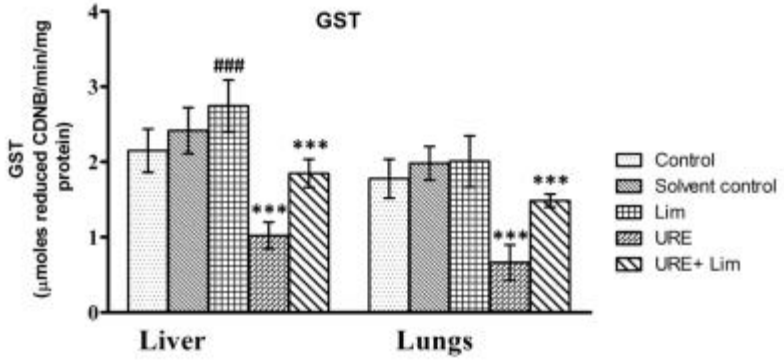

Figure 4.21: Glutathione S-transferase levels in different treatment groups of mice GST activity calculated as μ moles of reduced CDNB/min/mg of protein. Data presented as mean ± SD; (n = 5). Data was also analyzed for statistical comparison using ANOVA followed by Bonferroni test. A significance of (***) P< 0.01, (###) P< 0.01 and (##) P<0.05 was considered significant.

4.3.2.2.3. Modulatory effects of Lim and URE on catalase activity

As compared to negative control, administration of URE has significantly decreased the CAT activity in liver and lungs by 47.2% and 50.8% respectively. Co-administration of Lim with URE has significantly increased the CAT activity to 37.0% and 107.8% respectively as compared to positive (URE) control (Figure 4.22).

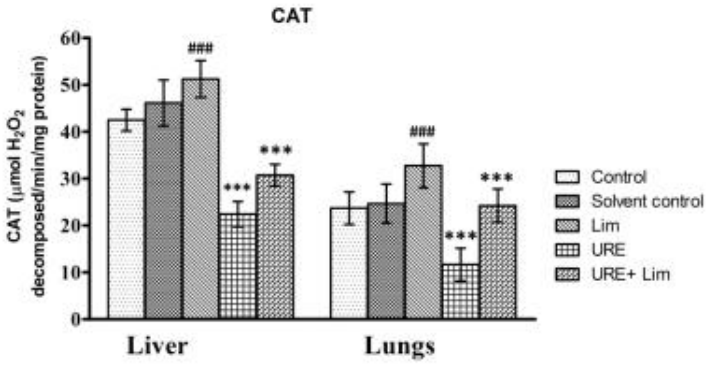

Figure 4.22: Catalase activity in different treatment groups of mice. Catalase activity calculated as decomposition of H_2O_2 in µmol/mg of protein. Data presented as mean ± SD; (n = 5). Data was also analyzed for statistical comparison using ANOVA followed by Bonferroni test. A significance of (***) P< 0.01 and (###) P< 0.01 was considered significant.

4.3.2.2.4. Modulatory effects of Lim and URE on SOD activity

As compared to negative control, administration of URE has significantly decreased the CAT activity in liver and lungs by 50.1% and 80% respectively. Co-administration of Lim with URE has significantly increased the CAT activity to 66.5% and 263.2% respectively as compared to positive (URE) control (Figure 4.23).

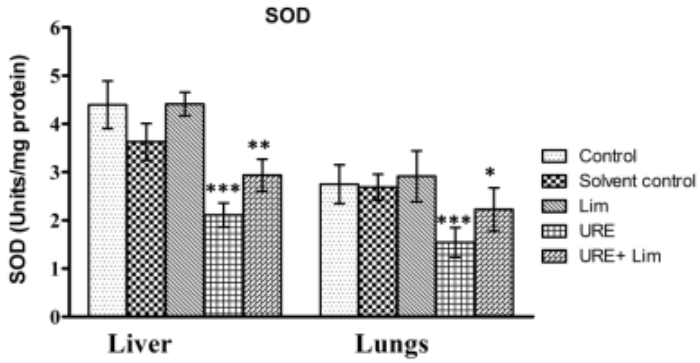

Figure 4.23: Superoxide dismutase activity in different treatment groups of mice. SOD activity in Units/mg of protein. Data presented as mean ± SD; (n = 5). Data was also analyzed for statistical

comparison using ANOVA followed by Bonferroni test. A significance of (***) P< 0.01, (**) P< 0.05 and (*) P< 0.10 was considered significant. Calculated values without symbolic notations within each row/column statistically insignificant at 5% level of probability.

4.3.2.2.5. Modulatory effects of Lim and URE on GR activity

As compared to negative control, administration of URE has significantly decreased the CAT activity in liver and lungs by 56.7% and 38.8% respectively. Co-administration of Lim with URE has significantly increased the CAT activity to 82.3% and 54.4% respectively as compared to positive (URE) control (Figure 4.24).

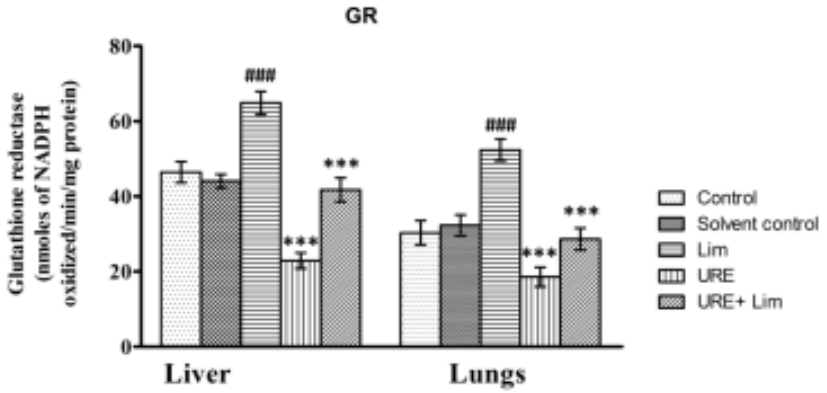

Figure 4.24: Glutathione reductase activity in different treatment groups of mice. GR activity in nmoles NADPH oxidation/min/mg of protein. Data presented as mean ± SD; (n = 5). Data was also analyzed for statistical comparison using ANOVA followed by Bonferroni test. A significance of (***) P< 0.01 and (###) P< 0.01 was considered significant. Calculated values without symbolic notations within each row/column statistically insignificant at 5% level of probability

4.3.2.2.6. Modulatory effects of Lim and URE on GPx activity

As compared to negative control, administration of URE has significantly decreased the CAT activity in liver and lungs by 30.2% and 39.6% respectively. Co-administration of Lim with URE has significantly increased the CAT activity to 27.2% and 58.9% respectively as compared to positive (URE) control (Figure 4.25).

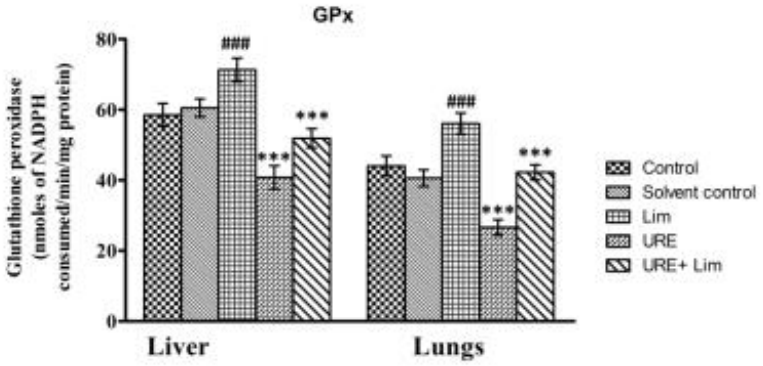

Figure 4.25: Glutathione peroxidase activity in different treatment groups of mice. Glutathione peroxidase activity in nmoles NADPH reduction/min/mg of protein. Data presented as mean ± SD; (n = 5). Data was also analyzed for statistical comparison using ANOVA followed by Bonferroni test. A significance of (***) P< 0.01 and (###) P< 0.01 was considered significant. Calculated values without symbolic notations within each row/column statistically insignificant at 5% level of probability.

4.3.2.2.7. Modulatory effects of Lim and URE on DTD activity

As compared to negative control, administration of URE has significantly decreased the DTD activity in liver and lungs by 52.5% and 48.7% respectively. Co-administration of Lim with URE has increased the DTD activity to 65.9% and 104.8% (significantly) respectively as compared to positive (URE) control (Figure 4.26).

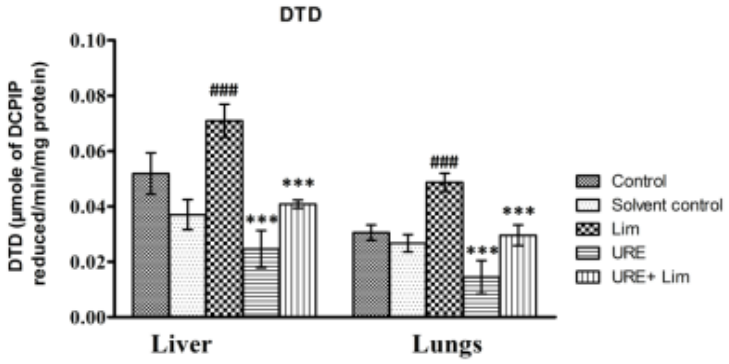

Figure 4.26: DT-diaphorase activity in different treatment groups of mice. DT-diaphorase activity in µmole of DCPIP reduction/min/mg of protein. Data presented as mean ± SD; (n = 5). Data was also analyzed for statistical comparison using ANOVA followed by Bonferroni test. A significance of (***) P< 0.01 and (###) P< 0.01 was considered significant. Calculated values without symbolic notations within each row/column statistically insignificant at 5% level of probability.

4.3.2.2.8. Modulatory effects of Lim and URE on CYP450 levels

As compared to negative control, administration of URE has significantly decreased the CYP450 activity in liver and lungs by 45.6% and 39.2% respectively. Co-administration of Lim with URE has increased the CYP450 activity to 118.1% and 209.1% (significantly) respectively as compared to positive (URE) control (Figure 4.27).

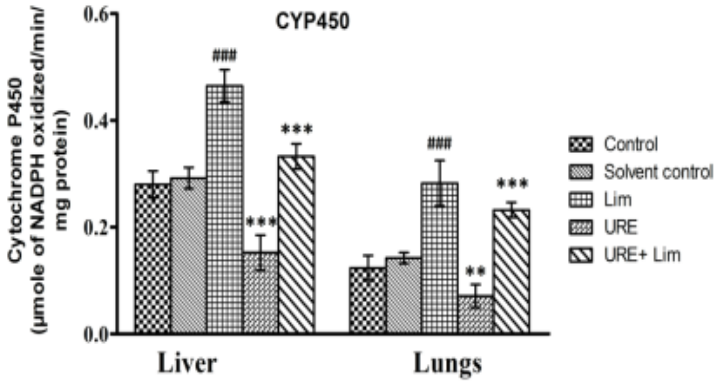

Figure 4.27: Cytochrome P450 levels in different treatment groups of mice. Cyt P450 activity in µmoles NADPH oxidation/min/mg of protein. Data was also analyzed for statistical comparison using ANOVA followed by Bonferroni test. A significance of (***) P< 0.01, (###) P< 0.01 and (**) P< 0.05 was considered significant Calculated values without symbolic notations within each row/column statistically insignificant at 5% level of probability.

4.3.2.2.9. Modulatory effects of Lim and URE on LPO (MDA content)

As compared to negative control, administration of URE has significantly increased the LPO activity in liver and lungs by 73.2% and 104.2% respectively. Co-administration of Lim with URE has significantly decreased the LPO activity to 26.3% and 25.0% respectively as compared to positive (URE) control (Figure 4.28).

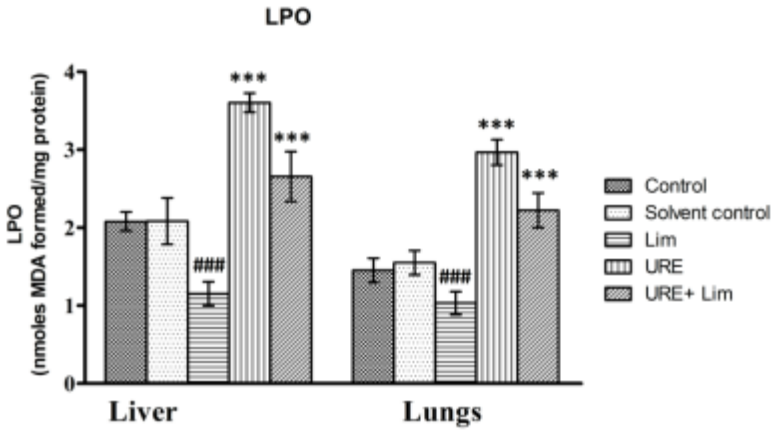

Figure 4.28: Lipid peroxidation levels in different treatment groups of mice. Lipid peroxidation levels in nmoles of MDA formed /mg of protein. Data was also analyzed for statistical comparison using ANOVA followed by Bonferroni test. A significance of (***) P< 0.01 and (###) P< 0.01 was considered significant. Calculated values without symbolic notations within each row/column statistically insignificant at 5% level of probability.

4.3.2.2.10. Modulatory effects of Lim and URE on LDH activity

As compared to negative control, administration of URE has significantly increased the LDH activity in liver and lungs by 125.3% and 110.1% respectively. Co-administration of Lim with URE has significantly decreased the LDH activity to 63.3% and 71.9% respectively as compared to positive (URE) control (Figure 4.29).

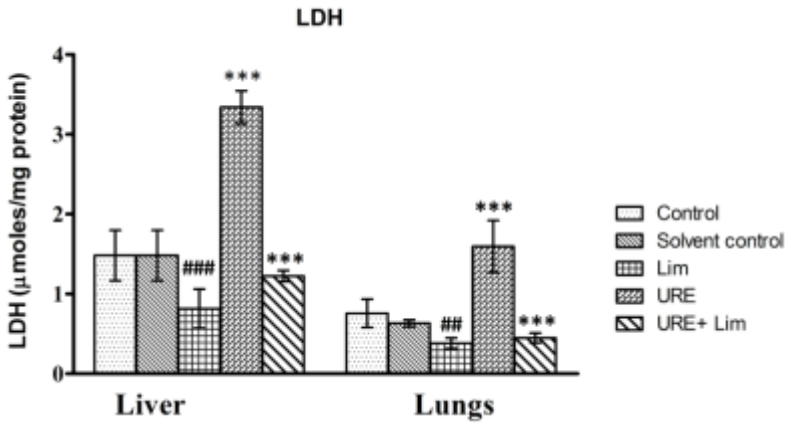

Figure 4.29: Lactate dehydrogenase level in different treatment groups of mice. Lactate dehydrogenase levels in µmoles/mg of protein. Data was also analyzed for statistical comparison using ANOVA followed by Bonferroni test. A significance of (***) P< 0.01, (###) P< 0.01 and (##) P< 0.05 was considered significant. Calculated values without symbolic notations within each row/column statistically insignificant at 5% level of probability.

4.3.2.3. Visualization of the apoptosis by AO/EtBr staining:

Apoptosis data obtained from AO/EtBr staining method is shown. The results analysis showed that percentage of apoptotic and dead cells were reduced in combined treatment of URE + Lim (20.9 ± 7.3) as compared to URE (38.8 ± 9.4) alone group (Table 1). AO penetrates into living cells, emitting green fluorescence after intercalation with DNA, the results analysis showed that in control and Lim group, the ratio of live cells were more as compared to URE group (1.6 fold increase) where the cells were stained with orange-yellow and red due to loss of membrane integrity and shrunken nuclear material which allows penetration of EtBr stain. The combined treatment of URE + Lim has significantly reduced the apoptotic cells (0.8 fold decrease) (Figure 4.30).

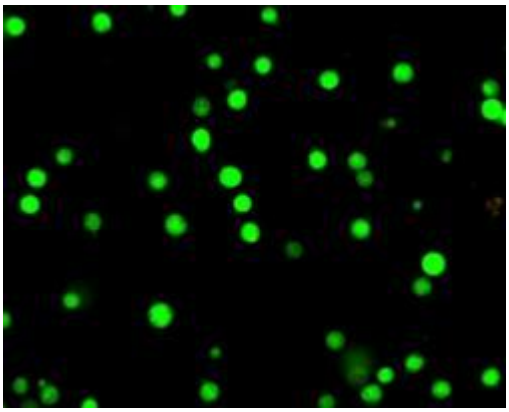

(A) Control

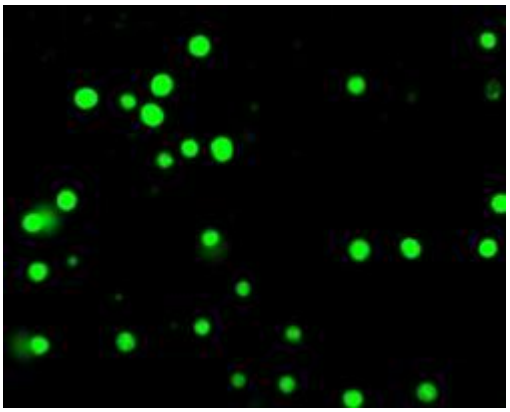

(B) Lim

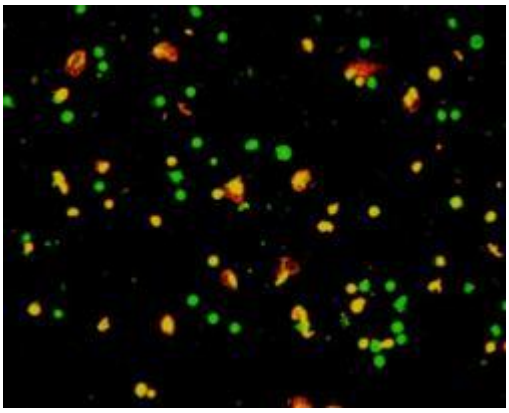

(C) URE

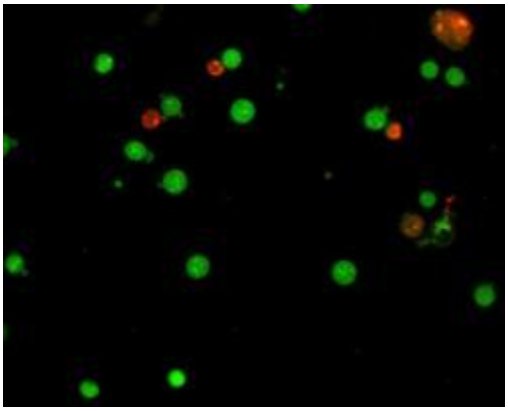

(D) URE + Lim

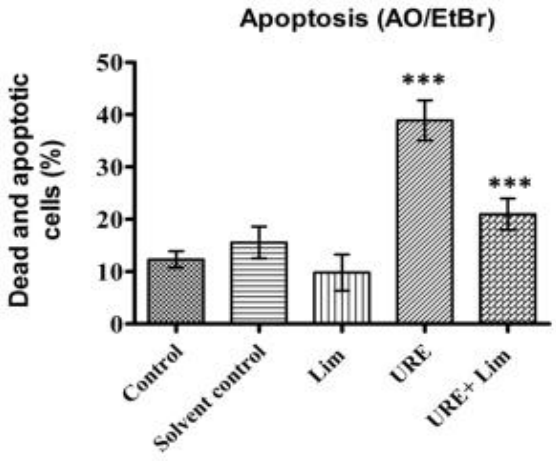

Figure 4.30: Effect of Lim and URE on apoptosis of bone marrow cells a) photomicrographs depicting live, apoptotic and dead cells. b) bar diagram showing the percentage of apoptotic and dead cells. Each data point represents mean ± SD of 1000 cells from five independent experiments. (*) $p<0.10$ vs control; (**) $p < 0.05$; (**) $p < 0.01$ represents the linear (pairwise) change.

4.3.2.3. Histopathological studies

The histopathological analysis was carried out using H&E staining in lungs, liver, kidney, intestines and testis of mice for all the control and treated groups.

The histopathological changes in lungs of control, URE and Lim, exposed mice (individually or in combination) are shown in Figure 4.31. URE treated lung showed alveolar spaces filled with edema fluid as compared to normal control and Lim treated mice where lungs section showed normal bronchiole and alveolar spaces and no infiltration or edema is seen. On the other hand, combined doses of URE + Lim treated lung showed significant changes where alveolar spaces were partially filled with edema fluid.

The hepatic section from the URE treated liver showed portal triad with damaged hepatocytes in the periportal area with the presence of inflammatory cells as compared to control, and Lim treated mice, where, portal triad showed normal hepatocytes and no inflammatory cells were observed. The combined treatment of URE + Lim has significantly reduced the damaged hepatocytes in the portal area with no evidence of inflammatory cells. (Figure 4.32).

The histopathological changes in testis of control, URE and Lim treated mice are shown in Figure 4.33. URE treated testis showed few apoptotic bodies (2 to 4/HPF) in the basal layers of the seminiferous tubules in comparison to control and Lim treated groups which did not show any significant changes in the morphology. The combined effect of URE+ Lim has significantly reduced the degree of apoptosis and restored the normal tissue morphology.

The histopathological changes in intestines of control, URE and Lim, treated mice are shown in Figure 4.34. URE treated animal showed a significant increase in the number of apoptotic bodies (8 to 10 /HPF) in epithelial cells of intestinal crypts as compared to control and Lim treated group, which showed few (0 to 1 / HPF) apoptotic bodies in epithelial cells. The presence of apoptotic bodies were significantly reduced (2 to 3 /HPF) when mice were treated with the combined dose of URE + Lim.

The histopathological changes in kidneys of control, URE and Lim, treated mice are shown in Figure 4.35. In the case of renal tissue of control and Lim treated mice, the glomerulus surrounded by renal tubules showed normal histological morphology as compared to URE treated group animal where the periglomerular space show presence of hyaline casts, indicating the leakage of proteinaceous material through the glomerulus. However, unlike in URE treated group, animals treated with URE + Lim resulted in the restoration of the normal cortical architecture (evidenced by the clear and occasional tubules that showed the presence of small hyaline casts with a lesser degree of protein leakage through the glomerulus.

4.3.2.3.1. Histopathological observation in lungs

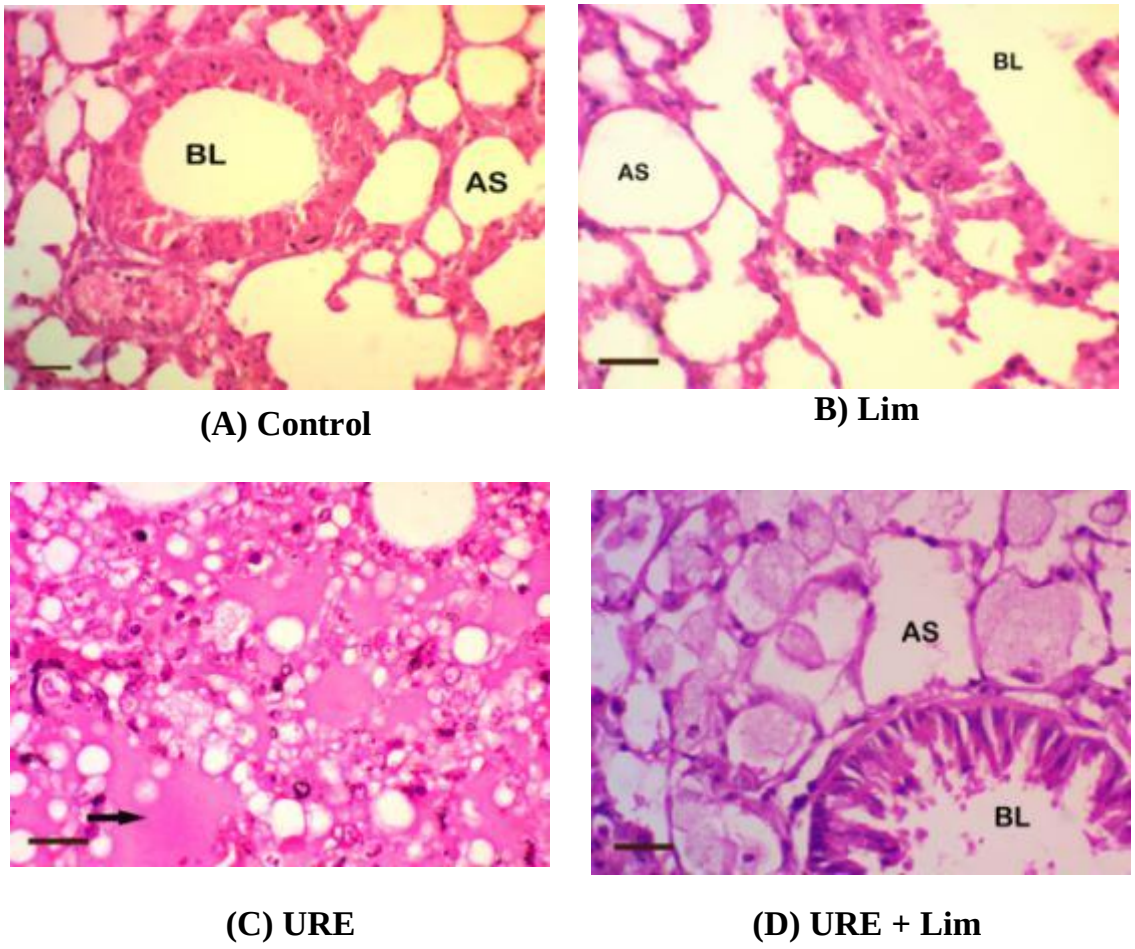

(A) Control **B) Lim**

(C) URE **(D) URE + Lim**

Figure 4.31: High power photomicrograph of histopathological analysis of control, URE and Lim treated mice lung tissue, (H&E X 40x). A and B: Control and Lim group showed normal bronchiole and adjacent alveolar spaces. No infiltration or edema is seen. C) URE treated lung showed alveolar spaces filled with edema fluid. D) URE + Lim treated lung showed alveolar spaces partially filled with edema fluid. The changes seen in this sample are less than that seen in URE treated animals. BL = Bronchial Lumen, AS = Alveolar Space.

4.3.2.3.2. Histopathological observation in liver

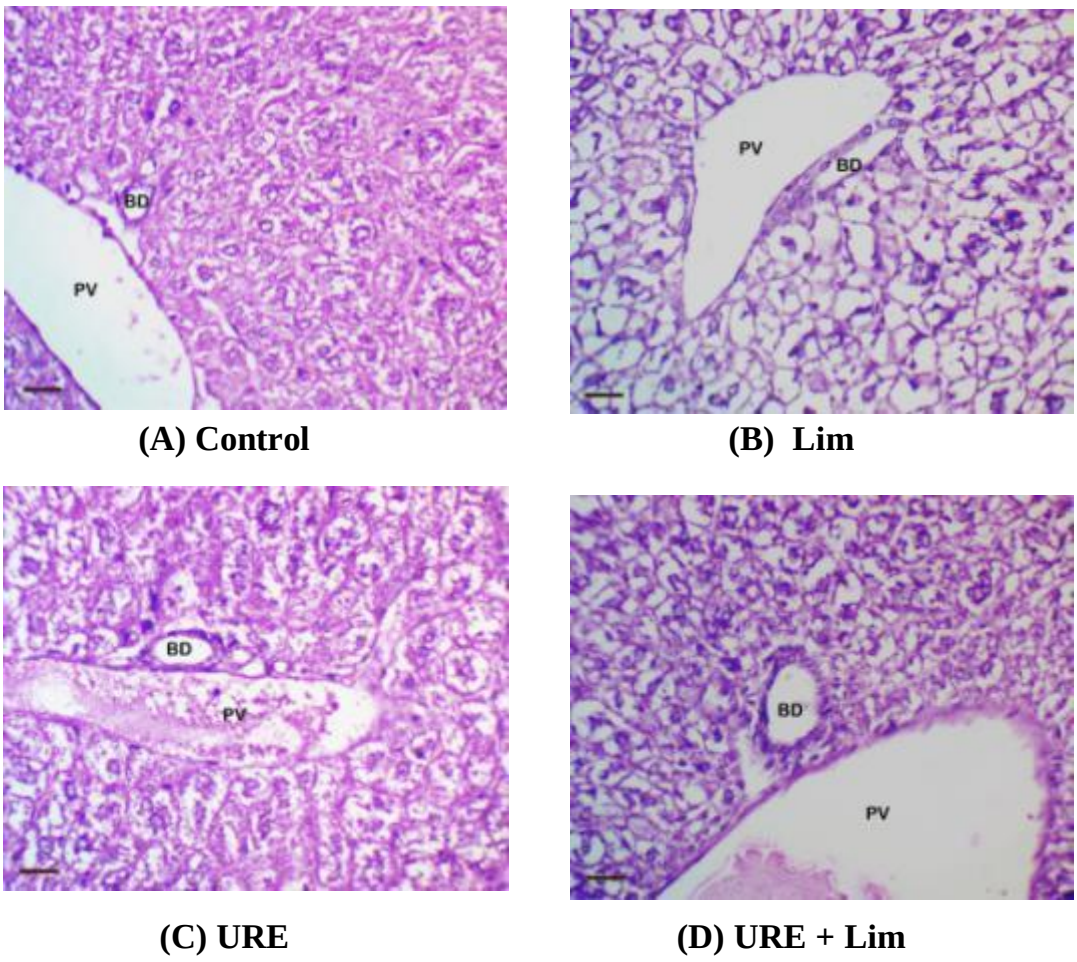

(A) Control **(B) Lim**

(C) URE **(D) URE + Lim**

Figure 4.32: High power photomicrograph of histopathological analysis of control, URE and Lim treated mice liver tissue, (H&E X 40x). Portal triad from the control and Lim treated liver showed normal portal triad structures with adjacent normal hepatocytes in the periportal area. No inflammatory cells are present. C) URE: URE treated liver showed portal triad with damaged hepatocytes in the periportal area. Inflammatory cells are present. D) URE + Lim: Liver showed portal triad with attenuated hepatocytes in the periportal area. No inflammatory cells are present. PV = Portal Vein, BD = Bile Duct.

4.3.2.3.3. Histopathological observation in testis

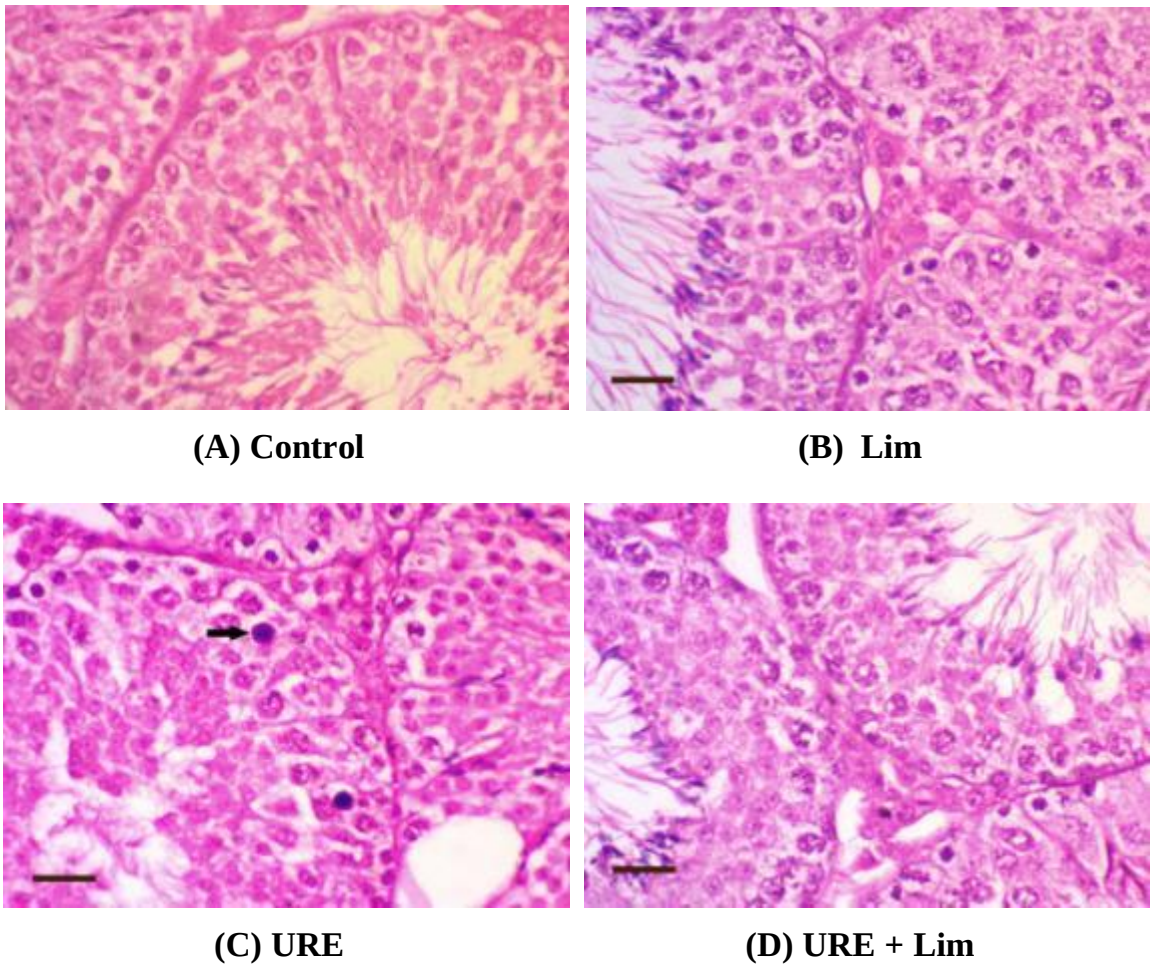

Figure 4.33: High power photomicrograph of histopathological analysis of control, URE and Lim treated mice testes, (H&E X 40x). A and B: Testis from control group animal showed the normal histological appearance of seminiferous tubules. No apoptotic bodies were seen. B) Lim: Testis from an animal treated with Lim showed the normal histological appearance of seminiferous tubules. No apoptotic bodies were seen. C) URE: Testis from URE treated animal showed few apoptotic bodies (2 to 4/HPF) in the basal layers of the seminiferous tubules. D) URE + Lim: Testis from URE + Lim treated animals showed the normal histological appearance of seminiferous tubules. No apoptotic bodies were seen.

4.3.2.3.4. Histopathological observation in intestines

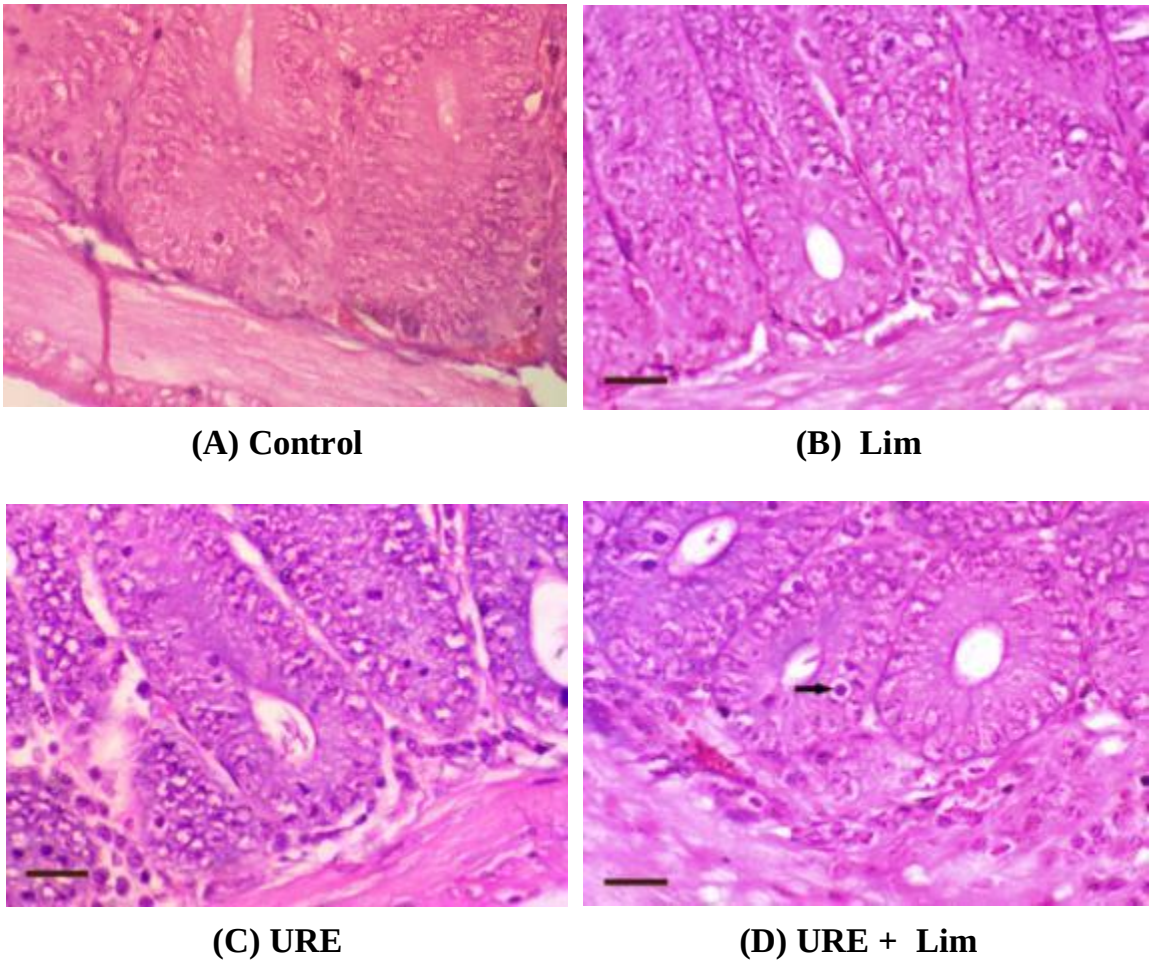

Figure 4.34: High power photomicrograph of histopathological analysis of control, URE and Lim treated mice intestines, (H&E X 40x). A and B: Intestinal crypts from the animal in control and Lim showed few (1 to 2 / HPF) apoptotic bodies in epithelial cells. C) URE: Intestinal crypts from the animal in URE group showed an increase in a number of apoptotic bodies (5 to 7 /HPF) in epithelial cells. D) URE + Lim: Intestinal crypts from the animal in URE + Lim group showed comparatively reduced the number of apoptotic bodies (2 to 3 /HPF) in epithelial cells.

4.3.2.3.5. Histopathological observation in kidneys

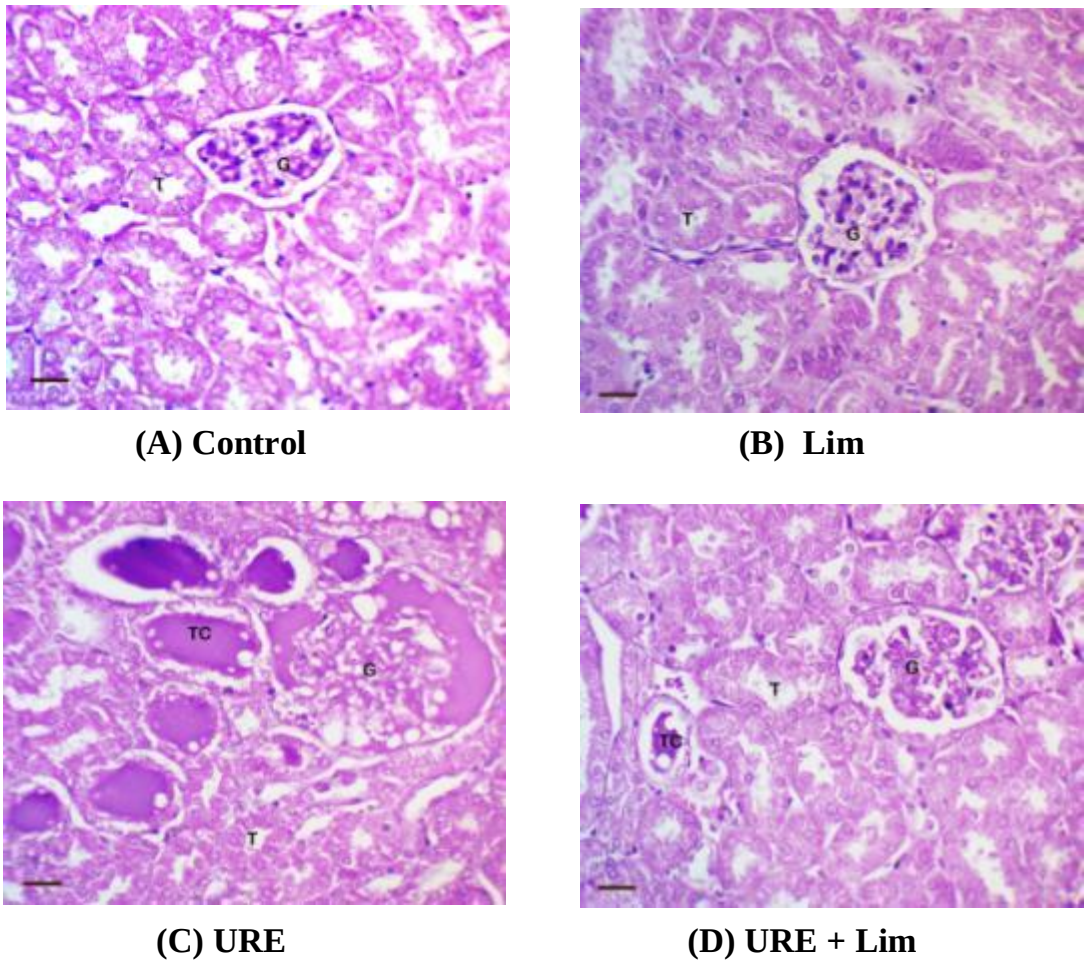

(A) Control **(B) Lim**

(C) URE **(D) URE + Lim**

Figure 4.35: High power photomicrograph of histopathological analysis of control, URE, Lim treated mice kidneys, (H&E X 40x). A) and B): Kidney from control and Lim group animal showed normal renal tissue with a glomerulus surrounded by renal tubules. C) URE: Kidney from URE treated group animal showed renal tissue with a glomerulus surrounded by renal tubules. The periglomerular space and several tubules show the presence of hyaline casts indicating leakage of proteinaceous material through the glomerulus. D) URE + Lim: Kidney from URE + Lim treated group animal showed renal tissue with a glomerulus surrounded by renal tubules. The periglomerular space is clear and occasional tubules showed the presence of small hyaline casts. The degree of protein leakage appeared to be significantly less in this sample. G = Glomerulus, T = Tubules, TC = Tubular Cast.

4.3.2.4. Evaluation of DNA damage by comet assay

The genotoxic potential of normal and exposed animals was evaluated by performing comet assay using the whole blood from mice as shown in Figure 4.36. In control group animals, no comets were observed indicating an intact DNA structure as compared to URE treated mice which showed a significant increase (3.1 fold) in the comet length, measured in the form of the olive tail moment. Co-administration of URE and Lim significantly reduced (0.9 ~1 fold) the DNA damage as compared to URE treatment alone, indicated by comparatively reduced comet tail length (Figure 4.36).

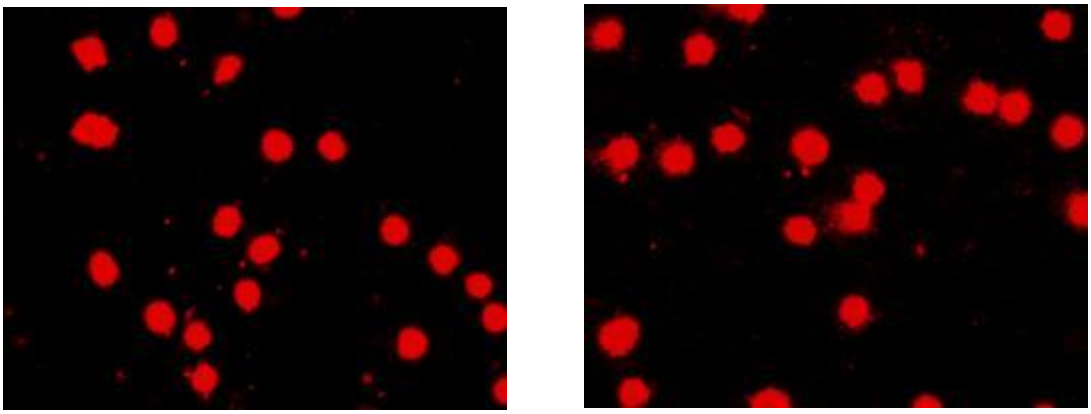

(A) Control **(B) Lim**

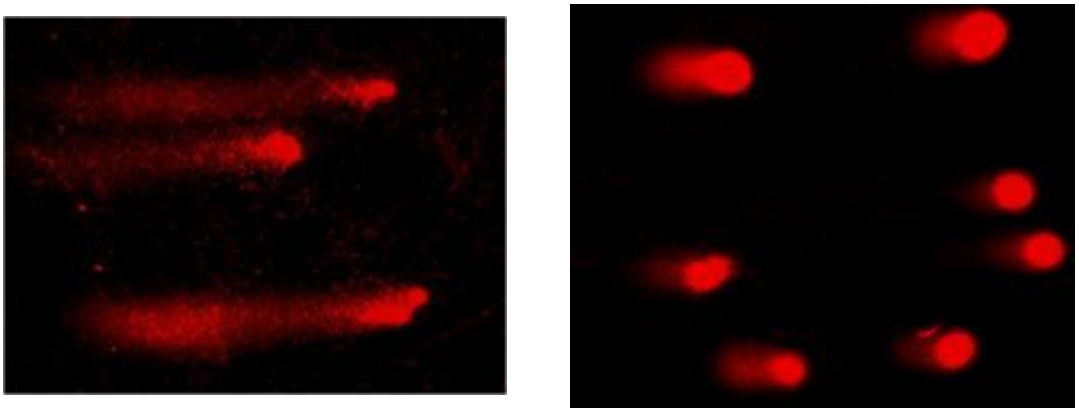

(C) URE **(D) URE + Lim**

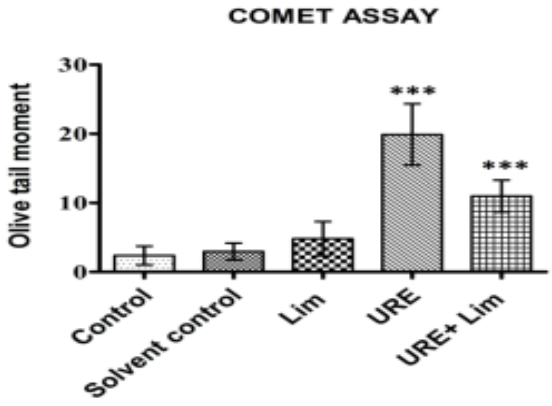

Figure 4.36: Effect of Lim on URE-induced DNA damage in mice. a)- A) Control, (B) Lim, (C) URE, (D) URE + Lim. b) Bar graph showing the olive tail moment of comets observed in different treatment groups. Each data point represents mean ± SD of 250 cells from fi five independent experiments. (*) $p < 0.10$ vs control; (**) $p < 0.05$; (**) $p < 0.01$ represents the linear (pairwise) change.

4.3.2.5. Evaluation of apoptosis by Annexin V (FITC) and PI staining method

The extent of apoptosis in bone marrow cells was evaluated by flow cytometric method using FITC-conjugated Annexin V/PI. The apoptotic rate by different treatment groups was quantified by Annexin V and PI staining. Treatment with URE resulted in significant increase in apoptosis by 76.3 % (only Annexin V positive) as compared to control group. Co-treatment of URE + Lim has significantly reduced the percentage of apoptotic cells by 28.9% (Figure 4.37-4.38).

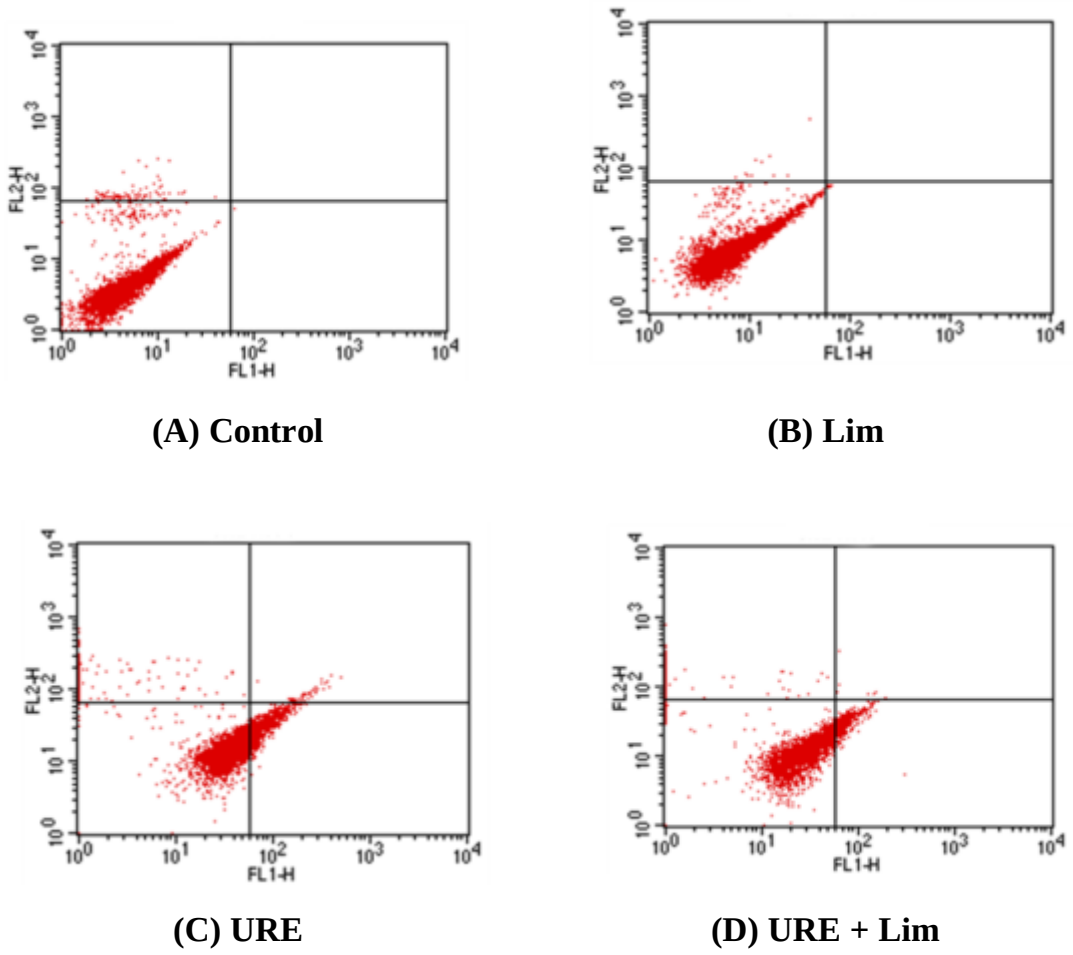

Figure 4.37: Effects of control, URE, Lim and its combination (URE+ Lim) exposure on apoptosis. The X-axis depicts Annexin- V positive cells and Y axis depicts PI positive cells.

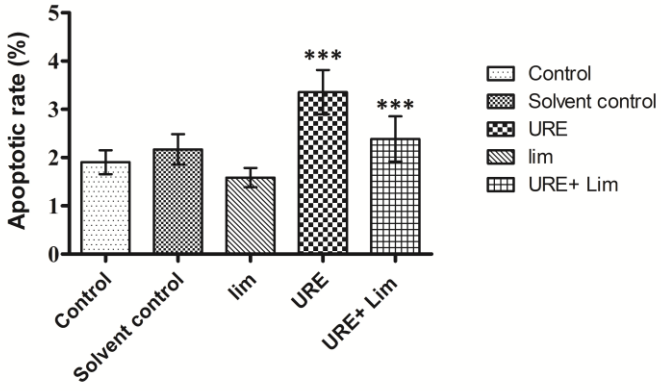

Figure 4.38: Comparison of the Annexin V and PI positive cells. The percentage of early/late apoptosis and necrosis were significantly more as compared with normal cells in the bar graph. Each data point represents mean ± SD; (n=5). (*) $p < 0.10$ vs. control; (**); (**) $p < 0.05$; (**) $p < 0.01$ represents the linear (pairwise) change.

4.3.2.6. Immunohistochemistry studies to analyze of p53, Bcl-2 and PARP protein in mice testis:

To evaluate the protective effects of TAX and Lim against URE on apoptotic and antiapoptotic proteins, expression levels of p53, Bcl-2 and PARP were observed in the basal, spermatid layers and in seminiferous tubules of the mice testes (Figure 29). The immunoreactivities of p53 protein in basal and in spermatid layer were found highest in the URE treated groups indicated by strong staining. Treatments of TAX and Lim in combination with URE significantly lower down the p53 immunoreactivity and showed mild to moderate p53 expression in seminiferous tubules. Similarly, the control group also showed mild to moderate p53 immunostaining throughout the tubule. The relatively less staining of p53 in groups treated with TAX and Lim in combination with

URE as compared to groups with URE treatment suggests that the TAX and Lim treatment reduced the levels of p53 and thus apoptosis in testes. (Figure 4.39)

The Bcl-2 expression in the control group and in groups treated with TAX and Lim in combination with URE show strong positive staining in the basal and spermatid layer of testes. On the other hand, groups treated with URE alone show very mild immunoreactivity in the basal layer. These staining patterns indicate that URE reduces expression of Bcl-2 in testes which further suggests that co-treatment of URE with TAX and Lim significantly restores the Bcl-2 expression to normal levels (Figure 4.40)

Immunostaining of PARP protein in the group treated with URE alone group showed strong immunoreactivity in both basal and spermatid layer of testis as compared to control group. Co-treatment of URE + TAX showed moderate immunoreactivity in the basal layer only in contrast to Co-treatment of URE + Lim which showed moderate immunoreactivity in both basal and spermatid layer in comparison to the group treated with URE alone. These staining patterns suggest that both TAX and Lim when treated with URE significantly reduce the expression of PARP protein in testes (Figure 4.41)

These results indicate that treatment of TAX and Lim in combination lower down URE induced cellular apoptosis by lowering down the expression of p53 and PARP protein and enhance cellular survival by increasing expression of the Bcl-2 protein.

4.3.2.6.1. Immunohistochemistry studies with p53

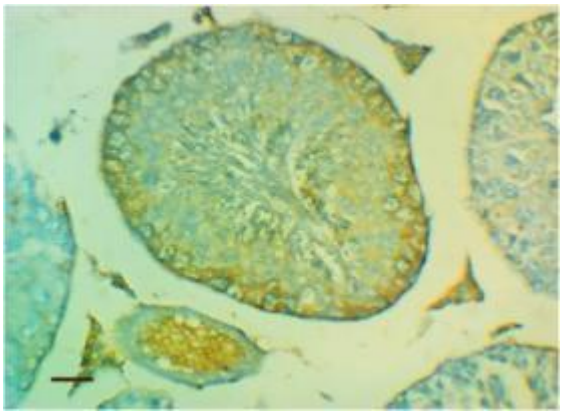

A) Normal control. Mild to moderately positive staining is seen throughout the tubule (IHC p53 x 400).

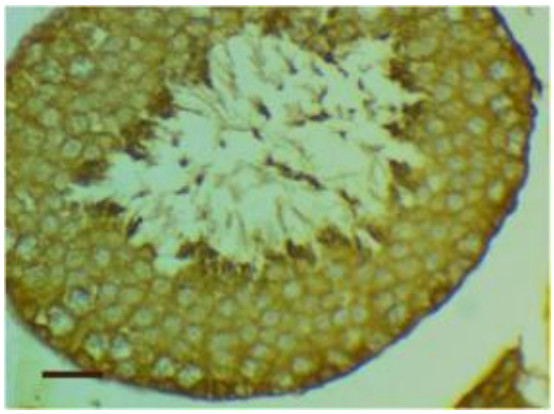

B) URE: A positive staining is seen in the basal layer. The spermatid layer shows p53 staining (IHC p53 x 400).

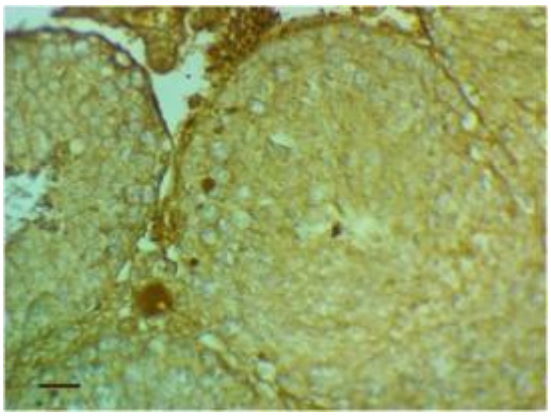

C) URE + TAX: Moderately positive staining is seen throughout the tubule (IHC p53 x 400).

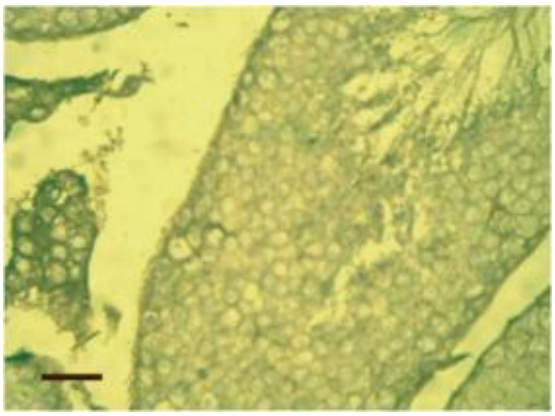

D) URE + Lim: Mild to moderately positive staining is seen throughout the tubule. (IHC P53 x 400

Figure 4.39: High power photomicrograph of a section of testis stained with immunohistochemical stain for p53, (IHC p53 x 400). A) Normal control: staining moderately, B) URE: stains positively, C) URE+TAX and D) URE + Lim: stains moderate to positively for p53 antibody

4.3.2.6.2. Immunohistochemistry studies with Bcl-2

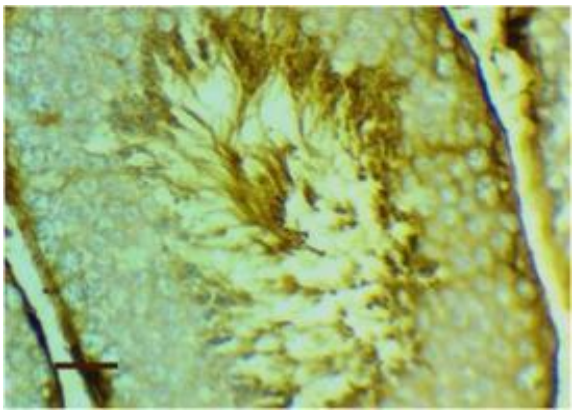

A) Normal control. Positive staining is seen in the basal layer and also in the spermatid layer (IHC Bcl-2 x 400).

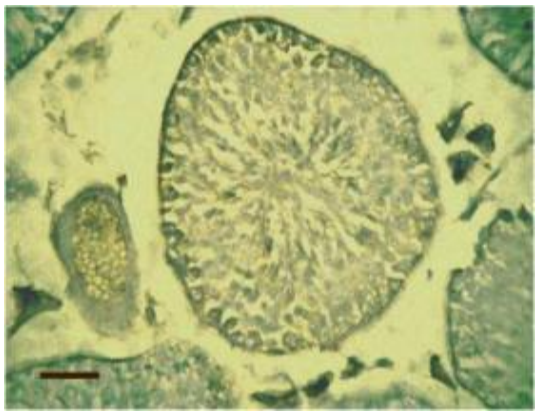

B) URE: A very mild staining is seen in the basal layer. The spermatid layer does not show any staining (IHC Bcl-2 x 400).

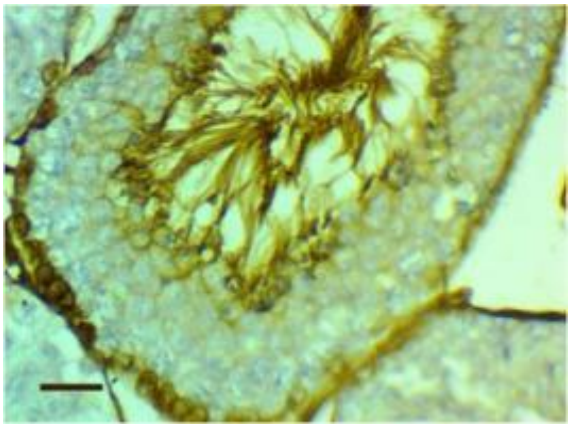

C) URE+TAX: Positive staining is seen in the basal layer and also in the spermatid layer (IHC Bcl-2 x 400).

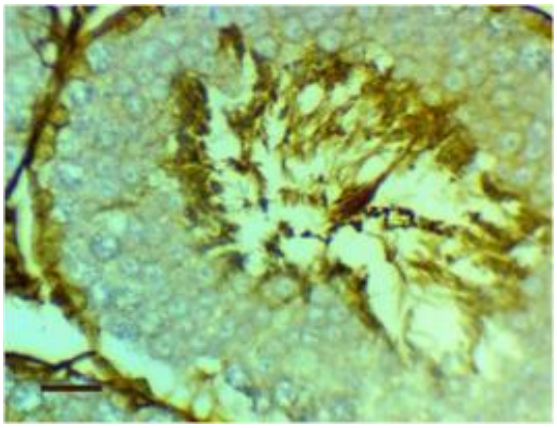

D) URE+Lim: Positive staining is seen in the basal layer and also in the spermatid layer. (IHC Bcl-2 x 400).

Figure 4.40: High power photomicrograph of a section of testis stained with immunohistochemical stain for Bcl-2, (IHC Bcl-2 x 400). A) Normal control: staining positively, B) URE: stains mildly, C) URE+TAX and D) URE+Lim: stains positively in the basal spermatid layer for the Bcl-2 antibody.

4.3.2.6.3. Immunohistochemistry studies with PARP

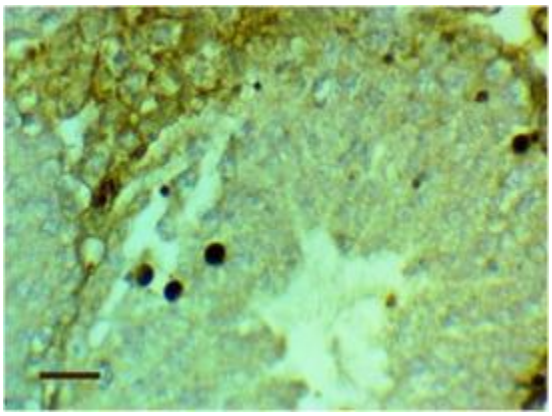

(A) Normal control. Moderately positive staining is seen in the basal layer. (IHC PARP1 x 400)

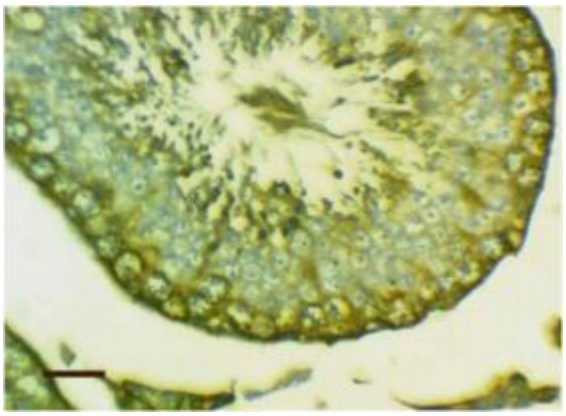

B) URE: Strong staining is seen in the basal layer and also in the spermatid layer. (IHC PARP1 x 400)

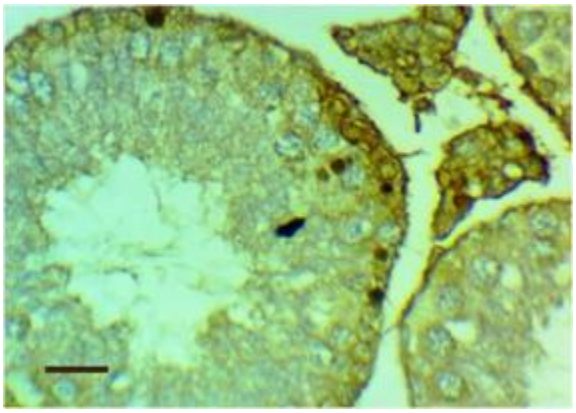

C) URE+TAX: Moderately positive staining is seen in the basal layer. (IHC PARP1 x 400)

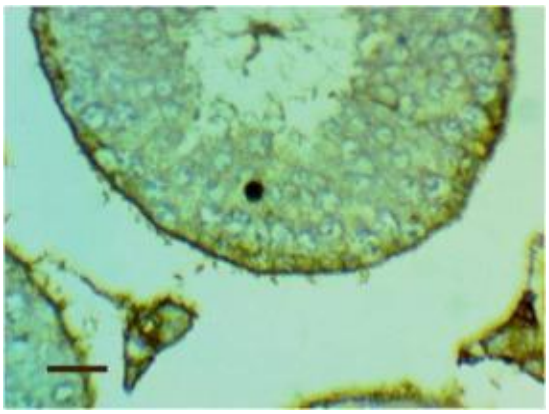

D) URE+Lim: Moderately positive staining is seen in the basal layer and also in the spermatid layer. (IHC PARP1 x 400)

Figure 4.41: High power photomicrograph of a section of testis stained with immunohistochemical stain for PARP, (IHC PARP1 x 400). A) Normal control: staining moderately in the basal layer, B) URE: stains positively in basal and spermatid layer, C) URE+TAX: stains moderate positively in the basal layer and D) URE+ Lim: stains moderate to positively in both basal and spermatid layer for the PARP antibody.

4.3.2.7. Western blot analysis of the expression of p53, and Bcl-2 protein

To study the apoptotic and antiapoptotic effects, we analyzed the expression levels of p53 and Bcl-2 proteins in tissue samples of liver for all the groups including control; group treated with URE alone and groups treated with TAX and Lim in combination with URE (Figure 4.4.2)

The expression of the apoptotic protein, p53 was highest in URE treated groups and lowest in the group treated with Lim alone. The p53 expression in control group was lower than URE alone treated group. On the other hand, the groups treated with TAX and Lim in combination with URE reduced the expression of p53 with respect to both control and URE alone treated groups.

Expression of Bcl-2 protein was highest in groups treated with Lim alone, followed by the control group. The URE alone treated group maximally reduced the expression of Bcl-2 in comparison to all the groups. Co-treatment of URE with TAX and Lim has significantly increased the Bcl-2 expression as compared with URE treatment.

The western blotting analysis clearly shows that both TAX and Lim in combination with URE reciprocally alter the expressions of p53 and Bcl-2 proteins in comparison to URE alone. The expression analysis of western blot suggests that both TAX and Lim can reduce URE induce cellular apoptosis and enhance cell survival by lowering the levels of p53 and by elevating the levels of anti-apoptotic protein Bcl-2.

4.3.2.7.1. Western blot and analysis for the expression of p53, and Bcl-2 protein:

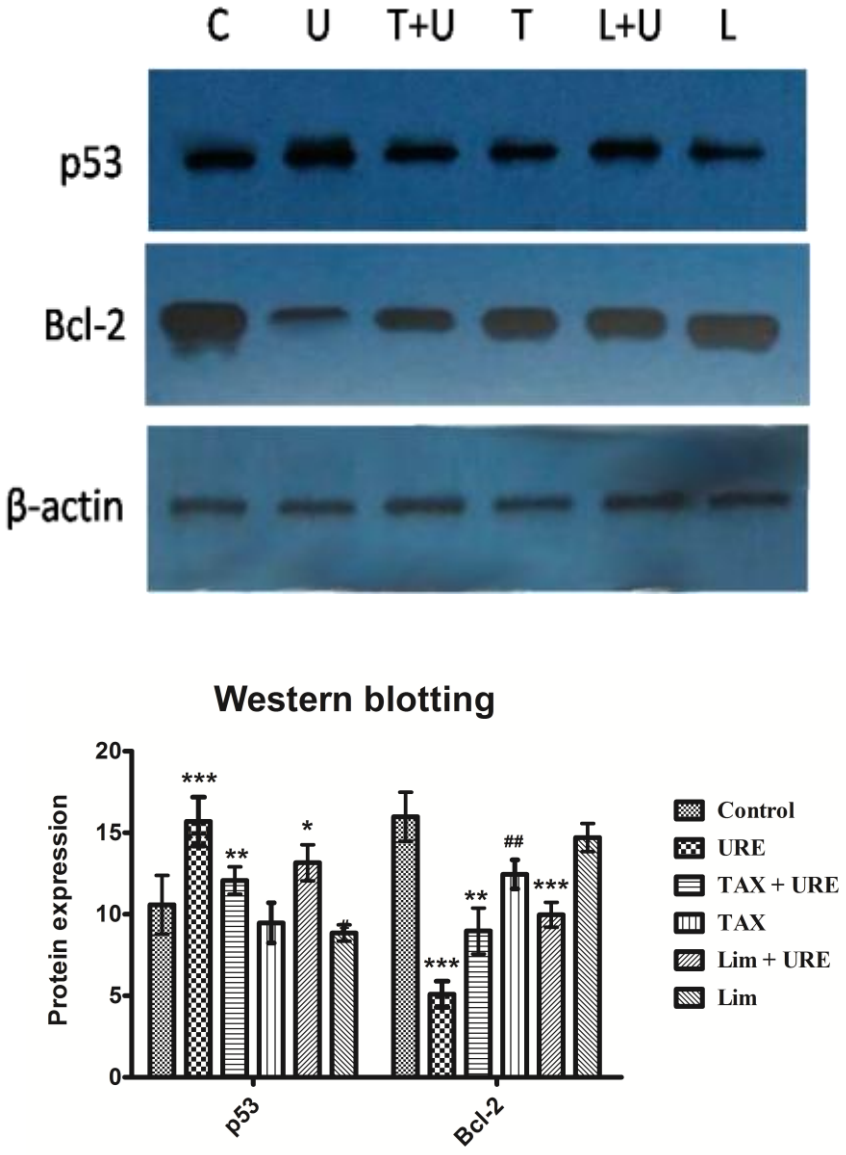

Figure 4.42: Western blot analysis: a) Expression profile of p53 and Bcl-2 proteins in liver tissues of mice with different treatment groups. b) bar diagram shows the mean band intensity. Each data point represents mean ± SD (n = 3). (##) $p < 0.05$ vs. control, (*) $p < 0.10$, (**) $p < 0.05$, (***) $p < 0.01$ vs. URE control. (C=control, U=URE, T+U=Tax + URE, T=Tax, L+U= Lim + URE, L=Lim).

4.4. Discussion

Urethane is a by-product found ubiquitously in almost all fermented beverages and in varieties of fermented products including cheese, yogurt, bread, etc. It is known to cause chromosome breakage, lethal mutations (Robson, 1941) and increases frequencies of sister chromatid exchange (Cheng et al., 1981). URE is reported to cause malignancies in various organs of mice which include liver, lungs, blood (Williams and Nery, 1971) and testes (Sotomayor et al., 1994). URE acts as a promutagen, and most of its effects are observed after its metabolization (Rogers, 1955), where the metabolic products interacts with DNA and RNA (Williams and Nery, 1971). Although URE can induce tumors in various organs, it predominantly induces malignancies in liver and lungs (Kaye, 1960; Bateman, 1976). Age-dependent studies on URE exposure to mice indicate that the frequency of development of liver and lung malignancies is relatively more in newborns or very young animals in comparison to adult mice (De Benedictis et al., 1962; Chieco-Bianchi et al., 1963). Different reports suggest that development of malignancies in lung tissues on exposure to URE is due to intrinsic properties of lung tissues and URE promotes this property (Field and Lang, 1988). Further, a study on mutational analysis of URE in the development of lung cancer suggests that URE induces point mutations which lead to the development of lung cancer (Tomisawa et al., 2003). Similarly, development of liver malignancies upon exposure to URE is due to the presence of susceptible genes mapped to chromosomes 7, 8 and 12 (Gariboldi et al., 1993).

In the present study, we have analyzed the antioxidant performance of TAX and Lim against URE induced oxidative stress by the assessment of various biochemical

enzymes. Further, to determine the antiapoptotic effects of both TAX and Lim against URE induced cellular apoptosis, we have performed AO/EtBr staining and flow cytometry by Annexin V- FITC staining. URE genotoxicity is associated with DNA damage. Hence comet assay has been performed to analyze the effects of URE alone and in combination with TAX and Lim on DNA damage. Also, we have examined the effects of URE and phytochemicals treatment on the histopathology of vital organs by hematoxylin and eosin (H&E) staining. Further western blot (in the liver) and immunohistochemistry (in testes) have been performed to check the expression of key regulatory apoptotic (p53), antiapoptotic (Bcl-2) and DNA repair protein (PARP).

Antioxidant enzymes are endogenous cellular defense system which neutralizes harmful ROS and free radicals and maintains cellular redox status. ROS and free radicals species are associated with myriads of pathological conditions including cancer, Alzheimer's disease, diabetes, atherosclerosis, the aging process, etc. Thus, antioxidant enzymes play an essential role in the maintenance of systemic health. The antioxidant enzyme system includes GST, GPx, GR, SOD and CAT. The glutathione S-transferases (GST) are phase II detoxification cytosolic enzymes. Their functions include electrophilic substitution of free radicals to GSH, peroxidation, and isomerisation (Sheehan et al., 2001). GSH is a tripeptide sequence of glutamine, cysteine, and glycine (Glu-Cys-Gly), which attenuates oxidation of thiol groups either by interacting directly with free radicals or indirectly by interacting with GST. Glutathione peroxidase (GPx) is an enzyme that neutralizes hydrogen and lipid peroxide radicals. Glutathione reductase (GR) catalyzes the reduction of oxidized glutathione (GSSG) to reduced glutathione (GSH) and thus maintains the cellular GSH levels (Chang et al., 1978). SODs are

metalloproteins that neutralize superoxides, while catalases are responsible for hydrogen peroxide turnover. Increased levels of these antioxidant enzymes and proteins are indicative of a reduction in oxidative stress condition. While the elevated levels of markers like MDA, and CYP450 indicate oxidative stress (Krishnamurthy and Wadhwani, 2012). TAX is dietary phytochemical with known antilipoperoxidant and antiradical properties, (Burda et al., 2001) and is structurally similar to quercetin. In our studies, co-administration of TAX with URE enhances the levels of GSH, GST, Catalase, SOD, GPx and GR and mitigates the genotoxic effects of URE in liver and lungs. Our findings are in agreement with previous reports where TAX enhanced tissue antioxidant enzyme activities (SOD, CAT, GPx and GR) and GSH levels in mice colon upon treatment of carcinogen 1, 2-dimethylhydrazine (Manigandan et al., 2014). Similarly, in another independent study, TAX is reported to elevate the levels of CAT, GPx, GR and SOD in zebrafish larvae exposed to cadmium (Manigandan, Jayaraj, et al., 2015). In our studies, TAX lowers the MDA and LDH levels in liver and lungs upon URE exposure. Similar reports addressing the attenuation of MDA levels (Manigandan et al., 2014; Manigandan, Jayaraj, et al., 2015) and LDH levels (Svobodová et al., 2006; Manigandan et al., 2015) strongly support that TAX attenuates free radicals by not only increasing the levels of antioxidant enzymes but also by inhibiting the processes associated with generation of free radicals. In our studies, Lim significantly increases the levels of GSH, GST, Catalase, SOD, GPx and GR and mitigates the genotoxic effects of URE in liver and lungs. These findings are also in accordance with previous reports where Lim is reported to increase GSH (Reicks and Crankshaw, 1993), and GST levels in liver (Van Lieshout et al., 1998; Murali et al., 2013). Reports with enhanced

levels of catalase, peroxidases and SOD in murine lymphocytes (Roberto et al., 2010; Murali et al., 2013) further supports our findings. In our studies, Lim decreases lipid peroxidation, and these observations are in agreement with recent reports where Lim decreases lipid peroxidation in streptozotocin-induced diabetic rats (Murali et al., 2013). We also observed that co-administration of Lim with URE reduced LDH leakage as compared to URE alone. Our findings are in concurrence with recent reports on antioxidative effects of Lim on doxorubicin-induced stress in kidney of Wistar rats, where Lim treatment not only reduced LDH leakage, it also reduced MDA levels and enhanced the levels of GSH, GST, CAT, SOD, GPx and GR (Rehman et al., 2014).

Apoptosis is a process of cellular death associated with distinctive morphological characteristics (Biola et al., 1998) including membrane blebbing without leakage of cellular components. The apoptotic cells loose water and undergo shrinkage along with its nucleus, and the chromatin condenses and forms patches which crescent along with the nuclear membrane (Cohen, 1993). These distinct structural features enable to distinguish apoptotic cells from normal cells by the use of different staining techniques (Ribble et al., 2005; Kasibhatla, 2006). A cell may be viable, or it may undergo to necrotic or early or late apoptotic stages. The different stages of cells can be analyzed on the basis of integrity and permeability of plasma membrane. Annexins are a family of small proteins with specificity to phosphatidylserine. Phosphatidylserine translocates to the plasma membrane during apoptosis and necrosis, and this translocation acts as an indicator whether the cell is viable or in apoptotic or necrotic stage by using fluorescent Annexins (Vermes et al., 1995). Mitochondria play a crucial role in cellular apoptosis and cytoplasmic release of mitochondrial proteins upon induction of oxidative stress

and triggers a series of events which leads to cellular apoptosis (Kroemer et al., 2007). One such mechanism involves the mitochondrial Cytochrome c-cardiolipin complex which produces peroxide radicals by catalyzing peroxidation of membrane lipids, and ultimately series of biochemical events lead to the release of cytochrome c and further triggers mitochondrial-induced apoptosis by activation of caspase cascade (Vladimirov et al., 2009). TAX is reported to quench and abrogate peroxide radicals produced from cardiolipin-Cytochrome c complex (Demin et al., 2008), and free radicals produced by respiratory chain, and lipid peroxidation. Thus TAX, by quenching mitochondrial free radicals inhibits mitochondrial apoptosis by inhibiting the release of Cytochrome c. In our studies TAX significantly decreased the levels of URE induced cellular apoptosis indicating that TAX is a neutralizing generation of free radical in mitochondria. It is reported that URE activates transcription nuclear factor (NF-κB) (Stathopoulos et al., 2007). NF-κB is an important modulator of oxidative stress (Li and Karin, 1999; Wang et al., 2002) and thus plays an important role in the progression of apoptosis (Siomek et al., 2014). TAX is reported to regulate activation of NF-κB and induces antioxidative effects (Wang et al., 2006). Similarly, Lim is also reported to inhibit translocation of NF-κB (D'Alessio et al., 2013; Rehman et al., 2014). These studies strengthen our findings of prevention of URE induced apoptosis by TAX and Lim. In an independent study associated with URE induced cellular damage, it was demonstrated that one of the probable mechanism of URE induced cellular apoptosis involves activation and phosphorylation of MAP kinases, particularly p38 MAP kinase (Cekanova et al., 2009). Recently it has been demonstrated that treatment with Lim significantly inhibited the expression of caspase 3, caspase 9 and phosphorylation of p38. The study also

demonstrated that by such inhibition, Lim prevents apoptosis in H_2O_2 induced stress in an epithelial cell of human lens and Lim treatment significantly decreased the number of apoptotic cells in comparison to H_2O_2 induced cells where the rate of apoptosis was high (Bai et al., 2016). These findings are consistent with our findings where Lim on co-administration with URE significantly reduced cellular apoptosis as compared to URE alone.

DNA damage acts as an indicator of genotoxicity which can be assessed by DNA fragmentations and breaks. Single-cell gel electrophoresis also known as comet assay is a common, sensitive, and rapid method used for the detection of DNA damage where the tail intensity of comet with respect to its head represents the number of DNA breaks (Collins, 2004). In the present study, on analyzing DNA damage we found that test group co-supplemented with TAX and URE showed significant protection against URE induced DNA damage as compared to the test groups which were treated with URE alone. In different studies based on DNA nicking assay, TAX is reported to protect DNA damage from hydroxyl radicals in plasmid DNA (Liang et al., 2013), from 1 , 2-dimethylhydrazine induced DNA damage in mice (Manigandan et al., 2014), and from cadmium-induced DNA damage in zebrafish larvae (Manigandan, Jayaraj, et al., 2015). These reports addressing the attenuation of DNA damage by TAX further support our findings that TAX protects DNA from URE induced damage. In our studies also we found that Lim induces protection from URE induced DNA damage. These findings are also in agreement with reports where Lim treatment reduced the DNA damage induced by hydrogen peroxide (Bacanli et al., 2015). Tissue damage can be analyzed using finely sectioned and mounted histological samples of the respective tissue. These

sections can also be used to analyze expression of the particular protein using specific antibodies. We analyzed the histological tissue sections of lungs, liver, testes, kidney and intestines to study the protective effects of TAX and Lim co-administration with URE. URE exposure causes tissue damage in the kidney (Greenberg, 1968), liver (Weiss and de los Santos, 1960), lungs (Ramos et al., 2015), small intestines (Dustin, 1947), and testes (Russell et al., 1987). Our studies show inflammatory cells in the portal vein of the liver in the groups exposed to URE alone, while reduction of inflammatory cells was observed in groups treated with TAX and Lim in combination with URE. Similarly, significant tissue damages were observed in other organs. The kidney tissue damage was marked by the presence of hyaline cast in the periglomerular space, and several tubules, the intestinal and testicular tissues showed an increase in a number of apoptotic bodies, and formation of a large abscess in the lung parenchymal tissues were observed within in the groups treated with URE alone. However, tissue sections of groups treated with TAX and URE, and Lim with URE showed remarkable protection against these tissue injuries. These findings clearly show that both TAX and Lim can potentially reduce the damaging effects of URE.

In our earlier study, we had performed molecular docking of dietary phytochemical library against p53, Mdm2, Bcl-2 and PARP proteins. The aim of the study was to target these proteins as they play a crucial role in induction and regulation of apoptosis. The Mdm2-p53 interaction is one of the most exploited protein-protein interaction in chemotherapeutic development (Shangary and Wang, 2008). The p53-Bcl-2 interaction (Mihara et al., 2003) is also reported to play an important role in cell survival (Deng et al., 2006) and with the recent findings that p53 can interact with Bcl-2 and Mdm2 with

the same binding domain (Ji-Hyang Ha et al., 2013), the dual function of p53 in apoptosis as well as in cell survival is suggested. PARP is a DNA repair enzyme, and it is associated with Poly (ADP-ribosyl)ation. It is reported that overactivation of PARP leads to necrosis (Zong et al., 2004) and this overactivation of PARP is in response to increased oxidative stress (Montero et al., 2013; Wiman, 2013). Thus, targeted inhibition of these proteins may rescue normal cells from undergoing apoptosis. To validate our computational docking experiments, we performed immunohistochemistry (testes) and western blot (liver) of the groups treated with URE alone as well as in combination with TAX and Lim. The testes immunohistochemistry shows mild to moderate staining for p53 upon co-administration of URE and TAX and also in URE and Lim as compared to the group treated with URE alone, where positive staining of p53 is observed. A similar trend was also observed in western blot analysis. These findings suggest that both TAX and Lim reduced the p53 levels in testes and kidney. These findings are in agreement with our molecular docking experiments where both TAX and Lim showed satisfactory binding affinities for p53 protein, indicating that they may inhibit the protein-protein interaction of p53 with other antiapoptotic proteins including Bcl-2 (Mihara et al., 2003). The immunohistochemistry and western blot analysis for Bcl-2 staining and expression clearly shows that both TAX and Lim enhanced the levels of Bcl-2 in testes and liver in comparison URE treatment alone. Recently, Lim was reported to increase Bcl-2 expression in the epithelial cells of the human lens (Bai et al., 2016). This report is consistent with our computational and experimental findings where Bcl-2 shows prominent affinity to Lim, and thus, its expression is increased. The immunohistochemistry of PARP in testes demonstrates

positive staining of PARP protein in URE induced groups, while the mild stain is observed in the groups where URE is administered along with TAX or Lim. Our immunohistochemistry data supports our computational docking experiments, where both TAX and Lim show a prominent binding affinity for PARP protein, with TAX showing the highest binding affinity for PARP suggesting that both TAX and Lim may inhibit PARP hyperactivity under cellular stress and induce protection against PARP-mediated cellular death.

4.5. Conclusion

URE is a potent clastogenic, mutagenic and carcinogenic agent. In the present study, we have shown that lethal effects of URE can cause extensive damage to an organism at DNA, biochemical, and tissue levels. Phytochemicals are known for their antioxidant potentials and thus, in the present study we have analyzed the protective effects of two dietary phytochemicals; TAX and Lim on URE induced damaging effects. In this study, we found that these phytochemicals significantly induce protection against URE induced damage at all the three levels i.e. DNA, biochemical, and tissue levels. Our findings in this study at biochemical and at DNA levels in mouse model correlate with our findings from the *Drosophila* model, where phytochemicals showed significant protection against URE exposure. Thus, by correlating these two studies we can say that *Drosophila* can be used as an alternative to mouse model in such kind of studies. Also our findings from immunohistochemistry and western blot correlate with our computational docking experiments, suggesting that *in silico* approach can be useful in the screening of large libraries and thus, may be beneficial for identification of lead compounds.

Chapter 5 : Summary

Environmental contaminants and radiations induce lethal mutations leading to DNA damage. Human exposure to environmental radiations is unavoidable. Moreover, with the recent applications of ionizing radiations in medical diagnostics and treatment, exposure to harmful levels of radiation is more frequent. Radiations are potent agents of DNA damage as they induce clusters of DNA lesions which are repaired less efficiently by endogenous DNA repair mechanism (Lomax et al. 2013). Similarly, human exposure to chemical mutagens is increasing with their applications in many different products. The mutagenic nature of many commercially used chemicals is not known, as effects of most chemical mutagens are observed after metabolization (Guengerich, 2000). Exposure to these mutagenic and genotoxic agents lead to the development of many pathophysiological conditions. To counteract these conditions, several synthetic chemotherapeutics drugs are available globally but they either fail to be efficient in the long run, or they induce other fatal side effects. Thus, there has always been a requirement of such potent ingredients which produce no side effects. Phytochemicals are low molecular weight secondary metabolites synthesized by plants. They are potent antioxidants with potentials to scavenge free radicals, inhibit enzymes producing ROS, elevate endogenous antioxidants and upregulate expression of antioxidant enzymes (Vieira da Silva et al. 2016). Phytochemicals have many other pathophysiological significances (Craig 1997). Understanding the biological significance of phytochemicals, the present study is focused on screening and evaluating dietary phytochemicals with potential antimutagenic and antigenotoxic properties. Besides, we

have also computationally screened phytochemicals that can target crucial proteins involved in the development and progression of cancer.

p53 is a tumor suppressor protein, and almost 50% of cancers are associated with mutations in the protein (Vogelstein et al. 2000). The functional significance of p53 includes regulation of cell cycle, transcription of many proteins involved in cell proliferation, regulation of apoptosis, autophagy, immunoregulation, regulation of ROS, etc. Mdm2 is a regulatory protein of p53 which interacts and induces p53 turnover. Bcl-2 (anti-apoptotic protein) is another protein of Bcl-2 family, associated with cancer progression (Hockenbery et al. 1990). Members of Bcl-2 family interact with p53 and recently it was reported that this binding is conserved in the Bcl-2 anti-apoptotic protein family (Lee et al. 2014). Poly(ADP-ribosyl)ation protein (PARP) is protein associated with DNA replication, repair, and transcription process. It mainly catalyzes the process of appending Poly(ADP-ribose) on to the target protein (D'Amours et al. 1999). Due to the crucial functions of these proteins we targeted these proteins in our study. We screened a library of phytochemicals against them and studied the molecular docking interactions of the top hits that were common to these three proteins. By our molecular docking studies, we finally selected TAX and Lim using GLIDE molecular docking tool. Later, to cross validate the screening results we also performed docking of these top hits with the another docking software, GOLD. Both GLIDE and GOLD docking tools use different algorithms for computing their energy calculations. Both TAX and Lim showed good binding affinity against the target proteins, TAX showed higher affinity with the proteins as compared to Lim.The docking scores, hydrogen bonds and hydrophobic interactions between p53-TAX complex and Mdm2-TAX complex showed

that TAX has a higher affinity for Mdm2 protein and it strongly disrupts Mdm2-p53 interaction.These findings are in concurrence with the molecular docking and simulation studies (Verma et al. 2013) where similar results are observed.In our docking studies, TAX showed a maximum affinity for PARP protein with highest docking scores, three hydrogen bonds, and nine hydrophobic interactions. The crucial amino acid residues involved in PARP-TAX interactions are also reported to favor interactions of other PARP inhibitors (Salmas et al. 2015; Ekhteiari et al. 2016) in similar kind of studies. Our Glide docking scores for TAX-PARP complex lie in the range of Glide docking scores of known chemical inhibitors (Salmas et al. 2015), suggesting that TAX may disrupt Poly(ADP-ribosyl)ation reaction catalyzed by PARP. TAX also showed good binding affinity with Bcl-2 protein. It interacts with a region that binds to p53 (Ji-Hyang Ha et al. 2013). Based on structural analysis of Bcl-2 and Mdm2 proteins it is observed that both share the binding region of a p53 transactivation domain and thus TAX with high binding affinity for Mdm2 and Bcl-2 can act as a dual inhibitor (Anon 2106). Lim also interacts with the target proteins however their docking scores are relatively low, but owing to the small size and hydrophobic nature of Lim it can serve as a potential inhibitor. Lim interacts with p53 and Mdm2 with strong hydrophobic interactions that are important for Mdm2-p53 interactions (Liu et al. 2010; Verma et al. 2013). Lim also occupies the hydrophobic region of the Bcl-2 protein (Lugovskoy et al. 2002) and its hydrophobic interactions with residues of the Bcl-2 protein are similar to those of some known and established BH3 inhibitors of the Bcl-2 (Zacarías-Lara et al. 2016). Interaction of Lim and PARP involves strong hydrophobic associations. Lim blocks the crucial residues involved in inhibition of PARP (Li et al. 2016) by forming

hydrophobic interactions between them indicating that chemically Lim may behave as another potent inhibitor of PARP. Lim is of relatively small size and has potentials to form hydrophobic interactions only. Thus, Lim can easily dissociate water molecules from the binding pocket of PARP (Bellocchi et al. 2005) and chemically form a strong association with PARP protein. Also in our docking experiments, the Lim molecule interacts with PARP by binding to a pocket which is exploited by many of the selective PARP inhibitors (Steffen et al. 2013) suggesting the potentials of Lim inhibit PARP activity. Using *in silico* docking tools, we demonstrated the potentials of dietary phytochemicals that showed interaction with different proteins and thus they can change the flux of cell signaling cascades particularly those involved in the development of malignancies.

We further evaluated the antigenotoxic and antioxidative potentials of screened dietary phytochemicals. We assessed the effects of BC and TP against γ radiation; QC, GA and Lim against URE and coffee against CPH. To assess the potential of these dietary phytochemicals we used *Drosophila* model. The utility of this model is that one can perform both, the genotoxic and the mutagenic assays. Also, the SLRL test employed in this study can be useful to detect the effects of promutagens that cause mutagenic effects only after metabolization (Lee et al. 1983). Another benefit of using SLRL assay is that we can assess the lethal effects in different germ cells and even a single lethal mutations (even if it is recessive) can be dissected out (Würgler 1980; Lee et al. 1983). As *Drosophila* model shares the core biochemical pathways with humans (Gonzalez 2013), it offers robust test systems to detect both mutagenicity as well as antimutagenic effects of test agents. QC is known to exert antigenotoxic effects against H_2O_2 induced

DNA damage (Duthie et al. 1997), it also neutralizes effects of UV-A (Erden Inal et al. 2001), UV-B (Fahlman & Krol 2009). QC is known to exert prominent antimutagenic effects by scavenging free radicals (Geetha et al. 2005). QC (Sotibrán et al. 2011) and Lim (Idaomar et al. 2002; Fernandez-Bedmar et al. 2011) are reported to reduce oxidative stress against URE induced mutation in somatic cells of *Drosophila*. QC reduces genotoxic stress induced by γ radiations in human lymphocytes (Devipriya et al. 2008). Similarly, GA is also reported to induce phytoprotection in rat liver microsomes against damage induced by γ radiation (Gandhi & Nair 2005) and ethyl methane sulfonate (EMS) at a lower concentration in germ cells of *Drosophila* (Stanic et al. 2011). BC reduces mutagenic effects induced by γ radiation (Manda & Bhatia 2003), UV radiation (Biesalski & Obermueller-Jevic 2001), CPH (Salvadori et al. 1992), doxorubicin (Dias et al. 2009) by scavenging free radicals and reducing oxidative stress. TP's are also reported to enhance antioxidant levels (Yen & Chen 1995), provide protection against radiation-induced damage (Morley et al. 2005). Similarly, CF also ameliorates somatic mutations induced by URE, CPH and mitomycin C (Abraham & Graf 1996), CF is also reported to enhance cellular redox potentials by enhancing associated enzyme activities (Abraham & Singh 1999). These data are in concurrence with our studies where QC, GA, and Lim reduced URE induced genotoxicity, TP and BC attenuated γ radiation induced genotoxicity and CF lowered CPH induced genotoxic effects in both adult and larval feeding experiments. Also, on evaluating the biochemical effects of these phytochemicals, the overall reduction in oxidative stress was observed. All phytochemicals in combination with respective mutagen URE or γ radiation or CPH increased the levels of GSH and activities of GST,

CAT and SOD, while decreased the MDA content in comparison to positive control groups. Assessment of life span in *Drosophila* is another advantage of this model as it has short life span and short generation time and it can provide a faster test system for assessment of life span (Bauer et al. 2004). Using longevity assay we observed that all the phytochemicals when administered in combination to mutagens enhanced the mean life span of the flies on mutagen alone. These findings are supported by similar reports where administration of phytochemicals has induced longevity in *Drosophila* (Spindler et al. 2013; Fernandez-Bedmar et al. 2011). Thus, our findings suggest that dietary phytochemicals not only reduce genotoxicity and oxidative stress, but can also enhance the mean lifespan of fruitflies. We also assessed the antimutagenic, antigenotoxic and inhibitory effects of TAX and Lim against URE induced toxicity in mouse model. We performed biochemical assays to determine oxidative stress, AO/EtBr staining and Annexin V flowcytometry assay to detect apoptosis, comet assay to determine DNA damage, tissue histology to determine tissue damage, immunohistochemistry and western blot assays to determine expression of crucial proteins involved in apoptotic pathways. In our studies both TAX and Lim significantly enhanced levels of GSH, GST, CAT, SOD, GR, GPx and CYP450 indicating protection against URE induced oxidative stress. Besides enhancing antioxidative enzymes and proteins, TAX and Lim in combination with URE also reduced the intracellular levels of MDA and LDH indicating that the subject phytochemicals not only enhance the antioxidative status, but they also lower down the cellular process associated with generation of oxidative stress in URE induced toxicity. These findings are in agreement with similar reports where treatment of TAX enhance the antioxidative status (Manigandan et al. 2014), reduce

LDH (Svobodová et al. 2006) and MDA levels (Manigandan et al. 2015). Reports on upregulation of antioxidative enzymes levels and downregulation of LDH, MDA levels upon Lim treatment (Rehman et al. 2014) further supports our findings that Lim and TAX can potentially reduce cellular oxidative stress. URE induces cellular apoptosis by increasing oxidative stress, by activation of NF-κB (Stathopoulos et al. 2007) and p38 map kinase (Cekanova et al. 2009). TAX ameliorates mitochondrial oxidative stress (Demin et al. 2008), and NF-κB activation (Wang & Tournier 2006). Similarly, Lim also regulates NF-κB activation (D'Alessio et al. 2013; Rehman et al. 2014) and it also inhibits phosphorylation of p38 map kinase (Cekanova et al. 2009) and thus it can be clearly deduced that both TAX and Lim can reduce cellular apoptosis induced by URE. Our results are also consistent with these reports and both TAX and Lim significantly reduced URE induced apoptosis. URE is known to induce mutations by chromosome breakage and DNA damage (Robson 1941; Liu et al. 2016). Comet assay is a sensitive method for the analysis of DNA damage. In the present studies, both TAX and Lim significantly reduced the URE induced DNA damage. These findings are in consistence with the recent reports of TAX (Liang et al. 2013; Manigandan et al. 2014; Manigandan et al. 2015),and Lim (Bacanli et al. 2015) assisted DNA protection against cellular stress. Production of free radicals, DNA damage and enhanced apoptosis by URE exposure results in severe tissue damage. Histological studies on hazardous effects of URE in different organs report that URE causes excessive tissue damage in liver, lungs, kidneys, testis, intestines brain, etc. In our study, we also observed severe damage in different tissues upon URE exposure. However a significant reduction was observed in tissue samples treated with TAX, Lim, and URE. Immunohistochemistry and western

blot analysis were used to study the expression of p53, Bcl-2 and PARP proteins in testis and expression of p53 and Bcl-2 proteins in liver tissues. Both in the testis and liver, the mice treated with URE alone showed high levels of p53 while the expression of Bcl-2 protein was significantly less. However, treatment of TAX and Lim along with URE showed reduced levels of p53 and enhanced expression of Bcl-2 protein in comparison to URE alone. It is known that p53 and Bcl-2 have an inverse relationship (Chan et al. 2000), and high levels of p53 induce apoptosis and high levels of Bcl-2 supports cell survival. A recent report suggests that Lim can upregulate Bcl-2 expression (Bai et al. 2016). These findings are in consistence with our findings, where TAX and Lim modulate URE induced apoptosis and promotes cell survival. Also, these findings corroborate our computational docking experiments, where both TAX and Lim show good binding affinity with DNA binding domain of p53 and BH1-BH3 domain of Bcl-2. The p53 interacts with Bcl-2 protein by its DNA binding domain (Mihara et al. 2003), while Bcl-2 interacts with p53 by its BH1-BH3 cavity (Ji-Hyang Ha et al. 2013). Thus, our computational experiments are in agreement with these reports indicating that both TAX and Lim are inhibiting the p53-Bcl-2 interaction. Further, IHC of PARP in mice treated with URE alone showed positive staining while those treated with TAX and Lim along with URE showed mild staining indicating a reduction in expression of PARP protein. Studies have shown a direct correlation between oxidative stress, p53, and overactivation of PARP which leads to cell death (Montero et al. 2013; Zong et al. 2004). These reports also support our immunohistochemistry findings, where p53 and PARP expression is elevated in URE induced oxidative stress and treatment of TAX and Lim along with URE reduced expression of both p53 and PARP. These findings

correlate with our computational docking experiments, where both TAX and Lim inhibits PARP and thus lower down its hyper activation under URE induced oxidative stress. The present study utilizes a three-tier approach to evaluating the antioxidative and antimutagenic performance of dietary phytochemicals. Initially, the study focuses on the screening of phytochemicals using computer-aided tools to inhibit the activities of some crucial proteins associated with development and progression of malignancies. Thereafter, the study resolves antigenotoxic and antimutagenic effects of dietary phytochemicals against the hazardous effects of physical (γ radiations) and chemical (URE and CPH) agents using SLRL, biochemical and longevity assays in *Drosophila* model. Lastly, the study dissects the beneficial effects of selected phytochemicals against URE induced cellular and tissue damage in an animal model using biochemical, DNA damage, apoptotic, histological and western blotting assays. Using these three different approaches, the present study aims to establish a correlation between them to reduce consumption of time, energy, and resources in screening and selection of particular beneficial compound. The present study correlates computational screening and mouse model to establish the importance of virtual screening and how it can be beneficial in the detection of noble compounds. The study correlates *Drosophila* model and mouse models on the basis of assays performed and results produced and hence it can be concluded that *Drosophila* can be used as an alternative to mouse model and thereby can help in reduction, refinement and replacement of animal models without influencing the outcome of the study. The study also demonstrates the beneficial effects of dietary phytochemicals over synthetic compounds which mostly produce side effects, may also lead to cellular resistance.

Bibliography

Abolaji, A.O., J.P. Kamdem, E.O. Farombi, et al. (2013). Drosophila melanogaster as a Promising Model Organism in Toxicological Studies: A Mini Review. *Archives of Basic & Applied Medicine 1*, 33–38.

Abraham, S.K. (1994). Antigenotoxicity of coffee in the drosophila assay for somatic mutation and recombination. *Mutagenesis 9*, 383–386.

Abraham, S.K. (1989). Inhibition of in vivo genotoxicity by coffee. *Food and Chemical Toxicology 27*, 787–792.

Abraham, S.K. (1995). Inhibitory effects of coffee on transplacental genotoxicity in mice. *Mutation Research Letters 347*, 45–52.

Abraham, S.K., and U. Graf. (1996a). Protection by coffee against somatic genotoxicity in drosophila: Role of bioactivation capacity. *Food and Chemical Toxicology 34*, 1–14.

Abraham, S.K., and U. Graf. (1996b). Protection by coffee against somatic genotoxicity in Drosophila: role of bioactivation capacity. *Food and chemical toxicology 34*, 1–14.

Abraham, S.K., L. Sarma, and P.C. Kesavan. (1993a). Protective effects of chlorogenic acid, curcumin and beta-carotene against gamma-radiation-induced in vivo chromosomal damage. *Mutation research 303*, 109–112.

Abraham, S.K., L. Sarma, and P.C. Kesavan. (1993b). Protective effects of chlorogenic acid, curcumin and β-carotene against γ-radiation-induced in vivo chromosomal damage. *Mutation Research Letters 303*, 109–112.

Abraham, S.K., and S.P. Singh. (1999). Anti-genotoxicity and glutathione S-transferase activity in mice pretreated with caffeinated and decaffeinated coffee. *Food and Chemical Toxicology 37*, 733–739.

Abraham, S.K., S.P. Singh, and P.C. Kesavan. (1993). Buthionine sulfoximine mediated enhancement of γ-radiation induced mutation frequency in Drosophila melanogaster. *Mutation Research Letters 301*, 255–259.

Abrahamson, S. (1980). How many loci on the X- chromosome of drosophila melanogaster can mutate to recessive lethals? *Environmental Mutagenesis 453*, 447–453.

Abrahamson, S., and E.B. Lewis. (1971). The Detection of Mutations in Drosophila melanogaster. *In* Chemical Mutagens, 461–487. Springer US, Boston, MA.

Adams, M.D., S.E. Celniker, R.A. Holt, et al. (2000). The genome sequence of Drosophila melanogaster. *Science (New York, N.Y.) 287*, 2185–95.

Aebi, H. (1984). Catalase in vitro . Methods in Enzymology. *Methods in enzymology 105*, 121 –126.

Amaral, J.D., J.M. Xavier, C.J. Steer, et al. (2010). The role of p53 in apoptosis. *Discovery medicine 9*, 145–152.

Ames, B.N. (1971). The Detection of Chemical Mutagens with Enteric Bacteria. *In* A. Hollaender [ed.], Chemical Mutagens: Principles and Methods for Their Detection Volume 1, 267–282. Springer US, Boston, MA.

Anon. (2016). Bcl-2-MDM2 Dual Inhibitors Based on Universal Pyramid-Like α-Helical Mimetics. *Journal of medicinal chemistry 59*, 3152–3162.

Apidianakis, Y., and L.G. Rahme. (2011). Drosophila melanogaster as a model for human intestinal infection and pathology. *Disease models & mechanisms 4*, 21–30.

Arruda, D.C., D.C. Miguel, J.K.U. Yokoyama-Yasunaka, et al. (2009). Inhibitory activity of limonene against Leishmania parasites in vitro and in vivo. *Biomedicine and Pharmacotherapy 63*, 643–649.

Auerbach, C. (1947). The induction by mustard gas of chromosomal instabilities in Drosophila melanogaster. *Proceedings of the Royal Society of Edinburgh. Section B: Biology 62*, 307–320.

Baars, A.J. (1980). Biotransformation of Xenobiotics in Drosophila melanogaster and Its Relevance for Mutagenicity Testing. *Drug Metabolism Reviews 11*, 191–221.

Bacanli, M., A.A. Basaran, and N. Basaran. (2015). The antioxidant and antigenotoxic properties of citrus phenolics limonene and naringin. *Food and Chemical Toxicology 81*, 160–170.

Bai, J., Y. Zheng, G. Wang, et al. (2016). Protective Effect of D-Limonene against Oxidative Stress-Induced Cell Damage in Human Lens Epithelial Cells via the p38 Pathway. *Oxidative Medicine and Cellular Longevity 2016*, 1–12.

Bakkali, F., S. Averbeck, D. Averbeck, et al. (2008). Biological effects of essential oils - A review. *Food and Chemical Toxicology 46*, 446–475.

Bass, T.M., D. Weinkove, K. Houthoofd, et al. (2007). Effects of resveratrol on lifespan in Drosophila melanogaster and Caenorhabditis elegans. *Mechanisms of Ageing and Development 128*, 546–552.

Bateman, A.J. (1976). Mutagenic action of urethane. *Mutation Research 39*, 75–95.

Bauer, J.H., S. Goupil, G.B. Garber, et al. (2004). An accelerated assay for the identification of lifespan-extending interventions in Drosophila melanogaster.

Proceedings of the National Academy of Sciences of the United States of America 101, 12980–12985.

Bellocchi, D., A. Macchiarulo, G. Costantino, et al. (2005). Docking studies on PARP-1 inhibitors: Insights into the role of a binding pocket water molecule. *Bioorganic and Medicinal Chemistry 13*, 1151–1157.

Ben-Amotz, A., S. Yatziv, M. Sela, et al. (1998). Effect of natural beta-carotene supplementation in children exposed to radiation from the Chernobyl accident. *Radiation and environmental biophysics 37*, 187–93.

De Benedictis, G., G. Maiorano, L. Chieco-Bianchi, et al. (1962). Lung Carcinogenesis by Urethane in Newborn, Suckling, and Adult Swiss Mice. *British journal of cancer 16*, 686–689.

Bergmeyer HU, Bernt E, H.B. (1974). Lactate dehydrogenase. *Methods of enzymatic analysis 2*, 574–579.

Bernards, A., and I.K. Hariharan. (2001). Of flies and men - Studying human disease in Drosophila. *Current Opinion in Genetics and Development 11*, 274–278.

Bhandari, P., and L.S. Shashidhara. (2001). Studies on human colon cancer gene APC by targeted expression in Drosophila. *Oncogene 20*, 6871–6880.

Bhatti, S., J. O'Keefe, and C. Lavie. (2013). Coffee and tea: perks for health and longevity? *Current Opinion in Clinical Nutrition & Metabolic Care 16*, 688-697

Bier, E., and W. McGinnis. (2008). Model organisms in the study of development and disease. *Molecular Basis of Inborn Errors of Development*, 25–48.

Biesalski, H.K., and U.C. Obermueller-Jevic. (2001). UV light, beta-carotene and human skin--beneficial and potentially harmful effects. *Archives of biochemistry and biophysics 389*, 1–6.

Biola, a, M. Pallardy, and J. Bre. (1998). Apoptosis : Identification of dying cells. *Cell biology and toxicology 14*, 111–120.

Bohacek, R.S., C. McMartin, and W.C. Guida. (1996). The art and practice of structure-based drug design: A molecular modeling perspective. *Medicinal Research Reviews 16*, 3–50.

Bonini, N.M. (1999). A genetic model for human polyglutamine-repeat disease in Drosophila melanogaster. *Philosophical transactions of the Royal Society of London. Series B, Biological sciences 354*, 1057–1060.

Boone, C.W., G.J. Kelloff, and W.E. Malone. (1990). Identification of Candidate Cancer Chemopreventive Agents and Their Evaluation in Animal Models and Human Clinical Trials: A Review. *Cancer Research 50*, 2–9.

Boots, A.W., G.R.M.M. Haenen, and A. Bast. (2008). Health effects of quercetin: From antioxidant to nutraceutical. *European Journal of Pharmacology 585*, 325–337.

Bordone, L., and L. Guarente. (2005). Calorie restriction, SIRT1 and metabolism: understanding longevity. *Nat Rev Mol Cell Biol 6*, 298–305.

Botas, J. (2007). Drosophila researchers focus on human disease. *Nature genetics 39*, 589–91.

Bournias-Vardiabasis, N., and J. Flores. (1983). Drug Metabolizing enzymes in Drosophila melanogaster : Teratogenicity of Cyclophosphamide in vitro. *Teratogenesis, Carcinogenesis, and Mutagenesis 3*, 255–262.

Bownes, M., and M. Seiler. (1977). Developmental effects of exposingDrosophila embryos to ether vapour. *Journal of Experimental Zoology 199*, 9–23.

Brumby, A.M., and H.E. Richardson. (2005). Using Drosophila melanogaster to map human cancer pathways. *Nature reviews. Cancer 5*, 626–639.

Budanov, A. V. (2014). The role of tumor suppressor p53 in the antioxidant defense and metabolism. *Sub-cellular biochemistry 85*, 133–59.

Burda, S., S. Burda, W. Oleszek, et al. (2001). Antioxidant and Antiradical Activities of Flavonoids. *Journal of Agricultural and Food Chemistry 49*, 2774–2779.

Bürkle, A. (2005). Poly(ADP-ribose): The most elaborate metabolite of NAD+. *FEBS Journal 272*, 4576–4589.

C Jagetia, G. (2007). Radioprotective Potential of Plants and Herbs against the Effects of Ionizing Radiation. *Journal of clinical biochemistry and nutrition 40*, 74–81.

Cämmerer, B., and L.W. Kroh. (2006). Antioxidant activity of coffee brews. *European Food Research and Technology 223*, 469–474.

Carlberg, I., and B. Mannervik. (1975). Purification and characterization of the flavoenzyme glutathione reductase from rat liver. *The Journal of biological chemistry 250*, 5475–80.

Caspari, E., and C. Stern. (1948). The Influence of Chronic Irradiation with Gamma-Rays at Low Dosages on the Mutation Rate in Drosophila Melanogaster. *Genetics 2*, 75–95.

Cekanova, M., S.H. Lee, R.L. Donnell, et al. (2009). Nonsteroidal anti-inflammatory drug-activated gene-1 expression inhibits urethane-induced pulmonary tumorigenesis in transgenic mice. *Cancer Prevention Research 2*, 450–458.

Chacko, S.M., P.T. Thambi, R. Kuttan, et al. (2010). Beneficial effects of green tea : A literature review. *Chinese Medicine*, 1–9.

Chan, W., K. Cheung, and J. Schorge. (2000). Bcl-2 and p53 Protein Expression,

Apoptosis, and p53 Mutation in Human Epithelial Ovarian Cancers. *The American Journal of Pathology 156*, 409–417.

Chander, S.K., a G. Lansdown, Y. a Luqmani, et al. (1994). Effectiveness of combined limonene and 4-hydroxyandrostenedione in the treatment of NMU-induced rat mammary tumours. *British Journal of Cancer 69*, 879–882.

Chandley, A.C., and A.J. Bateman. (1962). Timing of spermatogenesis in Drosophila melanogaster using tritiated thymidine. *Nature 193*, 299–300.

Chang, C., D.T. Simmons, M. a Martin, et al. (1979). Identification and partial characterization of new antigens from simian virus 40-transformed mouse cells. *Journal of Virology 31*, 463–71.

Chang, J.C., L.H. van der Hoeven, and C.H. Haddox. (1978). Glutathione reductase in the red blood cells. *Annals Of Clinical Laboratory Science 8*, 23–29.

Chen, J., V. Marechal, and a J. Levine. (1993). Mapping of the p53 and mdm-2 interaction domains. *Molecular And Cellular Biology 13*, 4107–4114.

Cheng, M., M.K. Conner, and Y. Alarie. (1981). Multicellular in vivo sister-chromatid exchanges induced by urethane. *Mutation Research 88*, 223–231.

Chieco-Bianchi, L., G. De Benedictis, G. Tridente, et al. (1963). Influence of Age on Susceptibility to Liver Carcinogenesis and Skin Initiating Action by Urethane in Swiss Mice. *British Journal of Cancer 17*, 672–680.

Choudhary, A., B. Zachek, R.F. Lera, et al. (2016). Identification of Selective Lead Compounds for Treatment of High-Ploidy Breast Cancer. *Molecular cancer therapeutics 15*, 48–59.

Chu, E.H.Y. (1974). Induction and Analysis of Gene Mutations in cultured mammalian somatic cells. *Genetics 78*, 115–132.

Cinkilic, N., E. Tüzün, S.K. Çetintaş, et al. (2014). Radio-protective effect of cinnamic acid, a phenolic phytochemical, on genomic instability induced by X-rays in human blood lymphocytes in vitro. *Mutation Research 770*, 72–79.

Circu, M.L., and T.Y. Aw. (2010). Reactive oxygen species, cellular redox systems and apoptosis. *Free Radical Biology & Medicine 48*, 749–762.

Cohen, J.J. (1993). Apoptosis. *Immunology Today 14*, 126–130.

Collins, A.R. (1999). Oxidative DNA damage, antioxidants, and cancer. *BioEssays 21*, 238–246.

Collins, A R. (2004). The comet assay for DNA damage and repair: principles, applications, and limitations. *Molecular Biotechnology 26*, 249–261.

Cooke, M.S., M.D. Evans, M. Dizdaroglu, et al. (2003). Oxidative DNA damage:

mechanisms, mutation, and disease. *FASEB journal : Official publication of the Federation of American Societies for Experimental Biology 17*, 1195–214.

Craig, W.J. (1997). Phytochemicals: Guardians of our Health. *Journal of the American Dietetic Association 97*, S199–S204.

Van Cruchten, S., and W. Van den Broeck. (2002). Morphological and biochemical aspects of apoptosis, oncosis and necrosis. *Anatomia, Histologia, Embryologia 31*, 214–223.

Csokay, B., N. Prajda, G. Weber, et al. (1997). Molecular mechanisms in the antiproliferative action of quercetin. *Life Sciences 60*, 2157–2163.

D'Alessio, P.A., R. Ostan, J.F. Bisson, et al. (2013). Oral administration of d-Limonene controls inflammation in rat colitis and displays anti-inflammatory properties as diet supplementation in humans. *Life Sciences 92*, 1151–1156.

D'Amours, D., S. Desnoyers, I. D'Silva, et al. (1999). Poly(ADP-ribosyl)ation reactions in the regulation of nuclear functions. *The Biochemical journal 342*, 249–268.

Darzynkiewicz, Z., X. Li, and J. Gong. (1994). Assays of cell viability: Discrimination of cells dying by apoptosis. *Methods in Cell Biology 41*, 15–38.

Davis, J.M., E.A. Murphy, and M.D. Carmichael. (2009). Effects of the dietary flavonoid quercetin upon performance and health. *Current Sports Medicine Reports 8*, 206–213.

DeLeo, a B., G. Jay, E. Appella, et al. (1979). Detection of a transformation-related antigen in chemically induced sarcomas and other transformed cells of the mouse. *Proceedings of the National Academy of Sciences of the United States of America 76*, 2420–2424.

Delgado-Andrade, C., J.A. Rufián-Henares, and F.J. Morales. (2005). Assessing the antioxidant activity of melanoidins from coffee brews by different antioxidant methods. *Journal of Agricultural and Food Chemistry 53*, 7832–7836.

Demin, E.M., E. V Proskurnina, and Y.A. Vladimirov. (2008). Antioxidant effects of dihydroquercetin and rutin in peroxidase reactions catalyzed by cytochrome c. *Moscow University Chemistry Bulletin 63*, 297–302.

Deng, X., F. Gao, T. Flagg, et al. (2006). Bcl2's flexible loop domain regulates p53 binding and survival. *Molecular and cellular biology 26*, 4421–34.

Devasagayam, T.P. a, J.P. Kamat, H. Mohan, et al. (1996). Caffeine as an antioxidant: Inhibition of lipid peroxidation induced by reactive oxygen species. *Biochimica et Biophysica Acta - Biomembranes 1282*, 63–70.

Devipriya, N., A.R. Sudheer, M. Srinivasan, et al. (2008). Quercetin ameliorates gamma radiation-induced DNA damage and biochemical changes in human peripheral

blood lymphocytes. *Mutation research 654*, 1–7.

Dias, C.D., B.C. Araújo, E.S. Dutra, et al. (2009a). Protective effects of β-carotene against the genotoxicity of doxorubicin in somatic cells of Drosophila melanogaster. *Genetics and Molecular Research 8*, 1367–1375.

Djilani, A., and A. Dicko. (2012). The therapeutic benefits of essential oils. *Nutrition, Well-Beig and Health*, 155–78.

Donà, M., I. Dell'Aica, F. Calabrese, et al. (2003). Neutrophil restraint by green tea: inhibition of inflammation, associated angiogenesis, and pulmonary fibrosis. *The Journal Of Immunology 170*, 4335–4341.

Dubrova, Y.E. (2016). Mutation induction in the mouse and human germline. *Russian Journal of Genetics 52*, 17–28.

Dustin, P. (1947). The Cytological Action of Ethylcarbamate (Urethane) and Other Carbamic Esters in Normal and Leukaemic Mice, an in Rabbits. *British Journal of Cancer 1*, 48–59.

Duthie, S.J., A.R. Collins, G.G. Duthie, et al. (1997). Quercetin and myricetin protect against hydrogen peroxide-induced DNA damage (strand breaks and oxidised pyrimidines) in human lymphocytes. *Mutation Research 393*, 223–231.

Ehrnhoefer, D.E., M. Duennwald, P. Markovic, et al. (2006). Green tea (-)-epigallocatechin-gallate modulates early events in huntingtin misfolding and reduces toxicity in Huntington's disease models. *Human Molecular Genetics 15*, 2743–2751.

Eischen, C.M., and G. Lozano. (2009). p53 and MDM2: antagonists or partners in crime? *Cancer Cell 15*, 161–2.

Ekhteiari Salmas, R., A. Unlu, M. Bektaş, et al. (2016). Virtual screening of small molecules databases for discovery of novel PARP-1 inhibitors: combination of in silico and in vitro studies. *Journal of Biomolecular Structure and Dynamics 1102*, 1–17.

Ekins, S. (2007). Computational toxicology: risk assessment for pharmaceutical and environmental chemicals. *John Wiley & Sons Vol 1*.

El-Habit, O.H.., H.. Saada, K.S. Azab, et al. (2000). The modifying effect of β-carotene on gamma radiation-induced elevation of oxidative reactions and genotoxicity in male rats. *Mutation Research 466*, 179–186.

Elegbede, J. A, T.H. Maltzman, C.E. Elson, et al. (1993). Effects of anticarcinogenic monoterpenes on phase II hepatic metabolizing enzymes. *Carcinogenesis 14*, 1221–1223.

Ellman, G.L. (1959). Tissue sulfhydryl groups. *Archives of Biochemistry and*

Biophysics 82, 70–77.

Elmore, S. (2007). Apoptosis : A Review of Programmed Cell Death. *Toxicologic Pathology 35*, 495–516.

Emadi, A., R.J. Jones, and R. a Brodsky. (2009). Cyclophosphamide and cancer: golden anniversary. *Nature reviews. Clinical oncology 6*, 638–647.

Erden Inal, M., A. Kahraman, and T. Köken. (2001). Beneficial effects of quercetin on oxidative stress induced by ultraviolet A. *Clinical And Experimental Dermatology 26*, 536–9.

Ernster, L., L. Danielson, and M. Ljunggren. (1962). Dt diaphorase I. Purification from the soluble fraction of rat-liver cytoplasm, and properties. *Biochimica et Biophysica Acta 58*, 171–188.

Eustermann, S., H. Videler, J.C. Yang, et al. (2011). The DNA-binding domain of human PARP-1 interacts with DNA single-strand breaks as a monomer through its second zinc finger. *Journal of Molecular Biology 407*, 149–170.

Fahlman, B.M., and E.S. Krol. (2009). Inhibition of UVA and UVB radiation-induced lipid oxidation by quercetin. *Journal of Agricultural and Food Chemistry 57*, 5301–5305.

Fakiha, K.G., and M. A Bibars. (2010). Mutageneic and antimutagenic effects of some plant extracts in Drosophilla melanogaster. *Nature and Science 8*, 77–82.

Favreau, L. V, and C.B. Pickett. (1991). Transcriptional regulation of the rat NAD(P)H:quinone reductase gene. Identification of regulatory elements controlling basal level expression and inducible expression by planar aromatic compounds and phenolic antioxidants. *Journal of Biological Chemistry 266*, 4556–4561.

Ferguson, L.R. (2001). Role of plant polyphenols in genomic stability. *Mutation Research - Fundamental and Molecular Mechanisms of Mutagenesis 475*, 89–111.

Fernandez-Bedmar, Z., J. Anter, S. de La Cruz-Ares, et al. (2011). Role of Citrus juices and distinctive components in the modulation of degenerative processes: genotoxicity, antigenotoxicity, cytotoxicity, and longevity in Drosophila. *Journal of Toxicology and Environmental Health-Part a-Current Issues 74*, 1052–1066.

Field, K.J., and C.M. Lang. (1988). Hazards of urethane (ethyl carbamate): a review of the literature. *Laboratory animals 22*, 255–262.

Frei, B., and J. Higdon. (2003). Antioxidant activity of tea polyphenols in vivo: evidence from animal studies. *The Journal of nutrition*, 3275S–3284S.

Frei, H., J. Clements, D. Howe, et al. (1992). The genotoxicity of the anti-cancer drug mitoxantrone in somatic and germ cells of Drosophila melanogaster. *Mutation*

Research 279, 21–33.

Friesner, R. a, J.L. Banks, R.B. Murphy, et al. (2004). Glide: a new approach for rapid, accurate docking and scoring. 1. Method and assessment of docking accuracy. *Journal of medicinal chemistry 47*, 1739–49.

Friling, R.S., A. Bensimon, Y. Tichauer, et al. (1990). Xenobiotic-inducible expression of murine glutathione S-transferase Ya subunit gene is controlled by an electrophile-responsive element. *Proceedings of the National Academy of Sciences of the United States of America 87*, 6258–62.

Frölich, A., and F.E. Würgler. (1990). Genotoxicity of ethyl carbamate in the Drosophila wing spot test: dependence on genotype-controlled metabolic capacity. *Mutation Research Letters 244*, 201–208.

Galenza, A., J. Hutchinson, B. Hazes, et al. (2015). Glucose modulates Drosophila longevity and immunity independent of the microbiota. *Biology open 5*, 165–173.

Gandhi, N.M., and C.K.K. Nair. (2005a). Protection of DNA and membrane from gamma radiation induced damage by gallic acid. *Molecular and Cellular Biochemistry 278*, 111–117.

Gariboldi, M., G. Manenti, F. Canzian, et al. (1993). Advances in Brief Chromosome Mapping of Murine Susceptibility Loci to Liver Carcinogenesis 1. *Cancer*, 209–211.

Geetha, T., V. Malhotra, K. Chopra, et al. (2005). Antimutagenic and antioxidant / prooxidant activity of quercetin. *Indian Journal of Experimental Biology 43*, 61–67.

Gertz, M., G.T.T. Nguyen, F. Fischer, et al. (2012). A molecular mechanism for direct sirtuin activation by resveratrol. *PLoS ONE 7*, 1–12.

Ghosh, D., U.B. Das, and M. Misro. (2002). Protective role of α-tocopherol-succinate (provitamin-e) in cyclophosphamide induced testicular gametogenic and steroidogenic disorders: a correlative approach to oxidative stress. *Free Radical Research 36*, 1209–1218.

Giacomotto, J., and L. Ségalat. (2010). High-throughput screening and small animal models, where are we? *British Journal of Pharmacology 160*, 204–216.

Gladstone, M., and T. Tin. (2011). Chemical genetics and drug screening in Drosophila cancer models. *Journal of Genetics and Genomics 38*, 497–504.

Goldstein, M., and M.B. Kastan. (2015). The DNA damage response: implications for tumor responses to radiation and chemotherapy. *Annual Review Of Medicine 66*, 129–43.

Gonzalez, C. (2013). Drosophila melanogaster: a model and a tool to investigate

malignancy and identify new therapeutics. *Nature Reviews Cancer 13*, 172–183.

Graf, U., S.K. Abraham, J. Guzmán-Rincón, et al. (1998). Antigenotoxicity studies in Drosophila melanogaster. *Mutation Research 402*, 203–209.

Graf, U., and D. Singer. (1992). Genotoxicity testing of promutagens in the wing somatic matuation and recombination test in Drosophila melanogaster. *Rev. Int. Contam. Ambient 8*, 15–27.

Graf, U., F.E. Würgler, A.J. Katz, et al. (1984). Somatic mutation and recombination test inDrosophila melanogaster. *Environmental Mutagenesis 6*, 153–188.

Grasberger, B.L., T. Lu, C. Schubert, et al. (2005). Discovery and cocrystal structure of benzodiazepinedione HDM2 antagonists that activate p53 in cells. *Journal of medicinal chemistry 48*, 909–12.

Greenberg, S.R. (1968). The Renal Response to Directly-administered Urethane. *Urologia Internationalis 23*, 309–314.

Greene, J.C., A.J. Whitworth, I. Kuo, et al. (2003). Mitochondrial pathology and apoptotic muscle degeneration in Drosophila parkin mutants. *Proceedings Of The National Academy of Sciences, 100,* 4078-4083.

Greeve, I., D. Kretzschmar, J. Tscha, et al. (2004). Age-dependent neurodegeneration and alzheimer-amyloid plaque formation in transgenic drosophila. *The Journal of Neuroscience 24*, 3899–3906.

Gul, K., A. Tak, A. K. Singh, et al. (2015). Chemistry, encapsulation, and health benefits of β-carotene - A review. *Cogent Food & Agriculture 1*, 1018696.

Habig, W.H., M.J. Pabst, and W.B. Jakoby. (1974). Glutathione S transferases. The first enzymatic step in mercapturic acid formation. *Journal of Biological Chemistry 249*, 7130–7139.

Halgren, T.A., R.B. Murphy, R.A. Friesner, et al. (2004). Glide: A New Approach for Rapid, Accurate Docking and Scoring. 2. Enrichment Factors in Database Screening. *Journal of Medicinal Chemistry 47*, 1750–1759.

Halliwell, B. (1991). Reactive oxygen species in living systems: Source, biochemistry, and role in human disease. *The American Journal of Medicine 91*, S14–S22.

Haqqi, T.M., D.D. Anthony, S. Gupta, et al. (1999). Prevention of collagen-induced arthritis in mice by a polyphenolic fraction from green tea. *Proceedings of the National Academy of Sciences of the United States of America 96*, 4524–4529.

Haraguchi, H., Y. Mochida, S. Sakai, et al. (1996). Protection against oxidative damage by dihydroflavonols in Engelhardtia chrysolepis. *Biosci Biotechnol Biochem 60*, 945–948.

Havaki, S., A. Kotsinas, E. Chronopoulos, et al. (2015). The role of oxidative DNA damage in radiation induced bystander effect. *Cancer Letters 356*, 43–51.

Heres-Pulido, M.E., I. Dueñas-García, L. Castañeda-Partida, et al. (2004). Genotoxicity of tamoxifen citrate and 4-nitroquinoline-1-oxide in the wing spot test of Drosophila melanogaster. *Mutagenesis 19*, 187–193.

Hill, A., D. Gotham, J. Fortunak, et al. (2016). Target prices for mass production of tyrosine kinase inhibitors for global cancer treatment. *BMJ Open 6*.

Ho, J.H., Y.L. Chang, and C.H.Y.O.N.G.L. Ee. (2004). Protective effects of quercetin and vitamin C against oxidative stress-induced neurodegeneration. *Journal of Agricultural and Food Chemistry 52*, 7514–7517.

Hockenbery, D., G. Nunez, C. Milliman, et al. (1990). Bcl-2 is an inner mitochondrial membrane protein that blocks programmed cell death. *Nature 348*, 334–336.

Hothorn, L. (1991). Kirkland, D. J. (ed.): Statistical evaluation of mutagenicity test data. UKEMS subcommittee on guidelines for mutagenicity testing. Report. Part III, Cambridge University Press, Cambridge 1989. *Biometrical Journal 33*, 460–460.

Hour, T.C., Y.C. Liang, I. Sen Chu, et al. (1999). Inhibition of eleven mutagens by various tea extracts, (-)epigallocatechin-3-gallate, gallic acid and caffeine. *Food and Chemical Toxicology 37*, 569–579.

Huang, Q., and H.M. Shen. (2009). To die or to live: The dual role of poly(ADP-ribose) polymerase-1 in autophagy and necrosis under oxidative stress and DNA damage. *Autophagy 5*, 273–276.

Huyan, X.-H., Y.-P. Lin, T. Gao, et al. (2011). Immunosuppressive effect of cyclophosphamide on white blood cells and lymphocyte subpopulations from peripheral blood of Balb/c mice. *International immunopharmacology 11*, 1293–7.

IARC. (1974). IARC monographs. *International Agency for Research on Cancer Monograph 1982*, 417–515.

Idaomar, M., R. El Hamss, F. Bakkali, et al. (2001). Genotoxicity and antigenotoxicity of some essential oils evaluated by wing spot test of Drosophila melanogaster. *Mutation Research 513*, 61–68.

Issaeva, N., P. Bozko, M. Enge, et al. (2004). Small molecule RITA binds to p53, blocks p53-HDM-2 interaction and activates p53 function in tumors. *Nature medicine 10*, 1321–8.

Ives, P. (1959). The mutation rate in Drosophila after high doses of gamma radiation. *Proceedings of the National Academy of Sciences 45*, 188–92.

Iwakuma, T., and G. Lozano. (2003). MDM2, an introduction. *Molecular cancer research : MCR 1*, 993–1000.

Jackson, G.R., I. Salecker, X. Dong, et al. (1998). Polyglutamine-expanded human huntingtin transgenes induce degeneration of drosophila photoreceptor neurons. *Neuron 21*, 633–642.

James D. Adams, JR, L.K.K. (1993). Acrolein-induced oxygen radical formation. *Free Radical Biology & Medicine 15*, 187–193.

Jänicke, R.U., D. Sohn, and K. Schulze-Osthoff. (2008). The dark side of a tumor suppressor: anti-apoptotic p53. *Cell death and differentiation 15*, 959–976.

Jennings, B.H. (2011). Drosophila – a versatile model in biology & medicine The fruit fly Drosophila melanogaster is a versatile model organism. *Materials Today 14*, 190–195.

Ji-Hyang Ha, J.S. Shin, M.K. Yoon, et al. (2013). Dual-site interactions of p53 protein transactivation domain with anti-apoptotic bcl-2 family proteins reveal a highly convergent mechanism of divergent p53 pathways. *Journal of Biological Chemistry 288*, 7387–7398.

Jia, S.S., G.P. Xi, M. Zhang, et al. (2013). Induction of apoptosis by D-limonene is mediated by inactivation of Akt in LS174T human colon cancer cells. *Oncology Reports 29*, 349–354.

Jiao, Z., Y. Dong, and Q. Chen. (2014). Ethyl carbamate in fermented beverages: Presence, analytical chemistry, formation mechanism, and mitigation proposals. *Comprehensive Reviews in Food Science and Food Safety 13*, 611–626.

Jimenez-Del-Rio, M., C. Guzman-Martinez, and C. Velez-Pardo. (2010). The effects of polyphenols on survival and locomotor activity in drosophila melanogaster exposed to iron and paraquat. *Neurochemical Research 35*, 227–238.

Joshi, A., and L.D. Mueller. (1997). Adult crowding effects on longevity in Drosophila melanogaster: Increase in age-independent mortality. *Current Science 72*, 255–260.

Kada, T., K. Tutikawa, and Y. Sadaie. (1972). In vitro and host-mediated "rec-assay" procedures for screening chemical mutagens; and phloxine, a mutagenic red dye detected. *Mutation Research 28*, 165–174.

Kamath, P.R., D. Sunil, A.A. Ajees, et al. (2016). N'-((2-(6-bromo-2-oxo-2 H -chromen-3-yl)-1 H -indol-3-yl)methylene)benzohydrazide as a probable Bcl-2/Bcl-xL inhibitor with apoptotic and anti-metastatic potential. *European Journal of Medicinal Chemistry 120*, 134–147.

Kanakry, C.G., S. Ganguly, M. Zahurak, et al. (2013). Aldehyde dehydrogenase expression drives human regulatory t cell resistance to posttransplantation cyclophosphamide. *Science Translational Medicine 5*.

Kannan, K., and S. Jain. (2000). Oxidative stress and apoptosis. *Pathophysiology 7*, 153–163.

Kasibhatla, S. (2006). Acridine Orange/Ethidium Bromide (AO/EB) staining to detect apoptosis. *Cold Spring Harbor Protocols 2006*, pdb.prot4493-prot4493.

Kavanagh, K.T., L.J. Hafer, D.W. Kim, et al. (2001). Green tea extracts decrease carcinogen-induced mammary tumor burden in rats and rate of breast cancer cell proliferation in culture. *Journal of Cellular Biochemistry 82*, 387–398.

Kaye, A.M. (1960). A Study of the Relationship between the Rate of Ethyl Carbamate (Urethan) Catabolism and Urethan Carcinogenesis. *Cancer Research 20*, 237–241.

Kerr, J.F.R., and A.H.W. and A.R. Currie. (1972). Apoptosis: A basic biological phenomenon with wide-ranging implications in human disease. *British Journal of Cancer 26*, 239–257.

Khan, N., and H. Mukhtar. (2007). Tea polyphenols for health promotion. *Life Sciences 81*, 519–533.

Khazaeli, A.A., W. Van Voorhies, and J.W. Curtsinger. (2005). Longevity and metabolism in Drosophila melanogaster: Genetic correlations between life span and age-specific metabolic rate in populations artificially selected for long life. *Genetics 169*, 231–242.

Kim, Y.J. (2007). Antimelanogenic and antioxidant properties of gallic acid. *Biological & pharmaceutical bulletin 30*, 1052–1055.

Kirkin, V., S. Joos, and M. Zo. (2004). The role of Bcl-2 family members in tumorigenesis. *Biochimica et biophysica acta 1644*, 229–249.

Kitchen, D.B., H. Decornez, J.R. Furr, et al. (2004). Docking and scoring in virtual screening for drug discovery: methods and applications. *Nature reviews. Drug Discovery 3*, 935–49.

Klebe, G. (2000). Virtual Screening: an alternative or complement to high throughput screening: Proceedings of the Workshop 'New Approaches in Drug Design and Discovery', special topic 'Virtual Screening', Schloß Rauischholzhausen, Germany, March 15–18, 1999. Springer Science & Business Media; 2000 Nov 30.

Krishnamurthy, P., and A. Wadhwani. (2012). Antioxidant enzymes and human health. *In* Antioxidant Enzymes, 3–18.

Kroemer, G., L. Galluzzi, and C. Brenner. (2007). Mitochondrial membrane permeabilization in cell death. *Physiology Reveiw*, 99–163.

Kurth, E.F., and F.L. Chan. (1951). Dihydroquercetin as an antioxidant. *Journal of the American Oil Chemists' Society 28*, 433–436.

Kushner, B.H., M.P. LaQuaglia, N. Wollner, et al. (1996). Desmoplastic small round-cell tumor: Prolonged progression-free survival with aggressive multimodality therapy. *Journal of Clinical Oncology 14*, 1526–1531.

Lappas, C.M., and N.T. Lappas. (2012). D-Limonene modulates T lymphocyte activity and viability. *Cellular Immunology*.

Laskowski, R.A., and M.B. Swindells. (2011). LigPlot + : Multiple Ligand À Protein Interaction Diagrams for Drug Discovery. *Journal of chemical information and modeling 51*, 2778–2786.

Lee, D.H., J.H. Ha, Y. Kim, et al. (2014). A Conserved Mechanism for Binding of p53 DNA-Binding Domain and Anti-Apoptotic Bcl-2 Family Proteins. *Molecules and cells 37*, 264–9.

Lee, S.B., K.H. Cha, D. Selenge, et al. (2007). The chemopreventive effect of taxifolin is exerted through ARE-dependent gene regulation. *Biological & pharmaceutical bulletin 30*, 1074–9.

Lee, W.R. (1975). Comparison of the mutagenic effects of chemicals and ionizing radiation using Drosophila melanogaster test systems. *In Radiation research. Biomedical, chemical, and physical perspectives 8*, 8293250.

Lee, W.R., S. Abrahamson, R. Valencia, et al. (1983a). The sex-linked recessive lethal test for mutagenesis in Drosophila melanogaster. *Mutation Research 123*, 183–279.

Lee, W.R., S. Abrahamson, R. Valencia, et al. (1983b). The sex-linked recessive lethal test for mutagenesis in Drosophila melanogaster. A report of the U.S. Environmental Protection Agency Gene-Tox Program. *Mutation research 123*, 183–279.

Li, J., N. Zhou, P. Cai, et al. (2016). In silico screening identifies a novel potential PARP1 inhibitor targeting synthetic lethality in cancer treatment. *International Journal of Molecular Sciences 17*, 1–11.

Li, N., and M. Karin. (1999). Is NF-κB the sensor of oxidative stress? *The FASEB Journal 13*, 1137–1143.

Liang, L., C. Gao, M. Luo, et al. (2013). Dihydroquercetin (DHQ) induced HO-1 and NQO1 expression against oxidative stress through the Nrf2-dependent antioxidant pathway. *Journal of Agricultural and Food Chemistry 61*, 2755–2761.

Van Lieshout, E.M. m, G.H. Posner, B.T. Woodard, et al. (1998). Effects of the sulforaphane analog compound 30, indole-3-carbinol, D-limonene or relafen on glutathione S-transferases and glutathione peroxidase of the rat digestive tract. *Biochimica et Biophysica Acta - General Subjects 1379*, 325–336.

Lindsley, D.L., and E.H. Grell. (1968). Genetic variations of Drosophila melanogaster.

Liu, B., Y. Chen, and D.K.S. Clair. (2008). ROS and p53 : A versatile partnership. *Free Radical Biology & Medicine 44*, 1529–1535.

Liu, J., Z. Liu, S. Man, et al. (2016). Inhibition of urethane-induced lung carcinogenesis in mice by a Rhizoma paridis saponin involved EGFR/PI3K/Akt pathway. *RSC Advances 6*, 1–16.

Liu, M., C. Li, M. Pazgier, et al. (2010). D-peptide inhibitors of the p53-MDM2 interaction for targeted molecular therapy of malignant neoplasms. *Proceedings of the National Academy of Sciences of the United States of America 107*, 14321–6.

Livingstone, F.B. (1973). The genetics of human populations. *American Journal of Physical Anthropology 39*, 141–144.

Lomax, M.E., L.K. Folkes, and P. O'Neill. (2013). Biological consequences of radiation-induced DNA damage: Relevance to radiotherapy. *Clinical Oncology 25*, 578–585.

Lötscher, M., M. Recher, K.S. Lang, et al. (2007). Induced prion protein controls immune-activated retroviruses in the mouse spleen. *PloS ONE 2*, e1158.

Lowry, O.H., N.J. Rosebrough, A.L. Farr, et al. (1951). Protein measurement with the Folin phenol reagent. *The Journal of biological chemistry 193*, 265–275.

Lozano, G., and R. Montes de Oca Luna. (1998). MDM2 function. *Biochimica et Biophysica Acta (BBA) - Reviews on Cancer 1377*, 55–59.

Lu, D.-Y. (2015). Anticancer Drug Combinations, Studies from Different Pathways. *Cell & Developmental Biology 4*, 3–4.

Lugovskoy, A.A., A.I. Degterev, A.F. Fahmy, et al. (2002). A novel approach for characterizing protein ligand complexes: molecular basis for specificity of small-molecule Bcl-2 inhibitors. *Journal of the American Chemical Society 124*, 1234–1240.

Majno, G., and I. Joris. (1995). Apoptosis, oncosis, and necrosis. An overview of cell death. *The American journal of pathology 146*, 3–15.

Makara, G.M. (2006). Hit discovery and hit-to-lead approaches. *Drug Discovery Today 11*, 741–748.

Maltzman, T.H., L.M. Hurt, C.E. Elson, et al. (1989). The prevention of nitrosomethylurea-induced mammary tumors by d-limonene and orange oil. *Carcinogenesis. 10*, 781-783.

Manda, K., and A.L. Bhatia. (2003). Pre-administration of beta-carotene protects tissue

glutathione and lipid peroxidation status following exposure to gamma radiation. *Journal of Environmental Biology 24*, 369–72.

Manigandan, K. and, R.L. Jayaraj, K. Jagatheesh, et al. (2015). Taxifolin mitigates oxidative DNA damage in vitro and protects zebrafish (Danio rerio) embryos against cadmium toxicity. *Environmental Toxicology and Pharmacology 39*, 1252–1261.

Manigandan, K., R.L. Jayaraj, and N. Elangovan. (2014). Taxifolin ameliorates 1 , 2-dimethylhydrazine induced cell proliferation and redox avulsions in mice colon carcinogenesis. *Biomedicine & Preventive Nutrition 4*, 499–509.

Manigandan, K., D. Manimaran, R.L. Jayaraj, et al. (2015). Taxifolin curbs NF-κB-mediated Wnt/β-catenin signaling via up-regulating Nrf2 pathway in experimental colon carcinogenesis. *Biochimie 119*, 103–112.

Manna, P., J. Das, J. Ghosh, et al. (2010). Contribution of type 1 diabetes to rat liver dysfunction and cellular damage via activation of NOS, PARP,IκBα/NF-κB, MAPKs, and mitochondria-dependent pathways: Prophylactic role of arjunolic acid. *Free Radical Biology and Medicine 48*, 1465–1484.

Marchenko, N.D., and U.M. Moll. (2014). Mitochondrial death functions of p53. *Molecular & cellular oncology 1*, e955995-8.

Marklund, S., and G. Marklund. (1974). Involvement of the superoxide anion radical in the autoxidation of pyrogallol and a conveniente assay for superoxide dismutase. *Eur J Biochem 47*, 469–474.

Markowitzz, E.H. (1970). Gamma ray-induced mutations in Drosophila Melanogaster oocytes: the phenomenon of dose rate. *Genetics 64*, 312–322.

Maser, R.S., K.J. Monsen, B.E. Nelms, et al. (1997). hMre11 and hRad50 nuclear foci are induced during the normal cellular response to DNA double-strand breaks. *Molecular and cellular biology 17*, 6087–96.

Mayne, S.T. (1996). Beta-carotene, carotenoids, and disease prevention in humans. *The FASEB Journal 10*, 690–701.

Meek, D.W. (2004). The p53 response to DNA damage. *DNA Repair 3*, 1049–1056.

Merad-Boudia, M., A. Nicole, D. Santiard-Baron, et al. (1998). Mitochondrial impairment as an early event in the process of apoptosis induced by glutathione depletion in neuronal cells: Relevance to Parkinson's disease. *Biochemical Pharmacology 56*, 645–655.

Mezzoug, N., A. Elhadri, A. Dallouh, et al. (2007). Investigation of the mutagenic and antimutagenic effects of Origanum compactum essential oil and some of its constituents. *Mutation Research 629*, 100–110.

Michael, D., and M. Oren. (2003). The p53-Mdm2 module and the ubiquitin system. *Seminars in Cancer Biology 13*, 49–58.

Mihara, M., S. Erster, A. Zaika, et al. (2003). P53 Has a Direct Apoptogenic Role At the Mitochondria. *Molecular Cell 11*, 577–590.

Mihara, M., S. Erster, A. Zaika, et al. (2003). p53 Has a Direct Apoptogenic Role at the Mitochondria Results p53 Rapidly Accumulates at Mitochondria of Primary Thymocytes Undergoing γIR-. *Molecular Cell 11*, 577–590.

Missirlis, F., J.P. Phillips, and H. Jäckle. (2001). Cooperative action of antioxidant defense systems in Drosophila. *Current Biology 11*, 1272–1277.

Missirlis, F., J.P. Phillips, H. Jäckle, et al. (2003). Drosophila and antioxidant therapy design. *Free Radical Biology & Medicine 33*, 147–151.

Mladenović, M., S. Matić, S. Stanić, et al. (2013). Combining molecular docking and 3-D pharmacophore generation to enclose the in vivo antigenotoxic activity of naturally occurring aromatic compounds: Myricetin, quercetin, rutin, and rosmarinic acid. *Biochemical Pharmacology 86*, 1376–1396.

Moll, U.M., and O. Petrenko. (2004). The MDM2-p53 Interaction. *Molecular Cancer Research 1*, 1001 LP-1008.

Monente, C., J. Bravo, A.I. Vitas, et al. (2015). Coffee and spent coffee extracts protect against cell mutagens and inhibit growth of food-borne. *Journal of Functional Foods 12*, 365–374.

Montero, J., C. Dutta, D. van Bodegom, et al. (2013). p53 regulates a non-apoptotic death induced by ROS. *Cell Death and Differentiation 20*, 1465–74.

Morgan, T.H. (1910). Sex Limited Inheritance in Drosophila. *Science 32*, 120–122.

Morgan, T.H. (1909). What are "factors" in mendelian explanations? *American Breeders Association Reports 5*, 365–368.

Morley, N., T. Clifford, L. Salter, et al. (2005). The green tea polyphenol epigallocatechin gallate and green tea can protect human cellular DNA from ultraviolet and visible radiation-induced damage. *Photodermatology Photoimmunology and Photomedicine 21*, 15–22.

Moron, M.S., Depierre, J.W. and Mannervik, B. (1979). Levels of glutathione, glutathione reductase and glutathione S-transferase activities in rat lung and liver. *Biochimica et Biophysica Acta 582*, 67–78.

Mothersill, C., and C. Seymour. (2001). Radiation-induced bystander effects: past history and future directions. *Radiation research 155*, 759–767.

Muller, H.J., and E. Altenburg. (1929). The frequency of translocations produced by X-

rays in Drosophila. *Genetics 15*, 283–311.

Murali, R., A. Karthikeyan, and R. Saravanan. (2013). Protective effects of D-limonene on lipid peroxidation and antioxidant enzymes in streptozotocin-induced diabetic rats. *Basic & clinical pharmacology & toxicology 112*, 175–81.

Murata, S., C. Zhang, N. Finch, et al. (2016). Predictors and modulators of synthetic lethality : an update on parp inhibitors and personalized medicine. *BioMed Research International 2016*, 1–12.

Nazir, A., I. Mukhopadhyay, D.K. Saxena, et al. (2001). Chlorpyrifos-induced hsp70 expression and effect on reproductive performance in transgenic Drosophila melanogaster (hsp70-lacZ) Bg9. *Archives of Environmental Contamination and Toxicology 41*, 443–449.

Negishi, T., S. Arimoto, C. Nishizaki, et al. (1989). Inhibitory effect of chlorophyll on the genotoxicity of 3-ainino-l-methyl-5H-pyrido[4,3-b]indole (Trp-P-2). *Carcinogenesis 10*, 145–149.

Nigro, J.M., S.J. Baker, a C. Preisinger, et al. (1989). Mutations in the p53 gene occur in diverse human tumour types. *Nature 342*, 705–708.

Nishikimi, M., N. Appaji Rao, and K. Yagi. (1972). The occurrence of superoxide anion in the reaction of reduced phenazine methosulfate and molecular oxygen. *Biochemical and Biophysical Research Communications 46*, 849–854.

O'Connor, L., A. Strasser, L.A. O'Reilly, et al. (1998). Bim: A novel member of the Bcl-2 family that promotes apoptosis. *EMBO Journal 17*, 384–395.

Ogura, K., J. Magae, Y. Kawakami, et al. (2009). Reduction in mutation frequency by very low-dose gamma irradiation of Drosophila melanogaster germ cells reduction in mutation frequency by very low-dose gamma irradiation of drosophila melanogaster germ cells. *Radiation Research Society 171*, 1–8.

Ohkawa, H., N. Ohishi, and K. Yagi. (1979). Assay for lipid peroxides in animal tissues by thiobarbituric acid reaction. *Analytical Biochemistry 95*, 351–358.

Omura, T., and R. Sato. (1964). The carbon monoxide-bindng pigent of liver microsomes. I. Evidence for its hemoprotein nature. *The Journal of Biological Chemistry 239*, 2370–8.

Orsucci, D., M. Mancuso, and G. Siciliano. (2008). Mitochondria, oxidative stress and PARP-1 network: a new target for neuroprotective effects of tetracyclines? *The Journal of Physiology 586*, 2427–2428.

Ortega-Arellano, H.F., M. Jimenez-Del-Rio, and C. Velez-Pardo. (2011). Life span and locomotor activity modification by glucose and polyphenols in Drosophila melanogaster chronically exposed to oxidative stress-stimuli: Implications in

Parkinson's disease. *Neurochemical Research 36*, 1073–1086.

Ow, Y.-Y., and I. Stupans. (2003). Gallic acid and gallic acid derivatives: effects on drug metabolizing enzymes. *Current Drug Metabolism 4*, 241–248.

Pacher, P., and C. Szabó. (2007). Role of poly(ADP-ribose) polymerase 1 (PARP-1) in cardiovascular diseases: The therapeutic potential of PARP inhibitors. *Cardiovascular Drug Reviews 25*, 235–260.

Paglia, D.E., and W.N. Valentine. (1967). Studies on the quantitative and qualitative characterization of erythrocyte glutathione peroxidase. *The Journal of Laboratory and Clinical Medicine 70*, 158–169.

Pandey, U.B., and C.D. Nichols. (2011). Human Disease Models in Drosophila melanogaster and the Role of the Fly in Therapeutic Drug Discovery. *Pharmacological Reviews 63*, 411–436.

Parsons, P.A. (1980). Acetic acid vapour as a resource: threshold differences among three Drosophila species. *Experientia 36*, 1363.

Patenkovic, A., M. Stamenkovic-Radak, T. Banjanac, et al. (2009). Antimutagenic effect of sage tea in the wing spot test of Drosophila melanogaster. *Food and Chemical Toxicology 47*, 180–183.

Phillips, M. (1990). The effects of a range of anti-cancer drugs in the mutation test in Drosophila. *Mutation Research 228*, 171–176.

Ramesha, C.S. (2000). How many leads from HTS? – Comment. *Drug Discovery Today 5*, 43–44.

Ramos, C.A.F., R. de C. da S. Sá, M.F. Alves, et al. (2015). Histopathological and biochemical assessment of D-limonene-induced liver injury in rats. *Toxicology Reports 2*, 482–488.

Rehman, M.U., M. Tahir, A.Q. Khan, et al. (2014). D-limonene suppresses doxorubicin-induced oxidative stress and inflammation via repression of COX-2, iNOS, and NFκB in kidneys of Wistar rats. *Experimental Biology and Medicine 239*, 465–76.

Reicks, M.M., and D. Crankshaw. (1993). Effects of D-limonene on hepatic microsomal monooxygenase activity and paracetamol-induced glutathione depletion in mouse. *Xenobiotica 23*, 809–819.

Reiter, L.T., and E. Bier. (2002). Using Drosophila melanogaster to uncover human disease gene function and potential drug target proteins. *Expert Opinion on Therapeutic Targets 6*, 387–399.

Reiter, L.T., L. Potocki, S. Chien, et al. (2001). A systematic analysis of human disease-associated gene sequences in drosophila melanogaster. *Genome Research*, 1114–

1125.

Ribble, D., N.B. Goldstein, D. a Norris, et al. (2005). A simple technique for quantifying apoptosis in 96-well plates. *BMC biotechnology 5*, 12.

Rice-Evans, C. (1995). Plant polyphenols: free radical scavengers or chain-breaking antioxidants? *Biochemical Society Symposium 61*, 103–116.

Roberto, D., P. Micucci, T. Sebastian, et al. (2010). Antioxidant activity of limonene on normal murine lymphocytes: Relation to H2O2 modulation and cell proliferation. *Basic and Clinical Pharmacology and Toxicology 106*, 38–44.

Robson, A. and. (1941). The discovery of mustard gas mutagenesis. *Genetics 134*, 393–399.

Rogers, S. (1955). Studies of the mechanism of action of urethan in initiating pulmonary adenomas in mice. I. The indirect nature of its oncogenic influence. *Journal of the National Cancer Institute 15*, 1675–1683.

Romero-Jiménez, M., J. Campos-Sánchez, M. Analla, et al. (2005). Genotoxicity and anti-genotoxicity of some traditional medicinal herbs. *Mutation Research 585*, 147–155.

Rosenkranz, H.S., B. Gutter, and W.T. Speck. (1976). Mutagenicity and DNA-modifying activity: a comparison of two microbial assays. *Mutation Research 41*, 61–70.

Russell, L.B., P.R. Hunsicker, E.F. Oakberg, et al. (1987). Tests for urethane induction of germ-cell mutations and germ-cell killing in the mouse. *Mutation Research 188*, 335–342.

Ruvolo, P.P., X. Deng, and W.S. May. (2001). Phosphorylation of Bcl-2 and regulation of apoptosis. *Leukemia 15*, 515–522.

Sadiq, M.F., and F.A. Al Quraishe. (2005). The effect of trifluoperazine on the induction of sex linked recessive lethals by cyclophosphamide in *drosophila melanogaster*. *Drug and Chemical Toxicology 27*, 169–178.

Salah, N., N.J. Miller, G. Paganga, et al. (1995). Polyphenolic flavanols as scavengers of aqueous phase radicals and as chain-breaking antioxidants. *Archives of Biochemistry and Biophysics 322*, 339–346.

Salmas, R.E., A. Unlu, M. Yurtsever, et al. (2015). In silico investigation of PARP-1 catalytic domains in holo and apo states for the design of high-affinity PARP-1 inhibitors. *Journal of Enzyme Inhibition and Medicinal Chemistry 6366*, 1–9.

Salvadori, D.M.F., L.R. Ribeiro, M.D.M. Oliveira, et al. (1992). The protective effect of

ß-carotene on genotoxicity induced by cyclophosphamide. *Mutation Research 265*, 237–244.

Salvadori, D.M.F., L.R. Ribeiro, Y. Xiao, et al. (1996). Radioprotection of β-carotene evaluated on mouse somatic and germ cells. *Mutation Research 356*, 163–170.

Santivasi, W.L., and F. Xia. (2014). Ionizing radiation-induced DNA damage, response, and repair. *Antioxidants & Redox Signaling 21*, 251–259.

Saraste, A., and K. Pulkki. (2000). Morphologic and biochemical hallmarks of apoptosis. *Cardiovascular Research 45*, 528–537.

Sathishkumar, N., S. Sathiyamoorthy, M. Ramya, et al. (2012). Molecular docking studies of anti-apoptotic BCL-2, BCL-XL, and MCL-1 proteins with ginsenosides from Panax ginseng. *Journal of Enzyme Inhibition And Medicinal Chemistry 27*, 685–92.

Schlatter, J., and W.K. Lutz. (1990). The carcinogenic potential of ethyl carbamate (urethane): Risk assessment at human dietary exposure levels. *Food and Chemical Toxicology 28*, 205–211.

Scovassi, F.A.A.I. (2014). Poly(ADP-ribose): A signaling molecule in different paradigms of cell death. *Biochemical Pharmacology 92*, 157–163.

Seong, K.M., C.S. Kim, S.W. Seo, et al. (2011). Genome-wide analysis of low-dose irradiated male Drosophila melanogaster with extended longevity. *Biogerontology 12*, 93–107.

Shangary, S., and S. Wang. (2008). Targeting the MDM2-p53 Interaction for Cancer Therapy. *Clinical Cancer Research 14*, 5318–5324.

Shaughnessy, D.T., K. McAllister, L. Worth, et al. (2015). Mitochondria, energetics, epigenetics, and cellular responses to stress. *Environmental Health Perspectives 122*, 1271–1278.

Sheehan, D., G. Meade, V.M. Foley, et al. (2001). Structure, function and evolution of glutathione transferases: implications for classification of non-mammalian members of an ancient enzyme superfamily. *Biochemical Journal 360*, 1–16.

Sheikh, M., and A. Fornace. (2000). Death and decoy receptors and p53-mediated apoptosis. *Leukemia 14*, 1509–1513.

Shitashige, M., M. Toi, T. Yano, et al. (2001). Dissociation of Bax from a Bcl-2/Bax heterodimer triggered by phosphorylation of serine 70 of Bcl-2. *Journal of biochemistry 130*, 741–8.

Siddiqui, W.A., A. Ahad, and H. Ahsan. (2015). The mystery of Bcl-2 family: Bcl-2 proteins and apoptosis: an update. *Archives of Toxicology 89*, 289–317.

Simić, D., B. Vuković-Gačić, and J. Knežević-Vukčević. (1998). Detection of natural bioantimutagens and their mechanisms of action with bacterial assay-system. *Mutation Research 402*, 51–57.

Simic, M.G., D.S. Bergtold, and L.R. Karam. (1989). Generation of oxy radicals in biosystems. *Mutation Research 214*, 3–12.

Singh, M.P., M. Mishra, A. Sharma, et al. (2011). Genotoxicity and apoptosis in Drosophila melanogaster exposed to benzene , toluene and xylene : Attenuation by quercetin and curcumin. *Toxicology and Applied Pharmacology 253*, 14–30.

Singh, M.P., M.M.K. Reddy, N. Mathur, et al. (2009). Induction of hsp70, hsp60, hsp83 and hsp26 and oxidative stress markers in benzene, toluene and xylene exposed Drosophila melanogaster: Role of ROS generation. *Toxicology and Applied Pharmacology 235*, 226–243.

Singh, N.P., M.T. McCoy, R.R. Tice, et al. (1988). A simple technique for quantitation of low levels of DNA damage in individual cells. *Experimental Cell Research 175*, 184–191.

Sinha, A.K. (1972). Colorimetric assay of catalase. *Analytical Biochemistry 47*, 389–394.

Sinha, R.P., and D.-P. Häder. (2002). UV-induced DNA damage and repair: a review. *Photochemical & Photobiological Sciences 1*, 225–236.

Siomek, A., D. Gackowski, A. Szpila, et al. (2014). Epigenetic modifications and NF-kB pathway activity in Cu,Zn-SOD-deficient mice. *Molecular and Cellular Biochemistry 397*, 187–194.

Slater, T.F. (1987). Free radicals and tissue injury. *British Journal of Cancer 55*, 5–10.

Snyder, R.D. (2009). An update on the genotoxicity and carcinogenicity of marketed pharmaceuticals with reference to in silico predictivity. *Environmental and Molecular Mutagenesis 50*, 435–450.

Sobels, F.H. (1974). The advantages of drosophila for mutation studies. *Mutation research 26*, 277–284.

Sobels, F.H., and E. Vogel. (1976). Assaying potential carcinogens with drosophila. *Environmental Health Perspectives Vol.15*, 141–146.

Sobels, F.H., E. Vogel, and C. Mutagenesis. (1976). The capacity of drosophila for detecting relevant genetic damage. *Mutation Research 41*, 95–105.

Sosa, V., T. Moliné, R. Somoza, et al. (2013). Oxidative stress and cancer: An overview. *Ageing Research Reviews 12*, 376–390.

Sotibrán, A.N.C., M.G. Ordaz-Téllez, and R. Rodríguez-Arnaiz. (2011). Flavonoids and

oxidative stress in Drosophila melanogaster. *Mutation Research 726*, 60–65.

Sotomayor, R.E., G.A. Sega, and F. Kadlubar. (1994). Induction of DNA damage by urethane in mouse testes: DNA binding and unscheduled DNA synthesis. *Environmental and Molecular Mutagenesis 24*, 68–74.

Soussi, T., and P. May. (1996). Structural aspects of the p53 protein in relation to gene evolution: a second look. *Journal of Molecular Biology 260*, 623–637.

Spindler, S.R., P.L. Mote, J.M. Flegal, et al. (2013). Influence on Longevity of Blueberry, Cinnamon, Green and Black Tea, Pomegranate, Sesame, Curcumin, Morin, Pycnogenol, Quercetin, and Taxifolin Fed Iso-Calorically to Long-Lived, F1 Hybrid Mice. *Rejuvenation Research 16*, 143–151.

Stamenkovic-Radak Marina, Savic T, V.M. and A.M. (2005). Antigenotoxic effects of royal jelly in the sex linked recessive lethal test with drosophila melanogaster. *Acta Veterinaria (Beograd) 5*, 626–639.

Stanic, S., S. Matic, G. Đelic, et al. (2011). Study of Genotoxicity and Antigenotoxicity of the Cotinus coggygria Scop . Methanol Extract by Drosophila melanogaster Sex Linked Recessive Lethal Test 1. *Russian Journal of Genetics 47*, 770–774.

Stathopoulos, G.T., T.P. Sherrill, D.-S. Cheng, et al. (2007). Epithelial NF-kappaB activation promotes urethane-induced lung carcinogenesis. *Proceedings of the National Academy of Sciences of the United States of America 104*, 18514–9.

Steffan, J.S., L. Bodai, J. Pallos, et al. (2001). Histone deacetylase inhibitors arrest polyglutamine-dependent neurodegeneration in Drosophila. *Nature 413*, 739–743.

Steffen, J.D., J.R. Brody, R.S. Armen, et al. (2013). Structural Implications for Selective Targeting of PARPs. *Frontiers of Oncology 3*, 301.

Stevens, J.F., and C.S. Maier. (2008). Acrolein: Sources, metabolism, and biomolecular interactions relevant to human health and disease. *Molecular Nutrition and Food Research 52*, 7–25.

Stilwell, G.E., S. Saraswati, J.T. Littleton, et al. (2006). Development of a Drosophila seizure model for in vivo high-throughput drug screening. *European Journal of Neuroscience 24*, 2211–2222.

Sueoka, N., M. Suganuma, E. Sueoka, et al. (2006). A New Function of Green Tea: Prevention of Lifestyle-related Diseases. *Annals of the New York Academy of Sciences 928*, 274–280.

Sun, J. (2007). D-Limonene: Safety and Clinical Applications. *Alternative Medicine Review 12*, 259–264.

Suzuki, B.Y.D.T., L.K. Piternick, S. Hayashi, et al. (1967). Temperature-sensitive mutations in Drosophila melanogaster, I. Relative frequencies among gamma-ray and chemically induced sex-linked recessive lethals and semilethals. *Proceedings of the National Academy of Sciences of the United States of America 57*, 902–912.

Svobodová, A., D. Walterová, and J. Psotová. (2006). Influence of silymarin and its flavonolignans on H2O2-induced oxidative stress in human keratinocytes and mouse fibroblasts. *Burns 32*, 973–979.

Szabad, J., I. Soós, G. Polgár, et al. (1983). Testing the mutagenicity of malondialdehyde and formaldehyde by the Drosophila mosaic and the sex-linked recessive lethal tests. *Mutation Research 113*, 117–133.

Tapon, N., K.F. Harvey, D.W. Bell, et al. (2002). salvador promotes both cell cycle exit and apoptosis in Drosophila and is mutated in human cancer cell lines. *Cell 110*, 467–478.

Tice, R.R., E. Agurell, D. Anderson, et al. (2000). Single Cell Gel / Comet Assay : Guidelines for In Vitro and In Vivo Genetic Toxicology Testing. *Environmental and molecular mutagenesis 35*, 206–21.

Tomisawa, M., H. Suemizu, Y. Ohnishi, et al. (2003). Mutation analysis of vinyl carbamate or urethane induced lung tumors in rasH2 transgenic mice. *Toxicology Letters 142*, 111–117.

Del Toro-Arreola, S., E. Flores-Torales, C. Torres-Lozano, et al. (2005). Effect of D-limonene on immune response in BALB/c mice with lymphoma. *International Immunopharmacology* 5,829-38.

Toshiyuki, M., and J.C. Reed. (1995). Tumor suppressor p53 is a direct transcriptional activator of the human bax gene. *Cell 80*, 293–299.

Toupet, K., V. Compan, C. Crozet, et al. (2008). Effective gene therapy in a mouse model of prion diseases. *PloS one 3*, e2773.

Trachootham, D., W. Lu, M.A. Ogasawara, et al. (2007). Mechanisms of cell death in oxidative stress. *Antioxidants & redox signaling 9*, 49–89.

Trachootham, D., W. Lu, M.A. Ogasawara, et al. (2008). Redox regulation of cell survival. *Antioxidants & redox signaling 10*, 1343–1374.

Trimble, B.Y.B.K., and J.H. Doughty. (1974). The amount of hereditary disease in human populations. *Ann. Hum. Genet 38*, 199–223.

Tse, C., A.R. Shoemaker, J. Adickes, et al. (2008). ABT-263: A potent and orally bioavailable Bcl-2 family inhibitor. *Cancer Research 68*, 3421–3428.

Tsujimoto, Y., J. Cossman, E. Jaffe, et al. (1985). Involvement of the bcl-2 gene in human follicular lymphoma. *Science 228*, 1440 LP-1443.

Tuppen, H.A.L., E.L. Blakely, D.M. Turnbull, et al. (2010). Mitochondrial DNA mutations and human disease. *Biochimica et Biophysica Acta 1797*, 113–28.

Uedo, N., M. Tatsuta, H. Iishi, et al. (1999). Inhibition by D-limonene of gastric carcinogenesis induced by N-methyl-N'-nitro-N-nitrosoguanidine in Wistar rats. *Cancer Letters 137*, 131–136.

Ugur, B., K. Chen, and H.J. Bellen. (2016). Drosophila tools and assays for the study of human diseases. *Disease Models & Mechanisms 9*, 235–44.

Varshney, R., and R.K. Kale. (1990). Effects of calmodulin antagonists on radiation-induced lipid peroxidation in microsomes. *International Journal of Radiation Biology 58*, 733–743.

Vassilev, L.T. (2007). MDM2 inhibitors for cancer therapy. *Trends in Molecular Medicine 13*, 23–31.

Vassilev, L.T., B.T. Vu, B. Graves, et al. (2004). In vivo activation of the p53 pathway by small-molecule antagonists of MDM2. *Science (New York, N.Y.) 303*, 844–8.

Verdonk, M.L., J.C. Cole, M.J. Hartshorn, et al. (2003). Improved protein-ligand docking using GOLD. *Proteins 52*, 609–23.

Verma, S., A. Singh, and A. Mishra. (2013a). Molecular dynamics investigation on the inhibition of MDM2-p53 interaction by polyphenols. *Molecular Informatics 32*, 203–212.

Verma, S., A. Singh, and A. Mishra. (2013b). Quercetin and taxifolin completely break MDM2-p53 association: Molecular dynamics simulation study. *Medicinal Chemistry Research 22*, 2778–2787.

Vermes, I., C. Haanen, H. Steffens-Nakken, et al. (1995). A novel assay for apoptosis. Flow cytometric detection of phosphatidylserine expression on early apoptotic cells using fluorescein labelled Annexin V. *Journal of Immunological Methods 184*, 39–51.

Vidal, M., S. Wells, A. Ryan, et al. (2005). ZD6474 Suppresses Oncogenic RET Isoforms in a Drosophila Model for Type 2 Multiple Endocrine Neoplasia Syndromes and Papillary Thyroid Carcinoma Thyroid Carcinoma. *Cancer Research*, 3538–3541.

Vieira da Silva, B., J.C.M. Barreira, and M.B.P.P. Oliveira. (2016). Natural phytochemicals and probiotics as bioactive ingredients for functional foods: Extraction, biochemistry and protected-delivery technologies. *Trends in Food Science and Technology 50*, 144–158.

Virág, L., and C. Szabó. (2002). The Therapeutic Potential of Poly(ADP-Ribose) Polymerase Inhibitors. *Pharmacological Reviews 54*, 375 LP-429.

Vladimirov, Y. a, E. V Proskurnina, E.M. Demin, et al. (2009). Dihydroquercetin (taxifolin) and other flavonoids as inhibitors of free radical formation at key stages of apoptosis. *Biochemistry. Biokhimiia 74*, 301–307.

Vogel, E. (1984). A comparison of genotoxic activity in somatic tissue and in germ cells of Drosophila melanogaster. *Mutation, Cancer, and Malformation*, 233–255.

Vogel, E. (1975). Mutagenic activity of cyclophosphamide, trofosfamide, and infosfamide in Drosophila melanogaster specific. Specific induction of recessive lethals in the absence of detectable chromosome breakage. *Mutation Research 33*, 221–228.

Vogel, E.W. (1987). Evaluation of potential mammalian genotoxins using Drosophila : the need for a change in test strategy. *Mutagenesis 2*, 161–171.

Vogelstein, B., D. Lane, and a J. Levine. (2000). Surfing the p53 network. *Nature 408*, 307–10.

Vogler, M. (2014). Targeting BCL2-Proteins for the Treatment of Solid Tumours. *Advances in Medicine 2014*, 1–14.

Vogler, M., D. Dinsdale, M.J.S. Dyer, et al. (2009). Bcl-2 inhibitors: small molecules with a big impact on cancer therapy. *Cell Death and Differentiation 16*, 360–367.

Vousden, K.H., and D.P. Lane. (2007). P53 in Health and Disease. *Nature reviews. Molecular Cell Biology 8*, 275–283.

Vujošević, M., and J. Blagojević. (2004). Antimutagenic effects of extracts from sage (Salvia officinalis) in mammalian system in vivo. *Acta veterinaria Hungarica 52*, 439–443.

Vuković-Gačić, B., S. Nikčević, T. Berić-Bjedov, et al. (2006). Antimutagenic effect of essential oil of sage (Salvia officinalis L.) and its monoterpenes against UV-induced mutations in Escherichia coli and Saccharomyces cerevisiae. *Food and Chemical Toxicology 44*, 1730–1738.

Vyas, S., and P. Chang. (2014). New PARP targets for cancer therapy. *Nature Reviews: Cancer 14*, 502–509.

Wallace, A.C., R.A. Laskowski, and J.M. Thornton. (1995). LIGPLOT: a program to generate schematic diagrams of protein-ligand interactions. *Protein Engineering 8*, 127–34.

Wang, T., X. Zhang, and J.J. Li. (2002). The role of NF-kappaB in the regulation of cell stress responses. *International Immunopharmacology 2*, 1509–1520.

Wang, X., and C. Tournier. (2006). Regulation of cellular functions by the ERK5 signalling pathway. *Cellular Signalling 18*, 753–760.

Wang, Y.H., W.Y. Wang, C.C. Chang, et al. (2006). Taxifolin ameliorates cerebral ischemia-reperfusion injury in rats through its anti-oxidative effect and modulation of NF-kappa B activation. *Journal of Biomedical Science 13*, 127–141.

Wang, Z., and T. Song. (2106). Bcl-2-MDM2 Dual Inhibitors Based on Universal Pyramid-Like α-Helical Mimetics. *Journal of medicinal chemistry 59*, 3152–3162.

Wang, Z.Y., S.J. Cheng, Z.C. Zhou, et al. (1989). Antimutagenic activity of green tea polyphenols. *223*, 273–285.

Ward, J.F. (1988). Dna damage produced by ionizing radiation in mammalian cells: identities, mechanisms of formation, and reparability w. E. C. And k. M. B. T.-p. In n. A. R. And m. Biology [ed.],. *Progress in Nucelic Acid Research and Molecular Biology Volume 35*, 95–125.

Weidmann, A.E. (2012). Dihydroquercetin: More than just an impurity? *European Journal of Pharmacology 684*, 19–26.

Weinreb, O., S. Mandel, T. Amit, et al. (2016). Neurological mechanisms of green tea polyphenols in Alzheimer's and Parkinson's diseases. *Journal of Nutritional Biochemistry 15*, 506–516.

Weiss, D.L., and R. de los Santos. (1960). Urethane-induced hepatic failure in man. *The American Journal of Medicine 28*, 476–481.

Weyemi, U., and C. Dupuy. (2012). The emerging role of ROS-generating NADPH oxidase NOX4 in DNA-damage responses. *Mutation Research 751*, 77–81.

Wienberg, J. (1977). BrdU-Giemsa-technique for the differentiation of sister chromatids in somatic cells of drosophila melanogaster. *Mutation Research 44*, 283–286.

Williams, K., and R. Nery. (1971). Aspects of the mechanism of urethane carcinogenesis. *Xenobiotica 1*, 545–50.

Willoughby, L.F., T. Schlosser, S.A. Manning, et al. (2013). An in vivo large-scale chemical screening platform using Drosophila for anti-cancer drug discovery. *Disease Models & Mechanisms 6*, 521–9.

Wiman, K.G. (2013). p53 talks to PARP: the increasing complexity of p53-induced cell death. *Cell Death And Differentiation 20*, 1438–9.

Wu, X., J.H. Bayle, D. Olson, et al. (1993). The p53-mdm-2 autoregulatory feedback loop. *Genes & Development 7*, 1126–1132.

Würgler, F.E. (1980). Mutagenicity testing with Drosophila. *Archives of Toxicology 46*, 77–87.

Würgler, F.E., and U. Graf. (1985). Mutagenicity Testing with Drosophila Melanogaster. *In* Basic and Applied Mutagenesis, 343–372. Springer US, Boston,

MA.

Würgler, F.E., U. Graf, and W. Berchtold. (1975). Statistical problems connected with the sex-linked recessive lethal test in Drosophila melanogaster. I. The use of the Kastenbaum-Bowman test. *Archiv für Genetik 48*, 158–78.

Yang, J., C. McCart, D.J. Woods, et al. (2007). A Drosophila systems approach to xenobiotic metabolism. *Physiological Genomics 30*, 223–31.

Ye, N., C.H. Chen, T. Chen, et al. (2013). Design, synthesis, and biological evaluation of a series of benzo[de][1,7]naphthyridin-7(8 H)-ones bearing a functionalized longer chain appendage as novel PARP1 inhibitors. *Journal of Medicinal Chemistry 56*, 2885–2903.

Yen, G.C., and H.Y. Chen. (1995). Antioxidant activity of various tea extracts in relation to their antimutagenicity. *Journal of Agricultural and Food Chemistry 43*, 27–32.

Ying, Y., B.J. Padanilam. (2016). Regulation of necrotic cell death : p53 , PARP1 and cyclophilin D-overlapping pathways of regulated necrosis ? *Cellular and Molecular Life Sciences 73*, 2309–2324.

Zacarías-Lara, O.J., J. Correa-Basurto, and M. Bello. (2016). Exploring the conformational and binding properties of unphosphorylated/phosphorylated monomeric and trimeric Bcl-2 through docking and molecular dynamics simulations. *Biopolymers 105*, 393–413.

Zhang, J., Q. Dai, D. Park, et al. (2016). Targeting DNA replication stress for cancer therapy. *Genes 7*, 1-16.

Zimmermann, F.K. (1973). Detection of genetically active chemicals using various yeast systems. *In* a. Hollaender [ed.], chemical mutagens: principles and methods for their detection. Volume 3, 209–239. Springer US, Boston, MA.

Zong, W.X., D. Ditsworth, D.E. Bauer, et al. (2004). Alkylating DNA damage stimulates a regulated form of necrotic cell death. *Genes and Development 18*, 1272–1282.